Cranfield University

Sarfraz Khaliq

Fibre optic long period fibre gratings for sensing applications

Centre for Photonics and Optical Engineering

School of Engineering

Department of Process and Systems Engineering

PhD

Cranfield University

Centre for Photonics and Optical Engineering

School of Engineering

Department of Process and Systems Engineering

PhD Thesis

Academic Year 2002-2003

Sarfraz Khaliq

Fibre optic long period gratings for sensing applications

Supervisors: Dr. Stephen W. James

Prof. Ralph P. Tatam

Submission Date: March 2003

This thesis is submitted in partial fulfilment of the requirements for the Degree of Doctor of Philosophy.

ABSTRACT

Long period gratings (LPGs) are formed by inducing a permanent periodic modulation of the refractive index (RI) of the core of an optical fibre. The transmission spectrum of the LPG contains a series of attenuation bands centered at discrete wavelengths. The exact form of the transmission spectrum and the central wavelengths of the attenuation bands, are sensitive to the period and the length of the LPG and to the local environment. The sensitivity of a LPG to a particular measurand is dependant upon the composition of the fibre and upon the order of the cladding mode to which the guided mode is coupled to and is thus different for each attenuation band.

The range of responses makes LPGs particularly attractive for sensor applications. In this thesis, three LPG based sensors that utilise the LPG's responses to the RI of its surrounding medium are demonstrated. An enhanced temperature sensor demonstrates a temperature sensitivity of 19.2nm/°C over a range of 1.1°C and a 14.8 % change in the attenuation band's minimum transmission value /°C over a range of 2.0°C.

A LPG has been shown to detect the RI changes in a curing epoxy resin, and are therefore suitable for monitoring the state of the epoxy's cure.

A liquid level is presented that is based on the partial immersion of the LPG into RI oil. This liquid level sensor overcomes the majority of the drawbacks associated with the current liquid level measuring techniques by providing continuous measurement in any environment. The relative changes in the minimum transmission values, CMTV, of the attenuation bands demonstrate a linear response, over ≈ 62% of the 40mm long LPG, with a sensitivity of 2% CMTV/ % length of the LPG. This corresponds to a sensitivity of 4.8% CMTV/ mm length of the LPG.

ACKNOWLEDGEMENTS

I would like to take this opportunity to thank the numerous people at the university and at home, who have made this Ph.D. thesis possible.

I am thankful to Dr. Steven James and Prof. Ralph Tatam for their help and ideas along with their repeated reading of draft copies of this thesis and publications arising from this work. My special gratitude goes to Dr. Steven James for allowing me to be his first PhD student; being a friend and helping me mature professionally. I greatly appreciate his patience with me, for being the source of wisdom that I called upon on many occasions and especially for his input to the computer modelling and Labview programs. Thanks goes to past and present members of the optics group for making lunch times as pleasant as possible in particular Dr. Gerald Byrne, and Dr. Nick Rees for helping me destroy evidence of the chips which often accompanied my sandwiches and for their useful discussions along with Dr. David Nobes, Dr. Roger Groves and Sammy Cheung. My sincere thanks go to Edmond Chehura and Dr. Gerald Byrne for keeping me company during the long, hard and lonely hours that were spent in the labs during the evenings and weekends. I am indebted to Stephen Staines for being able to design and manufacture, from my hand waving descriptions, various items used during the experiments presented in this thesis and for his general advise on home DIY. I must also thank Dr. Chen-Chun Ye for teaching me how to manufacture my own LPGs, so no matter how many I broke I could always make another.

My gratitude goes to my parents Abdul and Munawar Khaliq and my wife Yasmin whose unfailing support and encouragement allowed me to complete this research program. Extra special thanks to my children, Almaas and Bilal, for their continual support and for forgiving me for not being there, when they were making bows and arrows, at their school plays and sports days. To Yasmin for her love and understanding when morale was low and for ignoring me when the language got particularly bad. I would like to thank my brothers Imran and Urfan and also my sister Razwana for allowing me to complain bitterly to them when the work was not going according to plan. Finally, I would like to thank my nephew, Dr. Rabnawaz Aziz, for

making constructive suggestions, which have been incorporated into various chapters of the thesis.

Contents

Glossary of symbols and abbreviations

Symbols

β	propagation constant
b	normalised propagation constant
$\Delta\beta$	differential propagation constant
d	the rate of change
κ	coupling coefficient
k_0	wave number in free space
Δ	relative difference in the core-cladding refractive index
θ_c	critical angle
ε	applied strain
δ	detuning parameter
η	overlap integral between the core and cladding modes
ω	angular frequency
c	free space velocity of light
°C	degrees Celsius
n_1 (n_{core})	refractive index of optical fibre core
n_2 (n_{cl})	refractive index of optical fibre cladding
n_3 (n_{Ext})	refractive index of the external surrounding medium
n_{eff}	optical fibre core effective index
ΔL	extension of the fibre's length
Λ	periodicity of a long period grating
λ	central wavelength
λ_B	Bragg centre wavelength
λ_{cut}	cut-off wavelength of the fibre
λ_i	coupling wavelength
$\Delta\lambda$	change in wavelength

$E_{01}(r)$	electric field distribution of the fundamental guided modes
$E_{cl}^{(m)}(r)$	electric field distribution of the circularly symmetric cladding modes of the order m
T	temperature
z	perturbation in a fibre
⊗	light source
	detector

Abbreviations in the text

A	Amplitude of a sine wave
a	diameter of the fibre core
B-Ge	Boron-Germanosilicate
b	diameter of the fibre cladding
C	the ratio of the power coupled from one forward propagating mode to another in the presence of a perturbation
CCD	charge coupled device
CO_2	carbon dioxide
CW	continuous wave
d	wavelength offset
dB	decibels
DSC	dual shaped core
FBG	fibre Bragg grating
FOS	fibre optic sensor
FWHM	full-width half maximum
Ge	germanium
h	hours
H^+	hydrogen ion

L	length of the long period grating
l	length of long period grating immersed in liquid
Ltd	Limited (company)
LB	Langmuir Blodgett
LC	liquid crystal
LPG	long period grating
Nd:YAG	Neodymium doped Yttrium Aluminium Garret
P	power transmitted though a long period grating
PC	personal computer
PID	proportional, integral and derivative
Pt	platinum
R&D	research and development
RI	refractive index
s	seconds
T	normalised power transmitted by the fundamental guided mode through a long period grating
T_o	minimum transmission value of an attenuation band
Ti	Titanium
TIR	total internal reflection
UV	ultra-violet
UVGFS	ultra-violet grade fused silica
V	normalised frequency
WDM	wavelength division multiplexing, wavelength division multiplexer
x	rotational angle

Abbreviations in the figures

A	amplitude mask
B	V-grooved block

BBS	broadband light source
BD	UV beam dump
BS	beam splitter
C	fibre connector (FC301)
°C	degrees Celsius
CF	Corning Flexcore 1060nm fibre
κ_A	coupling efficiency of attenuation band A
κ_B	coupling efficiency of attenuation band B
L	cylindrical lens
LED	light emitting diode
LIF	lead in fibre
LOF	lead out fibre
LPG	long period grating
Ltd	limited (company)
mm	millimeters
m^{-1}	inverse meters
OF	optical fibre
PD	photo-diode
RF	receiving fibre
S	UV source (laser)
SF	fibre with special refractive index profiles
SMF	Corning SMF-28 fibre
Std	standard telecomms fibre
T_A	minimum transmission value of attenuation band A
T_B	minimum transmission value of attenuation band B
TF	transmitting fibre
TS	translation stage

List of Figures

List of Tables

Chapter 1 Introduction to fibre optic sensors

1.1 Introduction

The nature of the environment in which we live and work, and the fragile state of many aspects of the natural and man made environment, has been a major lesson for scientists over the last few decades. People are now more aware and involved in what goes on around them and they view the abilities of scientists and engineers with suspicion to provide an adequate solution to the problems that they directly or indirectly face. Monitoring of the various aspects of the environment, whether it is external or internal to us and involving chemical, physical or bio-medical parameters is an essential process for the well being of all.

Fibre optic sensor technology has potentially a major part to play in this process, both to complement existing technologies and to promote new solutions to difficult measurement issues.

1.2 Fibre optic sensor technology

Intensive research and development in the field of optical engineering over the last twenty years has given rise to an entirely new type of measurement device, the fibre optic sensor, FOS. FOSs boast a number of crucial advantages over traditional electrical and mechanical sensors: they are compact, robust, chemically inert, non-conductive, and are immune to electrical interference. As optical fibres are made of non-conducting dielectric materials it means that they can operate at zero potential, which makes them useful for operation in explosive environments, and, since the light is constrained to be within the fibre, the risk of explosion is further reduced. As well as acting as a sensing medium, the optical fibre can also be used for data transmission where their facility of having a low degree of signal attenuation and high transmission capacities may be exploited. In addition, they are compatible with the telecommunications and

optoelectronics industries, where the costs of the continually improving available technology are falling, and they may potentially take advantage of technological advances. Ideally, sensors need to be lightweight and should not compromise the structural integrity of the product whose properties they are going to sense. FOSs meet this criteria and offer another key advantage; they are insensitive to electro-magnetic interference and consequently do not require any bulky shielding. They also offer potential for fully distributed or high density multiplexing that will allow large numbers of sensor elements to be placed in series using the same length of fibre.

FOSs are generally classified as either intrinsic or extrinsic. In an intrinsic FOS, the sensing element is the optical fibre itself and its physical properties can be modified in response to an external physical or chemical influence, which is often called the measurand. Modulation of the fibre's properties directly perturbs the optical property of the light being guided within it. The properties of the light that can be changed are the intensity, frequency, phase, wavelength, modal distribution, or polarisation. Monitoring the modified properties of the light permits measurement of the measurand.

In an extrinsic FOS, the measurand again modulates the optical signal, but the perturbation of the properties of the light takes place in a region outside the optical fibre. The light still travels to the measurement region in an optical fibre, and often from the measurement region to the detector in another fibre; the fibres now act simply as light guides. A large number of techniques and schemes have been demonstrated and a large body of literature exists [1].

FOSs offer a variety of ranges and resolution and on most occasions show cross-sensitivity to other measurands, therefore, careful consideration has to be given to the technique that is selected for use. The range and resolution of a particular FOS may not be suited to every application or that particular details of the deployment may favour the properties of one scheme over another.

The interest in FOSs has increased in recent years because of the development of new optical fibres, optical components, sources and detectors, primarily for use with the communication industry, but exploited in sensor systems. The objective for optical fibres destined for communication purposes has always been to manufacture fibres with transmission properties that are independent of external environmental parameters such as temperature, pressure, humidity and strain. It is these exact areas of sensitivity that are exploited in FOSs for sensing applications. The research in this area has reached a level of maturity whereby FOSs systems are undergoing field trials and application tests [1, 2, 3, 4]. There are examples of commercially available FOSs such as fibre optic LDV and fibre current sensors and of these the most successful has been the fibre optic gyroscope (FOG) as a means of measuring rotation [5, 6]. However, there is currently an increasing commercial interest in FBG sensors with a large number of reports of field tests and application trials [2, 3].

1.3 Fibre gratings

Fibre gratings represent perhaps the most exciting development in the area of fibre optic research in recent years. Fibre gratings are widely exploited in the telecommunications industry, and many field trials of fibre grating sensors for the multiplexed sensing of parameters such as, temperature [3], strain [3], pressure [3], chemical concentration [3], load and vibration have been reported [3]. The fibre grating is a device that acts as a clearly defined and identifiable sensing region within the optical fibre. Fibre gratings are formed by inducing a permanent perturbation in the mode propagation constant in the core of germanosilicate optical fibre. This may be achieved by laterally exposing the fibre to a periodic pattern of UV irradiation, through the side of the fibre at a wavelength that is within the absorption band of germanium oxygen deficient centres, 193 - 281nm [7]. Since a grating or grating array can be directly written into a fibre's core without changing the fibre's geometry, fibre gratings as sensors and telecommunication devices are highly miniaturised and compatible with a wide range of important and unique applications [8]. These applications include being used as fibre laser mirrors [9], fibre filters [10, 11] and there is a particular interest in

using them for dense wavelength division multiplexing systems, WDM, to enhance the capacity of both existing long-haul networks and future local area networks [12]. Fibre gratings present themselves as ideal sensing solutions for real everyday applications and appear to be on the verge of large scale commercial exploitation across a broad range of sectors including civil engineering [13, 14, 15, 16], marine engineering [17, 18], medical [19] and military [20].

In accordance with the period of the grating, fibre gratings can be classified into two types, the short period fibre Bragg grating (FBG) and the long period grating (LPG). Section 1.4 will discuss the FBG and section 1.5 will introduce LPGs and highlight their main attributes.

1.4 Fibre Bragg gratings

FBGs, have a periodicity <1μm and are usually formed in the core of an optical fibre. When such a device is illuminated by a broadband optical source, a narrow-band spectral component corresponding to the Bragg resonance wavelength of the grating, λ_B, is reflected. The Bragg condition given by

$$\lambda_B = 2n_{eff}\Lambda \tag{1.1}$$

where n_{eff} is the effective refractive index of the propagation mode and the Λ is the grating period. All other wavelengths outside the narrow reflection band will be transmitted. It can be seen from equation 1.1 that environmentally induced changes in either n_{eff} or Λ will result in a shift in the reflected Bragg wavelength. The measurement of the wavelength shift is the foundation of the FBG based sensor and its primary measurands are temperature and strain [21]. Figure 1.1, illustrates the principle of operation of a FBG.

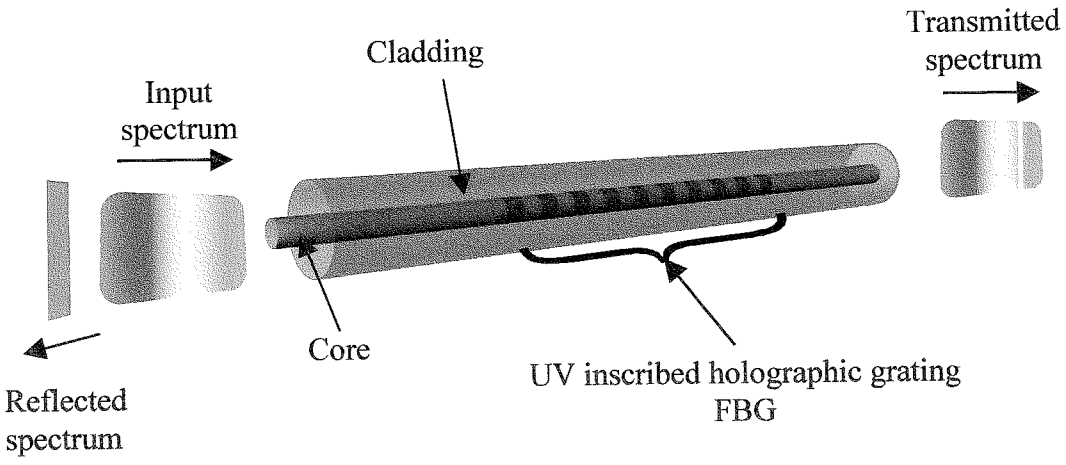

Figure 1.1: *Schematic diagram of a FBG illustrating that only the wavelength of light, λ_B, that satisfies the Bragg condition, is reflected.*

FBG sensors have attracted a considerable amount of interest within the FOS research community [2, 3]. The main reason for this is that FBG sensors offer a number of advantages over other FOS sensors including potentially low cost, unique wavelength multiplexing capacity, the transduction mechanism avoids the ambiguity of a phase measurement and is intensity independent. Over the past decade, FBGs have been extensively investigated for sensing applications [2]. The suitability of FBGs for the important application of strain sensing, whilst embedded in a composite aircraft structure, is gauged by the criteria suggested for an ideal sensor [22]. The criterion suggests that, ideally, a fibre optic sensor should be intrinsic in nature for minimum perturbation and stability. The sensor should be positioned locally so that it can operate remotely with insensitive leads [22]. It should have the ability to respond only to the strain field and ignore any changes in direction, be well behaved, and have reproducible responses [22]. The sensor should be robust for installation purposes and preferably of an all fibre construction for operational stability [22]. The sensor should be able to provide a linear response for absolute measurements and be insensitive to phase interruption at the structure's interface [22]. The sensor should consist of a single optical fibre for minimum perturbation and common mode rejection. If the sensor is single ended it would make installation and connection easier [22]. The sensor should be sufficiently sensitive to the measurand with an adequate measurement range and be

amenable to multiplexing to form sensing networks within a structure [22]. Finally, the sensor should be easily manufactured and adaptable to mass production [22].

For strain sensing, the FBG is the only type of sensor that fitted the criteria [23]. FBG sensors arrays have been used in the monitoring of large engineering structures such as buildings, bridges and aircraft [5].

FBGs may be incorporated into the structure to monitor it throughout its working lifetime. Preliminary accelerated ageing tests indicate that properly exposed and annealed FBGs are reliable for long term operation over periods greater than 25 years without degradation in performance [24]. FBGs may be used as an integral part of a control system that would correct for an environmental change being detected by the fibre optic system forming part of a so called 'fibre-optic smart structure' [3, 5].

Manufacturers are aware that their products gain added value when a structural monitoring system is incorporated within it [25], because the consumer can see that this can potentially extend the operating life of the product, optimise the maintenance schedule and improve its overall safety. The increased interest in the use of embedded sensors is attributed in the main to the potential reduction in cost and increased reliability of the component parts used in fibre optic systems. Although there exists some potential for further improvement in terms of performance and functionality, efforts are now engaged to realise cost effective FBG sensor systems and to explore more potential applications.

Long period gratings, LPGs, are emerging as an exciting new sensor technology, complementary to FBGs in offering the ability to simultaneously monitor a number of different measurands.

1.5 Long period fibre gratings

LPGs are a relatively new class of periodic structure, that were originally proposed in 1995 [26] and were developed, as were many optical sensor components, for use in communication systems [26]. LPGs employ a similar fabrication technology to that needed to produce the more widely used FBG. LPGs are never the less different to FBGs in that the periodicity of a LPG is typically tens to thousands of microns. When a LPG, in a single mode fibre, is illuminated by light of a broadband spectrum more than one part of the light will satisfy the phase matching condition thus allowing coupling between the guided fundamental mode and the forward propagating cladding modes. The high attenuation of the cladding modes results in the transmission spectrum of the LPG containing a series of attenuation bands, centred at discrete wavelengths, each attenuation band corresponding to coupling from a guided core mode to a different cladding mode. The principle of operation of a LPG is illustrated in Figure 1.2.

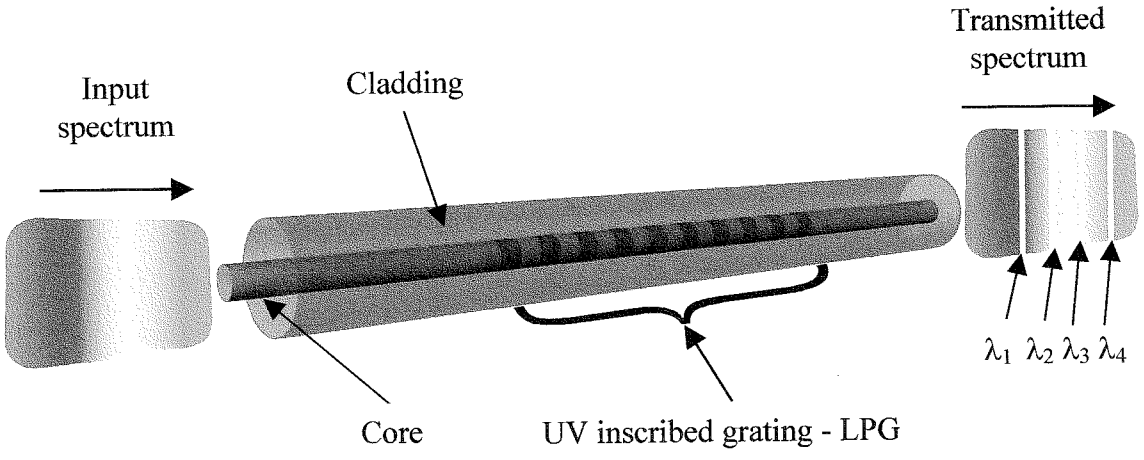

Figure 1.2: *Schematic diagram of a LPG illustrating the attenuation bands situated in the transmission spectrum at wavelengths λ_1 - λ_4 which satisfy the phase matching condition.*

The exact form of the transmission spectrum and the central wavelengths of the attenuation bands, are sensitive to the period of the LPG, the length of the LPG and to the local environment. In addition to the sensitivity to temperature and strain exhibited by FBGs, LPGs are also sensitive to an applied bend radius and the refractive index, RI,

of the material surrounding it [27].

During this research program, it is these properties of LPGs that will be characterised and exploited to demonstrate novel sensing schemes. The next section presents an outline of the major objectives of this thesis.

1.6 Thesis objectives

This research program focused on producing high quality fibre optic LPGs and characterised their response to a range of measurands. The results of the characterisations were exploited to demonstrate high performance sensing systems, for the measurement of temperature with an enhanced sensitivity, for the measurement of a liquid's level and for the detection of changes in the RI of the medium surrounding the fibre.

To facilitate the demonstration of such novel sensing schemes the thesis provides details of the supplementary work undertaken:

- the development of a compact and portable interrogation and demodulation system
- the design and development of a LPG fabrication system
- characterisation of the LPG's response to
    - temperature
    - strain
    - bending
    - and change in refractive index of the surrounding medium
- the thesis then demonstrates three novel sensing schemes
    - the measurement of liquid level
    - a highly sensitive temperature sensor

- monitoring the state of cure of an epoxy resin

The various applications of the LPG sensors considered here meant that the experimental instrumentation for this project needed to be portable; consequently, the initial phase of the work was to design and implement a portable and compact interrogation and demodulation system. This system is based on a low cost CCD spectrometer that is interfaced to a PC that controls, acquires and logs the data and enables the complete LPG spectrum to be viewed in real time. The CCD spectrometer used is limited to operation in the 400 – 1100nm range. In this thesis commercially available photosensitive optical fibre with a cut-off wavelength of 650nm was used which is lower than the fibres generally used in LPG experiments, which have cut-off wavelengths > 1200nm.

The system offers the facility to monitor, in real time, the formation of the LPG. This greatly aided the repeated manufacture of high quality LPGs and to that end two fabrication techniques, the point by point and the amplitude mask techniques were investigated.

To gain an understanding of the response of LPGs to the various measurands, the LPGs were exposed to changes in strain, temperature, bending curvature and in the RI of the medium surrounding it. FBGs have been considered the ideal strain sensor [23]. The strain sensitivity of LPGs is found to be up to two times that of a FBG [9], often LPGs can be strain insensitive which is an advantage for temperature sensing. The sensing of temperature is one of the measurands that has been extensively investigated [9, 28, 29, 30, 31, 32], LPGs show a sensitivity that is four times greater than that of a FBG. LPGs can also be insensitive to temperature, which makes them ideal candidates for strain sensing [28, 32].

The transmission spectrum of a LPG is highly sensitive to bending. The two observed responses are that the attenuation bands in the transmission spectrum shift with increasing bend curvature [33] and that the attenuation bands divide into two [34, 35], as illustrated in Figure 1.3. The wavelength separation between the two divisions

increases with increasing bend curvatures [34, 35].

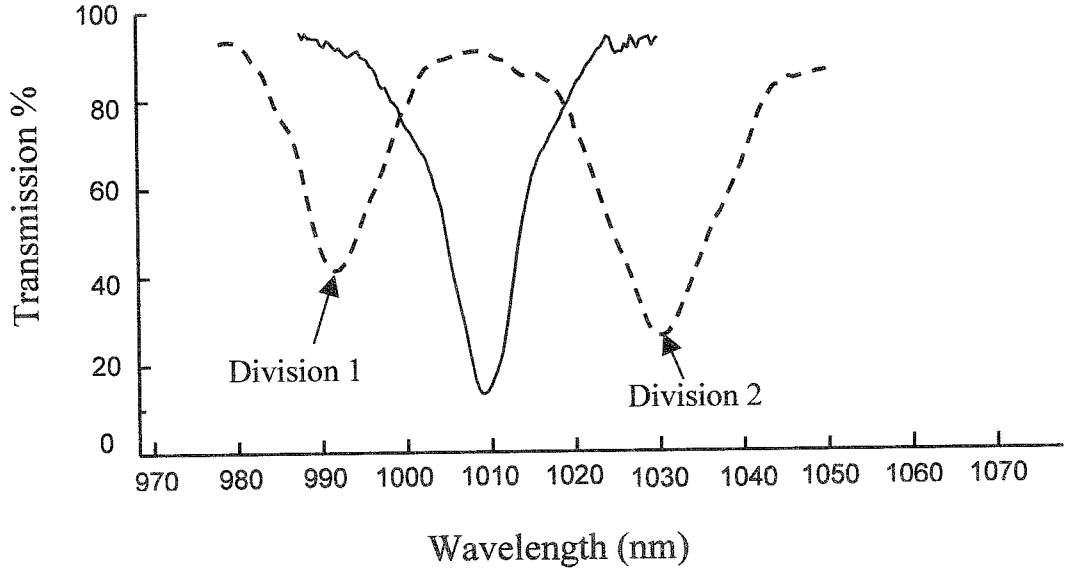

Figure 1.3: *A plot illustrating the dividing into two of an attenuation band when a curvature was applied to a straight LPG.* —— *Straight LPG,* ---- *LPG bent with a curvature of* $1.55m^{-1}$.

Structural bend sensors, based upon both of the observations have been demonstrated [33, 35, 36, 37]. In this thesis the author presents the characterisation of the response of a LPG's transmission spectrum to the orientation of the UV exposed side of the fibre relative to the plane of the bend curvature [38].

The response of a LPG's transmission spectrum to a change in the RI of its surrounding medium has been previously investigated [39, 40, 41]. In this thesis the characterisation of the RI response of a LPG with attenuation bands at wavelengths < 1200nm is presented and is exploited to demonstrate three novel sensing schemes. The thesis demonstrates a LPG based liquid level sensor, an enhanced temperature sensor and an in-situ means of monitoring the RI change occurring in a curing epoxy resin.

In many applications, knowledge of the volume of a liquid is required, for example, in fuel storage systems, and chemical processing. A wide range of liquid level sensing techniques already exist based around mechanical, electrical and optical techniques. A novel liquid level sensor is demonstrated in chapter 6 that overcomes the majority of the drawbacks associated with the current liquid level measuring techniques by providing continuous measurement in dangerous environments.

The thesis then presents, in chapter 6, an enhanced temperature sensor based on a LPG surrounded by a refractive index oil of a high thermo-optic coefficient that has a sensitivity that is two orders of magnitude higher than that shown by a LPG in air. This enables the sensor to act as a thermally tuned optical filter.

A proposed area of research was specifically aimed at advanced materials applications of LPG sensors. A wide range of industries use composite materials that are generally made of stacked laminate or woven fabrics of continuous carbon or glass or aramid fibre, pre-impregnated with an epoxy resin polymer system. The resin is heated under high pressure, so that it reacts chemically to produce a rigid cross - linked structure, known as the 'cure'. Current composite technology faces numerous problems, which leads to the inability to produce consistent batches of the material. The introduction of robust cure monitoring sensors would allow real-time modification of the curing process to compensate for the actual state of the composite during curing and lead to subsequent improvements in production. LPGs were used for the detection of the refractive index change in a curing epoxy resin with the goal of determining the effectiveness of using them to monitor the state of the epoxy's cure.

1.7 Thesis summary

Chapter 1 presented an introduction to fibre optic technology and detailed in general terms the operation of fibre optic sensors. The chapter introduced fibre gratings and in particular FBGs and LPGs and outlined the significant features of the thesis.

Chapter 2 discusses LPGs in detail and the theory involved with them. The Chapter also discusses the simple in-house model that allows the calculation of the coupling wavelengths for a given range of the LPG's periodicities and the results obtained from it.

Chapter 3 presents a review of the sensing applications of LPGs with a particular emphasis on their application as sensors for single and multi-parameter sensing.

Chapter 4 outlines the methods employed to bring about a permanent perturbation in the mode propagation constant in the core of the fibre. The chapter provides a detailed discussion of the fabrication process used to produce the LPGs in the laboratory at Cranfield. The chapter then discusses the need to anneal LPGs before use as sensors.

Chapter 5 details the characterisation of the LPG's response to measurands such as temperature, strain, bending and changes in the RI of the medium surrounding the LPG.

Chapter 6 presents the three novel LPG based sensing schemes that exploit the RI sensitivity of the LPG: the liquid level sensor, the sensor with enhanced temperature sensitivity and the sensor for monitoring the cure of an epoxy resin.

Chapter 7 presents the conclusions obtained from the work and discusses the work proposed for future investigations in this field.

1.8 Chapter summary

This first chapter has introduced fibre optic sensors and discussed the advantages that they offer over traditional mechanical and electrical sensors. The chapter introduced the relatively new class of FOS, the fibre grating, and discussed the advantages that they offer over conventional FOS. The chapter introduces the distinguishing features of the two different classes of fibre grating, the fibre Bragg grating and the long period grating. The objectives of the thesis are discussed and a summary of the thesis is presented.

References:

1 'Optical Fibre Sensors, principles and Components', Vol. 1, Artech House, Boston and London (1988), edited by J. Dakin and B. Culshaw.

2 A.D. Kersey, 'A review of recent developments in fibre optic sensor technology', Optical Fibre Technol., **2**, pp. 219 – 317, (1996).

3 Y.J. Rao, 'Recent progress in applications of in fibre Bragg grating sensors', Optics in lasers and Eng., **31**, pp. 297-324, (1999).

4 K.T.V. Grattan and T. Sun, 'Fibre optic sensor technology: an overview', Sensors and Actuators, **82**, pp. 40-61, (2000).

5 A.D. Kersey, M.A. Davis, H.J. Patrick, M. LeBlanc, K.P. Koo, C.G. Askins, M.A. Putnam and E. Joseph Friebele. 'Fibre grating sensors', J of Lightwave Technol., **15**, pp. 1442-1461, (1997).

6 'Handbook of Optical Fibre Sensing Technology', Wiley and Sons, Ltd., (2002) edited by Josè Miguel López-Higuera.

7 D.L. Williams, B.J. Ainslie, R. Kashap, G.D. Maxwell, J.R. Armitage, R.J. Campbell and R. Wyatt, 'Photosensitive index changes in germania doped silica glass fibres and waveguides ', Proc. SPIE, **2044**, pp. 55-68, (1993).

8 Y.J. Rao, 'In fibre Bragg grating sensors', Meas. Sci. Technol., **8**, pp. 355-375, (1997).

9 S. Vasiliev and O. Medvedkov, 'Long period refractive index fibre gratings: properties, applications and fabrication techniques', In Advances in Fibre Optics, Proceedings of SPIE, **4083,** pp. 212 – 223, (2000).

10 X. Shu, T. Allsop, B. Gwandu, L. Zhang and I. Bennion, 'Room-temperature operation of widely tunable loss filter', Electron. Lett., **37**, pp. 216 – 218, (2001).

11 R. Qian and H.F. Chen, 'Gain flattening fibre filters using phase shifted long period fibre gratings', Electron. Lett., **34**, pp. 1132 – 1133, (1998).

12 R.G. Smart, J.W. Sulhoff, J.L. Zyskind, J.A. Nagel and D.J. DiGiovanni, 'Gain peaking in a chain of 980nm pumped erbium-doped fibre amplifiers', IEEE-Photon. Tech. Lett., **6**, pp. 380-382, (1994).

13 R. Masskant, T. Alaive, R.M. Measures, G. Tadros, S.H. Rizkalla and A. Guha-Thakurta, 'Fibre - optic Bragg grating sensors for bridge monitoring', Cement and Concrete composites, **19**, pp. 21-23, (1997).

14 S.T. Vohra, B. Althouse, G. Johnson, S. Vuroillot and D. Inaudi, 'Quasi-static monitoring during the push phase of a box-girder bridge using fibre Bragg grating sensors ', in European Workshop on Fibre Optic Sensor, B. Culshaw and J.D.C. Jones (eds.) Proc. SPIE **3483**, pp. 283-287, (1998).

15 P. Ferdinand, O. Ferragu, J.L. Lechien, B. Lescop, S. Magne, V. Marty, S. Rougeault, G. Kotrotsios, V. Neuman, Y. Depeursinge, J.B. Vanuffelen, D. Varelas, H. Berthou, G. Pierre, C. Renouf, B. Jarret, Y. Verbrandt, W. Stevens, M.R.H. Voet and D. Toscano, 'Mine operating accurate stability control with optical-fibre sensing and Bragg grating technology', the European Brite/Euram stabilos project, J of Lightwave Technol., **13**, pp. 1303-1313, (1995).

16 R.L. Idriss, M.B. Kodindouma, A.D. Kersey and M.A. Davis, 'Multiplexed Bragg grating optical fibre sensors for damage evaluation in highway bridges', Smart Materials and Structures, **7**, pp. 209-216, (1998).

17 D.R. Hjelme, L. Bjerkan, S. Neegard, J.S. Rambach and J.V. Aarsnes, 'Applications of Bragg grating sensors in the characterisation of scaled marine vehicle models', Appl. Opt., **36**, pp. 328-336, (1997).

18 G. Wang, G.B. Havsgard, E. Urnes, K. Pran, S. Knusden, A.D. Kersey, M.A. Davis, T.A. Berkoff, A. Dandridge, and R.T. Jones, 'Digital demodulation and signal processing applied to fibre Bragg grating strain sensor arrays in monitoring transient loading effects on ship hulls', in 12th International Conference on Optical Fibre Sensors, OSA Technical Digest Series, **16**, pp. 646-649, Washington, DC, USA, (1997).

19 Y.J. Rao, B. Hurle, D.J. Webb, D.A. Jackson, L. Zhang and I. Bennion, 'In-situ temperature monitoring in NMR machines with a prototype in fibre Bragg grating sensor system', in 12th International Conference on Optical Fibre sensors, OSA, Technical Digest, Post-conference edition, **16**, pp. 646-649, Washington, DC, USA, (1997).

20 S.W. James, R.P.Tatam, S.R. Fuller and C. Crompton, 'Monitoring transient strains on a gun barrel using fibre Bragg grating sensors', Meas. Sci. and Technol., **10**, pp. 63-67, (1999).

21 W.W. Morey, G. Meltz and W.H. Glen, 'Fibre optic Bragg grating sensors', Proc. Fibre Optic and Laser Sensors VIII, Boston, pp. 98-107, (1989).

22 R.D. Turner, T. Valis, W.D. Hogg and R.M. Measures, 'Fibre Optic strain sensors for smart structures', J of Intelligent Materails Sys. Struct., **1**, pp 25-49, (1989).

23 R.M. Measures, 'Fibre optic sensing for composite smart structures', Composites Eng., **3**, pp. 715-750, (1993).

24 W.W. Morey, G.A. Ball and H. Singh, 'Applications of fibre grating sensors', Proc. of SPIE, **2839**, pp. 40-63, (1996).

25 M. J. O'Dwyer, 'Implementation and Appraisal of an In-Fibre Bragg Grating Quasi-Distributed Health and Usage Monitoring System with Applications to Advanced Materials', Ph.D. Thesis, Cranfield University (2000).

26 A.M. Vengsarkar, P.J. Lemaire, J.B. Judkins, V. Bhatia, T. Erdogan and J.E. Sipe, 'Long period fibre gratings as band rejection filters', OFC 1995, PD4-2, (1995).

27 V. Bhatia, 'Applications of long period gratings to single and multi-parameter sensing; Opt. Express, **4**, pp. 457-466, (1999).

28 K. Shima, K. Himeno, T. Saski, S. Okude, A. Wada and R. Yanauchi, 'A novel temperature insensitive long period fibre grating using a boron-doped-germanosilicated core fibre', Optical Fibre Conf. Tech. Dig. **6**, pp. 347-348, (1997).

29 V. Bhatia, D. Campbell and R. O. Claus, 'Simultaneous strain and temperature measurement with long-period gratings', Opt. Lett., **22**, pp. 648-650, (1997).

30 V. Bhatia, D.K. Campbell, T.D'Alberto, G.A. Ten Eyck, D. Sherr. K.A. Murphy and R.O. Claus, 'Standard optical fibre long period gratings with reduced temperature sensitivity for strain and refractive index sensing', In Tech. Dig. Conf. Opt. Fibre Comm. Dallas, TX. pp. 346 –347, (1997).

31 V. Bhatia, 'Properties and sensing applications of long period gratings', Ph.D. Thesis, Virginia Polytechnic and State University, Blackburg, Virginia, (1996).

32 J.B. Judkins, J.R. Pedrazzani, D.J. DiGiovanni and A.M. Vengsarkar, 'Temperature insensitive long period grating fibre gratings', Optical Fibre Conf. Tech. Dig. PD1, San Jose, USA (1996).

33 H.J. Patrick, C.C. Chang and S.T. Vohara, 'Long period fibre gratings for structural and bend sensing', Electron. Lett., **35**, pp.1773-1775, (1998).

34 C.C. Ye. 'Internal report', Cranfield University, 2000.

35 Y.Lin, L.Zhang, J.A.R. Williams and I. Bennion, 'Optical bend sensor based on measurement of resonance mode splitting of long period fibre grating', IEEE Photon. Technol. Lett., **12**, pp. 531-533, (2000).

36 C.C.Ye, C. Wei, S. Khaliq, S.W. James, P. E. Irving and R.P.Tatam, 'Bend sensing in structures using long period optical fibre gratings', SPIE, 5th European Conference on Smart Structures and Materials, **4073**, pp. 311- 315, Glasgow (U.K.), (2000).

37 J. Rathje, M. Svalgaard, J. Hübner and M. Kristensen, 'Sensitivity of a long period optical fibre grating bend sensor', OFC' 98, OSA Tech. Digest Series, **2**, pp. 238 – 239, (1998).

38 S. Khaliq, S.W. James, C.C. Ye, C. Wei, P. E. Irving and R.P. Tatam, 'Structural bend sensing using optical fibre long period gratings', IOP, Applied Optics and Opto-electronics Conference, Loughborough University (U.K.) pp. 20-24, Sept. (2000).

39 B.H. Lee, Y. Liu, S.B. Lee, S.S. Choi and J.N. Jang, 'Displacements of the resonant peaks of a long period grating induced by a change of ambient refractive index', Opt. Lett., **22**, pp. 1769 – 1771, (1997).

40 H.J. Patrick, A.D. Kersey and F. Bucholtz, 'Analysis of the response of long period fibre gratings to external index of refraction', J of Lightwave Technol., **16**, pp. 1606-1612, (1998).

41 O. Duhem, J.F. Henniont, M. Warrenghem and M. Douay, 'Demonstration of long period gratings efficient couplings with an external medium of refractive index higher than that of silica', Appl. Opt., **37**, pp. 7223 – 7228, (1998).

Chapter 2 Theory of fibre optic long period gratings

2.1 Introduction

This chapter discusses the principles of operation of LPGs in detail. The concept of the exchange of power between one or more modes in a perturbed optical fibre system is introduced. Coupled mode theory is used to explain the interaction between various modes and the phase matching condition for a periodic perturbation is presented. The transfer of power between co-directional propagating modes is discussed using the coupled mode equation.

2.2 Fibre optic long period gratings

LPGs are composed of a modulation of the propagation constants of the guided modes of an optical fibre and act to couple light between fibre modes. In general, this takes the form of a RI grating that is inscribed into the core of the optical fibre by structured UV irradiation. LPGs typically have a periodicity in the range 100μm - 1000μm and a gauge length of 20mm - 40mm. The short grating wave-vector promotes coupling between the propagating core mode and the co-propagating cladding modes. The high attenuation of the cladding modes, due to scattering losses at the cladding and air interface, results in the transmission spectrum of an optical fibre containing a LPG having a number of loss or attenuation bands centered at discrete wavelengths, each attenuation band corresponding to coupling to a different cladding mode. A typical transmission spectrum of a LPG is shown in Figure 2.1, showing a number of well-defined attenuation bands. The LPG had a length of 40mm and a period of 400μm, it was written in photosensitive fibre with a cut off wavelength of 650nm, using UV illumination at 266nm, through an amplitude mask [1].

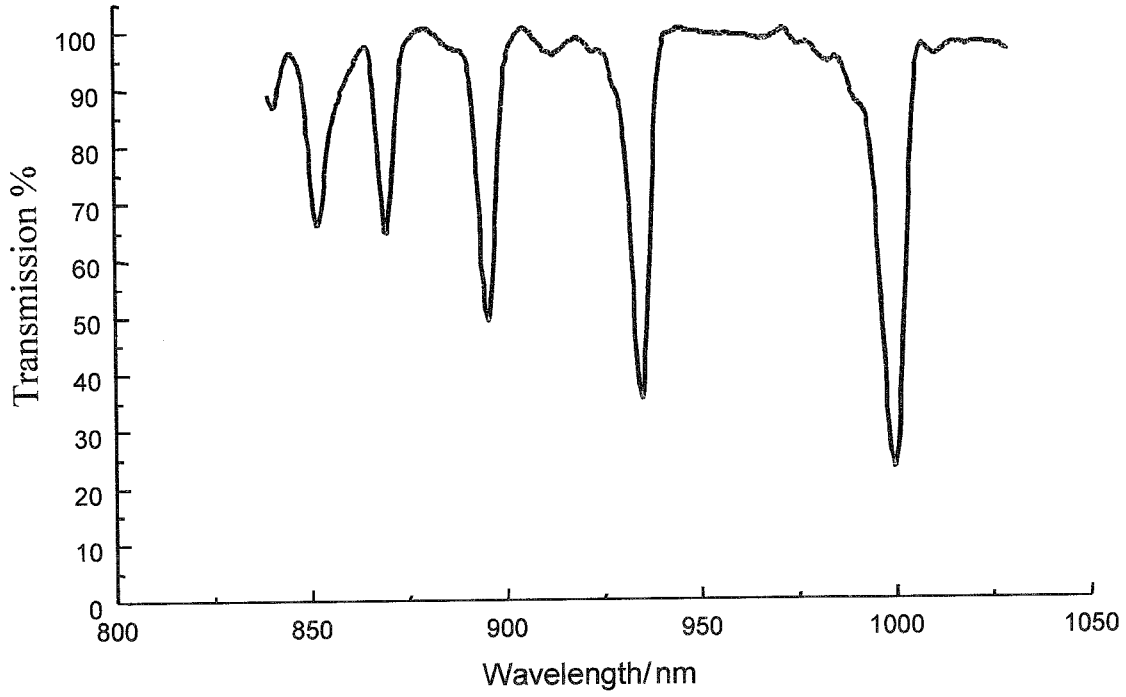

Figure 2.1: *Typical transmission spectrum of a LPG showing 5 of the attenuation bands. The LPG was of length 40mm and period 400μm, written in photosensitive fibre with a cut off wavelength of 650nm, using UV illumination at 266nm, through an amplitude mask* [1].

The centre wavelengths of the attenuation bands are determined by the phase-matching condition. The phase matching condition is governed by the difference in the effective RI of the cladding and core modes and by the period of the LPG [2] as will be shown in section 2.7.2. The minimum transmission, T_o, and the width of the attenuation bands are determined by the coupling efficiency between the core and the cladding modes and by the length of the LPG [3], and this will be discussed in section 2.6.1.

The exact form of the transmission spectrum and the centre wavelengths of the attenuation bands are sensitive to the local environment: temperature, strain, bend radius and RI of the medium surrounding the fibre. Changes in these environmental factors can modify the period of the LPG and/or the differential RI of the core and cladding modes. This then modifies the phase-matching conditions for coupling to the cladding modes and results in a change in the central wavelengths and minimum transmission of the attenuation bands.

The sensitivity to a particular measurand is dependent on the order of the cladding mode to which the guided optical power is coupled, the structure and the composition of the fibre and the period of the LPG, and is thus different for each attenuation band. This range of responses makes them particularly attractive for sensor applications, with the prospect for multi-parameter sensing using a single sensor element [4]. It is these distinguishing features that will be exploited in this thesis to demonstrate the novel sensing schemes.

2.3 Theory

In order to understand the properties of optical fibres, it is important to consider the wave-guide effect. Dielectric optical wave-guides have been extensively studied theoretically [5]. Optical fibres in their simplest form consist of a central core surrounded by a cladding layer whose RI is lower than that of the core. Such fibres are generally referred to as step-index fibers to distinguish them from graded-index fibres in which the RI of the core decreases gradually from the centre to the core boundary. Figure 2.2 shows a schematic cross section of typical optical fibres and the RI profiles.

The properties of the fibre are governed by its geometry. The diameter of the core, the RI between the core and the cladding, RI profile and the shape of the core all influence the characteristics of the fibre. Two parameters which characterise the fibre are the relative core-cladding index difference, Δ, and the normalised frequency, V, which are given in equations 2.1 and 2.2 respectively [6]:

$$\Delta = \frac{n_1 - n_2}{n_1} \tag{2.1}$$

$$V = k_0 a (n_2^2 - n_1^2)^{\frac{1}{2}} \tag{2.2}$$

where k_0, is the free space propagation constant at a wavelength of light λ, $k_0 = 2\pi/\lambda$, and a is the core radius. The parameter V determines the number of modes supported by the fibre. A step index fibre has been shown to support a single mode if $V < 2.405$ [6]. If the diameter of the core is reduced such that all but one of the modes is eliminated, then the fibre is referred to as a single mode fibre.

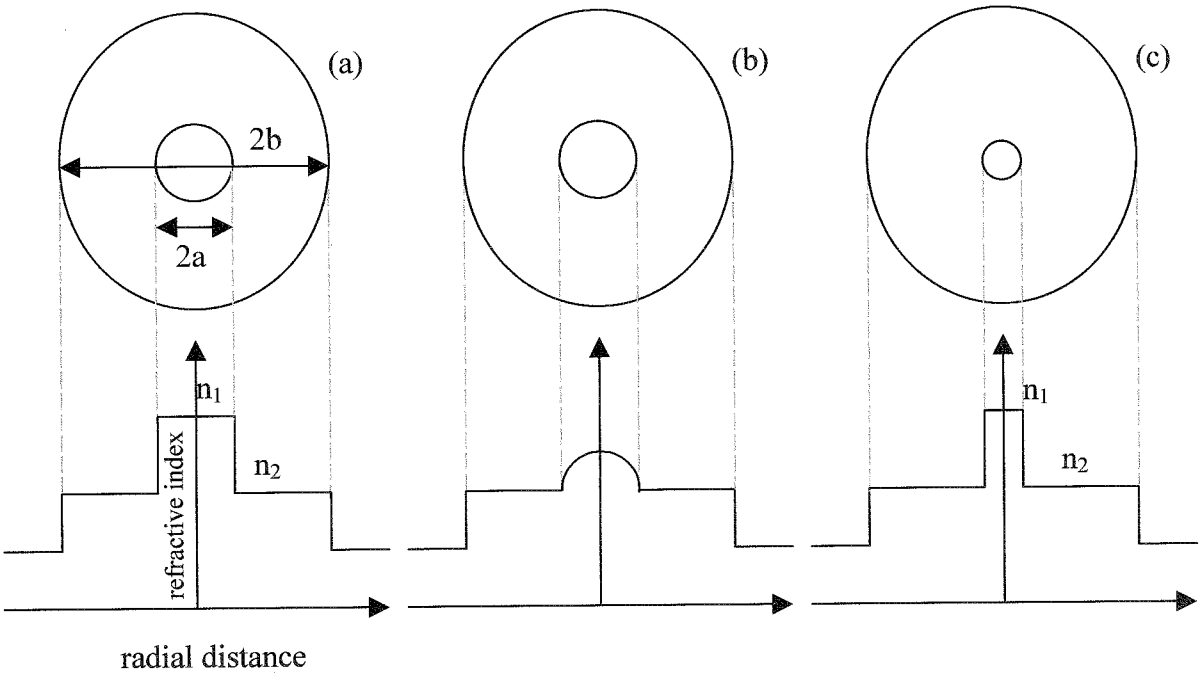

Figure 2.2: *Schematic of the cross section and the RI profile of (a) step-index multimode, (b) graded index fibre multimode and (c) single mode fibre where the RIs $n_1 > n_2$, a and b are the radii of the core and cladding respectively.*

2.4 Fibre modes

A simple model of the behaviour of light in a multimode fibre is illustrated in Figure 2.3. Light incident on the interface between the core and the cladding of the optical fibre undergoes total internal reflection, TIR, if the angle of incidence is greater than the critical angle, θ_c.

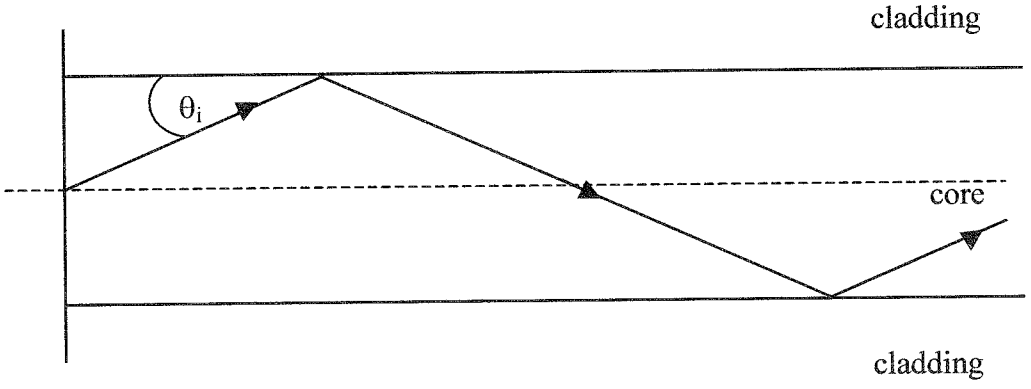

Figure 2.3: *Illustration of a light ray undergoing TIR when its angle of incidence θ_i is > than the critical angle θ_c.*

When this condition is satisfied the fibre can be used to guide light so that it propagates along the fibre, with the majority of the light confined within the core and an exponentially decaying tail extending into the cladding [7].

2.4.1 Guided and radiation modes

From a theoretical viewpoint, an optical fibre is a wave-guide and in a loss-less unperturbed optical fibre system and at any angular frequency, ω, optical fibres can support a finite number of guided modes. A mode in an optical fibre is a set of electromagnetic waves that participate in the propagation of energy in the fibre [8]. The guided modes travel in the fibre, without losing or gaining power, with discrete propagation constants, β, that are functions of the optical source's wavelength, the size, shape, and the nature of the optical fibre. The propagation constant can be determined by using Maxwell's equations and the electric and magnetic field boundary conditions

at the core and cladding interface [8]. It has been shown previously that the discrete values of propagation constants for the guided modes are confined to $n_2k_0 < |\beta| < n_1k_0$ [9]. Figure 2.4 illustrates the propagation constants of the forward ($\beta > 0$) and reverse propagating ($\beta < 0$) guided modes as functions of the optical frequency. The pictorial representation of the modal propagation constants in terms of frequency is termed the β plot [10]. The propagation constant is given by equation 2.3 [9].

$$\beta = \frac{\omega n_{eff}}{c} = \frac{2\pi n_{eff}}{\lambda} \tag{2.3}$$

where n_{eff} is the effective index of refraction, $n_2 | n_{eff} | n_1$, from the cladding to the core and c is the speed of light in a vacuum.

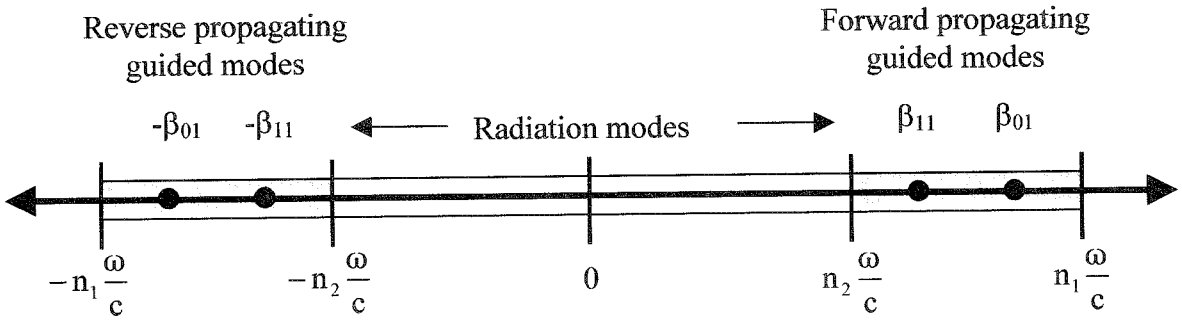

Figure 2.4: *Propagation constants of the forward and reverse propagating guided modes in an optical fibre. β_{01} and β_{11} are the propagating constants of the two lowest order forward propagating guided modes.* Diagram reproduced from [9].

Apart from the guided modes, another set of modes also satisfies the electromagnetic Maxwell's equations and the boundary values [12]. These modes are called radiation modes and owing to the imperfections within the wave-guide, result in the continuous loss of power from the guided modes [11]. The infinite number of radiation modes present possess a continuum of complex propagation constants in the range, $0 < |\beta| < n_2k_0$ [9], as illustrated in Figure 2.4. It is known that radiation modes extend to infinity and that they are strongly influenced by the outer cladding boundary.

Some of the radiation modes are trapped by the cladding due to the reflection at the cladding outer boundary. The subsequent modes that arise from the reflection of the radiation modes reflected at the cladding outer boundary are called cladding modes [12]. If the RI of the medium surrounding the cladding is n_3, the cladding modes propagation constants are bound within the range, $n_3 k_0 < |\beta| < n_2 k_0$.

The cladding modes are similar to the guided modes and, therefore, may travel in either forward or reverse direction. Cladding modes have discrete propagation constants as illustrated in Figure 2.5. Due to their higher density, they form almost a continuum [12]. The cladding modes attenuate rapidly due to bends in the fibre, scattering losses and absorption by the fibre's jacket. The coupling or transfer of energy from guided modes to discrete cladding modes forms the basic operating mechanism of long period gratings.

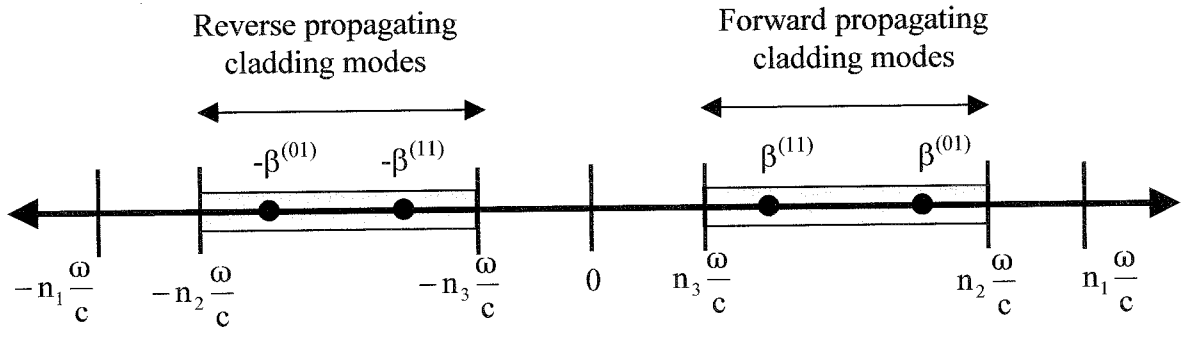

Figure 2.5: *Propagation constant distribution of the cladding modes in an optical fibre. The coloured region represents the cladding modes, where $\beta^{(01)}$ and $\beta^{(11)}$ are the propagation constants of the two lowest order forward cladding modes.* Diagram reproduced from [9].

2.5 Coupled mode theory

In section 2.4.1 it was discussed that, in a loss-less unperturbed optical fibre system, power is transferred in the form of modes, each mode propagates without losing or gaining power along the length of the fibre. However, in reality any small disturbance or irregularity in the system can cause power to couple between two or

more modes. An optical fibre can be perturbed by either bending the fibre, by modifying the RI or the diameter of the core or of the cladding, or by simply moving the fibre into close proximity with another wave-guide [12]. The techniques used to modify the RI or reduce the diameter of the core or cladding, respectively, are discussed in Chapter 4.

2.5.1 Co-directional coupling

In this section the approach used by Pierce [13] and by Taylor and Yariv [14] is followed to arrive at solutions to coupled mode equations for two modes propagating in the same direction, under the influence of a periodic perturbation. The coupled mode equations are also used to depict the importance of the phase matching condition between the two modes for significant exchange of power. The basic assumption of the coupled mode theory is that the coupling between the waveguides may be described as a perturbation in the polarisation of one waveguide due to the presence of the second. This analysis is only valid for weakly coupled waveguides, i.e. waveguides that are not too close together in space. Consider an optical fibre as shown in Figure 2.6, where the RI of the core is periodically perturbed with a period, Λ, along the fibre axis for a portion of the fibre's length, starting at z = 0 and ending at z = L.

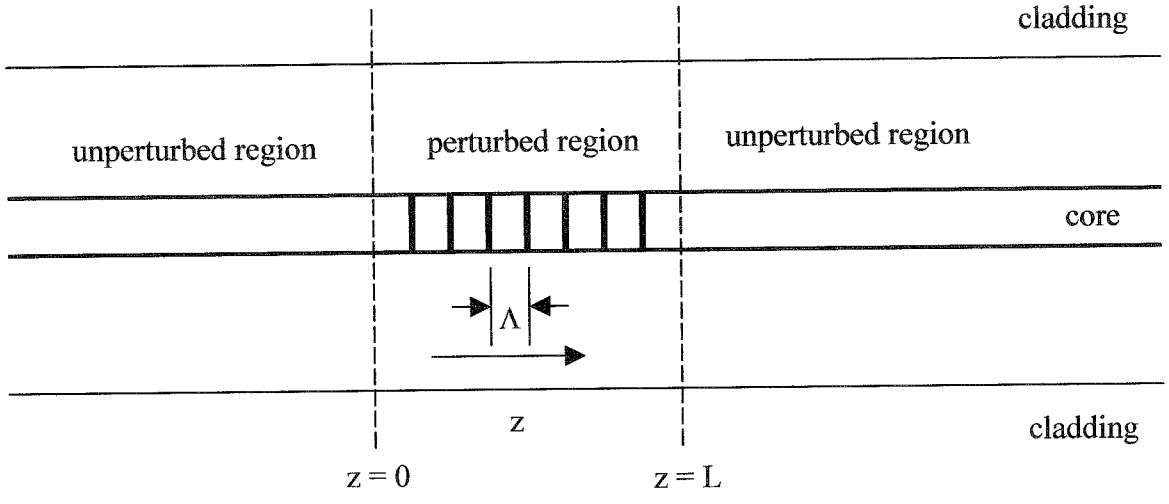

Figure 2.6: *Diagram of an optical fibre that has the RI of its core perturbed, with a periodicity Λ, over a length from a point z = 0 to z = L.*

Let two modes a_1 and a_2 travelling in the z direction with discrete propagation constants β_1 and β_2 respectively, be represented as [14]

$$a_1(z,t) = A_1(z)\, e^{j(\omega t - \beta_1 z)} \tag{2.4a}$$

$$a_2(z,t) = A_2(z)\, e^{j(\omega t - \beta_2 z)} \tag{2.4b}$$

where ω is the angular frequency and A_1 (z) and A_2 (z) are complex normalised amplitudes that are independent of z in an ideal loss-less unperturbed fibre. A perturbation of the fibre causes the two modes to exchange energy such that A_1 and A_2 become functions of the propagating distance [14]. The objective is to find the dependence of A_1 and A_2 upon z.

$$\frac{dA_1(z)}{dz} = \kappa_{12} A_2(z)\, e^{-j\Delta z} \tag{2.5a}$$

$$\frac{dA_2(z)}{dz} = \kappa_{21} A_1(z)\, e^{+j\Delta z} \tag{2.5b}$$

where κ_{12} and κ_{21} are termed the cross coupling coefficients and these control the amount of coupling between the two modes. Δ is the phase mismatch between the propagating modes and is usually the difference in their propagation constants [14]. In equations 2.5a & b the electric field of the perturbed portion of the fibre has been expressed as a linear combination of the two eigenmodes and substituted into the scalar wave equation for the perturbed system [15]. In the perturbed system, the slow varying approximation, SVA, is used to neglect the effect of 2nd order derivatives of the complex amplitudes. Integration over the cross-section of the fibre is then used to obtain the two-coupled 1st order differential equations [14]. The SVA requires that the amplitude of the mode change slowly over a distance of the order of the wavelength of the light and in the presence of a perturbation of period Λ, is modified to equation 2.6.

$$\Delta = \beta_1 - \beta_2 - \frac{2\pi}{\Lambda} \tag{2.6}$$

Since β_1 and β_2 are functions of the optical wavelength the phase mismatch, Δ has a strong spectral dependence. For synchronous transfer of power between the two modes the value of Δ should ideally be zero. Using equation 2.6, the phase matching condition between the two modes can be obtained, as in equation 2.7, where $\Delta\beta$ is their differential propagation constant.

$$\Delta\beta = \beta_1 - \beta_2 = \frac{2\pi}{\Lambda} \tag{2.7}$$

The total power carried by the modes a_1 and a_2 is given by $|A_1(z)|^2$ and $|A_2(z)|^2$ respectively. In an ideal loss-less system, there is no change in the total power in the coupling direction z, so the coefficients in equations 2.5a & b can be re-written as in equation 2.8, [14].

$$\kappa_{12} = -\kappa_{21}{}^* \tag{2.8}$$

Where * signifies the complex conjugate. If only one mode, a_2, is considered to carry power at the starting point of the perturbation in the fibre, z = 0, then the boundary conditions shown in equations 2.9 a & b are obtained.

$$a_1(0) = 0 \tag{2.9a}$$

$$a_2(0) = A \tag{2.9b}$$

These can be used to solve the coupled mode equations. Therefore, the complex modal amplitudes can be written as in equations 2.10 – 2.12 [16].

$$A_1(z) = A\frac{2\kappa_{12}}{\sqrt{4\kappa^2 + \Delta^2}} e^{-j\frac{(\Delta z)}{2}} \sin\left[\frac{1}{2}\left(\sqrt{4\kappa^2 + \Delta^2}\right)z\right] \tag{2.10}$$

$$A_2(z)=Ae^{j\left(\frac{\Delta z}{2}\right)}\left\{\cos\left[\frac{1}{2}\sqrt{4\kappa^2+\Delta^2}\ z\right]-j\frac{\Delta}{\sqrt{4\kappa^2+\Delta^2}}\sin\left[\frac{1}{2}\sqrt{4\kappa^2+\Delta^2}\ z\right]\right\} \tag{2.11}$$

where $$\kappa^2=|\kappa_{12}|^2 \tag{2.12}$$

The eigenmodes can now be obtained by substituting the value of the complex amplitudes A_1 (z) and A_2 (z) into equations 2.4a & b. The power in the two modes is given by equations 2.13 and 2.14,

$$P_1(z)=|A_1(z)|^2=P_0\frac{\sin^2\left[\kappa z\sqrt{1+\left(\frac{\delta}{\kappa}\right)^2}\right]}{1+\left(\frac{\delta}{\kappa}\right)^2} \tag{2.13}$$

$$P_2(z)=|A_2(z)|^2=P_0\frac{\cos^2\left[\kappa z\sqrt{1+\left(\frac{\delta}{\kappa}\right)^2}\right]+\left(\frac{\delta}{\kappa}\right)^2}{1+\left(\frac{\delta}{\kappa}\right)^2} \tag{2.14}$$

Where $\delta = \Delta/2$ is called the detuning parameter, which is dependent on the proximity of the operating wavelength to the phase-matching wavelength of the grating, and P_0 is the incident power in eigenmode P_2 ($P_0 = P_2(0) = |A|^2$). The two modes exhibit sinusoidal variation in the propagating power. The frequency and magnitude of power coupling is a function of the detuning ratio δ/k. Under the condition of phase mismatch ($\delta \neq 0$), the mode coupling is small and becomes negligible for $\delta/k \gg 1$. Under the condition of phase matching ($\delta = 0$), equations 2.13 & 2.14 can be modified to give equation 2.15 & 2.16,

$$P_1(z)=P_0\sin^2(kz) \tag{2.15}$$

$$P_2(z) = P_0 \cos^2(kz) \tag{2.16}$$

Which describes the interaction between the two modes throughout the coupling length. Where the perturbation in the fibre ends at z = L, then the modal interaction ceases. At that point the ratio C (C≤ 1) of the power in mode a_1 to that originally in a_2 can be determined from equations 2.13 & 2.14 to give equation 2.17 [17].

$$C = \frac{P_1(L)}{P_2(0)} = \frac{\sin^2\left[\kappa L \sqrt{1+\left(\frac{\delta}{\kappa}\right)^2}\right]}{1+\left(\frac{\delta}{\kappa}\right)^2} \tag{2.17}$$

At z = L the normalised power remaining in the mode a_2, T, is given by T = 1-C. For most applications the length L of the perturbed region is constant while the coupling coefficient κ is varied to achieve complete power transfer from mode a_1 to a_2 [10]. Although the maximum power transfer occurs when κL= mπ/2, where m is an integer, the device operation is usually optimised for m =1, which gives κ = π/2L.

2.6 Guided mode coupling using long period gratings

LPGs in the core of an optical fibre can be designed to couple the guided core modes to the cladding modes [10, 18] or to other guided modes [16, 19]. Thus far in this thesis, the discussion of LPGs has centered on those that couple the core modes to the cladding modes. This section introduces LPGs that have been designed to couple light from the fundamental LP_{01} mode to other forward-propagating guided modes in few-moded fibres.

LPGs that couple light from the fundamental LP_{01} mode to other forward-propagating guided modes were first fabricated to couple to the LP_{11} mode, these were originally known as rocking filters [19]. Since coupling in this case occurs from a

circularly symmetric to asymmetric mode, the grating needs to be blazed to attain optimum mode coupling [20]. For these particular LPGs the mode coupling occurs at wavelengths where the phase matching condition, $\Delta\beta = 2\pi/\Lambda$, is satisfied and the power is coupled from one guided mode to another [19]. The coupling wavelength can be varied by changing both the periodicity and the blaze angle of the grating. LPGs with 96% conversion efficiency have been demonstrated by changing the periodicity and the blaze angle [19]. LPGs that couple the fundamental guided mode to the circularly symmetric LP_{02} mode have also been demonstrated [16]. The LPGs had been written in two mode fibres with a periodicity of 209μm that resulted in a coupling wavelength of 619nm [16]. However, these LPGs do not require blazing because both LP_{01} and LP_{02} modes possess circular symmetry.

In general, LPGs that couple one forward guided mode to another though useful as modal couplers and for communication and sensing applications find a limited number of applications in optical systems [9]. Effective in-line spectral filters have been fabricated using these LPGs [21]. Dispersion compensation techniques in which the large negative dispersion of higher order spatial modes near their cut-off wavelength have been utilised to equalise the positive dispersion of the fibre link at 1.55μm [21]. A rocking filter designed to couple between the polarization components of the fundamental mode has been used to self switch a pulse of width 193 fs and a peak power of 1177W [22].

For the remainder of the thesis, unless otherwise stated, LPGs specifically refer to the LPGs that couple the guided mode to cladding modes. For most applications, LPGs are not blazed, so the RI modulation in the core has no transverse variation, and the perturbation is independent of azimuthal variation [20]. The overlap integral is thus non-zero only for pairs of modes that have the same azimuthal symmetry [20]. This causes the forward propagating guided mode with propagating constant β_{01}, the fundamental guided mode, to couple light to the azimuthally symmetric cladding modes travelling in the same direction ($\beta^{(m)} > 0$). These forward propagating $LP_{o,m}$ cladding modes of order m possess propagation constants that are donated by β^m, falling in the range $\omega n_3/c < \beta^m < \omega n_2/c$ ($n_2 > n_3$). The only non-zero coupling coefficients between the

core and the cladding modes involve cladding modes of azimuthal order m =1. Figure 2.7 plots the vector components of the electric field for the lowest order (m =1, v =1) cladding mode of a fibre as function of radial position. Where v is the cladding-mode number.

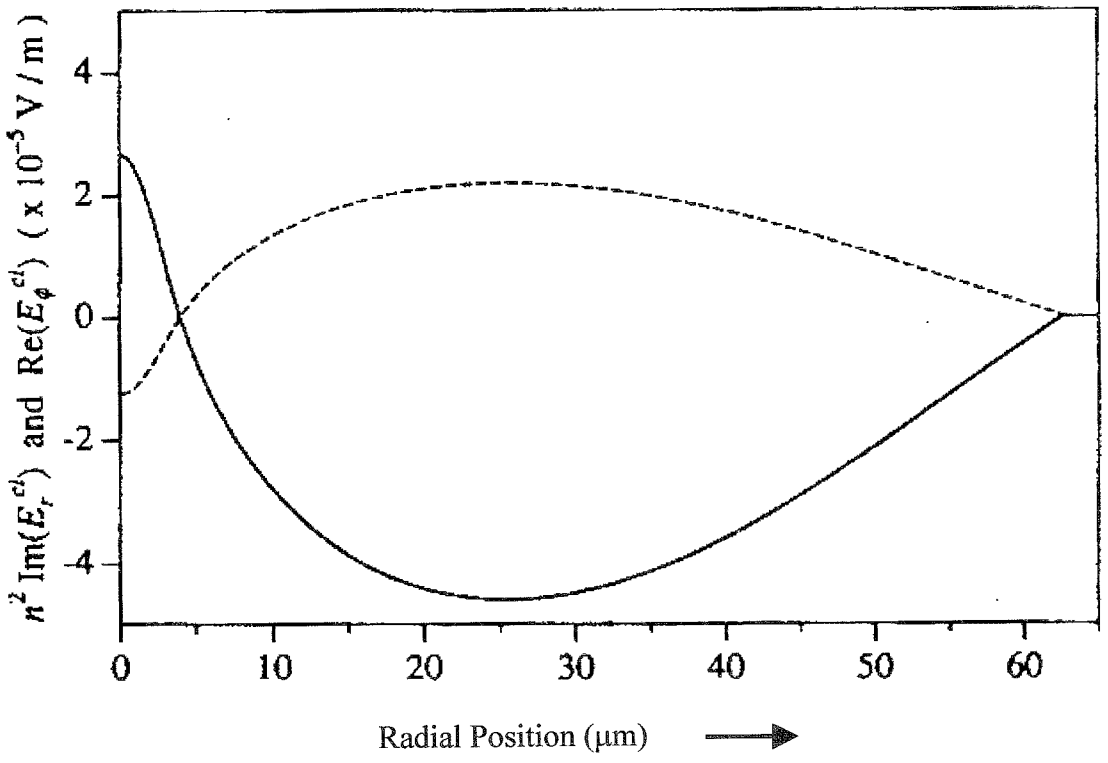

Figure 2.7: *Plot of the vector components of the electric-field for the lowest-order (v = 1) cladding mode of a fibre.* —— *radial component,* – – · *azimuthal component* [30].

The phase matching condition that was first introduced in equation 2.7 can be re-written as equation 2.18.

$$\Delta\beta^{(m)} = \beta_{01} - \beta^{(m)} = \frac{2\pi}{\Lambda} \qquad (2.18)$$

The spectral dependence of the propagation constants of the core and cladding modes results in a highly wavelength selective response of LPGs [10]. Figure 2.1 illustrates the transmission spectrum of a typical LPG.

The coupling of the fundamental guided mode to discrete cladding modes results in the distinct resonance bands or attenuation bands in the transmission spectrum. The bands have different values of peak loss or minimum transmission values and bandwidth due to dissimilar coupling coefficients that are functions of the modal overlap.

2.6.1 Important grating parameters

This sub-section considers important grating parameters such as the coupling coefficient, the bandwidth and the wavelength separation between the attenuation bands. The dependence of the transmission spectrum upon the length of the LPG and the coupling coefficient are also considered.

In section 2.5.1 the coupling between two modes propagating in the same direction was shown to be a strong function of the detuning ratio δ/k. The coupling coefficient $k^{(m)}$ for an attenuation band of order m has been shown to be a function of the peak index change Δn and the modal overlap between the guided mode and cladding modes over the region of perturbation [23]. Usually it is desired that the value of the detuning ratio should be as small as possible for maximum power transfer to occur which implies that the coupling coefficient should be optimised to improve the performance of the LPG. The coupling coefficient can be rewritten as in equation 2.19 [23]

$$\kappa^{(m)} = \frac{\pi |A_N|}{\lambda^{(m)}} \eta^{(m)} \tag{2.19}$$

where it has been assumed that the coupling coefficient is constant across the spectral width of the attenuation band of order m and is centred at a wavelength $\lambda^{(m)}$. A_N are the Fourier coefficients for a rectangular RI modulation of the core where the RI change $\delta n(z)$ in the (z) direction is written in terms of its Fourier series [24]. $\eta^{(m)}$ is the overlap integral when the RI modulation, that has no transverse variations, is considered to be small when compared with the unperturbed RI of the core. Since the coupling coefficient is directly proportional to the overlap integral, the modal distribution of the

cladding mode will have a strong influence on its magnitude. In addition, since the RI modulation has no azimuthal variation, the coupling of the guided mode can occur to only circularly-symmetric cladding modes and for all other cladding modes the overlap integral is zero. The overlap integral, $\eta^{(m)}$, is given by equation 2.20 [23],

$$\eta^{(m)} = \frac{\left| \int_0^a \Delta n \, E_{01}(r) \, E_{cl}^{(m)}(r) \, r \, dr \right|}{\sqrt{\int_0^\infty (E_{01}(r))^2 \, r \, dr \int_0^\infty (E_{cl}^{(m)}(r))^2 \, r \, dr}} \tag{2.20}$$

where $E_{01}(r)$ and $E_{cl}^{(m)}(r)$ are the electric field distributions of the fundamental guided modes and the circularly-symmetric cladding modes of order m, respectively [8]. From equation 2.20, it can be seen that enhancement in the magnitude of the peak index change Δn, results in an increased coupling coefficient.

The wavelength separation between two attenuation bands of order m and m+1, at wavelengths $\lambda^{(m)}$ and $\lambda^{(m+1)}$, respectively can be determined [10], where m is an integer. However, first it is necessary to calculate the wavelength of the m^{th} order attenuation band relative to the cut off wavelength of the fibre, λ_{cut}, [10]. This is achieved by using equation 2.21 [10, 25],

$$\lambda^{(m)} - \lambda_{cut} \approx \frac{\lambda_{cut}^2 \Lambda}{8 n_2} \frac{m^2}{b^2} \tag{2.21}$$

where the effective RI of the guided mode (n_{eff}) is assumed to be equal at $\lambda^{(m)}$ and λ_{cut} [10]. From equation 2.21 it can be seen that the wavelength separation between $\lambda^{(m)}$ and λ_{cut} is an increasing function of the order, m, and the periodicity, Λ, of the LPG. So for a given periodicity the wavelength separation will increase as higher order cladding modes are considered [9].

For the first few cladding modes, when m is small, $\lambda^{(m)}$ and λ_{cut} can be assumed to be very close and the wavelength separation $\delta\lambda^{(m,\,m+1)}$ between the attenuation bands of order m and m+1 can be obtained from equation 2.22 [10],

$$\delta\lambda^{(m,m+1)} = \lambda^{(m+1)} - \lambda^{(m)} \approx \frac{\lambda_{cut}^2}{8n_2}\frac{\Lambda}{b^2}\frac{2m+1}{} \qquad (2.22)$$

It can be seen that the wavelength separation between the attenuation bands increases as the value of m is increased which is consistent with the transmission spectrum of a typical LPG, as illustrated in Figure 2.1. Furthermore the wavelength separation between any two attenuation bands increases as the cladding radius, b, is reduced.

The coupled mode analysis is now used to determine the power transmitted through a LPG. The ratio C of the power coupled from one forward propagating mode to another in the presence of a perturbation has already been represented by equation 2.17. The detuning ratio for the cladding mode of order m is given by $\delta^{(m)}/\kappa^{(m)}$ and its magnitude should be minimised for maximum transfer of power from the guided mode to the cladding mode. The normalised power, T, transmitted by the fundamental guided mode through the LPG is then given by,

$$T = \frac{P^{(m)}(L)}{P_{01}(0)} = \frac{\cos^2\left[\kappa^{(m)} L\sqrt{1+\left(\frac{\delta^{(m)}}{\kappa^{(m)}}\right)^2}\right] + \left(\frac{\delta^{(m)}}{\kappa^{(m)}}\right)^2}{1+\left(\frac{\delta^{(m)}}{\kappa^{(m)}}\right)^2} \qquad (2.23)$$

which, at the phase matching wavelength, reduces to the expression for the minimum transmission value that is given in equation 2.24 [17],

$$T_0 = 1 - \sin^2\left(\kappa^{(m)} L\right) \qquad (2.24)$$

Equation 2.24 reveals that minimum power in the guided mode is transmitted at the

phase matched wavelength and depends on the coupling coefficient and the length of the LPG. So if the length of the LPG is known then the coupling coefficient and hence the peak RI change can be calculated. It is known that the optimum coupling for each cladding mode occurs at different values of Δn. So, during the fabrication of the LPG, for the selected cladding mode the value of Δn at which the transmission power at the coupling wavelength reduces to approximately zero, is calculated. When power is completely transferred to the cladding mode it corresponds to equation 2.25 [10].

$$\kappa^{(m)} L = \frac{\pi}{2} \qquad (2.25)$$

The fibre is exposed to the UV irradiation until the required Δn has been achieved. At the phase matched wavelength the complete power transfer gives C = 1 and T = 0. If a fixed length of the fibre is irradiated with UV then the total power transfer is obtained by increasing the peak RI change and hence the coupling coefficient. The exposure is stopped when the minimum transmission value or maximum loss in transmission reaches the value required for the application. For the situation when $\kappa^{(m)}L > \pi/2$, the power in the cladding mode starts to couple back into the fundamental guided mode, leading to an increase in the guided mode transmitted power. For a fixed value of the peak RI change, Δn, the complete power transfer occurs for a particular cladding mode and all other cladding modes are either under or over coupled. Hence, it is expected that all the attenuation bands will have different minimum transmission values, as illustrated in Figure 2.1. For an application, the desired attenuation band resident within the optical source's spectrum is monitored during the writing process. The writing process is complete when the desired attenuation band's minimum transmission has reached the required value [9].

2.7 Modelling fibre optic long period gratings

The parameters for determining the coupling between the modes of a LPG, the detuning parameter and the coupling coefficient, have been established in sections 2.5 and 2.6. It is useful to be able to predict the central wavelengths and the minimum

transmission values of the attenuation bands, prior to the fabrication of the LPG. With the data it would be possible to simulate the response of the attenuation bands to different environmental changes [26]. This can be achieved by creating a numerical model of the LPG. Although an exact theoretical treatment of optical waveguides is possible [23] it must be performed in cylindrical co-ordinates and becomes very complicated leading to 6 component equations of the homogenous wave equations [27]. Therefore, a simplified model of propagation within optical fibres is very advantageous and has been presented [11]. However, it should be noted that the model is very sensitive to the difference between the core and cladding refractive indices and this may vary from one batch of optical fibre to another as the fibre parameters change.

The three-layer model has been used to determine the cladding mode indices and Gloge's weakly guided approximation was used to calculate the index of the guided modes [11].

2.7.1 Fundamental guided mode analysis

This section introduces the technique used to calculate the guided mode indices. The amplitude of the guided modes decay rapidly as a function of increasing penetration into the cladding and causes it to possess negligible value at the outer cladding boundary, the analysis becomes simpler if the cladding is assumed to be infinite. In Figure 2.2c the radius of the core is a, n_1 is the RI of the core and n_2 is the RI of the cladding. Both n_1 and n_2 are functions of the operating wavelength λ [9, 28, 29]. The normalised index difference Δ between the core and cladding has been defined in equation 2.1 [6]. The commonly used waveguide parameters u and w are given by [11],

$$u = a\left(k_0^2 n_1^2 - \beta^2\right)^{\frac{1}{2}} \tag{2.26}$$

$$w = a\left(\beta^2 - k_0^2 n_2^2\right)^{\frac{1}{2}} \tag{2.27}$$

β is the wavelength dependent propagation constant of the guided mode that has been

defined in equation 2.3, which is limited in the interval $n_1k_0 \geq \beta \geq n_2k_0$, where $k_0 = 2\pi/\lambda$ is the wave number in free space.

The normalised frequency or the V number has been defined in equation 2.2 and can also be defined is terms of u and w where it is equal to $\{(u^2 + w^2)^{1/2}\}$. By matching the fields at the core-cladding boundary, we may deduce the functions u(V) or w(V) for each mode in the fibre. Furthermore, the propagation constants and other parameters of interest may be calculated from these functions. To proceed further it must be assumed, as Gloge did, that the modes within the optical fibre be considered weakly guided, as is the case in practice [11]. This state of weak guidance is defined by the condition

$$\left(\frac{n_1 - n_2}{n_2}\right) \ll 1 \tag{2.28}$$

Having assumed this condition it can be shown that the modes may be constructed whose transverse field is essentially polarised in one direction, the so called linearly polarised (LP) modes. In order to show how these modes relate to the normalised frequency, V a normalised propagation constant *b* has to be defined.

$$b(V) = 1 - \left(\frac{u^2}{V^2}\right) = 1 - \left(\frac{\left(\frac{\beta^2}{k_0^2}\right) - n_2^2}{\left(n_1^2 - n_2^2\right)}\right) \tag{2.29}$$

The normalised propagation constant in the weak coupling regime reduces to

$$b \approx \left(\frac{\left[\left(\frac{\beta}{k_0}\right) - n_2\right]}{\left(n_1 - n_2\right)}\right) \tag{2.30}$$

The index of the guided modes is calculated by using equations 2.29 and 2.30.

2.7.2 Cladding mode analysis

The important step in the theoretical investigation of LPGs is the determination of the effective indices of the circularly-symmetric forward propagating cladding modes. The analysis of the effective indices and the mode profiles of the cladding modes have been determined by using an exact vector-field treatment [30]. The exact vector-field treatment includes the presence of the core since it influences the electric field distribution of the cladding modes [30]. The electric field peaks within the core of the fibre and so there is an overlap between the mode propagating in the core and the cladding mode [30]. A comparatively simpler investigation of the cladding modes uses the approximation that the fibre can be considered as a step index structure ignoring the presence of the core [10, 12]. The fibre geometry to be analysed thus reduces from that shown in Figure 2.8a to that shown in Figure 2.8b. The core diameter 2a, in Figure 2.8a, is replaced by the cladding diameter 2b and the core index n_1 is substituted by the cladding index n_2. Additionally, if n_3 is the medium surrounding the fibre cladding, n_2 in Figure 2.8a it is replaced with n_3. The RI values n_1, n_2 and n_3 are still wavelength dependant [9, 28, 29].

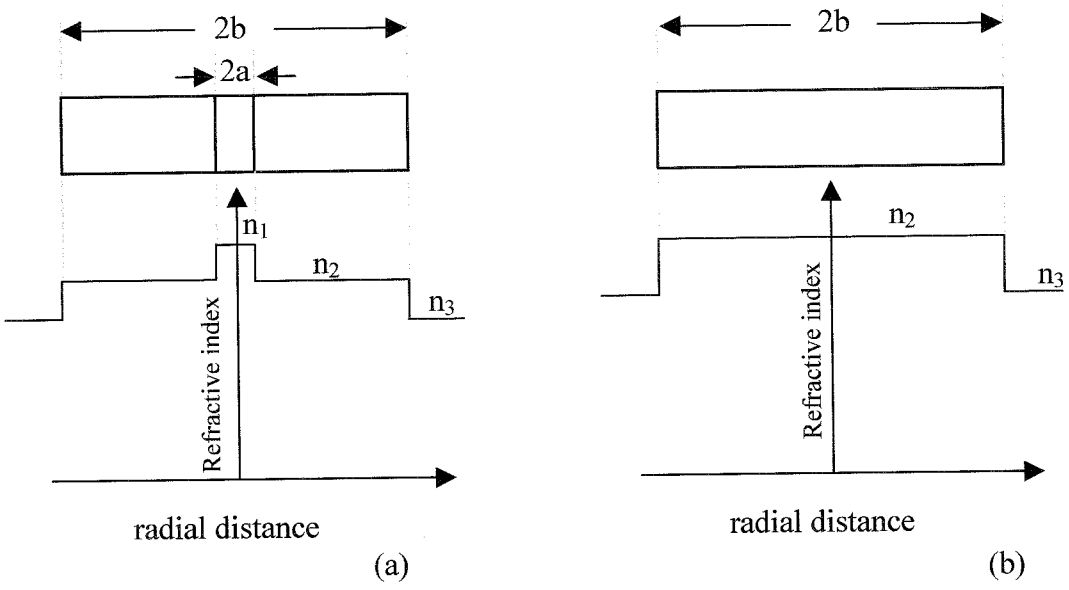

Figure 2.8a & b: *Schematic diagram of the cross section and the RI profile of the slab wave-guide equivalent of the step index fibre (a) considered with a core and (b) without a core for calculating the RI of the cladding mode.*

For a weakly-guided fibre with closely matched values of core and cladding refractive indices, this assumption has provided a fair approximation of the cladding mode propagation constants [10]. However, the greatest limitation of using the approximation is that, for a slab waveguide, the majority of the energy is away from where the core would have been and so there is little overlap between the propagating core and cladding modes. Thus, the approximation cannot be used to predict the coupling efficiency because equation 2.19 requires a value for the overlap integral.

The central wavelengths, λ_i, of the attenuation bands are given by the solutions of the phase matching equation [28, 29].

$$\lambda_i = (n_{eff}[\lambda_i] - n_{cl}^{(i)}[\lambda_i])\Lambda \qquad (2.31)$$

where $n_1(\lambda_i)$ is the effective RI of the core mode, $n_2^i(\lambda_i)$ is the effective RI of the $(i)^{th}$ cladding mode and Λ is the periodicity of the LPG. Since n_1, n_2 and n_3 are wavelength dependent this material dispersion combined with the waveguide dispersion leads to the wavelength dependence of n_1 and n_2^i used in equation 2.31. To determine the coupling wavelengths (λ_i), the effective refractive indices of the core and cladding modes are calculated, using equations 2.29 and 2.30, as functions of wavelength and this is used in the phase matching equation to solve for the wavelengths (λ_i) as a function of the periodicity. Using the simulation program [31], plots 2.9 and 2.10 are produced to illustrate the dependence of the coupling wavelength for low order cladding modes and high order cladding modes upon the period of the LPG.

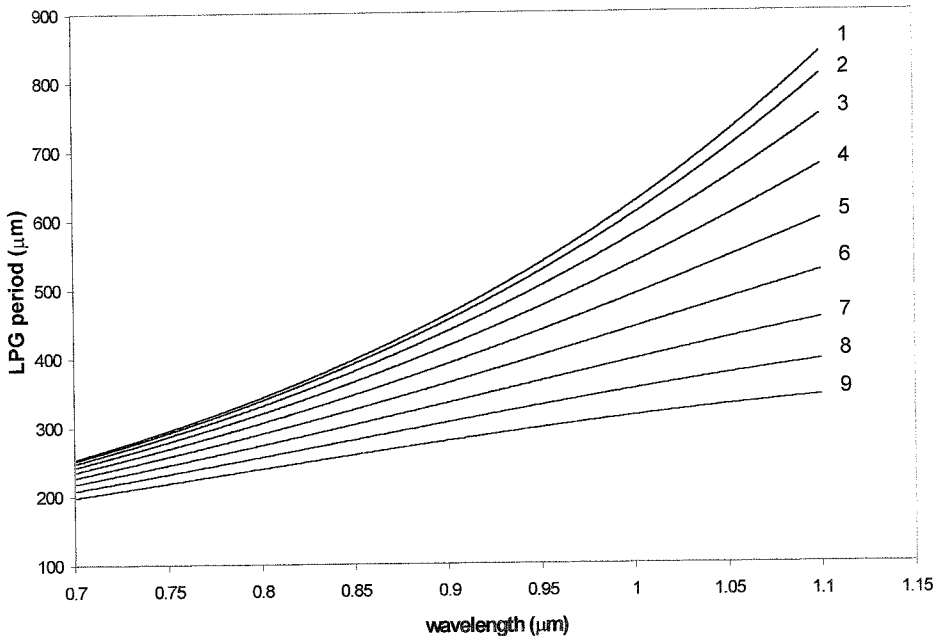

Figure 2.9: *Plot of the LPG's periodicity as a function of the coupling wavelength, for cladding modes 1-9.*

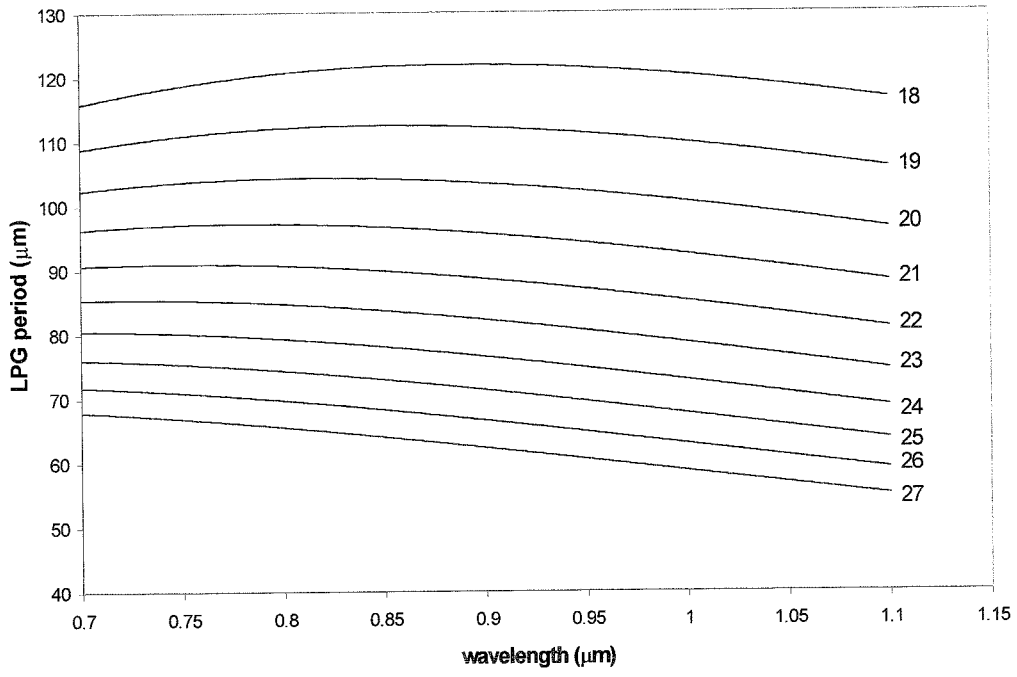

Figure 2.10: *Plot of the LPG's periodicity as a function of the coupling wavelength, for cladding modes 18-27.*

The plots indicate that coupling to low order-cladding modes is achieved using longer periods, while shorter periods facilitate coupling to higher order modes. The plots also show that by appropriate choice of the LPG's periodicity, it is possible to generate attenuation bands with positive or negative responses to the measurands. For positive responses to the measurands the LPG's period should be > 200μm and for negative responses the periodicity should be < 90μm. In addition, Figure 2.10 shows that for higher order cladding modes, coupling to one cladding mode, such as mode 18, can occur at two wavelengths, producing two attenuation bands [32]. Therefore, depending on the operating wavelength the attenuation band will exhibit either a positive or a negative response to the measurands. It should be noted that small changes in the coupling conditions could result in large changes in the separation of the two attenuation bands. For LPGs fabricated such that their period coincides with the peak of the curve, for example, mode 18, it has been observed that changes in the coupling conditions result in a change in the coupling efficiency, but not in the wavelength [33].

2.8 Chapter summary

This chapter has briefly detailed the principles of operation of a LPG and enhanced the discussion with a presentation of a LPG's transmission profile. The parameters that determine the central wavelengths and the minimum transmission values of the attenuation bands were introduced and their relationship to each other was discussed. A model used for predicting the coupling wavelengths as a function of the LPG's periodicity was discussed and results produced by it were presented.

Chapter 3 will present a review of the sensing applications of LPGs with a particular emphasis on their application as sensors for single and multi-parameter sensing.

References:

1 Transmission spectrum of a LPG fabricated by author at Cranfield University.

2 V. Bhatia, D.K. Campbell, D. Sherr, T.G. D'Alberto, N.A. Zabaronick, G.A. Ten Eyck, K.A. Murphy and R.A. Claus, 'Temperature insensitive and strain insensitive long period grating sensors for smart structures', Opt. Eng., **36**, pp. 1872-1876, (1997).

3 O. Duhem, J. Henninot, M. Warenghem and M. Douay, 'Demonstration of long period grating efficient coupling with an external medium of a refractive index higher than that of silica', Appl. Opt. **37**, pp. 7223-7228, (1998).

4 V. Bhatia, 'Applications of Long period gratings to single and multi parameter sensing', Opt. Exp., **4**, pp. 457 – 466, (1999).

5 J.A. Stratton, 'Electromagnetic Theory', McGraw-Hill, New York, 1941.

6 G.P. Agrawal, 'Non-linear fibre optics', Academic press, London, U.K., (1989).

7 J. Wilson and J.F.B. Hawkins, 'Optoelectronics an Introduction', 2nd edition McGraw-Hill, New York, 1987.

8 G. Keiser, 'Optical fibre communications', 2nd Edition, McGraw-Hill, New York, 1991.

9 V. Bhatia, 'Properties and applications of long period gratings', PhD. thesis, Virginia Polytechnic and State University, Blacksburg Virginia, (1998).

10 A.M. Vengsarkar, P.J. Lemaire, J.B. Judkins, V. Bhatia, J.E. Spie and T. E. Erdogan, 'Long period fibre gratings as band rejection filters', J. of Lightwave Technol., **14**, pp. 58 - 65, (1996).

11 D. Gloge, 'Weakly guiding fibres', Applied Optics, **10**, pp. 2252 -2258, (1971).

12 D. Marcuse, 'Theory of dielectric optical wave-guides', Academic Press, New York, (1974).

13 J.R. Pierce, 'Coupling of modes of propagation', Applied Physics, **25**, pp. 17-32 (1954).

14 H.F. Taylor and A. Yariv, 'Guided wave optics', Proc. of the IEEE, **62,** pp. 1044 - 1059, (1974).

15 A Yariv, 'Coupled mode theory for guided-wave optics', IEEE, J. of Quantum Electron., **9**, pp. 919 -934, (1973).

16 F. Bilodeau, K.O. Hill, B. Malo, D. Johnson and I. Skinner, 'Efficient narrowband LP_{01} <-> LP_{02} mode converters fabricated in photosensitive fibre: Spectral response', Electron. Lett., **27**, pp. 682 - 684, (1991).

17 D.G. Hall, 'Theory of wave-guides and devices', in Integrated Optical Circuits and Components, L.D. Huctheson: Editor, Marcel-Dekker, New York, (1987).

18 A.M. Vengsarkar, P.J. Lemaire, J.B. Judkins, V. Bhatia, J.E. Spie and T. E. Erdogan, 'Long period fibre gratings as band rejection filters', Proc. Conf. on Optical fibre Comm, paper PD4, (1995).

19 K.O. Hill, B. Malo, K. Vineberg, F. Bilodeau, D. Johnson and I. Skinner, 'Efficient mode-conversion in telecommunication fibre using externally written gratings', Electron. Lett., **26**, pp. 1270-1272, (1990).

20 D. Marcuse, 'Microdeformation losses in single mode fibres', Applied Optics, **23**, pp. 1082 - 1091, (1984).

21 C.D. Poole, J.M. Wiesenfeld, A.R. McCormick and K.T. Nelson, 'Broadband dispersion compensation by using the higher order spatial mode in a two-mode fibre', Opt. Lett., **17**, pp. 985 – 987, (1992).

22 D.C. Johnson, F. Bilodeu, B. Malo, K.O. Hill, P.G.J. Wigley and G.I. Stegeman, 'Long length long period rocking filters fabricated from conventional monomode telecommunications optical fibres', Opt. Lett., **17**, pp. 1635-1637, (1992).

23 A.W. Snyder and J. W. Love, Optical Waveguide Theory, Chapman and Hall, New York, 1983.

24 H. Taub and D. L. Schiling, 'Principles of Communication Systems', Mc Graw-Hill Book Company, New York, 1986.

25 M.R. Spiegel, 'Mathematical Handbook of Formulas and Tables', McGraw-Hill, New York, 1994.

26 R. Hou, Z. F. Hassemlooy, A. Hassan, A. Nabok and K.P. Dowker, 'Modelling of long period fibre grating response to refractive index higher than that of cladding', Meas. Sci. Technol., **12**, pp. 1709-1713, (2001).

27 D. Flannery, 'Fibre optic chemical sensing using Langmuir-Blodgett overlay waveguides', PhD. thesis, Cranfield University, (1998).

28 H.J. Patrick, A.D. Kersey, F. Bucholtz, K.J. Ewing, J.B. Judkins and A.M. Vengsarkar, 'Chemical sensor based on long period fibre grating response to index of refraction', presented at the Conf. Laser and Electro-Optics, Baltimore, MD, paper CThQ5, (1997).

29 H.J. Patrick, A.D. Kersey and F. Bucholtz, 'Analysis of the response of long period fibre gratings to external index of refraction', J. Lightwave Technol., **16**, pp. 1606 – 1771, (1998).

30 T. Erdogan, 'Cladding mode resonances in short and long period fibre grating filters', J. Opt. Soc., Am., A, **14**, pp. 1760 – 1773, (1997).

31 Dr. S.W. James of Cranfield University.

32 Y.G. Han, B.H. Lee, W.T. Han, U.C. Paek and Y. Chung, 'Resonance peak shift and dual peak separation of long period fibre gratings for sensing applications', IEEE Photon. Technol. Lett., **13**, pp. 699-701, (2001).

33 V. Grubsky and J. Feinberg, 'Long period fibre gratings with variable coupling for real time sensing applications', Opt. Lett., **25**, pp. 203-205, (2000).

Chapter 3 Review of the sensing applications of fibre optic long period gratings

3.1 Introduction

LPGs present themselves as very strong candidates for fibre sensor elements [1, 2, 3] because of their unique features. The measurand induces a response in the transmission spectrum, which manifests itself as a wavelength shift in the central wavelength of the attenuation bands. The wavelength shift is an absolute parameter and does not depend on the total light level that is present, losses in the connecting fibres and couplers, or the source power being used [4] and so provides LPG sensors with self-referencing capabilities.

The sensitivity of the LPG's transmission profile to changes in the external environment such as temperature, bending, strain and change in RI of the surrounding medium should be taken into account when a fibre optic sensing system is being designed. At any one time, a LPG based sensor will respond to changes in one or more of the external perturbations and to determine the effect of the desired measurand, the cross sensitivity between them must be minimised. A simple and economical solution to the problem of cross sensitivity is a sensor that is sensitive to a single measurand whilst being insensitive to the others. This can be achieved by appropriate choice of fibre composition and period which allows the LPG's sensitivity to a particular measurand to be enhanced, reduced or even become insensitive to it. This facilitates the isolation of the response due to the measurand of interest during simultaneous measurement of a number of measurands. Alternatively, since each attenuation band shows a different sensitivity to each measurand, monitoring the response of a number of attenuation bands simultaneously will allow the responses to be separated. This chapter reviews the sensing applications of fibre long period gratings.

3.2 Fibre optic long period gratings as single parameter sensors

3.2.1 Temperature sensitivity

The temperature response of the LPG's attenuation bands has manifested itself as a wavelength shift in the central wavelength of the attenuation band and also as a change in the coupling strength without a change in the attenuation band's central wavelength. The form of the response is dependent on the LPG's characteristics, Chapter 2 has discussed the conditions under which a change in coupling conditions results in the two different responses. LPGs are attracting interest as temperature sensors because of their high sensitivity, which, in air is in the range, – 0.14nm/°C to 0.38nm/°C [5]. This is upto ten times higher than that of fibre Bragg gratings [6]. The large range of temperature sensitivities arises because, as has already been discussed, the sensitivity of LPGs to environmental parameters is influenced by the order of the cladding mode to which coupling occurs, by the composition of the fibre and by the periodicity of the LPG.

This combination of influences allows the fabrication of LPGs that have a range of responses to a particular measurand, a single LPG may have attenuation bands that have a positive sensitivity to a measurand, others that possess a negative sensitivity and those that are insensitive to the measurand. This property has been widely exploited for controlling the temperature sensitivity of LPGs. For many telecommunications applications the spectral stability is of prime importance, and the ability to fabricate a LPG with an inherently insensitive temperature attenuation band is an attractive feature. This is useful for producing temperature insensitive strain sensors [7, 11]. For a temperature sensor, or a thermally tuned filter, a high temperature sensitivity of either sign is required [8, 9].

The sensitivity of a LPG to temperature, T, can be determined by expanding the phase matching equation [10] to give

$$\frac{d\lambda}{dT} = \frac{d\lambda}{d(\delta n_{eff})}\left(\frac{dn_{eff}}{dT} - \frac{dn_{cl}}{dT}\right) + \Lambda\frac{d\lambda}{d\Lambda}\frac{1}{L}\frac{dL}{dT} \qquad (3.1)$$

where λ is the central wavelength of the attenuation band, T is the temperature and $\delta n_{eff} = (n_{eff} - n_{cl})$.

The first term on the right hand side of equation 3.1 is the material contribution [10, 11]. The wavelength shift due to this contribution can be of either polarity and its magnitude is related to the change in the differential effective index of the core and the cladding arising from the thermo-optic effect. This contribution is dependent upon the composition of the fibre and is strongly dependent upon the order of the cladding mode. When coupling to low order cladding modes, accessed using LPGs with a periodicity > 100μm, the modes undergo small changes in their effective indices so the material effect dominates, since $dn_{eff}/dT > dn_{cl}/dT$ [10]. For coupling to higher order cladding modes, accessed using LPGs with a periodicity < 100μm, the modes undergo larger changes in their effective indices [10] so as dn_{cl}/dT approaches dn_{eff}/dT the material effect for standard germanosilicate fibres will become negligible [12]. The second term is the waveguide contribution, as it results from changes in the LPG's periodicity [12]. Since the wave-guide contribution has its basis in the thermal sensitivity of the LPG's periodicity, it's magnitude and sign depend upon the order of the cladding mode [10]. For coupling to low order cladding modes, $d\lambda/d\Lambda$ is positive, whilst for the higher order cladding modes it is negative, as can be seen from Figures 2.7 and 2.8. Thus, by appropriate choice of the LPG's periodicity, it is possible to balance the two contributions to the temperature sensitivity to produce a temperature insensitive attenuation band and also to produce attenuation bands with a positive or negative response to temperature appropriate to the specific application [13].

A LPG of period 40μm was found to have an attenuation band with sensitivity of 1.8pm/°C [12], an order of magnitude smaller than that of a FBG. Temperature insensitive LPGs have been demonstrated however, the used fibres for this purpose had special multi-layer RI profiles [11]. The special fibre design counterbalanced the material and waveguide contributions for specific cladding modes and over a specific range of periods the LPGs were found to be temperature insensitive [11]. The expense of the special fibres may be uneconomical in practical system designs [11].

In addition to using the parameters in equation 3.1 to design a temperature insensitive LPG [12], there has been much effort to further suppress the temperature sensitivity. One such method makes use of an athermal packaging, where the LPG is bonded to a substrate whose thermal expansion coefficient induces a strain that produces a wavelength shift of the opposite sign to that induced by the change in temperature. This temperature compensation technique reduced the thermal sensitivity of the LPG by approximately 45% by bonding the LPG in an aluminium cylinder [14]. Alternatively, coating the fibre with a material with a positive thermo-optic coefficient [15], has been shown to change the temperature sensitivity from –0.049nm/°C to 0.0007nm/°C [16]. Another technique modifies the composition of the fibre core by doping with B_2O_3 [17]. B_2O_3 has a negative thermal dependence and so counteracts the original positive temperature sensitivity of the LPG. Using this technique, the temperature sensitivity was changed from to -0.142nm/° C to 0.002nm/°C [17].

Metal-coated LPGs have been used to develop low power tuneable filters based upon resistive heating. This has been achieved by depositing Cu, [18] or Pt, [19] of thickness approximately 300nm onto the LPG. To provide good adhesion for the thin metal films they were laid on top of a 15nm layer of Ti, which had been deposited on the fibre by thermal evaporation [18] and DC magnetron sputtering [19]. The RI of the surrounding layer of Ti produced a 1nm wavelength shift in the attenuation bands and a small reduction in the coupling efficiency. The Cu coated fibre exhibited a 4nm wavelength shift for electrical power of 0.5W [18], while for the Pt based filter a 11nm wavelength shift was reported for 0.67W, with a linear efficiency of 16nm/W [19]. The index of refraction of Ti and Pt at 1.55μm are 4.04 and 5.31 respectively. These are

greater than that of silica thus, the metal coating was found to make the performance of the LPG insensitive to the RI of the medium surrounding the metal coating.

When a LPG is used as a temperature sensor or as a thermally tuned filter its temperature sensitivity may be difficult to determine when it is also being influenced by variations in strain or other measurands [2, 9]. One method of overcoming the problem of cross-sensitivity to other measurands is to enhance the LPG's temperature sensitivity. In standard telecommunications fibre the temperature sensitivity is in the range 0.03 to 0.10nm/°C, this can be enhanced, as has already been mentioned, by carefully choosing the order of the cladding mode, periodicity of the LPG and operating wavelength [2, 20]. Using those carefully chosen parameters the temperature sensitivity of LPGs fabricated in photosensitive B-Ge co-doped optical fibres of upto 2.75nm/°C has been reported [21].

The temperature sensitivity can be controlled by doping the inner cladding with dopants that have a negative temperature dependence of the RI, i.e. when the material effect < 0. Adjusting the doping levels of B_2O_3 in a GeO_2 fibre has changed the temperature sensitivity from –0.14nm/°C to 0.28nm/°C [17].

Temperature sensitivity enhancing techniques that are based upon surrounding the fibre by a material of large thermo-optic coefficients, resulting in the LPG responding to both changes in the temperature and to the temperature induced RI change of the surrounding medium [22, 23, 24, 25], are discussed in section 6.3 of Chapter 6.

Thus far in this discussion, the response to temperature has manifested itself as a shift in the central wavelength of the LPG's attenuation bands, while their coupling strength remains constant [2, 5, 8, 10]. A LPG whose attenuation band varies in coupling strength, but remains fixed in wavelength, in respect to changes in temperature has been demonstrated [26], the generation of such attenuation bands has been discussed previously in section 2.7.2 of Chapter 2. A sensor using this change showed, that over a 11°C temperature variation caused a 3% linear change in transmission. A

temperature change of 0.04°C was resolved using a detector that had a resolution of 0.01% [26].

This section has presented the response of LPGs to a change in its temperature. It has shown that the response to temperature of LPG based sensors can be tailored to possess a high positive or negative sensitivity, or to be temperature insensitive to match the needs of the application. Temperature insensitive LPGs can be used for strain measurements in thermally noisy environments [12]. The next section reviews LPG's response to strain.

3.2.2 Strain sensitivity

The sensitivity of a LPG to axial strain, ε, can also be predicted by expanding the phase matching equation and re-arranging to give:

$$\frac{d\lambda}{d\varepsilon} = \frac{d\lambda}{d(\delta n_{eff})}\left(\frac{dn_{eff}}{d\varepsilon} - \frac{dn_{cl}}{d\varepsilon}\right) + \Lambda\frac{d\lambda}{d\Lambda} \qquad (3.2)$$

Again, the sensitivity is comprised of the material and waveguide effects. The material effect, first term on the right hand side, arises from the change in dimension of the fibre and the strain-optic effect. The waveguide effect, the second term, can be significant and is a function of the slope of the dispersion term, $d\lambda/d\Lambda$, for a particular cladding mode [10]. Again, the two contributions to the total strain induced wavelength shift can be either positive or negative depending on the period of the LPG and the order of the cladding mode. For LPGs with a periodicity > 100μm, the material contribution is negative, while the waveguide contribution is positive. Appropriate choice of the LPG's periodicity, the composition and the geometry of the fibre will allow the generation of attenuation bands with positive, negative or zero sensitivity to strain [12] and those that vary in coupling strength, but remains fixed in wavelength [26].

A LPG of period 340μm, written in Corning Flexcore fibre exhibited an attenuation band with a strain sensitivity of 0.04pm/με [10] which is an order of magnitude less than that of a FBG. A LPG with a period of 40μm exhibited a large strain sensitivity of –2.2pm/με, since in this region, $\Lambda < 100\mu m$, both contributions to the strain sensitivity are negative [10]. The effect of strain has been demonstrated to decrease the coupling strength of the LPG, changing the minimum transmission of the LPG attenuation bands. When there was no strain the attenuation band had a coupling efficiency of over 80%, as the strain increased the coupling efficiency decreased linearly to 0% for an applied strain of 9410με [26].

Strain insensitive attenuation bands can be fabricated [2, 10, 11]. This is achieved in special fibres by careful selection of the period of the LPG, $\Lambda > 100\mu m$, as in this regime the material and waveguide contributions are equal and opposite.

The effectiveness of a strain sensor is a strong function of its temperature cross-sensitivity. It has been shown that in a thermally unstable environment it is impossible to differentiate between the effects of temperature and strain [10]. In order to eliminate the cross-sensitivity effects it has been proposed that the sensitivity to strain be enhanced [27].

In addition to the measurement of axial strain, the sensitivity of LPGs, fabricated in non-high birefringence fibre, to transverse loads has been investigated [28, 29]. When a transverse load was introduced onto the LPG the induced birefringence resulted in each attenuation band dividing into two smaller attenuation bands, corresponding to coupling to the two orthogonal polarisation states. The magnitude of the birefringence increased with the load. Since the wavelengths of the two components are related to the birefringence, the wavelength separation increases with applied load. A linear response was obtained, with a sensitivity of 500nm/kg/mm, which is 800 times that of a FBG [28].

Corrugated LPGs have been used to form torsion sensors [27]. A corrugated fibre experiencing torsion sees different twisting rates in the etched and unetched regions because of the difference in diameter. This results in a stress concentration at the etched boundary. The effect of torsion is to change the coupling strength, and to induce a wavelength shift [30].

This section has reviewed the response of LPGs to axial strain, transverse loads and has presented the use of LPGs as torsion sensors. It has highlighted that the sensitivity to strain can be enhanced or suppressed depending of the application's requirements. A LPG is also sensitive to bending and an overview is presented in the following section.

3.2.3 Sensitivity to bending

The transmission spectrum of a LPG has been found to be highly sensitive to bending. The bend sensitivity of LPGs manifests itself in one of two ways: as a shift in the central wavelength of the attenuation bands [31, 32], or as a splitting in two of each attenuation band, with the wavelength separation of the split components increasing with increasing curvature [33, 34]. The sensitivity to bending arises because it modifies the physical parameters of the LPG, an expansion of the outer edge of the LPG and a compression of the inner edge thus bringing about a non-periodic variation of the LPG's period, therefore the LPG can be considered as a non-uniform tilted grating [35]. A fuller theoretical analysis of the effects of bending is presented in [35]. Structural bend sensing is of great importance in a number of engineering areas, such as monitoring the bending of rotating helicopter rotor blades, in observing the bending of reinforcement girders in structures and in robotic manipulation [4].

The first observation of the influence of bending upon the transmission spectrum of a LPG noted that the shift in the central wavelength of the attenuation bands is accompanied by a reduction in the coupling strength and a broadening of their spectral width [31]. The sensitivity of the bend induced wavelength shift was subsequently observed to depend upon the orientation of the optical fibre with respect to the plane in

which the bend is applied, with the maximum and minimum sensitivities separated by 180° [32]. The origin of the orientation dependence is believed to be an eccentricity of the fibre core, with the core no longer at the neutral axis of the fibre. Fibres with eccentricities of up to 14μm have been used to form bipolar bend sensors [36].

The second manifestation, the splitting of the attenuation bands, illustrated in Figure 1.3 of Chapter 1, is attributed to a breaking of the symmetry of the system that results in two degenerate spatial modes of the fibre becoming non-degenerate. This effect has been observed in B-Ge co-doped photosensitive fibre [33, 34] and in fibres with large core eccentricities [37, 38]. This effect has also been observed to exhibit a dependence upon the orientation of the fibre [34, 37]. In this case the reference plane is defined by the orientation of the fibre during fabrication of the LPG, with the largest sensitivity corresponding to the surface of the fibre oriented towards the UV source on the outer surface of the bend, [34]. This is thought to be a result of an asymmetry introduced by a radially non-symmetric UV induced RI modulation. Such asymmetries have been used to account for similar effects in LPGs formed by CO_2 laser irradiation, where the asymmetry is more pronounced due to heating of the surface facing the laser beam [39].

As already discussed in section 2.7.2 of Chapter 2, for higher order cladding modes it is possible to couple to the same cladding mode at two different wavelengths. The wavelength separation of the two resulting attenuation bands shows high sensitivity to external measurands, and has been exploited to perform bend sensing [40]. The separation between the split attenuation bands increases with increasing bend curvature, separations as large as 70nm giving a bend sensitivity of $14nm/m^{-1}$ for an applied curvature of $5m^{-1}$, have been reported [41], offering sensitivities of up to fifty times that offered by the previously reported LPG bend sensors [42, 43].

This section has reviewed the responses of LPGs to bending and has explained the effects of bending reported in a various fibres. The following section reviews the response of the LPG's transmission spectrum to a change in the RI of its surrounding medium.

3.2.4 Sensitivity to the refractive index of surrounding medium

LPGs exhibit sensitivity to the RI of the material surrounding the cladding, n_{Ext}. The period of the LPG is unchanged under the effects of change in n_{Ext}, and the response is in the form of a wavelength shift of the attenuation bands and can be determined by rearranging equation. 3.1 to produce:

$$\frac{d\lambda}{dn_{Ext}} = \frac{d\lambda}{dn_{cl}} \frac{dn_{cl}}{dn_{Ext}} \tag{3.3}$$

Variation in n_{Ext} serves to change the effective index, n_{cl}, of the cladding modes. Since the coupling wavelength, λ for a particular cladding mode is dependent on the n_{cl} through the phase-matching condition, equation 3.1, a change in n_{Ext} will change λ. For each cladding mode the term dn_{cl}/dn_{Ext} is unique thus each attenuation band exhibits a different sensitivity. The sensitivity to the RI has manifested itself as a change in central wavelengths, as illustrated in Figure 3.1, and also as a change in the minimum transmission value of the attenuation bands as illustrated in Figure 3.2. Figures 3.1 and 3.2 illustrate respectively, the change in the central wavelength and the minimum transmission value of an attenuation band as a function of the RI of the medium surrounding the LPG.

Figure 3.1 shows that the greatest change in the central wavelength of the attenuation band to the change in the RI of the surrounding medium occurs as the RI approaches that of the cladding, 1.456, [44]. The wavelength shifts of up to a 100nm for a single attenuation band have been reported [9].

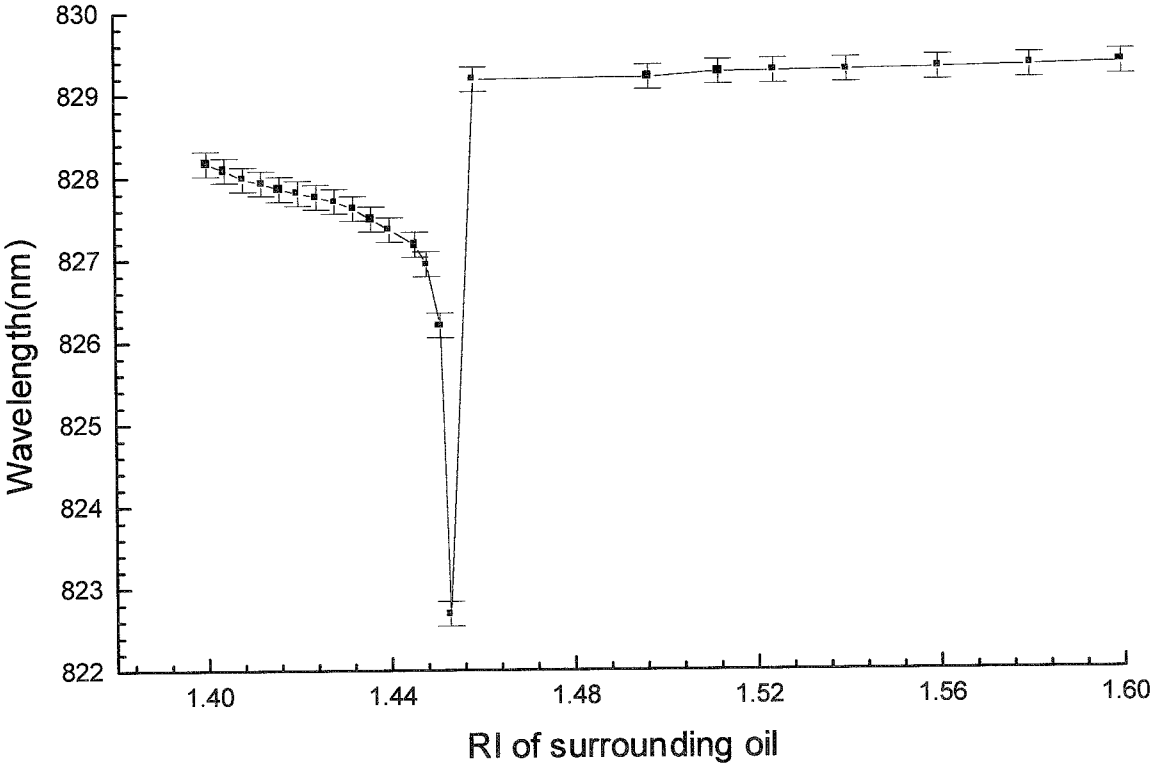

Figure 3.1: *Plot of wavelength as a function of the RI of the medium surrounding the LPG for an attenuation band* [45, 46, 47].

It can be seen from Figure 3.2 that the greatest change in the minimum transmission value also occurs when the RI of the medium surrounding the LPG approaches that of the cladding.

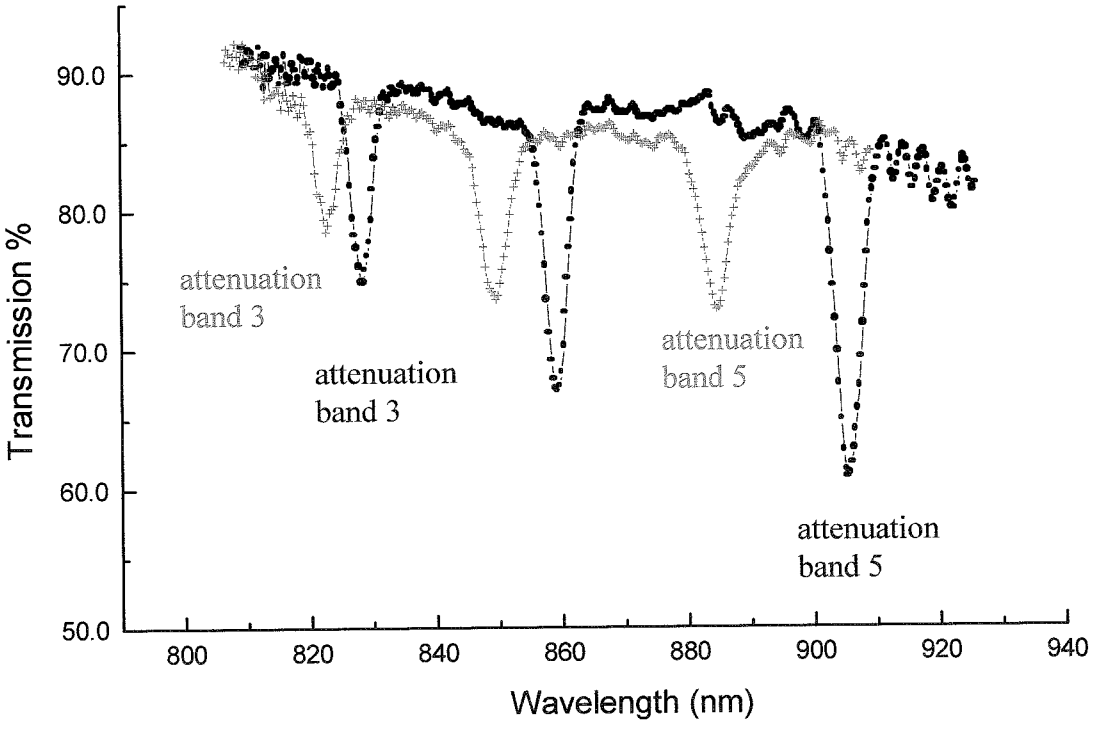

Figure 3.2: *Plots of transmission as a function of wavelength for the LPG when it was immersed in liquids of RI, • 1.400 and + 1.456* [45].

When the RI is equal to that of the cladding, the cladding appears to be of infinite extent, and thus supports no discrete modes. Broadband radiation-mode coupling losses are then observed, with no distinct attenuation bands. For a surrounding RI higher than that of the cladding, n_{Ext} >1.46, propagation modes are not supported. The existence of the attenuation bands under these conditions is attributed to the existence of attenuated cladding modes, arising from Fresnel reflections at the interface of the cladding and the external medium rather than total internal reflection [44]. The centre wavelengths of these attenuation bands show a considerably reduced sensitivity [44, 48, 49], but a change in the form of the transmission spectrum is observed, in that the coupling strength of the attenuation band is reduced [50], as illustrated in Figure 3.3. Figure 3.3 shows that when the RI of the medium surrounding the LPG is < RI of the cladding, the minimum transmission value of the attenuation band initially increases and then decreases as the RI approaches that of the cladding. When the RI of the surrounding medium is = to the RI of the cladding, the minimum transmission is at its

least value. Further increases in the RI of the surrounding medium show an initial increase in the minimum transmission value but stabilises at a value that is greatly reduced compared to its starting value.

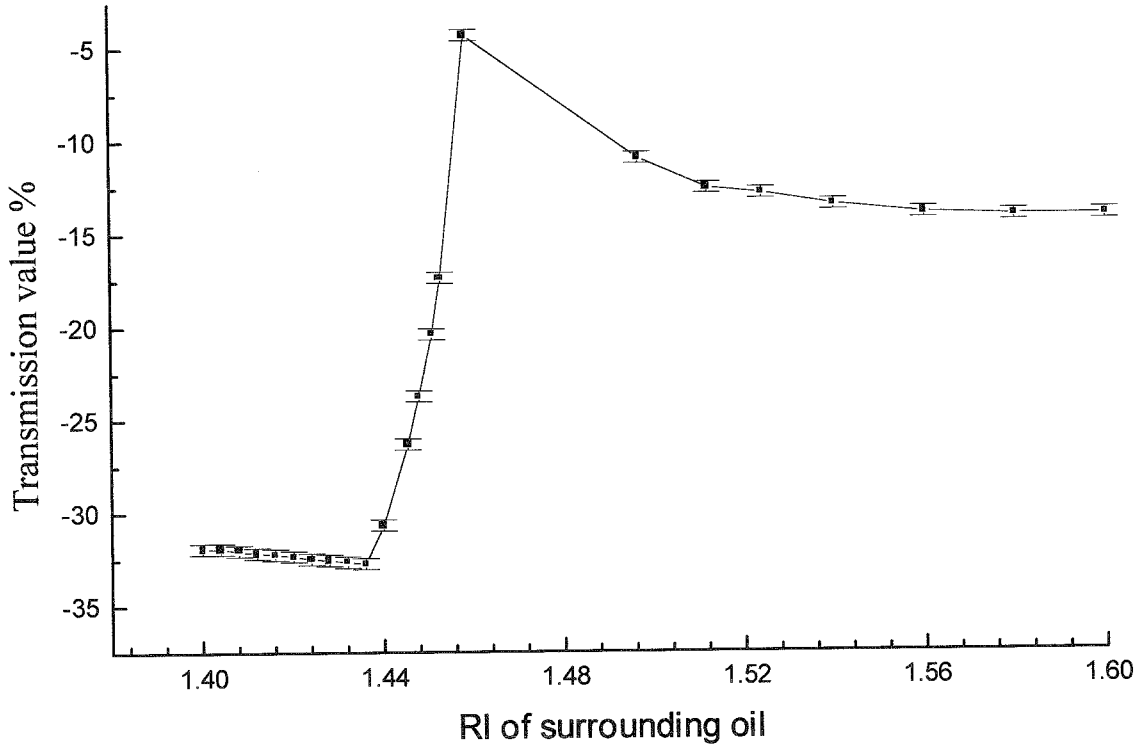

Figure 3.3: *A plot of the minimum transmission value as a function of RI for an attenuation band, the line is a guide for the eye only* [45, 47].

Clearly, for some applications where well controlled spectral characteristics are required, the RI sensitivity has a number of practical implications for the packaging and protection of a LPG. Care has to be taken to ensure that the properties of an adhesive used to attach a LPG to a substrate, or the properties of materials used to protect the LPG from mechanical damage or humidity, do not change the wavelengths of the attenuation bands from their original value, and that any changes in the RI of the surrounding material do not cause a change in the transmission of the LPG.

With this in mind, LPGs have been fabricated in fibres with complex structures to desensitise the LPG spectrum to the surrounding RI. LPGs fabricated in dual shaped core (DSC) dispersion shifted fibre exhibit an attenuation band that is insensitive to

external RI and to mechanical damage of the fibre surface [51]. The DSC fibre contains an inner-cladding region that has a higher RI than the remaining cladding layer. The RI insensitive attenuation band is believed to correspond to coupling to a mode of this inner cladding. These LPGs are prone to changes in their spectral characteristics by humidity, through RI changes of a coating polymer [15] or condensation on the bare fibre. When designing complex filters for gain flattening in optical amplifiers designers use the dispersion of different cladding modes to optimise the spectral widths of the individual gratings [52].

LPGs have been fabricated in an air-clad optical fibre, in which the cladding of the fibre is surrounded by a capillary tube, supported by thin silica webs. The evanescent field of the cladding modes does not extend beyond the capillary, with the result that all of the attenuation bands are insensitive to the external RI [53]. The advantage of such a LPG is that it is insensitive to environmental or ageing effects on the index of coating. This can improve the design flexibility of LPG gain flattening filters while simultaneously reducing the need for hermetic packaging of these devices [54]. A similar fibre structure, but in which the space between the capillary and the inner cladding is filled with a liquid crystal material, has been used to create a tuneable filter. In this case, the RI of a dye doped neumatic liquid crystal was controlled by realignment of the molecules using polarised laser illumination [22]. Similar systems could be controlled using electrical or thermal techniques.

The RI sensitivity of LPGs has been exploited to form RI sensors [55], used in biomedical engineering applications [56] and as a means of forming a tuneable spectral filter [22]. The use of LPGs for the measurement of solutions, dilutions and water-soluble industrial fluids is of interest in many quality control industrial processes in order to monitor the concentration stability and abnormal ageing effects. This has led to a unique application of LPG sensing to measure the concentration of chemical solutions [57, 58, 59], based on monitoring the wavelength shift of the attenuation bands. The operation of such sensors is limited to when n_{Ext} is in the range 1.40-1.46, because of the behaviour of the transmission spectrum in the region when the RI > 1.46.

While LPGs are sensitive over only a limited RI range, and their response is not species specific, it has been shown that LPGs may be used for on-line monitoring of the concentration of solutions of dangerous materials or materials in inaccessible locations for industrial production quality control [59]. LPGs have been used to measure the concentrations of solutions of sodium chloride [59], calcium chloride [59] and ethylene glycol [44, 59]. The measured sensitivities had resolutions that were equal to, or better than, than those offered by conventional Abbe refractomtery [59]. The use of LPGs to monitor the refining of kerosene, which requires that the concentration of organic aromatics such as benzene and xylene is measured, has been proposed. To demonstrate the feasibility, the concentration of a binary solution of xylene in heptane was measured with a minimum detectable volumetric concentration of 0.04%, corresponding to a RI change of $6x10^{-5}$. This is comparable to the accuracy of the standard technique of liquid chromatography and UV spectroscopy [55].

The studies discussed thus far in this section have concentrated upon the bulk immersion of the LPG into a solution. Overlay materials that exhibit changes in their RI in response to their local environment have been deposited onto LPGs [60, 61]. In this way, the LPG may be used to form, for example, a tuneable loss filter [60] a temperature insensitive filter [16] or a species-specific chemical sensor [61].

LPG based biosensors has been investigated by immobilising antibodies on the surface of the fibre, and monitoring the change in RI that occurs when an antigen bonds with the anti-body [61]. This allows use of a LPG to form a species-specific chemical sensor, again offering comparable performance to other techniques including surface plasmon resonance and interferometry, but with the prospect for on-line monitoring.

The effect of the thickness of the overlay material upon the LPG response has also been investigated [62]. A thin film of organic material has been deposited upon a LPG using the Langmuir-Blodgett technique, which allows high-resolution control (≈ 3nm) over the thickness of the film by depositing one molecular layer at a time. It was observed that, for films of RI higher than that of the cladding, the wavelength and amplitudes of the attenuation bands exhibited very high sensitivity to the optical

thickness of the overlay. This is obtained from films of thickness of a few hundred nm. For materials of index lower than that of the cladding, the sensitivity to thickness of the overlay is considerably reduced, an example of this response is shown in Figure 3.4. This is quite distinct from the behaviour under bulk immersion, in which the highest sensitivity is observed for indices lower than that of the cladding, as already seen in Figure 3.1. Materials suitable for deposition by the LB technique have been previously shown chemically sensitive [63, 64], offering the prospect for the development of a range of new species specific chemical sensors or optical modulators [62].

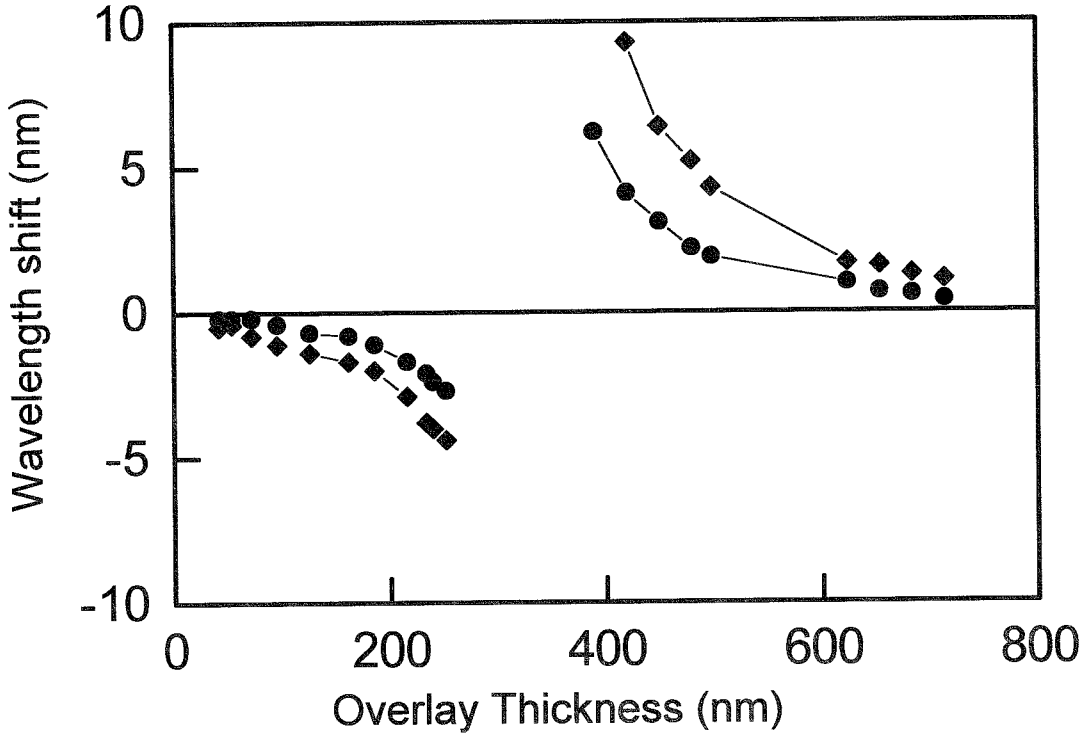

Figure 3.4: *Shift in the central wavelengths of the attenuation bands plotted as a function of the thickness of the overlay film.* ● *attenuation band corresponding to the coupling to the* 5^{th} *order cladding mode,* ■ *attenuation band corresponding to the coupling to the* 6^{th} *order cladding mode.* Diagram reproduced from [62].

The RI sensitivity of LPGs has been exploited to form other types of physical sensor. LPGs have been proposed to form a flow sensor to monitor the arrival of resin within a liquid composite moulding system [65, 66]. The measurement relies upon the reduction in the extinction ratio of the attenuation band that occurs when the LPG is surrounded by a material of higher RI.

The RI sensitivity has also been used to enhance and reduce the temperature sensitivity of LPGs. Surrounding the LPG by a liquid with large thermo-optic coefficient results in the LPG responding to both changes in temperature and to the temperature induced RI change of the surrounding medium [22, 24]. If the material has a negative thermal expansion coefficient, then for increasing temperature the wavelength shift induced by the change in RI of the coating causes a red shift in the wavelength of the attenuation band, this is discussed in section 6.3 of Chapter 6. If the attenuation band itself has positive temperature sensitivity, then the two effects add to increase the temperature response. If, however the material has a positive thermo-optic coefficient, then an increase in temperature causes a blue shift of the attenuation band, reducing the temperature response of the LPG.

Recoating a LPG with a UV curable acrylate based polymer of RI approximately equal to that of the cladding, and with a negative thermal expansion coefficient, increased the sensitivity of the LPG, which had been fabricated in a conventional dispersion shifted fibre, from 0.05nm/°C to 0.8 nm/°C 23]. This, however, was accompanied by a change in the coupling strength. Using an air clad optical fibre, described previously in this section, in which the air regions were filled by the same polymer, produced a similar sensitivity, but with no change in the minimum transmission of the attenuation bands [24]. In addition, it was noted that the novel fibre structure allowed the polymer to be protected from environmental effects, such as humidity, that may degrade its long-term performance. A similar system using a liquid crystal material produced a sensitivity of 2.10nm/°C [22]. For a LPG recoated with a material of positive thermo-optic coefficient, a temperature response as low as 0.0007nm/°C was obtained [16].

The sensitivity of the attenuation bands to the surrounding RI can be enhanced by manipulating the fibre parameters and choosing the appropriate period for the LPG for coupling to specific cladding modes [10]. Alternatively the thickness of the cladding around the LPG can be reduced [10, 67, 68]. The greatest sensitivity achieved is 130nm for a RI change of 2×10^{-3}, when the cladding's diameter was reduced from 125μm to 32μm [68]. It has also been observed that when the cladding diameter is reduced to 32μm only one resonant band remains in the spectrum's range of 900 to 1700nm. Thus it is possible to achieve a very broad tuning range without consideration of the overlap between different resonant bands [10, 69], making it a good candidate for widely tuneable fibre filters.

This section has reviewed the sensitivity of LPGs to changes in its surrounding RI in a range below and above that of the cladding. It has reviewed how the sensitivity to RI has been exploited to form RI sensors in medical, chemical and other engineering applications and also to produce a widely tuneable fibre filter. The next section overviews how a LPGs transmission spectrum can be adjusted to suit the requirements of the application.

3.3 Tuning the transmission spectrum of a long period grating

In many applications, such as gain flattening, it is necessary to control the central wavelengths of the attenuation bands to high a accuracy [70]. It has been observed that by post processing the LPG, the central wavelength can be fine- tuned to match the requirements of the application. Red shifts in the wavelengths have been achieved by reducing the diameter of the fibre's cladding around the LPG [67, 68, 70,], and by introducing a single, or multiple discrete phase shifts within the LPG's structure [71, 72, 73]. Since the resonance wavelength shifts are dependent on the cladding mode order, for the highest order cladding mode, wavelength shifts of up-to 130nm for a cladding diameter that is reduced from 125μm to 105μm have been reported [70].

An alternative means for tailoring the spectral response of the LPGs can be achieved by coating the LPG with a uniform metal overlay [18, 19]. A shift of 11nm in the central wavelength of the attenuation bands has been reported when a Platinum top layer of thickness 100nm [19] was used. This principle is the basis of a LPG based sensor that monitors the corrosion of a metal [74]. As the metal deteriorates, its thickness changes, which brings about a wavelength shift.

A wavelength shift in the LPG's attenuation bands has also been achieved by controlling the resistive heating [75]. When a LPG is coated with a non-uniform metal overlay, the localised thermal effects will produce a non-uniform heat distribution thus, control of the heating will control the amount of shift in wavelength. The shift to shorter wavelengths can be achieved by heating, straining and bending of the LPG. These methods have already been discussed in sections 3.2.1, 3.2.2 and 3.2.3, respectively.

Thus far, the main emphasis has been on considering LPGs as single parameter sensors of measurands such as temperature, strain, bending and to the change in the RI of its surrounding medium. LPGs have been introduced as sensors that are able to respond to more than one change in their environment, at any one time. The next section presents LPGs as multi-parameter sensors and discusses how the responses can be separated.

3.4 Multi-parameter sensing using long period gratings

LPGs are able to simultaneously respond to a number of environmental changes and it is possible to separate the responses. LPGs are therefore suitable for applications in which a variety of measurands have to be monitored simultaneously by a single sensor.

The simultaneous measurement of more than one external parameter is especially important in situations in which the output signal needs to be modified to compensate for the sensitivity to more than one external perturbation, or simply for

distributed and localised simultaneous sensing of a number of parameters. It has been shown that the differential shifts in two or more attenuation bands in a single LPG can be used for the simultaneous and independent measurement of temperature and strain [8], by the virtue of the difference in their sensitivities to the measurands. In addition, the observation of the bend induced splitting of the attenuation bands has allowed the simultaneous measurement of bend radius and temperature [34].

Strain and temperature can be simultaneously measured by using the wavelength shift in two fibre gratings that have different responses to temperature and strain [76, 77]. LPGs have been used in conjunction with FBGs to achieve this aim, where the difference in the ratio of the responses between the two devices was >15% [77].

Although the ability to simultaneously respond to more than one change is desirable, the response to each must be separable. As has been discussed previously, the sensitivity of LPGs to the various measurands is dependent upon the composition of the fibre, the period of the LPG and the order of the cladding mode to which coupling takes place. Appropriate choice of fibre composition and grating period allows the generation of attenuation bands that are insensitive to temperature or strain, facilitating independent measurement of these measurands [12]. Two LPGs, one with insensitivity to temperature and the other with insensitivity to strain, have been used to measure strain and temperature, respectively [17].

LPGs have been used in conjunction with FBGs to separate their temperature and strain responses [78] and also to demodulate the return from the LPG [79]. Two FBGs and a single LPG have been used to accurately determine the strain and temperature. The LPG had a higher temperature sensitivity and a lower strain sensitivity when it was compared to the FBGs. The two FBGs were fabricated such that their Bragg wavelengths sat on either side of the spectrum of an attenuation band of a LPG physically located on the source side of the two FBGs. Thus, the LPG acted to attenuate the reflections from the FBGs, the attenuation being dependent upon their relative central wavelengths. By virtue of the difference between the sensitivities of the FBGs and LPGs to strain and temperature a small decrease in the measured reflection of the

low wavelength FBG, accompanied by a small increase the reflection from the higher wavelength FBG, indicated a change in strain. While a large increase in the reflection from the low wavelength FBG, accompanied by a large decrease in the reflection from the longer wavelength FBG indicated a change in temperature. Measurement of the relative intensities of the reflections allowed independent measurement of temperature and strain [78]. A LPG was also used as an edge filter to facilitate an intensity based method to demodulate the reflection from a FBG [79].

A LPG has been used to simultaneously monitor changes in temperature and increases in its bend radius [34]. The temperature sensitivity of the LPG was shown to be independent of the bend radius [34]. The wavelength separation of the split components of the attenuation band is dependent on the bend radius [34]. The average wavelength of the attenuation bands was found to be dependent upon the temperature [34]. The average wavelength of the attenuation bands was also found to be independent of the bend radius [34]. Such a sensor could be used to determine the applied bend in a thermally unstable environment or the temperature in a situation where the sensor was constantly subjected to bending.

This section has highlighted and reviewed the suitability of LPGs for multi-parameter sensing. It has recognised the versatility of LPGs, which allows their combination with a number of FBGs for sensing purposes. Multiple LPGs have been used for sensing applications and these are now reviewed in the following section.

3.5 In-series long period grating sensors

There has been some interest in the use of concatenated LPGs for sensing applications [80]. When a pair of identical LPGs are fabricated in series within an optical fibre, separated by upto 100mm, a set of fringes are observed within the attenuation bands [80]. The formation of the fringes may be understood with reference to Figure 3.5.

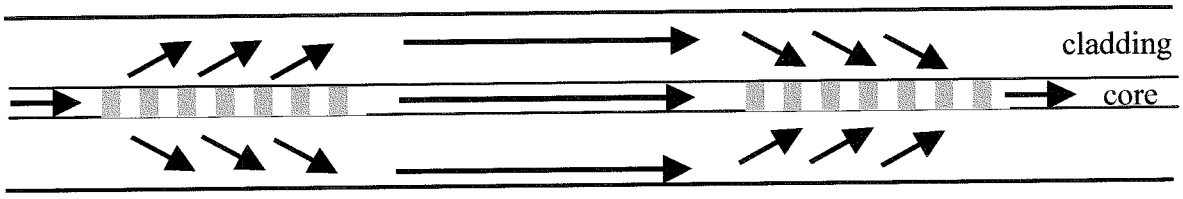

Figure 3.5: *Principle of operation of in-series LPGs.* Adapted from [81]

The first LPG couples light to the cladding mode. Light then propagates to the second LPG via two routes: in the core and in the cladding. By virtue of the difference in the effective refractive indices of the core and cladding modes, the light coupled into the cladding by the second LPG is phase shifted with respect to the light propagating in the core, giving rise to the interference pattern. The narrower bandwidth of the fringe facilitates greater resolution in the measurement of the wavelength than is possible with conventional LPGs.

In series LPGs have been used to sense bending [80], external index of refraction [81, 82], temperature and transverse load [81]. Bending the pair of in series LPGs, results in an increase in the attenuation of the cladding modes, with a concomitant reduction in the visibility of the fringes and a shift of the central wavelength [80, 82].

Transverse loading was observed to reduce the fringe visibility linearly, at a threshold load, then the fringe pattern disappeared [82]. Further increase of the load caused the pattern to reappear with a π phase shift [82].

The response of the in series LPGs to RI is a decrease in fringe visibility and a change in the central wavelengths, of similar form to that observed for single LPGs [82]. For refractive indices higher than that of the cladding, the fringes reappear, but with considerable reduced visibility. If, however, only the section of fibre between the LPGs is surrounded by the material of high RI, the minimum transmission of the

attenuation bands can show up to twice the sensitivity of a conventional LPG, for refractive indices in the range 1.50 to 1.55 [81].

Coating the end of a fibre containing a LPG with metal film results in the double pass of the light through the LPG, allowing the generation of the interference fringes [83]. This also allows the monitoring of the performance of the LPG in reflection, and avoids the necessity to fabricate identical LPGs. This has been used to form a temperature sensor [83]. A pair of cascaded LPGs, one with a low temperature sensitivity and the other with a suppressed strain sensitivity have been used to carry out the required simultaneous measurements of temperature and strain. The LPGs showed a temperature sensitivity of 0.28nm/°C, in a temperature range of 30°C to 150°C, and a strain sensitivity of 0.00042nm/με [17].

The use of two cascaded LPGs, with periods chosen such that one LPG had an attenuation band that was insensitive to temperature, while the other had a band that was insensitive to refractive index, has been shown to allow simultaneous, independent measurement of these two parameters. This potentially allows the temperature independent monitoring of chemical solutions with temperature dependent refractive indices [84].

3.6 Discussion

The review of long period fibre gratings has shown them an effective and versatile temperature, strain, RI and bend sensor. They have shown themselves as transducers that possess high sensitivity and because of their large spectral width they can be used with simple demodulation schemes. It has been shown that the induced wavelength shifts are a strong function of the LPG's periodicity and the order of the cladding mode. Strain and temperature LPG based sensors are seen to possess larger wavelength shifts than conventional FBG based sensing schemes. LPG multi-parameter sensing abilities are used for the simultaneous measurement of temperature and strain and of temperature and bending. The cross-sensitivity to these external parameters can be eliminated or at least greatly reduced and so allowing the use of strain insensitive

LPGs as effective temperature measuring devices in the presence of axial strain. Temperature insensitive LPGs are effective in the monitoring of strain and bending. Unlike the FBG based RI sensor, the LPG based RI sensor does not require etching of the cladding and is shown to have a wide range of applications in chemical and biomedical engineering. The sensitivity to RI has been used to tune LPG based filters and has also found use in the monitoring of corroding metal in a structure.

One drawback of LPGs is that the presence of multiple resonance attenuation bands and their large bandwidth limit the options for multiplexing arrays of sensors to the use of spatial division multiplexing, in which each LPG is located within a separate fibre and allocated its own detection system. Despite this draw-back the investigation of sensing applications for LPGs needs to continue as there are many applications that would benefit from the definite advantages and multi-parameter sensing abilities that LPGs offer.

3.7 Chapter summary

This chapter has discussed the origin of the sensitivity of LPGs to measurands such as temperature, strain, bending and RI, and how the attenuation bands have differing sensitivities to the various measurands. These different sensitivities offer the prospect for the development of sensor elements capable of monitoring simultaneously and independently a number of measurands. The ability to tune the sensitivity by virtue of the fibre composition and LPG period has also been discussed. The means for optimising the performance of the LPG by using techniques such as etching of the cladding diameter has been outlined for particular applications. A review of the LPG as a single parameter sensor of temperature, strain, bending and RI was presented. A brief summary of the properties of LPGs is presented and an indication of their sensitivity to the various measurands is given in Table 3.1.

- $\Lambda < 100\mu m$ the LPG couples to higher order cladding modes
- $\Lambda > 100\mu m$ the LPG couples to lower order cladding modes
- Sensitivity to the measurand is dependent on the order of the attenuation band.
- Higher order attenuation modes show the greatest sensitivity to the measurand.
- Suitable for multi-parameter sensing, including temperature and strain, temperature and bending and temperature and RI.

Table 3.1: *A summary of the sensitivity of the LPGs response to the measurands.*

Temperature	**Sensitivity**	**Λ (μm)**	**Fibre type**	**Reference:**
Un-modified response	-0.14 to 0.38nm/°C	>100	Std.	[5]
	1.8pm/°C	40	CF	[12]
	upto 2.75nm/°C	240	B-Ge	[21]
	0.093nm/°C	280	SMF-28	[85]
	3% change in MTV	50.1	PFBG-1355-T	[26]
Enhanced response	-0.14 to 0.28nm/°C	500	GeO_2	[17]
	0.05 to 0.8nm/°C	600	Std.	[23]
	2.10nm/°C		SF	[23]
Suppressed response	-0.049 to 0.0007nm/°C	430	Std., B-Ge	[16]
	-0.142 to 0.002 nm/°C	500	GeO_2	[17]
Strain				
Un-modified response	0.04ρm /με	340	CF	[10]
	-0.01 to –2.2pm/με	40	CF	[10]
	-0.22 to -0.23nmμε	280	SMF-28	[85]
	80% change in MTV	50.1	PFBG-1355-T	[26]
RI	Wavelength shift of the attenuation band as the bulk RI of the medium surrounding the LPG < that of the fibre cladding, upto 100nm when the surrounding RI ≈ cladding	200 200-350	BPG HF	[9, 44, 48, 49, 50]

RI	A change in the MTV of the attenuation band over the RI range 1.40- 1.7	200 200-350	BPG HF	[9, 44, 48, 49, 50]
Bending	A wavelength shift in the central wavelength of the attenuation band for increasing bend curvature ≈ 10nm/m^{-1}	225-325	Ge with HF	[31, 32]
	A splitting of the attenuation bands. The distance between the splits increases with increasing applied bend curvatures, a sensitivity of 14.5 nm/m^{-1}	500 400 490	 B-Ge B-Ge	[33, 34, 37, 38, 41, 42, 43]
	The magnitude of the splits is also dependent on the orientation of the UV exposed side of the fibre.	225-325	Ge with HF	[32, 34, 37, 41]

Key: Std. = Standard telecomms fibre, H = Hydrogen loaded fibre, CF = Corning Flexcor 1060nm fibre, B-Ge = Boron Germanosilicate co-doped fibre, SF = Fibres with special RI profiles, SMF-28 = Corning SMF-28 Fibre.

Chapter 4 will discuss in detail the various physical methods used to induce a LPG into the core of a fibre. There is a detailed consideration of the UV irradiation method and the two LPG fabrication configurations based on this are described.

References:

1 A.D. Kersey, M.A. Davis, H.J. Patrick, M. LeBlanc, K.P. Koo, C.G. Askins, M.A. Putman and E.J. Friebele, 'Fibre grating sensors', J. Lightwave Technol., **15**, pp. 1442 – 1461, (1997).

2 V. Bhatia and A.M. Vengsarkar, 'Optical fibre long period gratings sensors', Opt. Lett., **21**, pp. 692 – 694, (1996).

3 A.D. Kersey, 'A review of recent developments in fibre optic sensor technology', Optical Fibre Technol., **2**, pp. 241 – 317, (1996).

4 E. Udd, 'Fibre Optic Sensors', Wiley, USA, (1992).

5 S.A. Vasiliev and O.I. Medvedkov, 'Long period refractive index fibre gratings: properties, applications and fabrication techniques', In Advances in Fibre Optics, Proc. of SPIE, **4083**, pp. 212 – 223, (2000).

6 D.A. Krohn, 'Fibre Optic Sensors', 2nd Edition, Instrument Society of America, North Carolina, (1992).

7 K. Shima, K. Himeno, T. Saski, S. Okude, A. Wada and R. Yanauchi, 'A novel temperature insensitive long period fibre grating using a boron-doped-germanosilicated core fibre', Optical Fibre Conf. Tech. Dig. **6**, pp. 347-348, (1997).

8 V. Bhatia, D. Campbell and R. O. Claus, 'Simultaneous strain and temperature measurement with long-period gratings', Opt. Lett., **22,** pp. 648 (1997).

9 V. Bhatia, D.K. Campbell, T.D'Alberto, G.A. Ten Eyck, D. Sherr. K.A. Murphy and R.O. Claus, 'Standard optical fibre long period gratings with reduced temperature sensitivity for strain and refractive index sensing', In Tech. Dig. Conf. Opt. Fibre Comm. Dallas, TX. pp. 346 –347, (1997).

10 V. Bhatia, 'Properties and sensing applications of long period gratings', Ph.D. Thesis, Virginia Polytechnic and State University, Blacksburg, Virginia (1996).

11 J.B. Judkins, J.R. Pedrazzani, D.J. DiGiovanni and A.M. Vengsarkar, 'Temperature insensitive long period grating fibre gratings', Optical Fibre Conf. Tech. Dig. PD1, San Jose, USA (1996).

12 V. Bhatia, D.K. Campbell, D. Sherr, T.G. D'Alberto, N.A. Zabaronick, G.A. Ten Eyck, K.A. Murphy and R.A. Claus, 'Temperature insensitive and strain insensitive long period grating sensors for smart structures', Opt. Eng., **36**, pp. 1872-1876, (1997).

13 C.C. Ye, S.W. James and R.P. Tatam, 'The effect of annealing on the temperature sensitivity of long period gratings', Cranfield University, Internal report, (1999).

14 L Qin, Z.X. Wei, Q.Y. Wang, H.P. Li, W. Zheng and D.S. Gao, 'Compact temperature-compensating package for long period fibre gratings', Optical Materials, **14**, pp. 239-242, (2000).

15 A.A. Abramov, A. Hale and A.M. Vengsarkar, 'Recoated temperature insensitive long period fibre gratings', Optical Fibre Conf. Tech. Dig. **6**, PD3-1, (1997).

16 J.N. Jang, S.Y. Kim, S.W. Kim, M.S. Kim, 'Novel temperature insensitive long period grating by using the refractive index of the outer cladding', Optical Fibre Comm. Conf., **1**, pp. 29-31, (2000).

17 Y. G. Han, C.S. Kim, K.Oh, U.C. Paek and Y. Chung, 'Performance enhancement of strain and temperture sensors using long period fibre grating', Proc. 13th OFS Conf., SPIE, **3746**, Tu2-7, pp. 58-61, Kyongju, Korea, (1999).

18 O. Duhem, A. DaCosta, J.F. Henninot and M. Douay, 'Long period copper-coated grating as an electrically tuneable wavelength-selective filter', Electron. Lett., **35**, pp. 1014-1016, (1999).

19 D.M. Costaniti, H.G. Limberger, R.P. Salathe, C.A.P. Muller and S.A. Vasiliev, 'Tunable loss filter based on metal coated long period grating,' ECOC '98, pp. 391-392, Madrid (1998).

20 E.M. Dianov, A.S. Kurkov, O.I. Medvedkov, S.A. Vasiliev, 'Photoinduced long period grating as a promising sensor element', Proc. of Eurosensors X, The 10th Euopean Conf. on Solid State transducers, Leuven, Belgium, P5, pp -128, (1996).

21 X. Shu, T. Allsop, B. Gwandu, L. Zhang and I. Bennion, 'High temperature sensitivity of long period gratings in B-Ge co-doped fibre,' IEEE - Photon. Technol. Lett., **13**, pp. 818-820, (2001).

22 S. Yin, K-W. Chung and X. Zhu, 'A novel all optic tuneable LPG using a unique double cladding layer', Opt. Comm. **196**, pp. 181-186, (2001).

23 A.A. Abramov, B.J. Eggleton, J.A. Rogers, R.P. Espindola, A. Hale, R.S. Windeler and T.A. Strasser, 'Electrically tunable efficient broad band fibre filter', IEEE, Photon. Technol. Lett., **11**, pp. 445-447, (1999).

24 A.A. Abramov, A. Hale, R.S. Windeler and T.A. Strasser, 'Widely tunable long period fibre gratings', Electron. Lett., **35**, pp. 81- 82, (1999).

25 C.G. Atherton, A.L. Steele, and J.E. Hoad, 'Resonance conditions of long period gratings in temperature sensitive polymer ring optical fibre,' IEEE - Photon. Technol. Lett., **12**, pp. 65-67, (2000).

26 V. Grubsky and J. Feinberg, 'Long period fibre gratings with variable coupling for real-time sensing applications', Opt. Lett., **25**, pp. 203-205, (2000).

27 C-Y. Lin, L.A. Wang and G-W. Chern, 'Corrugated long-period fibre gratings as strain, torsion and bending sensors', J. Lightwave Technol. **19**, pp. 1159-1168, (2001).

28 Y. Liu, L. Zhang and I. Bennion, 'Fibre optic load sensors with high transverse strain sensitivity based on long-period gratings in B/Ge co-doped fibre', Electron. Lett., **35**, pp. 661-662, (1999).

29 L. Zhang, Y. Liu, J.A.R. Williams and I. Bennion, 'Design and realisation of long-period grating devices in conventional and high birefringence fibers and their novel applications as fibre optic load sensors', IEEE - J. Selected Topics in Quantum Electronics, **5**, pp. 1371-1378, (1999).

30 L.A. Wang, C.Y. Lin and G.W. Chern, 'A torsion sensor made of a corrugated long period fibre grating', Meas. Sci. Technol., **12**, pp. 793-799, (2001).

31 M.G. Xu, R. Maaskant, M.M. Ohn and A.T. Alavie, 'Independent tuning of cascaded LPG for spectral shaping', Electron. Lett., **33**, pp. 1893-1894, (1997).

32 H.J. Patrick, C.C. Chang and S.T. Vohra, 'Long period gratings for structural bend sensing', Electron. Lett., **34**, pp. 1773-1775, (1998).

33 Y. Liu, L. Zhang, J.A.R. Williams and I. Bennion, 'Optical bend sensor based on measurement of resonace mode splitting of long period fibre gratings', IEEE-Photon. Technol. Lett., **12**, pp. 531-533, (2000).

34 C.C. Ye, S.W. James and R.P. Tatam, 'Long period fibre gratings for simultaneous temperature and bend sensing', Opt. Lett., **25**, pp. 1007-1009, (2000).

35 D.A. González, J.L. Arce-Diego, A. Cobo and J.M. López-Higuera, 'Spectral modelling of curved long period fibre gratings', IOP, Meas. Sci. Technol., **12**, pp. 786-792, (2000).

36 H.J. Patrick, 'Self aligining, bi-polar bend transducer based on long period gratings written in eccentric core fibre', Electron. Lett., **36**, pp. 1763-1764, (2000).

37 J. Rathje, M. Krislensen and H. Hubner, 'Effects of core concentricity error on bend direction asymmetry for long period gratings', Bragg gratings, Photosensitivity and Poling in Glass Waveguides, Suart, USA, pp. 283-285, (1999).

38 J. Rathje, 'Long period gratings', Ph.D. thesis, Technical University, Lyngby, Denmark, (2000).

39 G.D. VanWiggeren, T.K. Gaylord, D.D. Davis, E. Anemogiannis, B.D. Garrett, M.I. Braiwish and E.N. Glytsis, 'Axial rotation dependence of resonances in curved CO_2 laser induced long period grating'' Electron. Lett., **36**, pp. 1354-1355, (2000).

40 H.J. Patrick, S.T. Vohra, 'Directional shape sensing using bend sensing of Long period grating', OFS –13, Proc. SPIE **3746**, pp. 561-564, (1999).

41 Y.Liu, L.Zhang and I. Bennion, 'Novel optical sensing applications of long period gratings', IOP, Applied Optics and Opto-electronics Conf. Loughborough University (U.K.) Sept. 2000

42 Y. G. Han, B.H. Lee, W. T. Han, U. C. Paek and Y. Chung, 'Resonance peak shift and dual peak separation of long period fibre gratings for sensing applications', IEEE - Photon. Technol. Lett., **13**, pp. 699-701 (2001).

43 J. Rathje, M. Svalgaard, H. Hubner, M. Kristensen, 'Sensitivity of a long period optical fibre grating bend sensor', OFC'98, OSA Tech. Dig. Series, **2**, pp. 238-239, (1998).

44 H.J. Patrick, A.D. Kersey and F. Bucholtz, 'Analysis of the response of long period fibre gratings to external index of refraction', J. Lightwave Technol., **16**, pp. 1606-1612, (1998).

45 Result from experiment conducted by author.

46 S. Khaliq, S.W. James and R.P. Tatam, 'Fibre optic liquid level sensor using long period gratings' Optics Lett., **26**, pp. 1224-1226, (2001).

47 S. Khaliq, S.W. James and R.P. Tatam, 'Enhanced sensitivity fibre optic long period grating temperature sensor', Meas. Sci. & Technol., **13**, pp. 792-795, (2002).

48 B.H. Lee, Y. Liu, S.B. Lee and S.S. Choi, 'Displacements of the resonant peaks of a long period fibre grating induced by a change of ambient refractive index', Opt. Lett., **22**, pp. 1769 - 1771, (1997).

49 R. Hou, Z. Ghassemlooy, A. Hassan, C. Lu and K.P. Dowker, 'Modelling of long period fibre grating response to refractive index higher than that of cladding, Meas. Sci. Technol. **12**, pp. 1709-1713, (2001).

50 O. Duhem, J.F. Henninot, M. Warenghem and M. Douay, 'Demonstration of long period grating efficient coupling with external medium of a refractive index higher than that of silica', Appl. Optics, **37**, pp. 7223-7228, (1998).

51 B.H. Lee and J. Nishii, 'Cladding-surrounding interface insensitive long period grating,' Electron. Lett., **34**, pp. 1129-1130, (1998).

52 T. Ergoden and D. Stegall, ' Impact of dispersion on the bandwidth of long period fibre grating filters,' Optical fibre Comm. Conf., **2**, pp. 280-282, OSA Tech. Dig. Series, (1998).

53 R.P. Espindola, R.S. Windeler, A.A. Abramov, B.J. Eggleton, T.A. Strasser and D.J. Di Giovanni, 'External refractive index insensitive air-clad long period grating', Elect. Lett., **35**, pp. 327-328, (1999).

54 R.S. Windler, J.W. Wagener and D.J. Digiovanni, 'Silica-air microstructured fibres: Properties and applications,' Optical Fibre Comm. Conf., San Diego, C.A. (1999).

55 T. Allsop, L. Zhang and I. Bennion, 'Detection of organic aromatic compounds in paraffin by a long period fibre grating optical sensor with optimised sensitivity', Opt. Comm., **191**, pp. 181-190, (2001).

56 T.A. Tran, J.A. Greene, K.A. Murphy, V. Bhatia, T. D'Alberto, R.O. Claus, B. Carman, D.M. Lyerly and T.D. Wilkins, 'Real-time immunoassays using fibre optic long period grating sensors,' Proc. SPIE, Conf. on the Biomedical Sensing, Imaging and Tracking Technol., **2676**, paper 27, (1996).

57 X. Shu and D. Huang, 'Highly sensitive chemical sensor based on the measurement of the separation of dual resonant peaks in a 100μm period fibre grating,' Opt. Comm., **171**, pp. 65-69, (1999).

58 H.J. Patrick, A.D. Kersey, F. Bucholtz, K.J. Ewing, B. Judkins and A.M. Vengsarkar, 'Chemical sensor based on long period grating response to index of refrcation', in Proc. Conf. Laser Electro-Opt., **11**, pp. (1997).

59 R. Falciai, A.G. Mignani and A. Vannini, 'Long period gratings as solution concentration sensors,' Sensors and Actuators B, **74**, pp. 74-77, (2001).

60 D.M. Costantini, C.A.P. Muller, S.A. Vasiliev, H.G. Limberger, and R.P. Salathe, 'Tunable loss filter based on metal coated long period fibre gratings', IEEE Photonics Technol. Lett., **11**, pp.1458 – 1460, (1999).

61 M.P. DeLisa, Z. Zhang, M. Shiloach, S. Pilevar, C.C. Davis, J.S. Sirkis and W.E. Bentley, 'Evanescent wave long period fibre Bragg grating as an immobilised antibody bio sensors', Anal. Chem., **72**, pp. 2895-2900, (2000).

62 S.W. James, N.D. Rees, G.J. Ashwell and R.P. Tatam, 'Optical fibre long period gratings with Langmuir Blodgett thin film overlays', Opt. Lett., **27**, pp. 686-688, (2002).

63 D. Flannery, S.W. James, R.P. Tatam and G.J. Ashwell, 'A pH sensor using Langmuir-Blodgett overlays on polished optical fibres, Opt. Lett., **22**, pp. 567-569, (1997).

64 D. Flannery, S.W. James, R.P. Tatam and G.J. Ashwell, 'Fibre optic chemical sensing using Langmuir-Blodgett overlay waveguides', Appl. Opt., **38**, pp. 7370-7374, (1999).

65 J.P. Dankers, J.L. Lenhart, S.R. Kueh, J.H. van Zanten, S.G. Advani and R.S. Parnas, 'Fibre optic flow and cure sensing for liquid composite moulding', Opt. Laser Eng. **35**, pp. 91-104, (2001).

66 S.R.M. Kueh, R.S. Parnas, S.G. Advani, 'A methodology for using long-period gratings and mold-filling simulations to minimise the intrusiveness of flow sensors in liquid composite moldings', Composi. Sci. Technol., **62**, pp. 311-327, (2002).

67 K.S. Chiang, Y. Liu, M.N. Ng and X. Dong, 'Analysis of etched long period fibre grating and its response to external' Electron. Lett., **36**, pp. 966-967, (2000).

68 S. Yin, O. Leonov, K.W. Chung, P. Kurtz, K. Reichard, H. Liu and Q. Zhang, 'Wavelength tuning range enhanced single resonant band fibre filter using a long period grating with ultra thin cladding layer', Optical Fibre Communications Conference, pp. 23 –25, (2000).

69 A.M. Vengsarkar, P.J. lemaire, J.B. Judkins, V. Bhatia, T. Erdogan and J.E. Spie, 'Long period fibre gratings as band rejection filters', J. Lightwave Technol., **14**, pp. 58-65, (1996).

70 S.A. Vasiliev, E.M. Dianov, D. Varelas and H. Limberger and R.P. Salathe, 'Postfabrication resonance peak positioning of long period cladding mode coupled gratings' Opt. Lett., **21**, pp. 1830-1832, (1996).

71 F. Bakhti, P. Sansonetti, 'Realisation of low back reflection wide band fibre bandpass filters using phase shifted long period gratings', Proc. Conf. Opt. Comms. (OFC'97) paper FB4, (1997).

72 J.R. Qian and H.F. Chen, 'Gain flattening fibre filters using phase shifted long period gratings,' Electron. Lett., **34**, pp. 1132-1133, (1998).

73 H. Ke, K.S. Chiang and J.H. Peng, 'Analysis of phase shifted long period fibre gratings, ' IEEE - Photon. Technol. Lett., **10**, pp. 1596-1598, (1988).

74 J.A. Greene, K.A. Murphy, T.A. Tran, V. Bhatia and R. O. Claus, 'Grating based optical fibre corrosion sensors', Proc. SPIE Conf. on Smart Sensing, Processing and Instrumentation, **2718**, paper A-19, (1996).

75 L.R. Chen, 'Tunable phase shifted long period gratings by refractive index shifting,' Canadian Conf. on Electrical and Computer Eng. **1**, pp. 453-457, (2001).

76 M.G. Xu, J.L. Archambault, L.Reekie and J.P. Dakin, 'Discrimination between strain and temperature effects using dual-wavelength fibre grating sensors,' Electron. Lett., **30**, pp. 1085-1087, (1994).

77 A.J. Rogers, V.A. Handerek, S.E. Kanellopoulos and J. Zhang, 'New ideas in non-linear distributed optical fibre sensing,' Proc. Soc. Photon-Opt. Instrum. Eng., SPIE, **2507**, pp. 162-174, (1995).

78 H.J. Patrick, G.M. Williams, A.D. Kersey and J.R. Pedrazzani, 'Hybrid fibre Bragg grating/ Long period fibre grating sensor for Strain/ Temperature discrimination', IEEE- Photonics Technol. Lett., **8**, pp. 1223-1225, (1996).

79 R. W. Fallon, L. Zhang. L. Everall, J.A.R. Williams and I. Bennion, 'All fibre optical sensing system: Bragg grating sensor interrogated by a long period grating', Meas. Sci. Technol., **9**, pp.1969- 1971(1998).

80 B.H. Lee and J. Nishii, 'Bending sensitivity of in-series long period fibre gratings', Opt. Lett., **23**, pp. 1624- 1626, (1998).

81 O. Duhem, J.F. Henninot and M. Douay, 'Study of in fibre Mach-Zehnder interferometer based on two spaced 3-dB long period gratings surrounded by a refractive index higher than that of silica', Opt. Comm., **180**, pp. 255-262, (2000).

82 Y.G. Han, B.H. Lee, W.T. Han, U.C. Paek and Y. Chung, 'Fibre optic sensing applications of a pair of long period fibre gratings', IOP, Meas. Sci. Technol., **12**, pp. 788-781, (20001).

83 B.H. Lee and J. Nishii, 'Self-interference of long-period fibre grating and its application as temperature sensor', Electron. Lett., **34**, pp. 2059-2060, (1998).

84 B.A.L. Gwandu, X. Shu. T.D.P. Allsop, W. Zhang, L. Zhang, I. Bennion, 'Simultaneous refractive index and temperature measurement using cascaded long-period grating in double-cladding fibre', Electron. Lett. **38**, pp. 695-696, (2002).

85 V. Bhatia, 'Applications of LPGs to single and multi-parameter sensing', Optics Express, pp. 457 – 466, (1999).

Chapter 4 Fabrication of fibre optic long period gratings

4.1 Introduction

This chapter discusses the methods used for generating a periodic modulation of the optical properties of the fibre and evaluates their merits and disadvantages. The chapter presents the UV based amplitude mask fabrication method used in manufacturing the LPGs used in this thesis. The LPGs require post processing by thermal annealing. Annealed fibre gratings exhibit linear wavelength response at high temperatures and that can be exploited to accurately tune the central wavelength of an attenuation band and for the development of sensor transducer elements. This chapter presents a discussion of the effects of annealing on the properties LPGs.

4.2 Generating a periodic modulation in the optical properties of the fibre

The fabrication of LPGs relies upon the introduction of a periodic modulation of the optical properties of the fibre. This may be achieved by permanent modification of the RI of the core of the optical fibre, by physical deformation of the fibre or by electrically controlling the behaviour of the core of a special fibre. The physical deformation of the fibre has been achieved mechanically [1], by tapering the fibre [2], by deforming the core [3, 4, 5], or the cladding [6]. The electrically induced change in the behaviour of a hollow-core fibre filled with liquid crystal allows the fibre to behave as a LPG [7]. The permanent modulation of the core RI has been achieved by the implantation of ions [8], irradiation by femtosecond laser pulses in the infrared [9], irradiation by focused CO_2 laser [10, 11, 12], by the spatial redistribution of the chemical composition of the glass due to thermo-induced diffusion of the fibre's dopants [13, 14], the periodic relaxation of the mechanical stress within the fibre [15, 16], electric discharges [17, 18, 19] and by exposure of the fibre to ultra-violet (UV) light [20, 21, 22, 23, 24, 25, 26].

4.3 Physical deformation of the fibre

4.3.1 Mechanically

The periodic index modulation of the LPG is induced via the photoelastic effect at the pressure points, when the fibre is pressed between a periodically grooved plate and a flat plate. Out-of-band losses of upto 15dB have been achieved, which is comparable with photo induced LPGs, but can be controlled by adjusting the pressure on the grooved plate. The position of the attenuation bands can be easily adjusted by changing the angle between the fibre and the grooves. The LPGs produced by this method are temporary, as once the pressure on the grooved plate is removed the transmission profile returns to its pre-pressure state. The transmission profile of a LPG produced by this method is cleaner possibly because the fibre does not have its buffer jacket removed, as this is said to reduce micro bending [1].

4.3.2 Tapering

A LPG has been produced by periodically tapering sections along the length of a already narrowed fibre. Out of band losses of upto 17db have been achieved after 35 periods have been deformed. Such a LPG is considered stable even at high temperatures because the perturbation is due to its macroscopic structure, unlike those induced by irradiation to UV. A length of fibre is heated in a travelling flame and then stretched to obtain a uniform fibre diameter of approximately 15μm [27]. A 0.8mm section of fibre is then further heated and elongated very slowly. This results in a microtaper structure that is repeated at equal spaced intervals along the narrowed fibre to form the LPG.

4.3.3 Deforming the fibre core

There are two methods of deforming the core to produce a LPG. The first deformation is achieved in a two-step process. In the first step, the unjacketed fibre is held firmly between two fixed points on a translation stage, the fibre has periodic incisions made into its cladding by exposing it to a focused single pulse of a CO_2 laser beam. This first step is shown in Figure 4.1. After the first incision has been made, the fibre is translated along by a distance equal to the grating period, Λ, and the process is repeated for the required number of incisions. The width of the cut depends on the size of the beam and the depth of the cut, dictated by the diameter of the cladding, is pre-determined and continually monitored [5]. The incisions do not bring about a change in the RI of the core because they do not extend into the core [5]. The required RI change is brought about in the second step, by locally heating each incision in the fibre to its melting point for a short time. The surface tension of the molten glass transforms the corrugation on the fibre surface into a sinusoidal deformation of the core. This second step is shown in Figure 4.2. The heating process causes sufficient perturbation of the core with just 14 grating periods to see coupling to the cladding mode. This is because the effective index changes that are produced by deforming the core ($\Delta n = 0.1$) are approximately an order of magnitude greater than the largest permanent index changes achieved in photo induced gratings [4]. The change in the LPG's response to external perturbations was measured and found to be comparable to photo-induced LPGs [28]. The LPGs produced by this method posses a large bandwidth, are highly efficient and reliable [3].

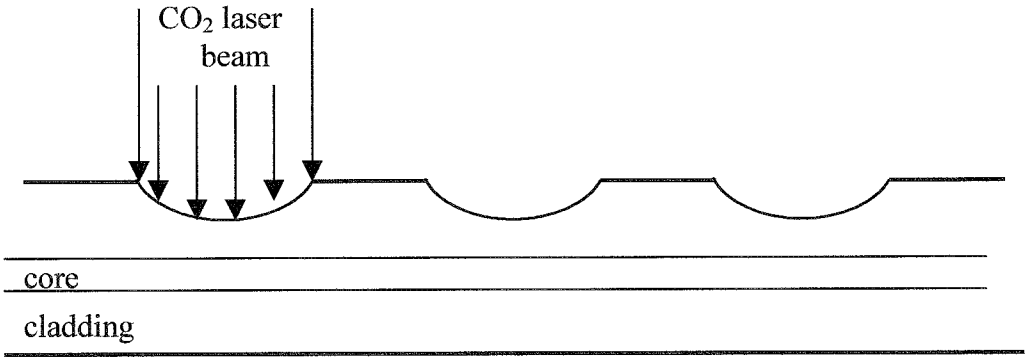

Figure 4.1: *Making periodic cuts in the surface of the cladding using a focused CO_2 laser beam.* Diagram reproduced from [3].

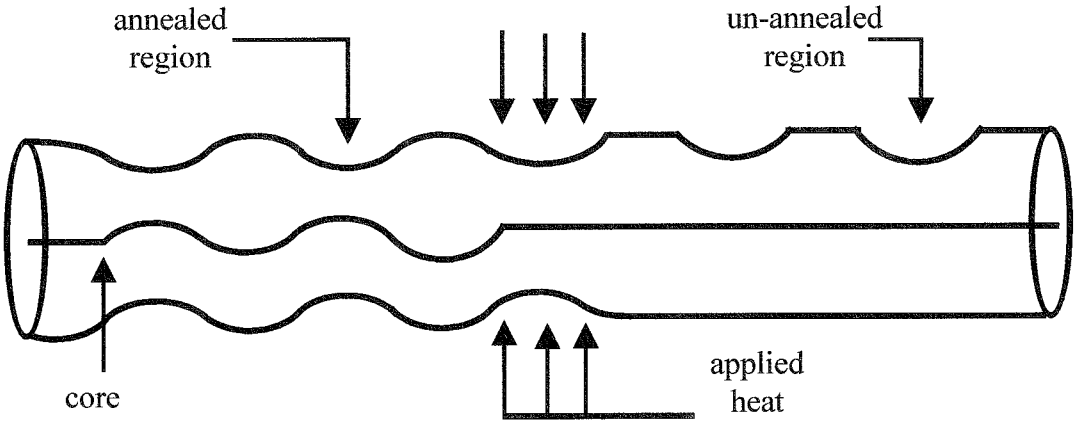

Figure 4.2: *Inducing the required change in the RI of the core by locally melting the fibre, using the arc of a fusion splicer. The surface tension of the molten glass transforms the corrugation on the fibre surface into a sinusoidal deformation of the core.* Diagram reproduced from [3].

The second method is based on inducing periodic micro-bends in the core by the use of electric arcs [5, 17]. The RI change induced by this method is due to the deformation of the fibre and by the release of the stress within the fibre. The region of the fibre in which the LPG is to be produced is devoid of its buffer jacket. The fibre is held straight between two fibre holders. A lateral stress is induced in the fibre, between the two holders, by displacing one of the fibre holders by $\approx$ 100μm in a direction orthogonal to the fibre's axis. A section of the fibre is heated by applying an electric arc; the fibre is slightly deformed because of the lateral stress thus creating a micro-bend. The length of the bend, which is typically less than 1μm, is controlled by the duration of the arc. Most of the originally applied lateral stress remains within the fibre so a series of micro-bends can be induced into the fibre without additional displacement of the fibre holders [5]. To fabricate the LPG the electrodes are moved along the fibre by a distance equal to the grating period, and the process is repeated. The resonance wavelengths of LPGs produced using this method are determined by the grating period and are not effected by the coupling strength. This is because the micro-bending method of changing the index of the core does not induce a change in the beat length of two coupled modes [5]. This simple method inscribes a permanent micro-bend structure into the optical fibre, which can be achieved in any type of fibre, including standard telecommunications single mode fibres. These LPGs have low insertion loss, high thermal stability, of up to 800°C without degradation of the LPG, where as with UV induced LPGs the LPGs erase at a few hundred degrees centigrade, 400°C. These also offers flexibility in control of filter parameters and profiles by using simple apodisation techniques [5]. The technique can provide practical, low cost all fibre filters and, or, mode converters for optical fibre communication and sensor systems [5].

4.3.4 Deforming the fibre cladding

The main mechanism accounting for the mode coupling in this type of LPG is the difference in the stress fields induced within the corrugated structure when an external stress is applied [6]. The LPG consists of two unit sections, one is the etched region, a section of fibre in which the cladding's diameter has been reduced, and the un-

etched region. The corrugated structure introduces a periodic change of index profiles along the length of the fibre. However, this corrugated structure has little contribution to the mode coupling when there is no external stress. When an external stress is applied along the fibre in an equilibrium condition, each of the two regions will experience different tensile stresses that are inversely proportional to the cross-section of the corresponding region [6]. Therefore, by the photoelastic effect, the differential strain results in a periodic index modulation. The strength of this index modulation can be controlled by the applied tensile stress [6].

4.4 Liquid crystal

The behaviour of a LPG is recreated in a hollow-core optical fibre that has the same structure as a commonly used single mode fibre except for the hollow core region. The structure of a hollow-core optical fibre is shown in Figure 4.3

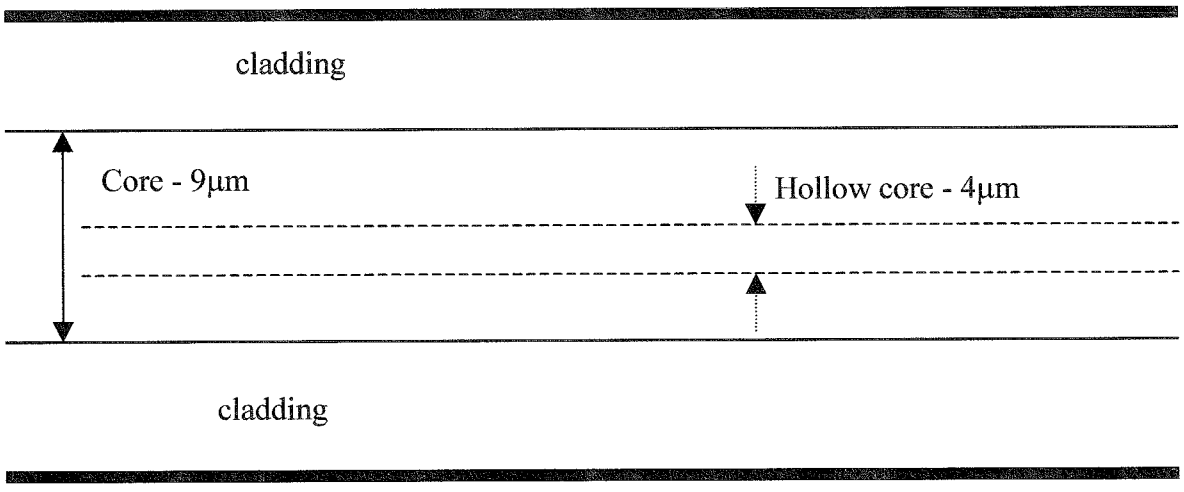

Figure: 4.3: *The structure of a hollow core optical fibre.*

The hollow core is filled with a nematic Liquid crystal, LC [7]. At rest the molecules of the LC tend to align in an axial direction [29], as shown in Figure 4.4(a). If a voltage is applied to the electrode, which is shown in Figure 4.4(b), the LC molecules align along the direction of the applied electric field. If a comb-structured electrode is used, a periodic electric field can generate a RI modulation inside the LC core because the effective index of the LC depends upon the direction of poling. Thus, the effective index for the guided optical radiation through the core changes with the direction change of the LC alignment and so the optical radiation through the region undergoes diffraction as in conventional LPGs [21]. The properties of the LC can be electrically controlled to manipulate a filter's characteristics [30].

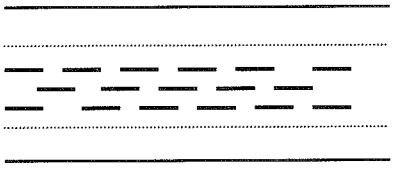

Figure 4.4a

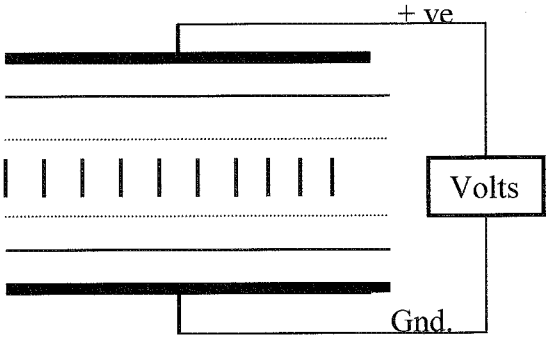

Figure 4.4b

Figures 4.4 a & b: *a) The nematic director aligning itself along the axis of the fibre.*
b) The nematic aligning itself along the direction of the applied electric field.

4.5 Modulation of the core's refractive index

4.5.1 Ion implantation

The RI modulation of the fibre's core is generated by high-energy ion implanting, using He^{2+} or H^{+} ions. For any change in the RI to occur, the ions must reach into the core of the fibre [8]. The change in the RI, of upto 1%, is developed by the compacting of the glass; the compaction is predominantly caused by the interaction of the introduced ions and the host material's atoms. It has been shown that the glass is compacted mainly at the end of the travelling range of the ions when they come to rest in the host material [31]. The end of range, or stopping distance, of the ions is determined by the mass of the ion, its launch speed and the physical properties of the material. The diameter of the cladding around the core is approx. 125μm and the He^{2+} ions cannot reach a sufficiently high launch speed that allows them to penetrate into the core. Therefore, the cladding's diameter is reduced to ≈ 53μm by etching with Hydrofluoric acid. This is not necessary for H^{+} ions as the ions can be launched at higher speeds. The pre-prepared fibre is mounted inside a microprobe target chamber [32] and the ion beam is focused onto the fibre. A schematic of the alignment of the mask and the fibre is shown in Figure 4.5.

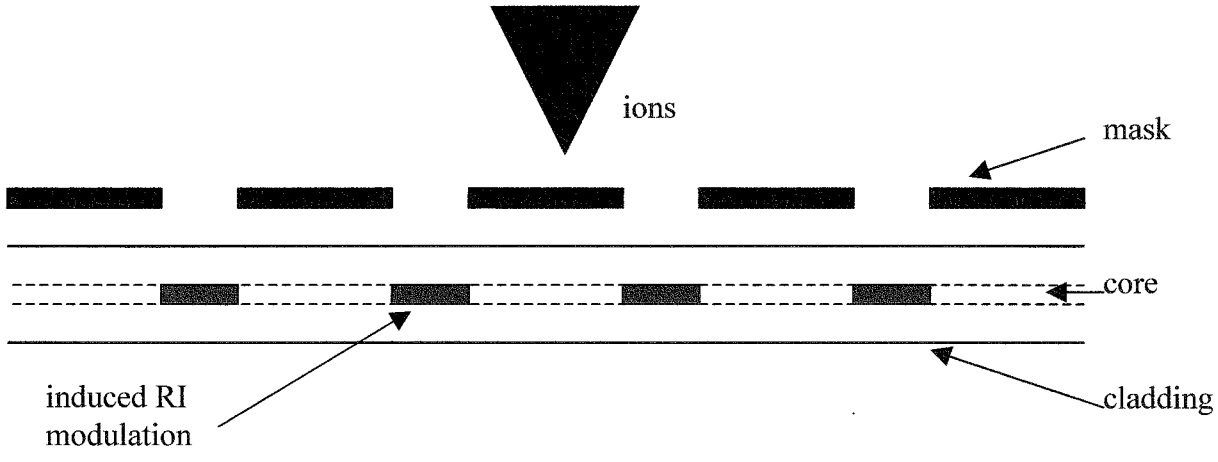

Figure: 4.5. *A schematic diagram of a LPG's fabrication, based on ion implantation through an amplitude mask.*

A tandem accelerator is used to increase the ion's acceleration energy to 5.1Mev, to enable the ions to be launched at a higher speed, so that they penetrate through the thinner cladding and into the fibre's core. The process uses an amplitude mask because the beam of ions cannot be sufficiently focused to irradiate individual areas of the core.

There are several advantages to using ion implantation rather than other techniques to produce LPGs. Firstly, the fabrication process is fundamentally independent of the precise nature of the fibre and so ion implantation makes it possible to fabricate optical fibre gratings in almost all kinds of silica-based optical fibre [33]. Secondly, at the ion doses that are required for the fabrication of the LPGs, the index change is approximately linear with ion dose. This linear change eliminates the necessity for complex irradiation schemes of the type required for UV irradiation of photosensitive fibres [34]. The implanting of ions into a fibre's core has been shown to produce significant changes in glasses [35, 36] which is stable to above 500°C and this presents significant advantages for temperature sensing applications [37].

4.5.2 Irradiation by Infrared femtosecond laser pulses.

The RI change in core of the fibre is induced by exposing it to the beam of an infrared femtosecond laser, at a wavelength of 800nm [9]. The process induces a modulation of the RI of the core by light that is not absorbed by the cladding or the buffer jacket. The induced RI change of ≈ 0.01, is brought about by a combination of factors, firstly, local densification in the glass, secondly, a non-linear reaction through a multiphoton process and thirdly, through conventional heating by the laser in the localised regions [9]. Since the densification of the glass might well result from thermal effects, the LPGs produced by this method, based on the point-by-point fabrication process, show a high thermal stability below 500°C. The thermal stability is achieved because the cause of the RI change is different from that of the UV induced RI change, this is discussed in detail in section 4.9.

4.5.3 Exposure to CO_2 laser pulses

A RI change, of 0.02%, is induced into the core of the fibre by directly exposing the fibre to 10.6μm wavelength CO_2 laser pulses [10]. The reported change in the RI is brought about by the relief of residual stress in the fibre and the densification of the glass and is not attributed to the removal of the fibre material. Since the fibre is directly exposed to the CO_2 laser pulses, the absorption of silica at 10.6μm results in the majority of the energy being converted to heat in the first 10-20μm of glass.

4.5.4 Thermal induction

It is possible to form LPGs in fibres that have been doped with chemical elements that have a high diffusion coefficient in silica glass [38]. In such fibres the periodical perturbations in the core/cladding interface can be easily created by local heating. This diffusion induced change of the RI of the core is approximately 3.6×10^{-4}. A LPG fabrication technique based on the thermal induced broadening of the RI profile in the fibre owing to the diffusion of Nitrogen to the cladding region has been proposed [13]. Nitrogen has a relatively small atomic weight and it diffuses rapidly into the silica cladding at elevated temperatures.

This process forms a LPG by locally heating the fibre with a shaped beam of a CO-laser [10, 11, 12] or by using a micro-arc discharge as a power source [17]. The thermo-activated diffusion of Nitrogen can only be effectively initiated at temperatures in access of 1400°C. Thermo-induced LPGs have higher temperature stability in comparison with conventional photo-induced LPGs and retain their spectral properties even at temperatures of upto 1200°C [13]. However at the same time thermo-induced LPGs have a few disadvantages. Firstly, during the fabrication process the physical deformation of the fibre causes spectrally independent losses. Secondly, the thermo-induced fabrication process depends heavily on the temperature of the heating source. To ensure that the grating produced is uniform the process requires high reproducibility of the heating time and temperature from point to point. It should also be noted that the

heat transfer along the fibre axis limits the minimum grating period to be approximately 200μm.

4.5.5 Periodic relaxation of residual stress

Releasing the tension that is introduced into the core of a fibre during its manufacturing process induces a RI change of approximately 0.1% [15, 16]. A high-silica core fibre consists of silica core and a Fluorine doped cladding. Fluorine is doped into the cladding to decrease the RI with respect to the core. The core glass has a higher softening temperature than that of the doped cladding. During the manufacturing of the fibre, when the fibre is drawn the glass of the core solidifies faster than that of the cladding. The drawing tension remains permanently in the core as a residual stress. This method relies upon periodically relaxing the residual stress [15, 16]. To produce a LPG using this process the buffer jacket in the selected region of the fibre is removed and the fibre is held securely between two clamps. The bare fibre is locally heated at a selected point along its axis using CO_2 laser illumination [15] or an electric arc [16]. The fibre is heated to the softening temperature of the cladding and the stress in the core is released, producing a increase in the local RI. The fibre is moved by a distance equal to the grating period, Λ, and the procedure is repeated until the required number of points have had their RI changed.

4.5.6 Electric discharge

An electric arc has been used to produce a perturbation of 1.8×10^{-3} in the RI of conventional dispersion shifted fibre having a core doped with germanium [39]. The perturbations responsible for the mode coupling brought about by using electric discharges could be induced by three mechanisms. The mechanisms exploited include the induction of microbends into the fibre [5], the periodic tapering of the fibre [2] the diffusion of dopants [13, 14] and the relaxation of internal stresses [17, 18]. The main mechanism for the formation of the LPGs is considered to be the rapid heating and cooling process that in turn results in changes in the glass density, viscosity, index of

refraction and Raleigh scattering [18, 40]. Electric discharges have been used to fabricate LPGs into standard untreated telecommunications fibres, Corning (SMF- 28) [41], however an investigation into the mechanisms that forms these LPGs has yet to be conducted [41].

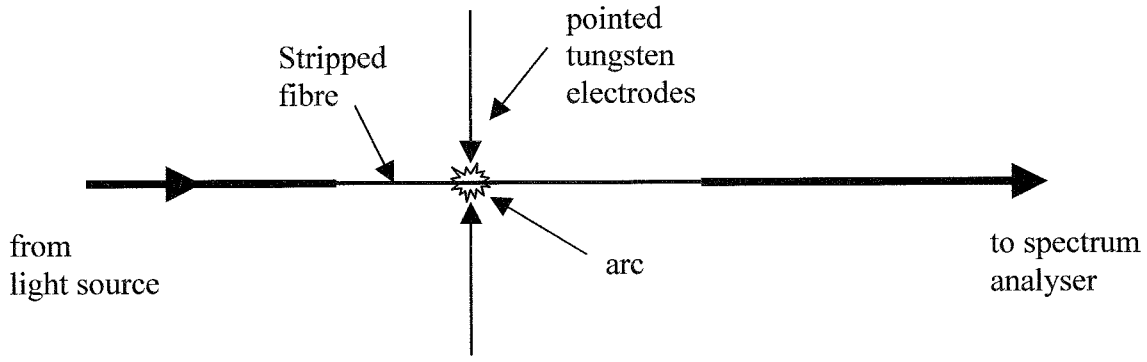

Figure 4.6: *A schematic diagram of the systematic fabrication of a LPG using an electric arc.*

Figure 4.6 illustrates the process used. The fibre is stripped of its buffer jacket and held longitudinally under tension, midway between two electrodes which are 2.54mm apart. The pointed tungsten electrodes, containing a minor amount of Thorium, are connected to a switched current source that produce an electric arc between them. The fibre is exposed to a high current arc, > 1.5mA, for a time, > 2sec. Using the point-by-point technique, the LPG was successfully fabricated in a length of fibre that was not doped with hydrogen. Fabricating the LPG in hydrogen loaded fibre and reducing the current and exposure times produced a LPG that was mechanically stronger. LPGs fabricated, using electric discharges, in S doped fibres or Ge-doped fibres have been shown to operate without any permanent degradation of their transmission spectrum at temperatures of upto 800°C [18]. LPGs fabricated in Ge-doped fibres have been shown to operate at temperatures of upto 1190°C for 30 mins [18]. However, the transmission spectrum suffered some irreversible degradation nevertheless, it does present an opportunity to monitor high temperatures with out the need for special fibres [18]. The irreversible change of the LPG's spectra at high temperatures is caused by the annealing of intrinsic stresses induced in the course of the fibre drawing and also by local heating

of the fibre during the writing process. Above ≈ 1000°C, this change can be due to viscous flow of the fibre and its plastic deformation [18].

Using standard telecommunication fibre, Corning (SMF- 28), it was found that the amplitude of the induced perturbations was so large that less than 20 steps, corresponding to a total length of 10-14mm, were required to obtain a 20dB isolation [41]. Comparing this with a photo-imprinted LPG in the same fibre that is loaded with Hydrogen, 100 steps are typically required which corresponds to a total grating length of 50mm. From a characterisation and simulation of LPGs fabricated using this method, it was found that the resonance wavelength of the gratings depended only on the period and was independent of the arc current [19]. The technique is a simpler and less expensive method of making LPG's because expensive lasers and their associated equipment are not required. These LPGs have low insertion loss, high thermal stability, they also offers flexibility in control of filter parameters and profiles by using simple apodisation techniques [19]. The technique can provide practical, low cost all fibre filters and, or, mode converters for optical fibre communication and sensor systems.

4.5.7 UV irradiation techniques

A popular method of producing LPGs is by the illumination of the core of a germanium-doped fibre with UV radiation through an amplitude mask, or directly exposing the fibre one point at a time [20, 21, 22, 23, 24, 25, 26]. The point-by-point configuration builds up the LPG one point at a time [42]. The amplitude mask configuration allows all or a large number of the elements of a LPG to be formed simultaneously [21]. The point by point configuration is time consuming but flexible when compared to the use of an amplitude mask, for it readily allows the fabrication of LPGs with a range of characteristics such as apodisation [43], chirp [43] and phase steps [43]. The amplitude mask configuration is popular when LPGs with reproducible properties are required and is more suited to mass production.

UV radiation at a wavelength close to the absorption peak of a germania related defects triggers a change in the RI of the core. Several processes are possibly occurring depending on the writing conditions. The most established explanation is that UV radiation causes bond breaking of point defects in the glass matrix [44, 45]. This increases the absorption in the UV spectrum which in-turn causes the RI in the core to increase [46]. The induced RI change can be increased by a factor of ten if UV radiation at a lower wavelength is used [47].

Another proposal is that the largest part of the UV induced index change is attributed to a structural change that is due to electron transfer from Ge related defects, which do not accompany a thermal process [48]. The photoexcitation of oxygen vacancy defects states forms paramagnetic GeE′ centres that contribute to index changes. Because the defects related to GeE′ centres relax even at temperatures below 100°C, the LPG's performance degrades thermally.

Until now in this discussion the wavelength of the UV source used to generate the periodic modulation of the optical properties of the fibre has been greater than 240 nm. A UV laser beam at a wavelength of 157nm has been used to fabricate LPGs by exposing the fibre to the UV through an amplitude mask [23, 24]. The choice of such a short wavelength was reasoned [49, 50, 51] after it was demonstrated that an improvement of 10 times in the RI change inside a low GeO_2 doped fibre could be achieved by shifting the laser's wavelength from 248nm to 193nm [47]. This was because the two photon absorption across the GeO_2 band gap was the photo sensitivity mechanism. This process, using the laser beam with a wavelength of 157nm, does not require the fibre to have undergone any photosensitivity enhancement, such as loading with hydrogen. This is because the use of such a low wavelength allows access to a new single photon process near the band edge of GeO_2 and fused silica. The LPGs produced in this way have attenuation bands that have a minimum transmission value of –17dB [23, 24].

The general requirements of the UV source for the writing of LPGs is less stringent than in the case of writing FBGs. For the writing of LPGs the requirements of the coherence length of the UV radiation are relaxed because the fabrication process does not require interferometric fringes. The mechanical stability requirements of the writing system are also relaxed because of the large period of the gratings. Although the UV based fabrication method is a well-established technology it has problems. It requires a complex and time consuming processes, including hydrogen loading for the enhancement of the photosensitivity of the fibre, UV writing and annealing. Another difficulty with UV induced LPGs is in the control of filter parameters. The resonance wavelength of the filter not only depends on the LPG's period but also on the amplitude of the index modulation [21, 22]. This dependence arises from the increase of the average core index by UV irradiation, which induces a change in the beat length of two coupled modes. So there is a need to carefully select a LPG's period, considering both the rejection wavelength and the efficiency of the LPG to be fabricated. This fact makes it more difficult to implement the apodisation technique for tailoring a filter profile. The non-uniform coupling strength induces position dependent variations of the local resonance wavelength, which results in the formation of an unintentional chirping effect [21, 22].

4.6 Practical implementation of UV irradiation for the fabrication of long period gratings

4.6.1 Fabrication using the amplitude mask technique

These methods use an amplitude transmission mask to allow the simultaneous generation of many periods of the modulation of the optical properties of the fibre. The amplitude mask technique simplifies the manufacturing process of the fibre gratings, because it allows easier alignment of the fibre for photoimprinting and reduces the stability requirements of the photoimprintng apparatus. The LPGs that are produced have high performance and the technique allows repeatable fabrication of gratings with controlled spectral response characteristics. With this method it is difficult to change the parameters of the LPG, but LPGs with similar parameters can be produced in a matter of minutes rather than in a few hours, as in the case of the point by point fabrication technique. This can be upto 2h depending on the LPG's length, photosensitivity, laser's power and number of points to be exposed.

Four types of amplitude mask are available for the production of gratings. These could be made out of chrome-plated silica [52], metal masks [53], dielectric masks [54] and microlens arrays [5]. The low damage threshold of chrome masks and dielectric masks necessitates a long writing time to compensate for the low power that needs to be used. Metal masks consist of slots which are precision laser machined out of thin copper sheets to spatially modulate the intensity of the writing beam or of the high energy beam used in ion implantation schemes. Metal masks are not so easily damaged as they have a high threshold level, > 1J/cm^2, and can withstand high intensity UV irradiation and so reduce the writing time considerably. However all amplitude masks block a significant part of the laser beam and so are not energy efficient and their use with high power lasers shortens their lifetime [53].

Focusing micro-optics constructed with UV grade fused silica is a more suitable material as it has a similar damage threshold to the fibres and furthermore it focuses the laser beam into a periodic pattern and thus requires much less energy from the laser. However, the extremely high cost of microlens arrays prohibits their use in LPG fabrication [53]. Microlens arrays constructed using low cost UV grade fused silica (UVGFS) fibres have been demonstrated [53]. Processes based on using dielectric masks and microlens array are discussed in the following sections.

A dielectric mask has been produced by selectively etching off the > 99% reflecting layers of a commercial KrF excimer laser mirror. A commercially available photo-resistant resin was baked onto the mirror, at 90°C for 30 mins. A focused argon laser beam was used to directly expose the pattern onto the resin. After developing the photoresist resin, the exposed areas of the laser mirror were etched using a solution of 5% HF acid in deionised water. The remaining resin was removed using solvents [53].

The LPGs were formed in hydrogen loaded fibre by exposing it to the output of a UV adapted Argon laser, of wavelength 248nm and intensity of 120mJ/cm^2 per pulse. Using this method a single pattern, 210mm LPG can be fabricated in less than a minute. Since the mask allows the rapid writing of LPGs with a high intensity laser output, attenuation in the fibre of up to 25dB can be observed.

The microlens array method relies on the use of commercially available UVGFS to construct a, simple and cheap, microlens array suitable for the mass production of LPGs. The array is constructed by cutting a length of low attenuation fibre that has a core diameter of 400μm and the cladding diameter is 440μm. The fibre's polyamide buffer jacket is removed using a butane flame; then the surface of the fibre is thoroughly cleaned with Acetone [5]. The fibre is cut into 20mm long pieces and then fixed, using a UV cured epoxy resin, onto an aluminium block, of dimensions, 50mm × 20mm × 10mm with a hole, 40mm × 10mm, cut into the centre of it. The aluminium block is placed between the fibre, to be exposed, and the UV beam of an Excimer laser. The hole in the block allows the beam to fall onto the mico-lens array and then onto the fibre. The periodicity of the LPG thus produced is determined by the cladding diameter, 440μm, of

the UVGFS fibre. Comparing two otherwise identical LPGs, one produced using the micro-lens array and the other a metal mask the LPGs, show significant differences. The attenuation of the micro-lens array LPG was −11.7dB after 50sec, under identical conditions for the other it was −10.9dB after 200sec [5]. This shows that the microlens array method is far more efficient. Since the array has a similar damage threshold as the fibre to be exposed less energy is used from the laser, however the array must be positioned near the fibre with micron precision.

4.6.2 Fabrication using the point-by-point technique

In the point by point technique for fabricating LPGs, the process moves onto the next exposure point by either moving the fibre while the source is fixed, or visa versa. It can take upto two hours to fabricate a LPG using this method. The system's flexibility allows the alteration of the parameters of the LPG, such as its grating length, grating pitch and duty cycle. It allows the forming of various grating shapes such as apodisation and chirp. The RI profile of the grating can be easily tailored to produce any desired spectral response because the UV pulse energy can be varied between points of induced index change [21].

4.7 In - house long period grating fabrication

The LPGs used in this thesis are fabricated by exposing the fibre to UV irradiation at a wavelength of 266nm through a copper amplitude mask. This section describes in detail the stages undertaken to produce the LPGs.

4.7.1 Fibre preparation

The fibre used was Boron-Germanium co-doped photosensitive fibre (Fibrecore PS 750) that had a cut-off wavelength of approximately 650nm. Before the fibre can be used to write a LPG the buffer jacket must be removed because it absorbs UV. The

buffer jacket is removed by placing the region on a microscope slide and then covering it with a, 5mm thick, layer of 'Nitromores', which is a Dichlomethene and methanol based paint stripper. After approximately a minute the buffer jacket can be seen to deform, the fibre is moved away from the glass slide, the buffer jacket and surplus paint stripper is removed using clean lens tissues doused in Isopropanol alcohol, IPA. Each end of the fibre is terminated using a FC301 connector.

4.7.2 The UV source

The UV irradiation source used in the laboratory was a Spectra Physics, Quanta-Ray, GCR 100 Series; injection seeded Neodymium doped Yttrium Aluminum Garnet (Nd:YAG), frequency-quadrupled, laser. The laser operates at a wavelength of 266nm, with a pulse width of 5nsec and a repetition rate of 10Hz. The laser system is allowed to warm up, for a period of one hour. The laser system needs to be run at the maximum flash lamp energy to ensure the optimum beam quality and to minimize the pulse to pulse energy fluctuations of the Nd:YAG crystal. Phase matching for the Nd:YAG, fourth harmonic generating crystal to achieve optimum conversion efficiency is accomplished by rotating the crystal. The optimum angle is temperature dependent, which requires that the angle of the crystal be adjusted periodically during warm up until thermal equilibrium is reached.

Figure 4.7 plots the power output of the laser as a function of time. The plot shows that after the warm up period when the angle of the fourth harmonic generating crystal is adjusted the UV output of the laser increases. The UV power stabilizes when the crystal is at its phase matching angle. The temperature of the crystal increases and the output power begins to diminish and so further adjustment of the crystal's angle is required to increase the UV output power. This process is repeated continually, at points A, B, C the output power has fallen to zero, and re-adjustment of the crystal's angle increases the output power. After 25 minutes, 15000 s, the power (1.1 Watts) is considered sufficiently stable to fabricate LPGs. The average stabilised UV output power was 1.1W and the beam's waist at the output of the laser was 10mm, the energy per pulse was 50mJ [55].

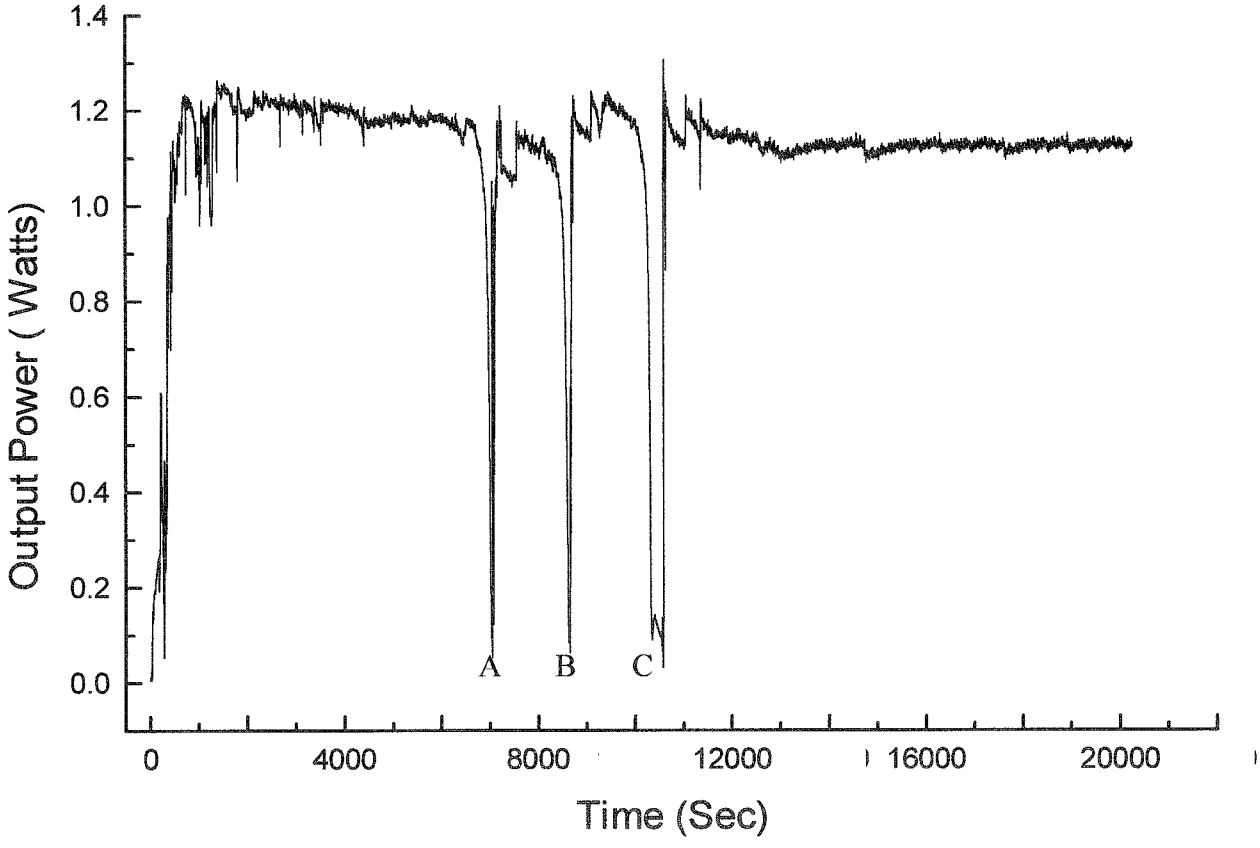

Figure 4.7: *Plot of the output of the laser as a function of time, during the stabilisation of the maximum output power prior to the fabrication of the LPGs.*

4.7.3 The interrogation system

The growth of the transmission spectrum was monitored online using the system shown in Figure 4.8.

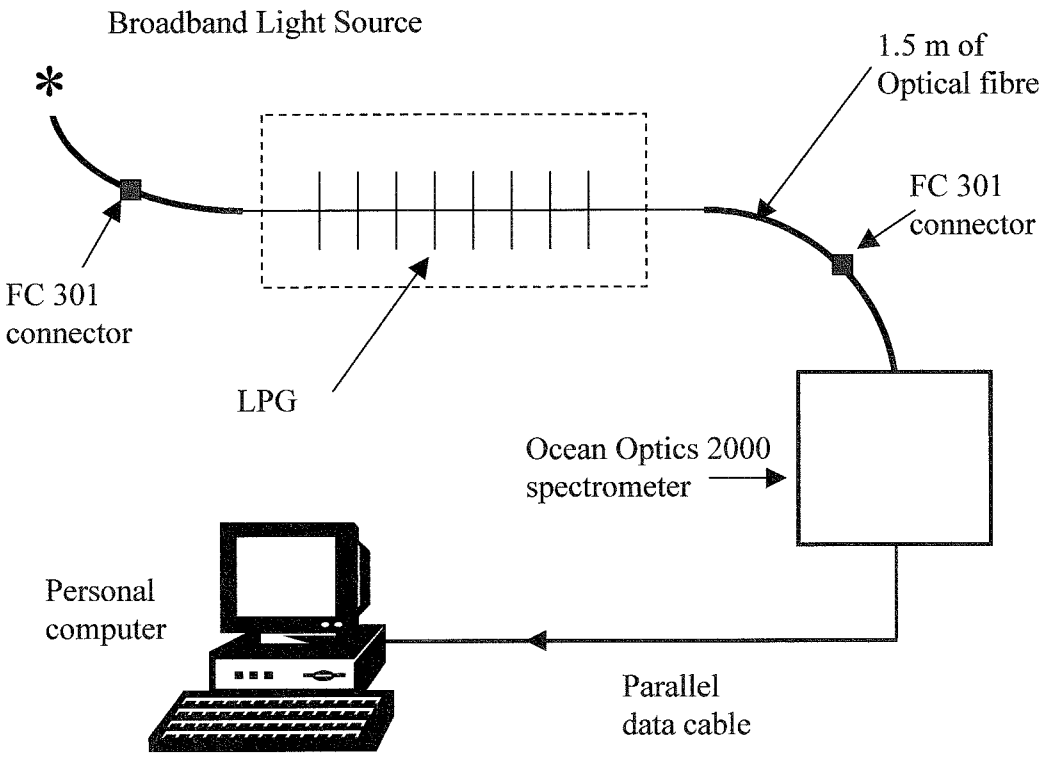

Figure 4.8: *General experimental configuration of the major components of the interrogation system used to monitor the transmission spectrum of the LPG.*

Figure 4.8 illustrates the general experimental configuration of the major components in the interrogation system. The broadband light source used was an Ocean Optics, fan cooled Tungsten Halogen light source, HL-2000. It has a spectral range of ≈220 – 1100nm within a power a stability of ± 0.05%. An Ocean Optics S2000 fibre coupled CCD spectrometer is coupled to the distal end of the fibre. The spectrometer is interfaced to the PC where a Labview program [56] allows the real time monitoring of the transmission profile. The spectrometer offers measurement of a spectrum extending from 500nm to 1100μm with a resolution of 0.7nm and a minimum integration time of 1ms.

The Labview program allows the transmission spectrum to be logged at a rate of up to 1Hz. The central wavelengths and the minimum transmission values of the attenuation bands were determined through a polynomial fit to the transmission spectrum of the band.

4.8 Fabrication System

The configuration of the UV based amplitude mask fabrication technique is shown in Figure 4.9. The process uses a copper amplitude mask [57]. The mask is 40mm long with a duty cycle of 50% and a periodicity of 400μm. It is fixed onto the blocks 5mm in front of the v-grooves.

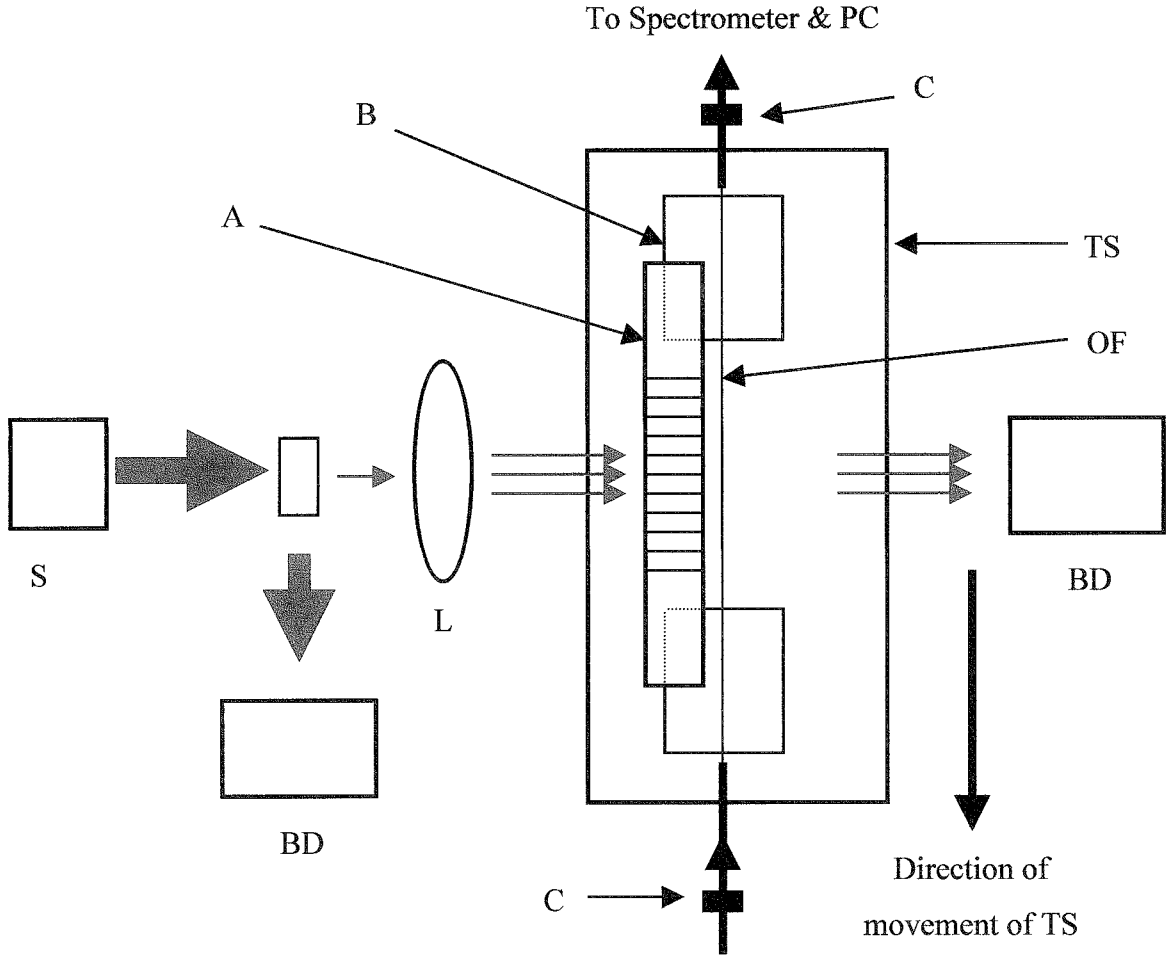

Figure 4.9: *General UV based fabrication set-up for inscribing a LPG into an optical fibre. A: Amplitude mask, S: UV laser, BS: 95 % / 5% beam splitter, L : cylindrical lens, B : V - grooved block, OF: Prepared photosensitive optical fibre, TS: Computer controlled stepping motor driven translation stage, BD: Beam dump, BBS: Broadband light source , C: Connector (FC 301)*

The output power of the previously stabilised UV laser is split using the 95% /5% beam splitter. The 95% portion of the laser beam is reflected into a beam dump whilst the remaining 5% is transmitted through and measured with an Ophir laser power meter, model N°. AN/2, and its associated UV detector head, model N°. 30(150) A-HE-SH, situated immediately after the beam splitter. Only the 5%, 50-60mW, of transmitted power is required for the process, as more than this will cause mechanical failure of the fibre. The cylindrical lens, of focal length 100mm, is positioned so that it focuses and orientates the UV into a beam, of length 10mm, behind the v-grooves. The lens had orientated the beam such that its axis was aligned with the motion axis of the translation stage. The beam was blocked, and the prepared fibre was orientated such that its axis was also aligned with the motion axis of the translation stage. The fibre was positioned so that the region to be exposed was directly behind the amplitude mask. Magnets were used to secure the untwisted fibre, straight and taut, in the v-grooved blocks. The v-grooved blocks were mounted onto a computer controlled stepping motor driven translation stage. The translation stage had a travel length of 50mm and a resolution of 2μm. The ends of the fibre were connected to the broadband light source as shown in Figure 4.8.

The fibre traverses in a direction parallel to the fibre's axis in front of the stationary UV beam. The computer program allows the input of the total number of steps of the translation stage, the distance moved during each step and the dwell time that defines the exposure time of the fibre to the UV beam. The translation stage is positioned at its starting point. Simultaneously the UV beam is unblocked and the computer program is executed; the developing LPG is viewed on the spectrometer & PC arrangement.

4.9 Annealing of fibre optic long period gratings

The thermal stability of LPGs is a key factor determining their performance in applications in telecommunications and sensing. The induced RI modulation contains an unstable portion, which is annealed at elevated temperatures. The removal of the unstable element of the RI modulation results in a change in the wavelength and

reflectivity of FBGs [20, 58, 59, 60]. The effect has also been reported for LPGs, where it causes a change in the central wavelength of the attenuation bands and the coupling efficiency [61, 62, 63]. Annealing the grating at a temperature in excess of the maximum expected operating temperature promotes long term stability in the device by fixing the spectral characteristics of the fibre grating [58, 60]. Annealed fibre gratings exhibit a linear wavelength response at high temperatures [60] that can be exploited for accurate wavelength tuning and the development of sensor elements.

The importance of thermal stabilisation techniques for successful use of FBGs is well acknowledged and has been thoroughly investigated [60, 64, 65, 66, 67, 68]. This has resulted in FBGs that do not require annealing [69]. The manufacturing process of these particular FBGs involves exposing the fibre to uniform near UV light before and after fabrication of the grating [69]. The exposure to near UV light is said to eliminate the unstable index modulation components in the fibre [69].

In general, the FBGs are not manufactured using the process detailed in [69] and so the thermal decay can be explained by a 'power law' [58] function of time with a small (<< 1) exponent. Consequently, the UV induced index change initially decays very rapidly, but the rate of decay decreases as time increases. The decay is also a strong function of temperature [58]. The decay mechanism is thought to be one in which carriers excited during fabrication are trapped in a broad distribution of trap states and the rate of thermal depopulation is a function of the trap depth. There is, however, some disagreement on two issues, the first concerns the stability of FBGs written in hydrogen loaded and non-hydrogen loaded fibres. The disagreement arises because FBGs written in hydrogen loaded fibres have been found to be less stable than [60, 49], and as stable [66] as those written in non-hydrogen loaded fibres. The second issue questions the applicability of the 'power law' as an explanation of the thermal decay in FBGs written in non-hydrogen loaded and hydrogen loaded fibres. The thermal decay of FBGs written in non-hydrogen loaded fibres can be accurately described by the 'power law' [58]. FBGs written in hydrogen loaded fibres however show a different thermal decay that does not follow the 'power law' model but can be characterised by a 'log time' model [58]. The known short-term behaviour of FBGs at elevated temperatures has been used

by accelerated ageing processes to predict the FBGs long-term behaviour at designated operating temperatures [47, 49, 70, 71, 72, 73, 74]. If a typical requirement of a FBG is that it should be able to operate for 25 years in a temperature range of -40 to 80°C [58]. The accelerated ageing process has predicted that a FBG that is aged to an equivalent time at 80°C of 2000 years, over the next 25 years the degradation of the UV induced index would be < 0.01% for a germanium-doped silica fibre [58], < 0.05% for a boron and germanium co-doped silica fibre [49] and < 0.3% for hydrogen loaded boron and germanium co-doped silica fibre [49].

The importance of thermal stabilisation techniques to the successful use of LPGs is even more important. This is because the wavelength at which the coupling from the core to the cladding modes takes place is directly dependent on the effective UV induced RI change, $\Delta n_{eff,}$ and on the difference in the RI of the core and the cladding, Δn. A decrease in these can cause a large shift in the central wavelengths of the attenuation bands in the transmission spectra of a LPG. For example, a 2% decrease in $\Delta n_{eff,}$ would have a negligible effect in a add/drop wavelength-division multiplexed (WDM) Bragg grating ($\Delta\lambda$ < 10 pm) where a similar decay in a LPG would shift the centre wavelength by ≈ 0.5nm. Such a shift is unacceptable for most applications, such as gain equalisation [75].

LPGs written in hydrogen loaded fibres with periods in the range of 300-600μm have been annealed at temperatures of 150, 180, 200 and 250°C, for 42, 24, 11 and 1.5hrs respectively. The attenuation bands displayed wavelength shifts, relative to their pre-annealing wavelengths, in the range – 60nm to + 12.3 nm. [62].

When two gratings where annealed for 2100h at 110°C, the change in the effective RI was observed to stabilise after 1000h, and, by 2100h, Δn_{eff} was found to vary by less than 10^{-7}. The stabilisation of Δn_{eff} for a FBGs at 110°C would occur after 20 - 40 hours. The stabilisation of LPGs takes longer when compared to FBGs because LPGs exhibit a higher sensitivity to index changes as small as 10^{-6}. When the LPGs are annealed at 250°C the stabilisation time decreases to 100h.

Using an adapted version of the ageing curve it was predicted previously that a 30mm long temperature in-sensitive LPG formed by UV irradiation in deuterium loaded fibre had a useful life of 25 years with wavelength shifts of < 0.02nm at 40°C and < 0.12nm at 60°C [76].

The annealing of LPGs also influences their temperature sensitivity. It has been shown that the pre-annealed sensitivity of the LPG was measured to be –0.28nm/°C and after annealing this was reduced to –0.16nm/°C [61].

4.10 Chapter summary

This chapter has discussed in detail each of the techniques used for inducing a periodic modulation of the optical properties of the fibre, with a comparison of their merits and disadvantages. A section was dedicated to UV irradiation as a means of inducing a periodic RI modulation of the fibre's core, which also discussed its practical implementation with respect to both fabrication configurations. The LPGs used through out this thesis were fabricated in-house and a detailed discussion of the UV based amplitude mask configuration was presented.

The importance of annealing the LPG prior to inclusion in a sensing system was discussed. To enhance this discussion the results of annealing experiments conducted on 8 LPGs, fabricated in commercially available boron germanium co-doped fibres, at different temperatures for various times are presented and discussed in section 5.3.4 of Chapter 5. Chapter 5 also presents and discusses the characterisation of a LPG to measurands such as temperature, strain, bending and changes in the bulk RI of its surrounding medium.

References:

1 S. Savin, M.J.F. Digonnet, G.S. Kino and H.J. Shaw, 'Tunable mechanically induced long period fibre gratings', Opt. Lett., **25**, pp. 710-712, (2000).

2 G. Kakarantzas, T.E. Dimmick, T.A. Birks, R. Le Roux and P. St. J. Russel, 'Miniature all fibre devices based on CO_2 microstructuring of tapered fibres', Opt. Lett., **26**, pp. 1137-1139, (2001).

3 C.D. Poole, H.M. Presby and J.P. Meester, 'Two mode fibre spatial-mode converter using periodic core deformation', Electron. Lett., **30**, pp. 1437-1438, (1994).

4 C. Narayanan, H.M. Presby, A.M. Vengsarkar, 'Band-rejection fibre filter using periodic core deformation',OFC 1996, San Jose, USA, pp. 267 – 268, (1996).

5 I.K. Hwang, S.H. Hwang, H.S. Yin- Kim, B.Y. Kim, 'Long period grating based on arc induced microbending', OECC 98, Tech. Dig. pp. 144 – 145, (1998).

6 C.Y. Lin, G.W. Chern and L.A. Wang, 'Periodical corrugated structure for forming sampled fibre Bragg gratings and long period grating with tunable coupling strength', J. Lightwave Technol., **19**, pp. 1212-1220, (2001).

7 J. Yoonchan, Y. Byungchoon, L. Byoungho, H.S. Seo, O.K. Sangsoo, 'Electrically controllable liquid crystal fibre gratings', Optical fibre Comm. Conf., **4**, pp. 19-21, March (2000).

8 M. Fujimaki , Y. Ohki, J.L. Brebner and S. Roorda, 'Fabrication of long period gratings by use of ion implantation', Opt. Lett., **25**, pp. 88-89, (2000).

9 Y. Kondo, K. Nouchi, T. Mitsuyi, M. Watanabe, P. Kazansky and K. Hirao, 'Fabrication of long period fibre gratings by focused irradiation of infrared femtosecond laser pulses', Opt. Lett., **24**, pp. 646-648, (1999).

10 D.D. Davis, T.K. Gaylord, E.N. Glytsis, S.G. Kosinski, S.C. Mettler and A.M. Vengsarkar, 'Long period fibre grating fabrication with focused CO_2 laser pulses', Electron. Lett., **34**, pp. 302-303, (1998).

11 L. Drozin, P.Y. Fonjallaz and L.K. Stensland, 'Long period fibre gratings written by CO_2 exposure of H_2 loaded standard fibres', Electron. Lett., **36**, pp. 742-743, (2000).

12 D.D. Davis, T.K. Gaylord, E.N. Glytsis, and S.C. Mettler, 'CO_2 laser induced long period gratings: spectral characteristics, cladding modes and polarisation independence', Electron. Lett., **34**, pp. 1416-1417, (1998).

13 E.M. Dianov, V.I. Karpov, M.V. grekov, K.M. Golant, S.A. Vasiliev, O.I. Medvekov, and R.R. Khrapko, 'Thermo-induced long period fibre grating', IOOC-ECOC 1997, **2**, pp. 53-56, (1997).

14 E. M. Dianov, V.I. Karpov, A.S. Kurkov and M.V. Grekov, 'Long period fibre gratings and mode-field converters fabricated by thermo-diffusion in phosphosilicate fibres', 24th European Conf. on Optical Comm. 1998, **1**, pp. 395-396, (1998).

15 M. Akiyama, K. Nishide, K. Shima, A. Wada and R. Yamauch, 'A novel long-period fibre grating using periodically released residual stress in pure-silica core fibre', OFC 1998 Tech. Dig., pp. 276-277, (1998).

16 T. Enmoto, M. Shigehara, S.I. Ishikawa, T. Danzuka and H. Kanamori, 'Long period fibre grating in pure-silica-core fibre written by residual stress relaxation', OFC. Tech. Dig., **6**, pp. 277 – 278, (1998).

17 S.G. Kosinski and A.M. Vengsarkar, 'Splice-based long period fibre gratings', OFC 98, paper THG3, Tech. Dig., pp. 278-279, (1998).

18 G. Rego, O. Okhotnikov, E. Dianov and V. Sulimov, 'High temperature stability of long period fibre gratings using and electric arc', J. Lightwave Technol., **19**, pp. 1574-1579, (2001).

19 P. Palai, M.N. Satanarayan, M. Das, K. Thyagarajan and B.P. Pal, 'Characterisation and Simulation of long period gratings fabricated using electric discharge', Opt. Comm., **193**, pp. 181-185, (2001).

20 A. Othonos, 'Fibre Bragg gratings', Rev. Sci. Instrum., **68**, pp. 4309-4341, (1997).

21 T. Erdogan, 'Fibre grating spectra', J. Lightwave Technol., **15**, pp. 1277-1294, (1997).

22 V. Bhatia and A.M. Vengsarkar, 'Optical fibre long period grating sensors', Opt. Lett., **21**, pp. 692 - 694, (1996).

23 K. Chen, P. Herman, J. Zhang and R. Tam, 'Fabrication of strong long period gratings in hydrogen free fibres with 157nm F_2 laser radiation', Opt. Lett., **26**, pp. 771-773, (2001).

24 K.P. Chen, P.R. Herman, R. Tam and J. Zhang, 'Rapid long period grating formation in hydrogen loaded fibre with 157nm F_2 laser radiation, Electron. Lett., **36**, pp. 2000-2001, (2000).

25 B. O. Guan, H.Y. Tam, S.L. Ho, S.Y. Liu and X.Y. Dong, 'Growth of long period gratings in H_2 loaded fibre after 193 nm UV inscription', IEEE - Photon. Technol. Lett., **12**, pp. 642-644, (2000).

26 J. Blows and D.Y. Tang, 'Gratings written with tripled output of Q-switched Nd:YAG laser', Electron. Lett., **36**, pp. 1837-1839, (2000).

27 T. A. Birks and Y.W. Li, 'The shape of fibre tapers', J. Lightwave Technol., **10**, pp. 432- 438, (1992).

28 C. Narayanan, H.M. Presby and A.M. Vengsarkar, 'Band-rejection fibre filter using periodic core deformation', Electron. Lett., **33**, pp. 280-281, (1997).

29 I.C. Khoo, 'Liquid Crystals', New York: John Wiley & Sons, 1994.

30 Y. Jeong, B. Yang, B. Lee, H.S. Seo, S. Choi and K. Oh 'Electrically controllable liquid crystal fibre gratings', Optical Fibre Comms. Conf., **4**, pp. 19-21, March (2001).

31 M. L. von Bibra, A. Roberts, P. Mulvaney and S.T. Huntingdon, 'Direct imaging of end of range compaction in Ion beam irradiated silica waveguides by atomic force microscopy' J. Appl. Phys. **87**, pp. 8429-8431, (2000).

32 T. R. Corle and G.S. Kino, 'Differential interference contrast imaging on real-time confocal scanning microscope and related imaging systems', Appl. Opt. **29**, pp. 3769-3774, (1990).

33 M. Verhaegen, L.B. Allard, J.L. Brebner, M. Essaid, S. Rooda and J. Albert, 'Photo refactive waveguides produced by ion implantation of fused silica', Nucl. Instrum. Methods Phys. Res. B, **106**, pp. 438-441, (1995).

34 V. Grubsky, A. Skorucak, D.S. Starodubov and J. Feinberg, 'Fabrication of long period fibre gratings with no harmonics', IEEE- Photon. Technol. Lett. **11**, pp. 87- 89, (1999).

35 P.D. Townsend, P.J. Chandler and L. Zhang, 'Optical effects of ion implantation', Canbridge University Press, Cambridge, pp. 233, (1994).

36 J. Albert, B. Malo, K.O. Hill, D.C. Johnson, J.L. Brebner and R. Leonelli, 'Refractive index changes in fused silica produced by heavy ion implantation followed by photobleaching', Opt. Lett., **17**, pp. 1652-1654, (1992).

37 E.P. Eernisse and C. B. Norris, 'Introduction rates and annealing of defects in ion-implanted SiO_2 layers on Si', J. Appl. Phys. **45**, pp. 5196-5205, (1974).

38 J.S. Harper, C.P. Bothman, S. Hornung, 'Tapers in single mode optical fibre by controlled core diffusion', Electron. Lett. **24**, pp. 245-246, (1998).

39 European patent application, N°: 97308597.0, Date of filing: 26th Oct 1997, by S.G. Kosinski and A.M. Vengsarkar.

40 S. Sakaguchi and D. Todoroki, 'Viscosity of silica core optical fibre', J. Non-Cryst. Solids, **244**, pp. 232-237, (1999).

41 N. Godbout, X. Daxhelet, A. Maurier and S. Lacroix, 'Long period fibre grating by electrical discharge', Optical Comm. 24th European Conference, **1**, pp. 397-398, (1998).

42 E.M. Dianov, D.S. Starodubov, S.A. Vasiliev, A.A. Frolov and O.I. Medvedkov, 'Refractive index gratings written by near UV radiation', Opt. Lett., **22**, pp. 221-223, (1997).

43 S.A. Vasiliev and O.I. Medvedkov, 'Long period refractive index fibre gratings: properties, applications and fabrication techniques', In Advances in Fibre Optics, Proc. of SPIE, **4083**, pp. 212–223, (2000).

44 M.G. Sceats, G.R. Atkins, S.B. Poole, 'Photolythic index changes in optical fibres', Ann. Rev. Mat. Sci., **23**, pp. 381-410, (1993).

45 A.V. Amossov and A.O. Rybaltovsky, 'Oxygen deficent centers in silica glasses. A review of their properties and structure', J. Non-Cryst. Sol., **179**, pp. 75-83, (1994).

46 P.S.J. Russell, L.J. Poyntz-Wright and D.P. Hand, 'Frequency doubling, absorption and grating formation in glass fibres: Effective defects or defective effects ?', in Proc., SPIE Fibre Laser Sources and amplifiers II, **1373**, pp. 126-139, (1990).

47 J. Albert, B. Malo, K.O. Hill, F. Bilodeau, D.C. Johnson and S. Thériault, 'Comparison of one photon and 2 photon effects in the photosensitivity of Germanium doped silica optical fibres exposed to intense ARF Excimer laser pulses', Appl. Phys. Lett. **67**, pp. 3529-3531, (1995).

48 E.M. Dianov, V.G. Plotnichenko, V.V. Koltashev, Y.N. Pyrkov, N.H. Ky, H.G. Limberger and R.P. Salathe, 'UV irradiation induced structural transformation of Germanosilicate glass fibre', Opt. Lett., **22**, pp. 1754-1756, (1997).

49 S.R. Baker, H.N. Rourke, V. Baker and D. Goodchild, 'Thermal decay of fibre Bragg gratings written in Boron and Germanium co-doped silica fibre', J. Lightwave Technol., **15**, pp. 1470-1477, (1997).

50 K.M. Davis, K. Miura, N. Sugimoto and K. Hirao, 'Writing waveguides in glass with a femtosecond laser', Opt. Lett., **21**, pp. 1729 - 1731, (1996).

51 K. Miura, J. Qui, H. Inouye, T. Mitsuyu and K. Hirao, 'Photowritten optical waveguides in various glasses with ultra short pulse laser', Appl. Phys. Lett., **71**, pp. 3329-3331, (1997).

52 A.M. Vengsarkar, P.J. Lemaire, J.B. Judkins, V. Bhatia, T. Erdogen and J.E. Sipe, 'Long period gratings as band rejection filters', IEEE - J. Lightwave Technol., **12,** pp. 58-65 (1996).

53 S.Y. Liv, H.T. Tam and M.S. Demokan, 'Long period gratings fabrication using microlens array', Electron. Lett., **35**, pp. 79-80, (1999).

54 H.J. Patrick, C.G. Askins, R.W. McElhona and E.J. Friebele, 'Amplitude mask patterened on a Excimer laser mirror for high intensity writing of long period gratings', Electron. Lett., **33**, pp. 1167-1168, (1997).

55 Handbook for Spectra-Physics GCR-100 Pulsed Nd: YAG laser.

56 Program produced by Dr. S.W. James and S. Khaliq, Cranfield University, Bedfordshire, U.K.

57 Manufactured by Dr. David Coutts, Department of Atomic & Laser Physics, Clarendon Laboratory, Oxford University, Park Road, Oxford.

58 T. Erdogan, V. Mizrahi, P.J. Lemaire and D. Monroe, 'Decay of ultraviolet induced fibre Bragg gratings', J. Appl. Phys. **76**, pp. 73-80, (1994).

59 A.M. Vengsarkar, P.J. Lemaire, J.B. Judkins, V. Bhatia, T. Erdogan and J.E. Sipe, 'Long period fibre gratings as band rejection filters', IEEE - J. Lightwave Technol., **15**, pp. 1478 - 1483, (1997).

60 H. Patrick, S.L. Gilbert, A. Lidgard, M.D. Gallagher, 'Annealing of Bragg gratings in hydrogen loaded optical fibre', J. Appl. Phys. **78**, pp. 2940 – 2945, (1995).

61 CC. Ye, S.W. James and R.P. Tatam, 'The effects of thermal annealing on the temperature sensitivity of long period gratings', Internal report, Cranfield University (1999).

62 Qin-Li, Wei-Zhan-Xiong, Wang-Quing-Ya, Li-Hui-Ping, Zhang-Yu-Shu, Goa-Ding-San, 'Abnormal shift of center wavelength in annealing long period gratings', Chinese Phys. Lett., **17**, pp. 28-30, (2000).

63 F. Bakhti, J. Larrey, P. Sansonetti, 'Annealing of long period gratings in standard hydrogen loaded fibre', Bragg Gratings, Photosensitivity, and Poling in Glass Fibres and Waveguides: Applications and Fundamentals. Tech. Dig. Williamsburg, VA. USA, pp. 350, Oct. 1997.

64 B. Poumellec, P. Niay, P. Bernage, M. Douay, J.F. Bayon and V.B. Soulimov, 'Densification mechanisms for type 1 gratings', in Proc. Cost 246 European Workshop on Bragg Gratings Reliability, Berene, Switzerland, pp. 177-200, (1995).

65 D.L. Williams and R.P. Smith, 'Accelerated life-time tests on UV written intra-core gratings in boron germania co-doped silica fibre', Electron. Lett., **31**, pp. 2120-2121, (1995).

66 R.J. Egan, H.G. Inglis, P. Hill, P.A. Krug and F. Ouellette, 'Effects of hydrogen loading and grating strength on the thermal stability of fibre Bragg gratings', in Proc. OFC, paper Tu03, pp. 83-84, (1996).

67 S. Kannan and P.J. Lemaire, 'Thermal reliability of Bragg gratings written in hydrogen sensitised fibres', in Proc. OFC. Paper Tu04, pp. 84-85, (1996).

68 I.Riant, S. Borne and P. Sansonetti, 'Dependence of fibre Bragg gratings thermal stability on grating fabrication process', in Proc. OFC. Paper Tu04, pp. 86-87, (1996).

69 E. Salik, D.S. Starodubov, V. Grubsky and J. Feinberg, ' Thermally stable gratings in optical fibres without temperature annealing', Intl. Conf. on Integrated Optics and Optical Fibre Comm. OFC/IOOC, Tech. Digest, **3**, paper ThD3-1, pp. 56-58, (1999).

70 T. Taunay, P. Niay, P. Bernage, M. Douay, W.X. Xie, D. Pureur, P. Cordier, J.F. Bayon, H. Poignant, E. Delevaque and B. Poumelec. 'Bragg grating inscriptions within strained monomode high NA Germania doped fibers 1. Experimentation', J. Phys. D, Appl. Phys., **30**, pp. 40-52, (1997).

71 G. Meltz, W.W. Morey, 'Bragg grating formation and germanosilicate fibre photosensitivity', Proc. SPIE **1516**, pp. 185-199 (1991).

72 H. Patrick, S.L. Gilbert, A. Lidgard and M.D. Gallagher, 'Annealing of Bragg gratings in Hydrogen loaded optical fibre', J. Appl. Phys.,**78**, pp. 2940-2945, (1995).

73 S. Kannan, J.Z.Y. Gou and P.J. Lemaire, 'Thermal stability analysis of UV induced fibre Bragg gratings', J. Lightwave Technol., **15**, pp. 1478-1483, (1997).

74 L. Dong and W.F. Liu, 'Thermal decay of fibre Bragg gratings of positive and negative index changes formed at 193nm in a Boron co-doped Germanosilicate fibre', Appl. Opt., **36**, pp. 8222 – 8224, (1997).

75 R. Kashyap, R. Wyatt and R. J. Campbell, 'Wideband gain flattened eribum fiber amplifier using a photosensitive fibre blazes grating', Electron. Lett., **29**, pp. 154-156, (1996).

76 S. Kannan, L. Copeland, J. Judkins, M. LuValle, P. Lemaire, 'Reliability of long period gratings', OFC. Tech. Dig., pp. 282-283, (1998).

Chapter 5 Characterisation of fibre optic long period gratings

5.1 Introduction

The transmission spectrum of a LPG consists of a series of attenuation bands, each situated at a different central wavelength. The exact form of the transmission spectrum and the central wavelengths of the attenuation bands are sensitive to the local environment experienced by the LPG and changes in response to temperature, strain, bending and change in the RI of the medium surrounding the LPG. The sensitivity to a particular measurand is dependent upon the order of the cladding mode to which the guided optical power is coupled to, and so is different for each attenuation band. This range of responses by a sensor element has enabled the LPG to pave the way for multi-parameter sensing using a single sensor element.

Before a LPG can be incorporated into a sensing scheme, it must be characterised to determine its sensitivity to the measurands that will influence it. This chapter will investigate the sensitivity of LPGs to each of the measurands, namely temperature, strain, bending and the change in the RI of the medium surrounding the LPG. The chapter will detail the characterisation experiments carried out on the LPGs to the measurands and discuss the results obtained.

5.2 Characterisation of temperature sensitivity

5.2.1 Introduction

The effect of temperature on the LPG spectrum reveals itself mainly in a change of the central wavelengths of the attenuation bands. The temperature sensitivity of the attenuation bands of LPGs depends on the order of the coupling-cladding mode and is usually in the range 0.03 to -0.1nm/°C for standard telecommunications fibre [1]. This section investigates the temperature sensitivity of a LPG written in boron co-doped fibres.

Annealing LPGs at a temperature in excess of their maximum operating temperature removes the unstable portion of the UV induced RI modulation [2], as discussed in section 4.9 of Chapter 4. For LPGs written in boron co-doped fibres it has been shown that, in addition to stabilising the spectral characteristics of the LPG, annealing results in a reduction of the temperature sensitivity [3]. This section investigates the effect of annealing on the temperature sensitivity of the LPG. Once the LPG had been annealed, the stability of the post annealing temperature sensitivity of the LPG is assessed by comparing the results obtained from two temperature sensitivity investigations that were conducted a week apart from each other.

5.2.2 Experiment

The LPG used in the temperature sensitivity investigations had been fabricated in boron-germanium co-doped photosensitive silica single mode optical fibre (Fibrecore PS750), which had a cut off wavelength of 650nm. The RI of the fibre had been modulated by exposure to UV irradiation, at a wavelength of 266nm, through an amplitude mask, as detailed in section 4.8 of Chapter 4. The LPG had a length of 40mm and a periodicity of 400μm.

The section of the fibre containing the long period grating was positioned in the middle of a cylindrical tube furnace, details are presented in section 5.2.2.1. The response of the transmission spectrum was observed, on a PC via a CCD coupled spectrometer, over a temperature range from room temperature to 200°C. A constant strain was applied to the LPG; the central wavelengths of the attenuation bands 2-5 and the temperature around the LPG were recorded using the general experimental configuration shown in Figure 4.8 of Chapter 4.

5.2.2.1 Tube furnace

The cylindrical tube furnace, supplied by Carbolite Furnaces Ltd., was 180mm long with an internal diameter of 15mm. The furnace had a temperature range of 900°C with an accuracy of ±1°C, and had been specially modified for operation at temperatures below 200°C. The furnace used a PID circuit to maintain the desired temperature with a stability of ± 1°C. The furnace had a uniform temperature zone of length 40mm in the middle of its ceramic inner tube. A photograph of the tube furnace is shown in figure 5.1.

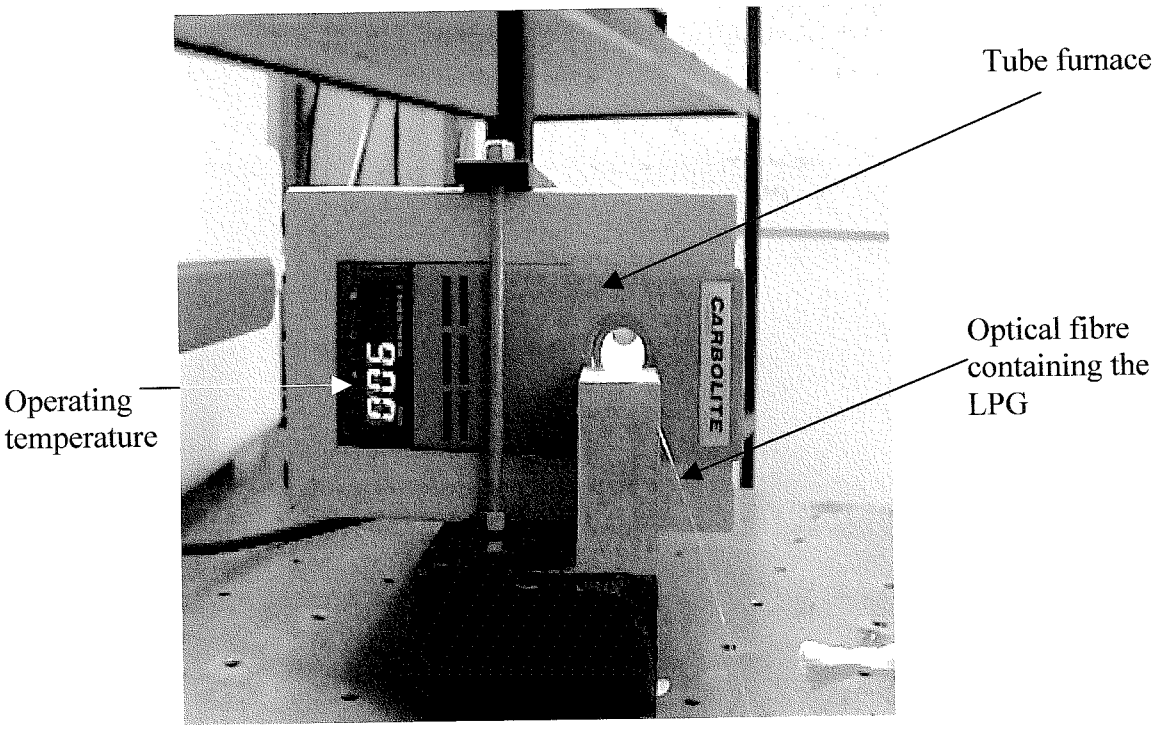

Figure 5.1: *This photograph shows the tube furnace running at its maximum temperature of 900°C.*

The temperature profile along the tube is displayed graphically in Figures 5.2 and 5.3.

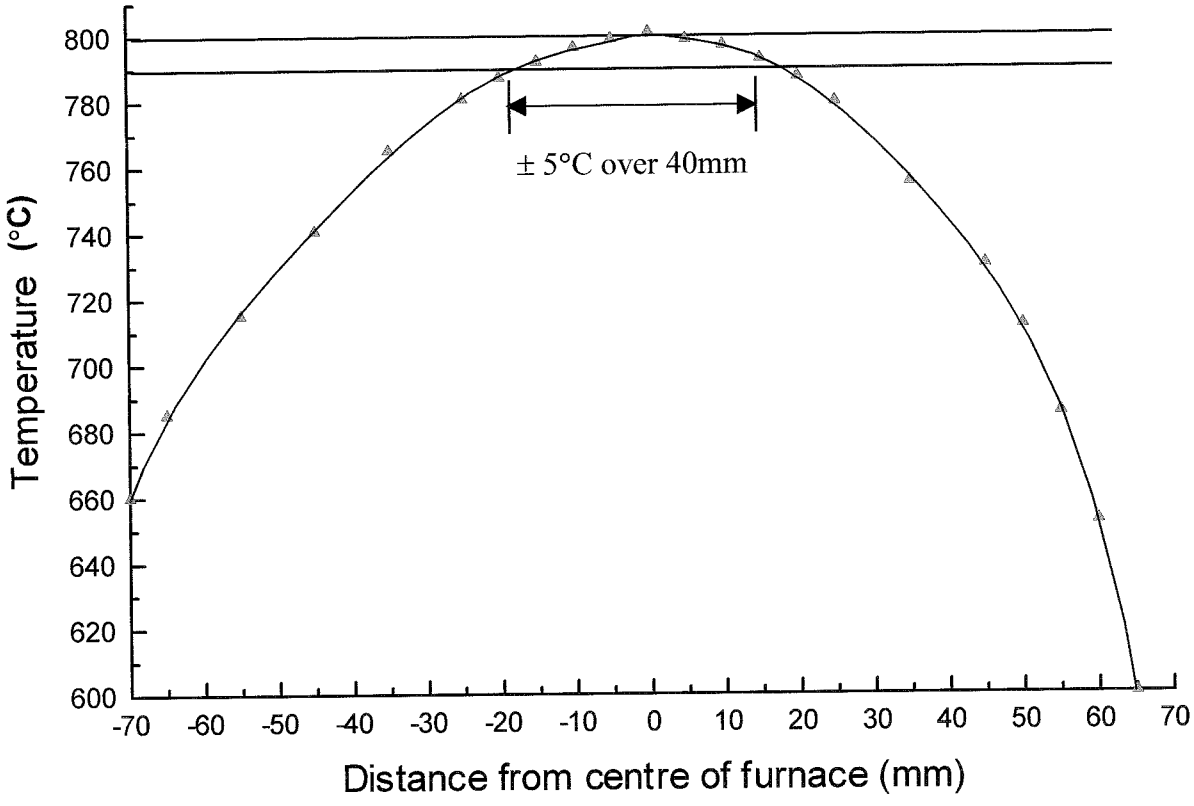

Figure 5.2: *Measurement of the temperature distribution along the axis of the tube furnace. At a set temperature of 800°C the temperature along the central 40mm of the tube varies by ±5°C.* The graph was supplied by Carbolite Ltd [4]

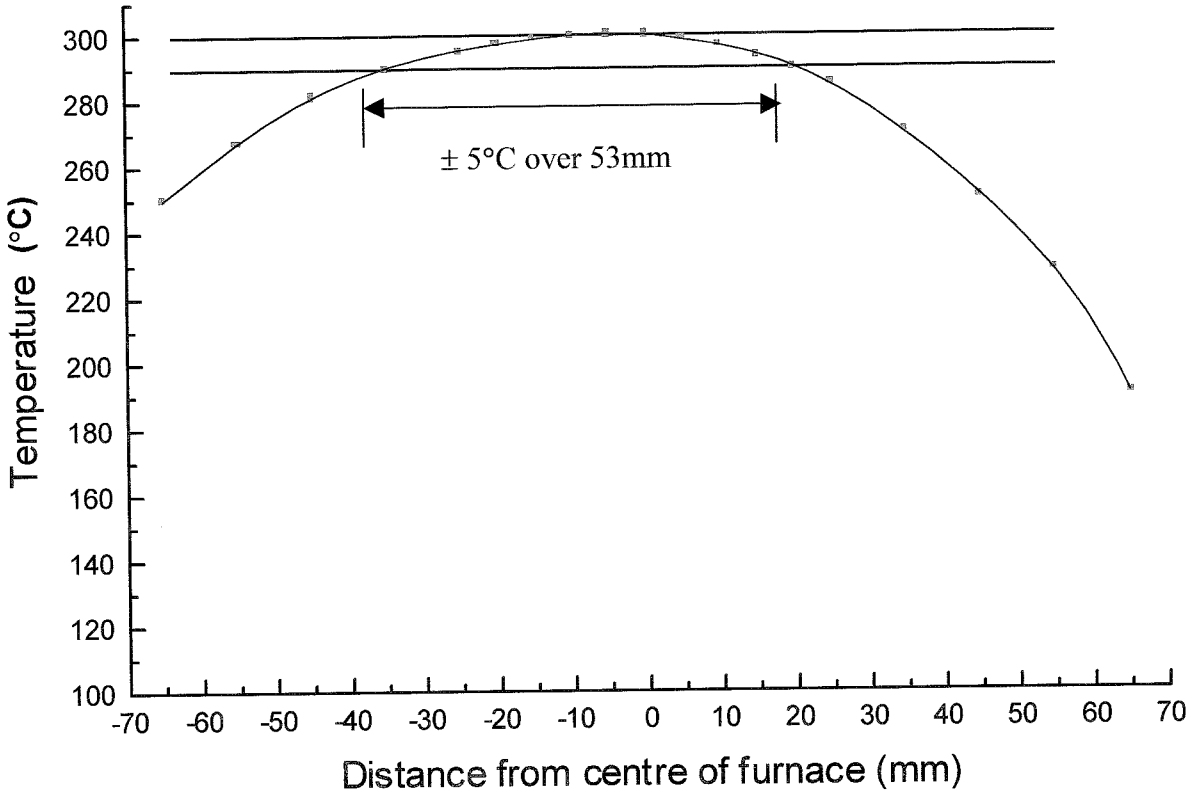

Figure 5.3: *Measurement of the temperature distribution along the axis of the tube furnace. At 300°C, the temperature along the central 53mm of the tube varies by ±5°C.* The graph was supplied by Carbolite Ltd [4].

5.2.2.2 Temperature sensing equipment

The furnace's own temperature sensor is positioned near the edge of the ceramic inner tube, and it was felt that this could not provide a sufficiently accurate measurement of the temperature of the region immediately around the LPG. To determine the temperature in the immediate vicinity of the LPG, a K-type thermocouple, that had been previously calibrated and found to have a temperature coefficient of – 0.044, was utilised. The thermocouple was positioned so that it was in close proximity, 2-3mm, to the LPG and was monitored using a 10 channel, Keithley 740, scanning thermometer. An IEEE 488 GPIB card was used to address the scanning thermometer and this allowed the temperature data to be read and saved by the Labview program.

5.2.2.3 Experimental configuration

The configuration of the annealing equipment is illustrated in Figure 5.4.

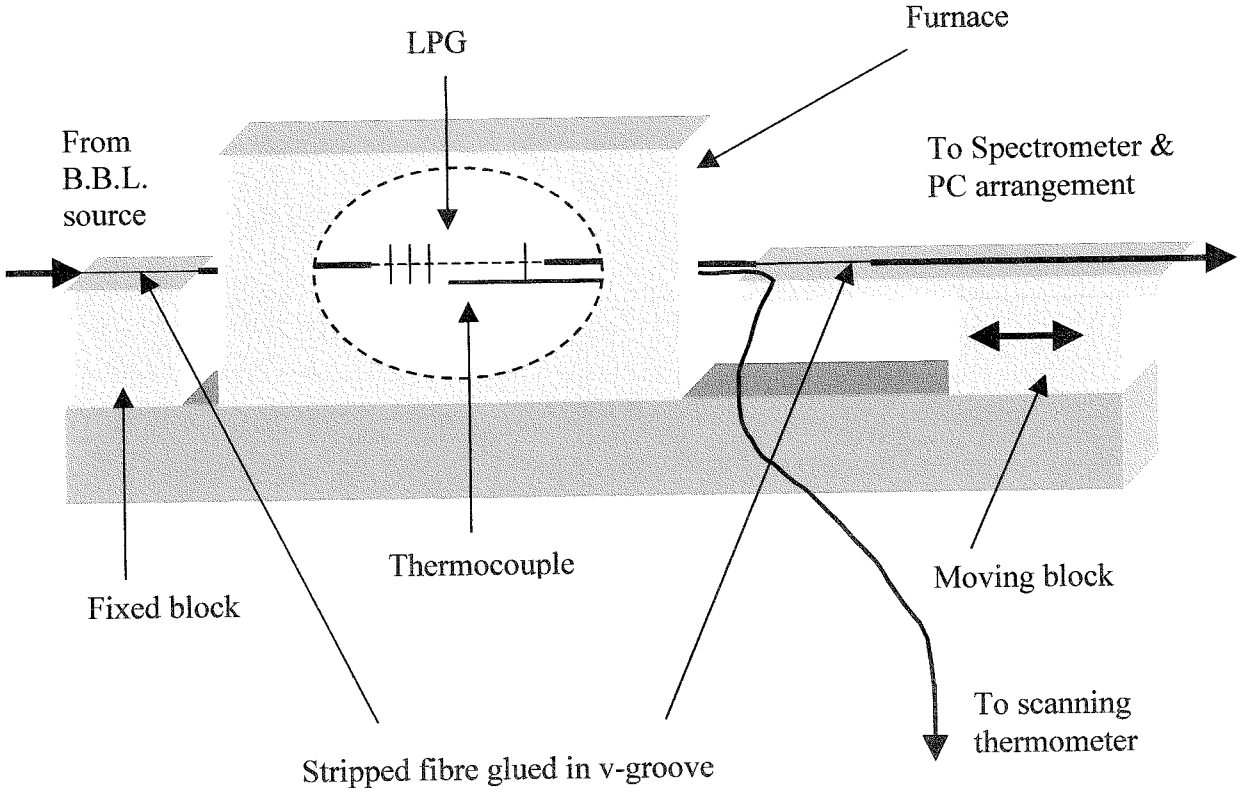

Figure 5.4: *The experimental configuration used to characterise the response of the LPG to the increase in the temperature around it.*

At room temperature, the LPG was positioned within the ceramic inner tube's uniform temperature zone. To reduce the temperature variations along the length of the ceramic inner tube the ends of the tube were fitted with insulating plugs. Two 30mm lengths of the buffer jacket surrounding the fibre were removed to bond them into the v-grooves of the fixed block and the moving block. The fibre was bonded into the grooves using a Cyanocrylate super glue so that the fibre did not move during the annealing procedure. Before the section of stripped fibre is bonded to the moving block, it is important to untwist and pre-tension the LPG. This ensures that the LPG is straight and taut, as a bend in the LPG would introduce a splitting of the attenuation bands, discussed in

section 3.7 of Chapter 3. The ends of the fibre were connected to the broadband light source and the spectrometer so that the transmission profile of the LPG could be observed on the PC as discussed in section 4.7.3 of Chapter 4. To ensure that the fibre had bonded, after 10 mins, a strain of 2000με was applied to the LPG and the central wavelengths of the attenuation bands were seen to decrease, upon release of the strain the LPG's attenuation bands returned to their pre-strain wavelengths. The central wavelengths and the minimum transmission values of the attenuation bands were recorded as a function of temperature.

5.2.3 Pre-annealing temperature sensitivity

The central wavelengths of attenuation bands 2-5 were recorded at 25°C. The furnace was then set to 200°C and the central wavelengths of attenuation bands 2-5 were monitored at a rate of 1Hz as the temperature increased. Initially the temperature of the furnace increased at a rate of 3.5°C/ s reaching a temperature of 160°C in 45s, the rate of change then decreased and the furnace stabilised at 200°C after a further 7 minutes. Whilst the temperature of the furnace was increasing to 200°C, the central wavelengths of all the attenuation bands, 2-6, were observed to decrease. To illustrate the observation the movement in the central wavelength of an attenuation band is shown in Figure 5.5. Figure 5.5 shows the location of attenuation band 6's central wavelength at temperatures of 30°C, 40°C, 80°C, 120°C and 180°C.

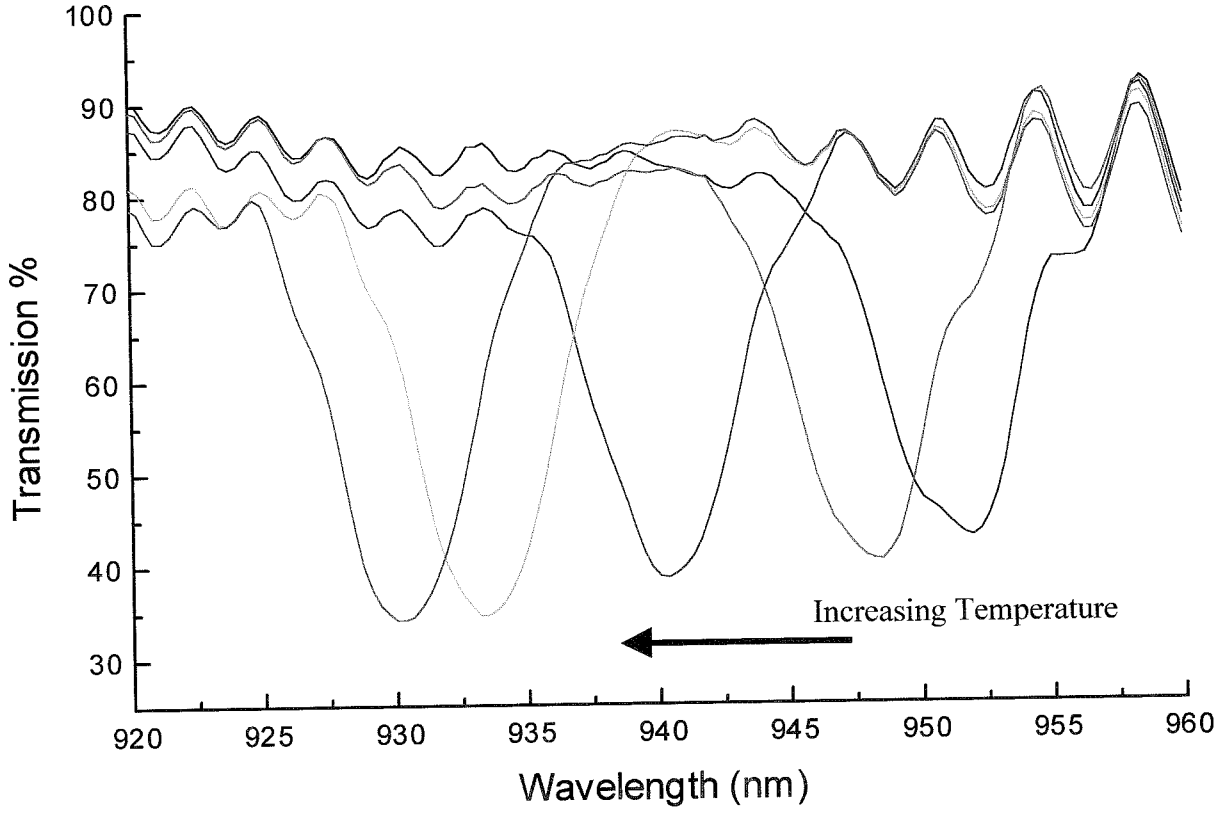

Figure 5.5: *Plot of transmission against wavelength of attenuation band 6 showing the change of the central wavelength to shorter wavelengths as the temperature increased.* — 30°C, — 40°C, — 80°C, — 120°C and — 180°C

The wavelength shift of each attenuation band, due to increasing temperature around the LPG, was determined with respect to the position of the attenuation band in air at a temperature of 25.0°C. Figure 5.6 plots the wavelength shift of attenuation band 6 as a function of increasing temperature.

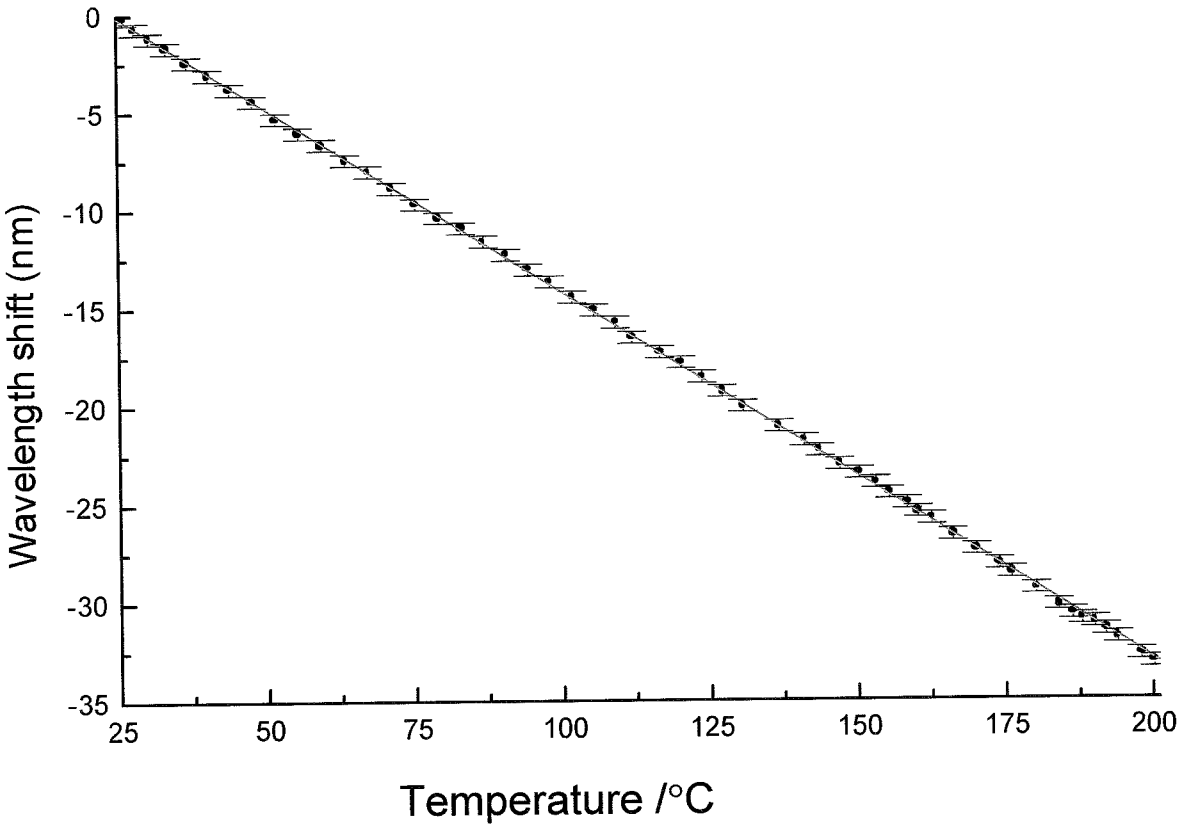

Figure 5.6: *Plot of wavelength shift as a function of increasing temperature for attenuation band 6 before the LPG was annealed.*

Attenuation band 6 shows a linear response over a temperature range of 25°C to 200°C. The temperature sensitivity of attenuation band 6 was determined using a linear regression. Attenuation band 6 showed a temperature sensitivity of 0.19nm /°C ± 2.8×10^{-4} nm /°C, the other attenuation bands also exhibited linear responses over the same temperature range with each band having a different sensitivity. The results of the characterisation to temperature are summarised in Table 5.1.

Table 5.1: *The pre-annealed temperature sensitivities of the LPG's attenuation bands 3-6.*

attenuation band 3	attenuation band 4	attenuation band 5	attenuation band 6
$0.12\pm2.9\times10^{-4}$nm/°C	$0.14\pm2.8\times10^{-4}$nm/°C	$0.15\pm3.6\times10^{-4}$ nm/°C	$0.19\pm2.8\times10^{-4}$ nm/°C

5.2.3.1 Discussion

Attenuation bands 3-6 have shown a linear response to temperature over a range of 25°C - 200°C. The attenuation bands have shown a pre-annealing temperature sensitivity in the range 0.12nm/°C to 0.19nm/°C. Previous reports of the temperature sensitivity of high order attenuation bands, for LPG's written in Hydrogen-loaded germanosilicate fibres, lie in the range of 0.046nm/°C to 0.154nm/°C, [5, 6, 7]. The demonstrated attenuation bands 3-6 have shown a temperature sensitivity that is higher than those reported in [5, 6, 7]. The greater sensitivity could arise from the variations in the guided and cladding mode's effective indices, the grating's periodicity, the operating wavelength and the fibre's composition. The next section presents the investigation of the effects of annealing on the temperature sensitivity of the attenuation bands and on the stability of the post-annealed temperature sensitivity of the attenuation bands.

5.2.4 Investigating the effect of annealing on LPGs

The effect of annealing the LPGs at temperatures of 100°C, 200°C and 500°C for times ranging from 0.5h up to 5.5h was investigated. The details of the times and temperatures are given in Table 5.2.

Table 5.2. *The annealing temperatures and durations for the 8 LPGs, A – H.*

	100°C	200°C	500°C
LPG	A for 5.5h B for 4.0h C for 2.5h	D for 5.0h E for 4.0h F for 3.0h	G for 0.25h H for 0.50h

Figure 5.7 shows a typical transmission profile of the LPGs, A-H. The six most prominent attenuation bands were labelled 1- 6.

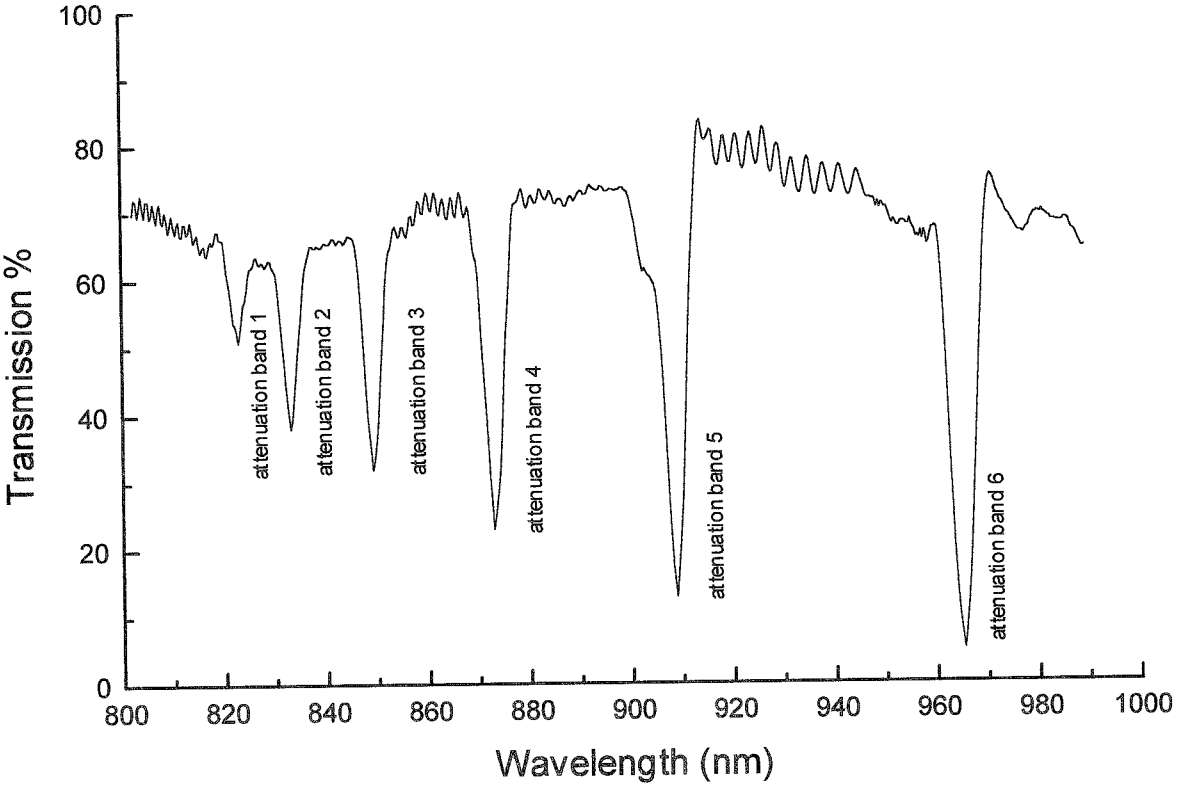

Figure 5.7: *Typical transmission profile of LPG A, demonstrating 6 attenuation bands. The LPG, of length 40mm and period of 400μm, was fabricated in photosensitive fibre, with a cut off wavelength of 650nm, using UV irradiation at 266nm through an amplitude mask.*

The furnace was set to the required annealing temperature and the following data was collected and saved by the Labview program at a rate of 1 Hz:

- the temperature at the LPG
- the central wavelength and the minimum transmission values of the attenuation bands
- the time
- and the transmission spectrum.

Figure 5.8 illustrates a typical plot of the wavelength response as a function of time of the attenuation bands through the whole process.

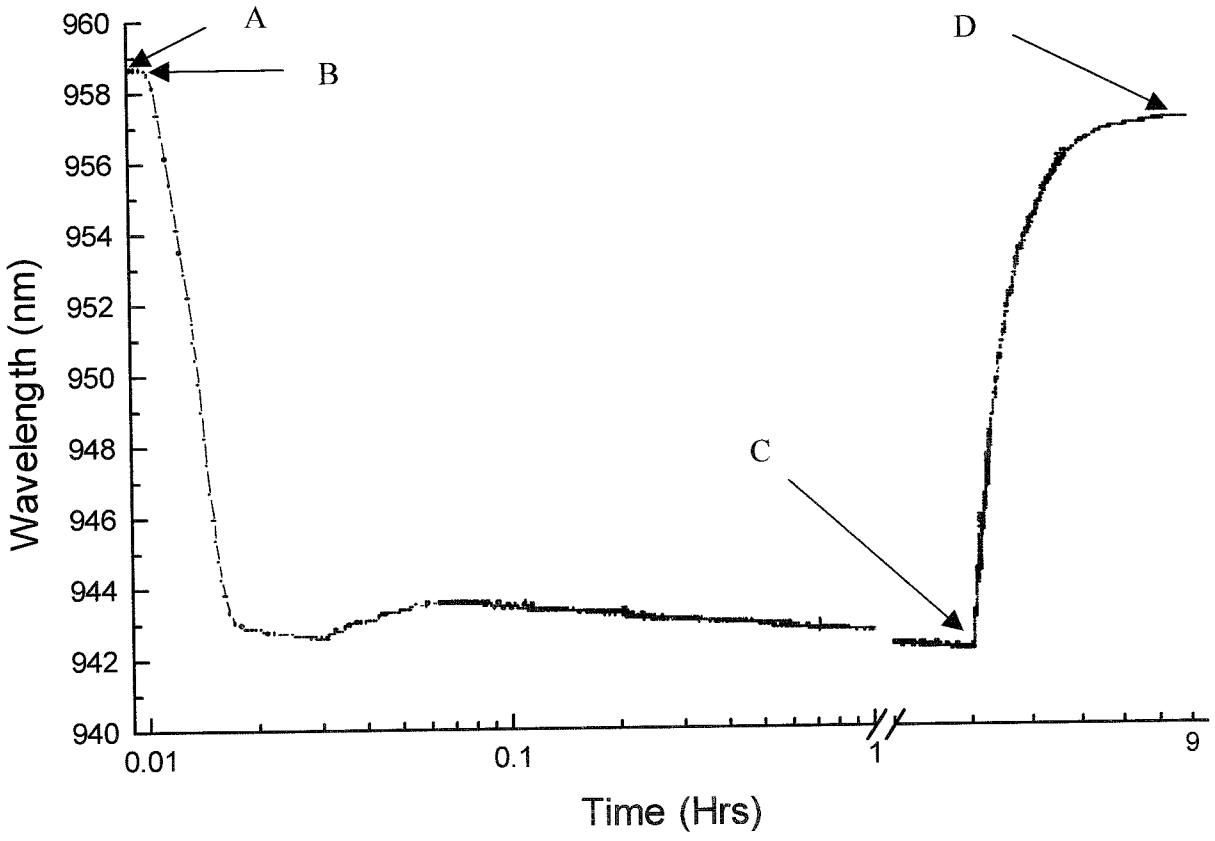

Figure 5.8: *The wavelength response, over the region A to D, as a function of time of LPG C's attenuation band 6.*

In region A, the system had stabilised at room temperature. At time B the furnace was set to 100°C and its temperature increased at a rate of 1.5°C /s. The central wavelength of the attenuation band decreased indicating a negative temperature sensitivity. As the furnace approached 100°C the rate of change of temperature slowed to 0.5°C /s. The temperature settled at 99.7°C and the LPG was annealed at temperatures between 99.7- 100.2°C. The plot shows that the wavelength decreased. At time C the furnace was set to cool to room temperature. In region D, at room temperature, the central wavelength was 956.99nm, a permanent shift of −1.71nm, with respect to the attenuation band's central wavelength before annealing. The LPG was allowed to settle for a further 12h at room temperature, after which the new central

wavelength and minimum transmission values of the attenuation bands and the temperature within the furnace were recorded.

5.2.4.1 Annealing at 100°C

The annealing procedure induced permanent wavelength shifts in the attenuation bands of up to –2.18 nm. Each attenuation band's wavelength shift is calculated with respect to its minimum transmission value at 25°C before annealing, the wavelength shifts are summarised in Table 5.3.

Table 5.3: *The permanent shift in the central wavelengths of attenuation bands 3-6, for LPGs A-C, induced by annealing at 100 °C for their respective duration.*

LPG No.	attenuation band 3	attenuation band 4	attenuation band 5	attenuation band 6	Annealed for
A	-1.3nm	-1.9nm	-2.2nm	-2.2nm	5.5Hrs
B	-1.3nm	-1.6nm	-1.6nm	-2.1nm	4.0Hrs
C	-1.2nm	-1.5nm	-1.5nm	-2.0nm	2.5Hrs

5.2.4.2 Annealing at 200°C

The transmission profiles of the LPGs, D, E and F, recorded before annealing, are similar to that shown in Figure 5.7. The experimental set-up and the annealing process are as described earlier in section 5.2.2.3. A summary of the results for annealing at 200°C is shown in Table 5.4.

Table 5.4: *The permanent shift in the central wavelengths of attenuation bands 3-6, for LPGs D-F, induced by annealing at 200 ℃ for their respective duration.*

LPG No:	attenuation band 3	attenuation band 4	attenuation band 5	attenuation band 6	Annealed for
D	– 5.2nm	– 6.4nm	– 6.6nm	– 7.7nm	5.0 hrs
E	– 5.4nm	– 6.1nm	– 5.9nm	– 7.4nm	4.0 hrs
F	– 4.1nm	– 4.9nm	– 5.1nm	– 6.2nm	3.0 hrs

5.2.4.3 Annealing at 500°C

LPG G was placed inside the furnace and the temperature was set to 500°C. Initially the central wavelength of the attenuation bands decreased. However as the furnace's temperature increased, the minimum transmission values of the attenuation bands began increasing and within 30s the attenuation bands had disappeared.

LPG H, which had been pre-annealed at 100°C for 2.5h, was also annealed at 500°C, for approx. 10min. Here again the central wavelengths decreased and then the minimum transmission values of the attenuation bands began increasing and within 60s, the attenuation bands had disappeared.

5.2.4.4 Discussion

The central wavelengths of all the attenuation bands decreased during annealing. The experiments have shown that the higher the temperature and the longer that the LPG is annealed for, the greater the permanent wavelength shift that is induced. The experiments have shown a limit to the maximum temperature at which the LPG can be annealed. At an annealing temperature of 500°C the partially pre-annealed LPG was erased after 60 sec, and the previously un-annealed LPG was erased after 30 sec. This shows that the pre-annealed LPG was stable at the higher annealing temperature for

twice as long as the un-annealed LPG. The permanent shifts in the central wavelengths of the attenuation bands are of the same order, as already reported. The choice of annealing temperature and duration must ensure that just the unstable portion of the UV induced RI modulation is removed [13, 14].

5.2.5 Post annealing temperature sensitivity

LPG F had been used for the pre-annealing temperature sensitivity experiment, it was subsequently annealed at 200°C for 3h and allowed to cool down to room temperature. The LPG then stabilised overnight at room temperature. The central wavelengths of the attenuation bands 3-6 were recorded when the LPG was at 25°C. The annealing process was observed to introduce a permanent change in the central wavelengths of the attenuation bands ranging from –4.1nm, for attenuation band 3 to –6.2nm for attenuation band 6.

Annealing at a temperature in excess of the maximum expected operating temperature is important for all types of fibre gratings as it stabilises their spectral characteristics by removing the unstable portion of the UV induced RI modulation [1, 2, 3, 8, 9, 10, 11, 12, 13, 14].

The post annealing temperature sensitivity of the attenuation bands was then determined, using the tube furnace, the temperature was increased in steps of 5°C, over a temperature range of 25°C- 200°C. The temperature of the furnace was allowed to stabilise at each set temperature for 1 minute after which the central wavelengths of attenuation bands 3-6 were recorded. The attenuation bands showed a linear response over the selected temperature range and the temperature sensitivity was again determined using a linear regression. Table 5.5 summarises the post annealing temperature sensitivity of the attenuation bands 3-6

Table 5.5: *The post annealing temperature sensitivities of attenuation bands 3-6.*

attenuation band 3	attenuation band 4	attenuation band 5	attenuation band 6
0.10 $\pm 5\times10^{-4}$ nm/°C	0.11 $\pm 5\times10^{-4}$ nm/°C	0.12 $\pm 9.\times10^{-4}$ nm/°C	0.14 $\pm 3\times10^{-4}$ nm/°C

The results show that the attenuation bands 3-6 exhibited a post annealing temperature sensitivity which ranged from 0.10nm/°C to 0.14nm/°C. It was observed that the post-annealing temperature sensitivities of the attenuation bands 3-6 had decreased when compared to their pre-annealing temperature sensitivities, detailed in table 5.1. It has been previously reported that annealing had reduced the temperature sensitivity of a LPG, written in standard telecommunications fibre, from 0.20nm/ °C to 0.15nm/ °C [15]. For LPGs written in boron co-doped fibres it has been reported previously that annealing at temperatures of upto 160 °C, had reduced the temperature sensitivity from -0.28nm/ °C to 0.16 nm/°C [16].

For the boron co-doped fibre used in the experiment, the measured temperature sensitivity is negative, as illustrated in Figure 5.6. The temperature sensitivity of a LPG's attenuation band (i) can be rewritten as [16],

$$\frac{d\lambda_i}{dT} = \Lambda\left[\left(n_{eff} - n_{cl}^{(p)}\right)\frac{1}{\Lambda}\frac{d\Lambda}{dT} + \frac{d\left(n_{eff} - n_{cl}^{(p)}\right)}{dT}\right] \qquad (5.1)$$

The term $\frac{1}{\Lambda}\frac{d\Lambda}{dT}$ represents the thermal expansion coefficient of the fibre core, which is independent of Λ. For the boron co-doped fibre used in these experiments the measured temperature sensitivity is negative and the thermal coefficient of silica is positive, this implies that the term $\Lambda d\left(n_{eff} - n_{cl}^{(p)}\right)/dT$ is negative, and dominates the equation. Annealing the LPG at an elevated temperature induces a change in the difference of refractive indexes ($n_{eff} - n_{cl}^{(p)}$), and its derivative with respect to temperature, resulting in a change in wavelength λ_p and the temperature sensitivity $d\lambda/dT$.

To investigate the stability of the spectral response of the LPG, a week later, a second post-annealing assessment of temperature sensitivity was made of the same

attenuation bands, by repeating the process of the first post-annealing assessment. The attenuation bands 3-6 again showed a linear temperature response over the measured temperature range. The temperature sensitivity of each attenuation band was again determined and compared with their respective temperature sensitivity from the first post annealing responses. It was observed that the temperature sensitivities of the assessments were consistent with each other. A representation of the consistency of the temperature sensitivity is shown in Figure 5.9, that plots wavelength shift as a function of increasing temperature in the range 30-200°C, for the reassessments of the LPG's temperature sensitivity after annealing.

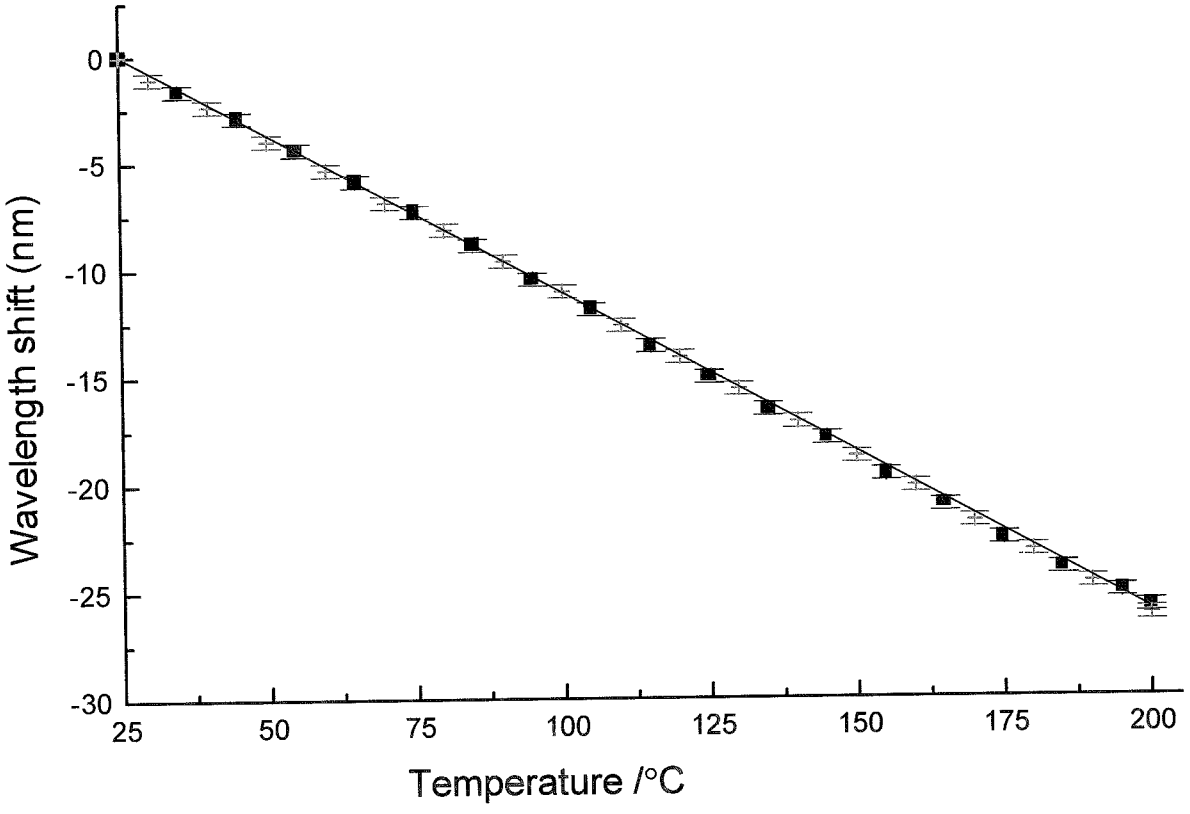

Figure 5.9: *Plot of wavelength shift as a function of increasing temperature for two different assessments of the LPG's temperature sensitivity after the LPG had been annealed at 200℃ for 3 h,* + *1st assessment,* ■ *2nd assessment conducted a week later. The linear regression shown in the plot is a guide for the eye only.*

The temperature sensitivity for the first assessment was 0.14nm/°C ± 0.002nm and for the second it was 0.14nm/°C ± 0.001nm. This indicates that once a LPG has been annealed the spectral characteristics of the LPG are stabilised. Subsequent reassessments of the LPG's temperature sensitivity at temperatures up to 200°C show that there is no further change.

5.2.5.1 Extending the measurement range beyond the annealing temperature

The temperature range of the measurements is extended to 300°C. Attenuation band 6 was selected for observation as it had showed the highest temperature sensitivity. The temperature of the furnace was stabilised at 200°C where the attenuation band showed a wavelength shift of approximately –25.5nm. The temperature was increased to 300°C and the furnace was allowed to stabilise for 60 sec. After a further 2 minutes the wavelength of the attenuation band began to decrease and 2 hour later the wavelength had decreased by 2nm. The change in wavelength indicated that the LPG was now being annealed at the higher temperature, thus confirming that the highest temperature in the assessment range must ideally be below the annealing temperature. The LPG was cooled to room temperature and allowed to settle for a further 12h. The annealing at 300°C had induced a permanent wavelength shift of –2.5nm. The temperature sensitivity of the LPG was again determined using the procedure detailed in section 5.2.5. The temperature was increased in steps of 20°C over a temperature range of 25°C - 300°C and the temperature sensitivity was found to be reduced from 0.14nm/°C ± 0.002nm to 0.11nm/°C ± 0.003nm.

5.2.5.2 Discussion

It has been shown that the annealing process introduces a permanent change in the central wavelength of the attenuation bands. The permanent shifts in the central wavelengths of the attenuation bands are of the same order, as already reported [3]. The overall decrease in wavelength is a function of the duration, the annealing temperature

and the order of the attenuation band. The work has also highlighted that a pre-annealed LPG is stable for longer at a temperature of 500°C. The choice of annealing temperature and duration must ensure that, just the unstable portion of the UV induced RI change is removed [3]. The annealing process also induced a decrease in the temperature sensitivity of the attenuation bands [3]. When compared to the attenuation bands' pre-annealing temperature sensitivities it had decreased by as much as 0.05nm/ °C. Once the LPG had been annealed it was found that any subsequent investigations of the temperature sensitivities, within the same temperature range, were consistent with each other provided that the measurement range remained below the annealing temperature. This indicates the importance of annealing at temperatures above the highest temperature to be measured.

5.3 Strain characterisation

5.3.1 Introduction

The application of axial strain to an optical fibre containing a LPG manifests itself as a change in the central wavelengths of the attenuation bands. The strain sensitivities of the attenuation bands of LPG are a function of the grating period and the order of the corresponding cladding mode to which coupling takes place. This section presents the characterisation of the LPG's response to applied strain.

5.3.2 Experiment

The LPG's parameters are detailed in section 5.2.2 and the configuration of the system used to apply an axial strain to the LPG under test is shown in Figure 5.10. The buffer jacket was removed from the entire section of fibre under test, as discussed in section 4.7.1 of Chapter 4, and using a Cyanocrylate super glue [17] the fibre's cladding was glued directly into the v-grooves of the blocks. Anchoring the fibre cladding rather than the jacket reduced the possibility of slippage while the fibre was being strained and

ensured that the applied strain was transferred uniformly between the glue points. The LPG was positioned centrally between the two v-grooved blocks and was held straight and taut to avoid any distortion of the LPG's transmission spectrum due to a curvature of the LPG [18]. One of the v-grooved blocks was fixed and the other was mounted on a linear translation stage that was manually driven by a micrometer screw gauge. The translation stage had an extension of 50mm and the micrometer screw gauge could be set to an accuracy of ± 0.5μm. The distance, L, between the inner edges of the two V-grooved blocks was measured using Vernier callipers and was found to be 185±0.5mm. By movement of the translation stage by a known amount, *l*, the strain applied to the LPG could be calculated using the ratio (*l* / L). The uncertainty in the fibre's length, resulted in a systematic error of ± 0.5%.

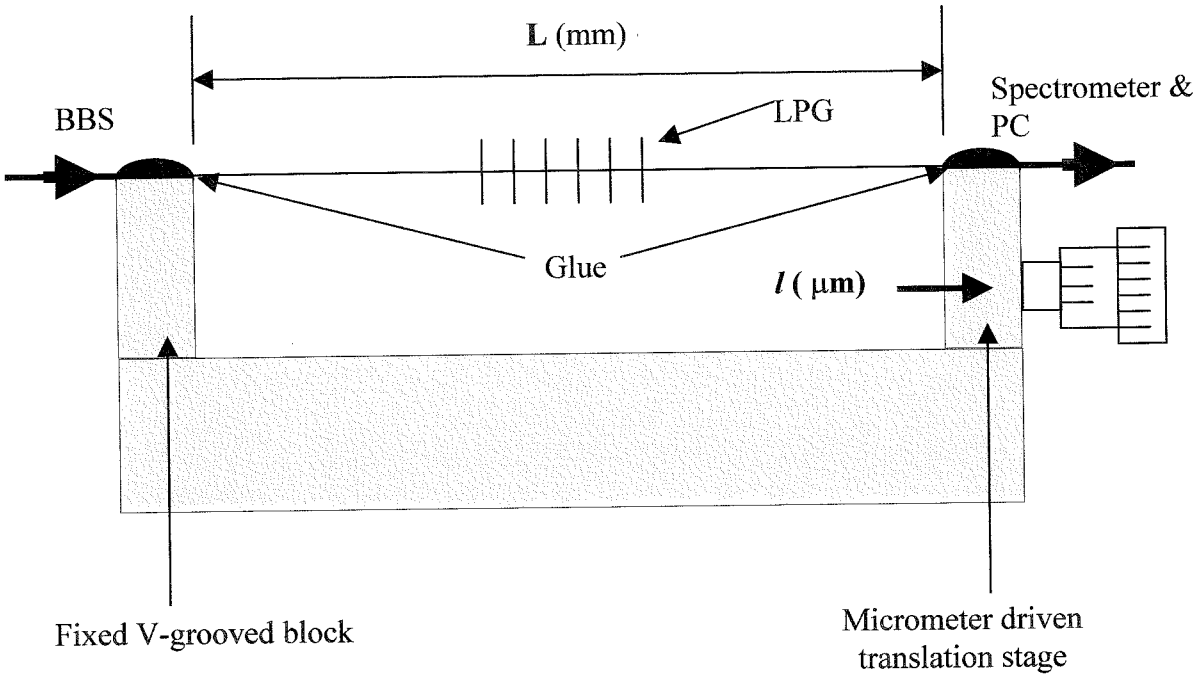

Figure 5.10: *The configuration of the system used to extend the LPG by a known amount.*

BBS: Broadband Source, LPG: Long period grating, L: Distance between the inner edges of the V-grooved blocks, l: Distance that the moveable block moves.

To ensure that the fibre was held securely in the v-grooves, under a thermal enclosure, the fibre was extended by 600μm, which equates to an applied strain of approximately 3243με. The attenuation bands were observed to decrease to lower wavelengths. After 10 minutes the attenuation bands had not shown any further change in their central wavelengths and the strain was released. The attenuation bands were seen to return to their original positions. If the attenuation bands had not returned to their original central wavelengths then it would indicate either hysterisis in the translation stage or creep of the fibre at the glue points. The zero strain condition was taken to be when the anchored fibre section just becomes taut and this could be repeatedly set to an accuracy of ±5με. The error of ±5με leads to an extension of approximately ±0.9μm which equates to a wavelength shift of 2.6nm. The system was surrounded by a thermal enclosure to reduce the effects of variance in the surrounding temperature. The thermal stability within the enclosure was measured using a thermocouple and was found to be less than 1°C which for attenuation bands 2-3, 5-6 equates to wavelength shifts in the range 0.10nm/°C to 0.14nm/°C. Such small variations in wavelength shifts cannot be detected, as the resolution of the CCD is 0.3nm at 1000nm.

5.3.3 Results

The central wavelengths of the attenuation bands were recorded at 25°C. The fibre was subjected to a maximum extension of 700μm in steps of 50μm which equates to a maximum strain of approximately 3780με, in steps of 270με respectively, at room temperature. Previous investigations had concluded that the LPG was prone to mechanical failure at strains of approximately 4000με. The breaking of the LPGs at the lower applied strain value was considered to be due to a weakness that had been introduced into the fibre during the fabrication process. The mechanisms of the degradation induced by UV-irradiation are unclear. It has been shown that fibre gratings exposed to pulsed UV irradiation showed a factor of 4 reduction in mechanical strength when compared to gratings exposed by a CW UV laser at 244nm [19, 20, 21, 22].

At each step, the transmission spectrum and the central wavelengths of attenuation bands 2-6 were recorded. The central wavelengths of attenuation bands 6 and 5 were observed to increase whilst those for attenuation bands 3 and 2 decreased and attenuation band 4 appeared to show no response. The sensitivity to strain for attenuation band's 2-3 and 5-6 can be determined by plotting their central wavelength shifts as function of applied strain. The central wavelength shift for each band was calculated with respect to the wavelength of that particular attenuation band at 25°C. The response of the attenuation bands 2-6 to applied strain are illustrated in Figure 5.11. Where the wavelength shift is plotted as a function of applied strain for attenuation band 2- 6.

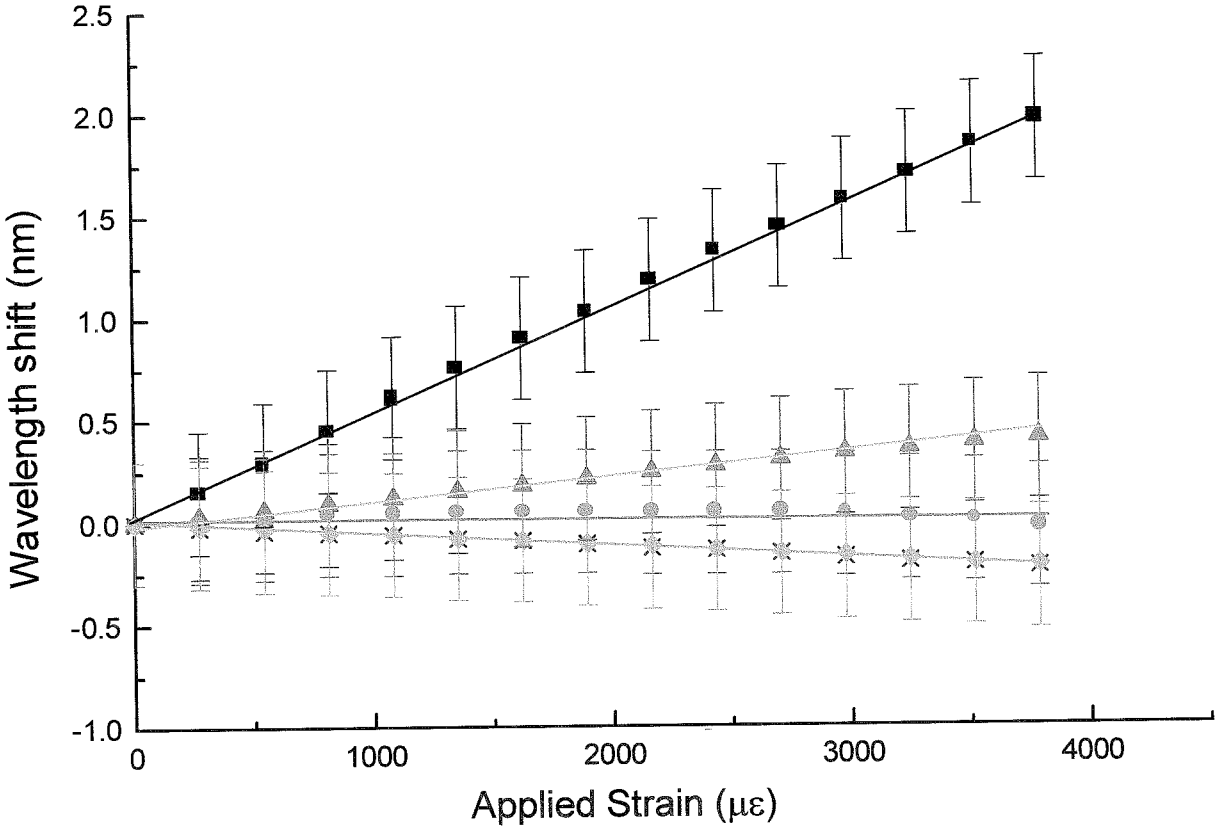

Figure 5.11: *Plot of wavelength shift as a function of applied strain for attenuation bands 2-6. The linear regressions shown in the plot are a guide for the eye only.* ◆ *attenuation band 2,* × *attenuation band 3,* ● *attenuation band 4,* ▲ *attenuation band 5 and* ■ *attenuation band 6.*

Figure 5.11 shows that the applied strain induced a linear central wavelength shift in attenuation bands 2-3, 5- 6 and attenuation band 4 showed no response to strain. The observed fluctuations in the wavelength for attenuation band 4 can be attributed to the less than 1°C temperature variation under the thermal insulator. The attenuation bands showed a sensitivity in the range 0.52 ± 0.02pm/με to –0.05pm/με. Table 5.6 summarises the sensitivity of the attenuation bands under investigation.

Table 5.6: *The strain sensitivities of attenuation bands 2-6.*

attenuation band 2 (pm/με)	attenuation band 3 (pm/με)	attenuation band 4	attenuation band 5 (pm/με)	attenuation band 6 (pm/με)
-0.06 ± 0.03	-0.06 ± 0.04	No observed response	0.11 ± 0.05	0.52 ± 0.02

5.3.4 Discussion

Attenuation bands 2 & 3 showed a negative sensitivity to strain whilst attenuation bands 5 & 6 showed a positive sensitivity. Attenuation band 4 did not show a sensitivity to strain, the drift observed in its central wavelength was attributed to the variance in temperature, of 0.5°C, under the thermal enclosure. The magnitude and the sign of the strain sensitivity are defined by the difference between the strain optic coefficients of the core and cladding regions and the periodicity of the LPG described in section 3.2.2 of Chapter 3. Attenuation band 4 has shown no sensitivity to strain but has demonstrated, in sections 5.2.3 to 5.2.5, a sensitivity to temperature of 0.11nm/°C. This attenuation band could be used to measure temperature, the effect of which could be subtracted from attenuation band 6 to facilitate independent measurements of strain.

For LPGs fabricated in hydrogen loaded germanosilicate Coring FLEXCOR fibres, possess strain coefficients in the range – 2.2pm/με to 1.521pm/με [5]. The results presented in section 5.3.3 are comparable with other previously reported results [5, 16].

5.4 Characterisation of the change in the refractive index of the medium surrounding the long period grating

5.4.1 Introduction

LPGs exhibit a sensitivity to the RI of the medium surrounding the cladding, n_{Ext}. [23, 24, 25, 26, 27, 28, 29, 30, 31, 32]. The RI sensitivity of LPGs arises from the dependence of the phase matching condition upon the effective RI of the cladding, n_{cl}. The effective indices of the cladding modes are dependent upon the difference between the RI of the cladding and that of the medium surrounding the cladding, n_{Ext}. The central wavelengths of the attenuation bands thus show a dependence upon the RI of the medium surrounding the cladding, if the cladding has the higher RI [23, 24, 25, 26]. When n_{Ext} has a RI higher than that of the fibre cladding, the central wavelengths of the attenuation bands show no change, but the minimum transmission values of the attenuation bands are observed to change [23, 24, 25]. This section investigates the response of the LPG's transmission spectrum to a change in the RI of the medium surrounding it.

5.4.2 Experiment

To facilitate the characterisation of the RI responses the LPG was immersed in a series of RI liquids, Cargille series 'A'. A receptacle, in which the LPG could be totally immersed in the liquids, had been designed and constructed for the investigation. The receptacle consisted of a well, which had been fabricated, in an aluminium block. The well was 5mm deep and 50mm long. V-grooves, used to support the fibre either side of the LPG, ran longitudinally into the well from either end of the block. The configuration of the receptacle is shown in Figure 5.12.

The buffer jacket was removed from the entire section of fibre under test, as discussed in section 4.7.1 of Chapter 4. The fibre was held straight and taut thus avoiding any distortion of the LPG's transmission spectrum due to a curvature of the

LPG [18]. The LPG was positioned in the middle section of the well. The stripped fibre, sitting in the V-grooves, was glued into the V-grooves using a Cyanocrylate super glue [17]. The anchoring of the fibre ensured that the applied strain on the LPG was kept constant.

Wax, supplied by Radio Spares, was used to seal the ends of the V-grooves to prevent the RI liquids from flowing out. The temperature of the RI liquids, in which the LPG was to be immersed, was maintained at 25°C by fixing the liquid receptacle to the middle of a thermo-electric heater/cooler. A cross section of the experimental configuration is shown in Figure 5.12. A thin layer of heat sinking compound was laid between the base of the well and the thermo-electric heater/cooler to assist in the uniform heating of the liquid receptacle and the RI liquids.

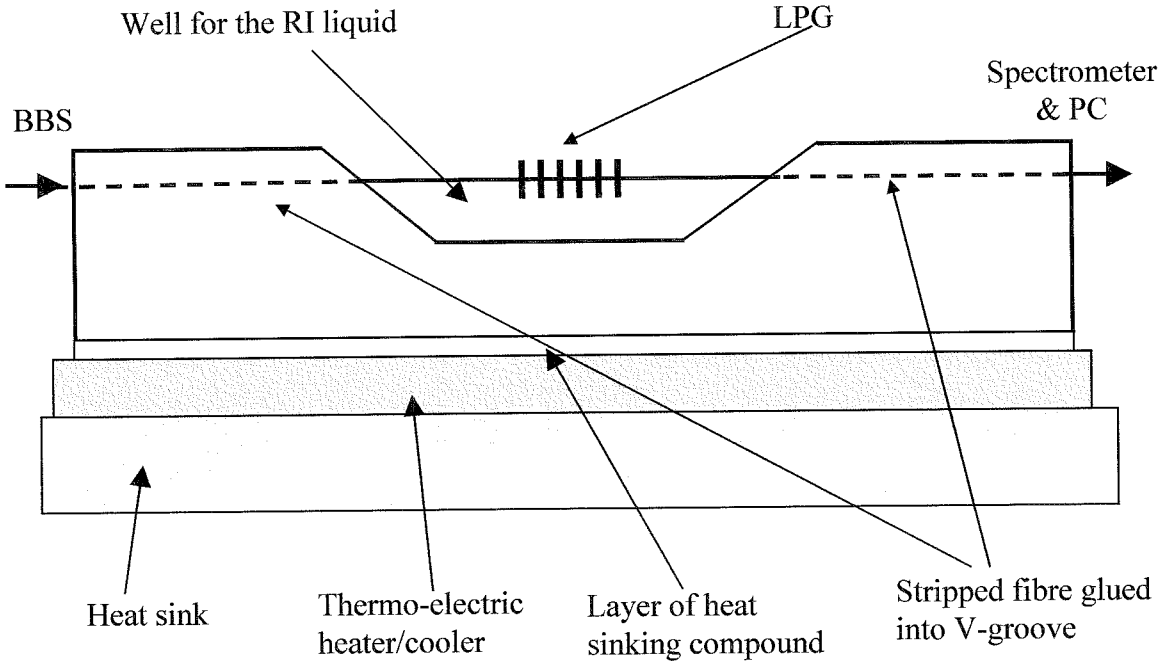

Figure 5.12: *The configuration of the LPG receptacle used to investigate the response of the LPG's transmission spectrum to changes in the RI of the surrounding medium.*

The temperature of the liquid was measured using a K-type thermocouple and an AD590 temperature sensor. The measuring devices were positioned into recesses, which would be filled with the RI liquid, located on either side of the LPG. The K-type thermocouple used in association with a digital thermometer, Keithley 740 scanning thermometer. The scanning thermometer had a resolution of 0.1°C. The AD590 was used in a feedback loop by a thermoelectric temperature controller, a TED 200 supplied by Profile, to maintain the thermo-electric heater at the required temperatures ± <1°C. The temperature range of the thermo-electric heater was limited by the size of the heat sink and the maximum output current of the TED 200, 2A. The TED 200 was able to maintain a temperature with a stability of ≤0.01°C. The settling behaviour of the TED 200 for a change in temperature was determined by the proportional, integral and derivative, PID, parameters which were adjusted to an aperiodic temperature settlement. Temperature changes in the environment immediately surrounding the experimental configuration were further minimised by enclosing it within a thermal enclosure.

The thermal stability within the enclosure was measured and found to be less than 1°C. For attenuation bands 2-3, 5-6 the temperature variation equates to wavelength shifts in the range < 0.10nm/°C to < 0.14nm/°C. Such small variations in wavelength shifts can not be detected, as the resolution of the CCD is 0.3nm at 1000nm.

The LPG was cleaned thoroughly between the application of each liquid. The LPG was flushed firstly with Iso-Propyl alcohol, IPA. Remaining traces of the RI liquid were removed by cleaning the LPG with lens tissue doused in IPA. The LPG was then dried with a lens tissue. The LPG was cleaned until the attenuation bands returned to their starting central wavelength values, as this indicated that there were no traces of RI liquid or IPA present on the LPG.

5.4.3 Results

The liquids chosen to surround the LPG ranged in RI from 1.400 to 1.600 ± 0.0002; the quoted values were given when measured at 25°C at a wavelength of 589.3nm [33]. A record of each attenuation band's central wavelength and minimum transmission value was made whilst the LPG was surrounded by air at 25°C under a thermal insulator. The LPG was surrounded by a RI liquid and allowed to settle at 25°C and the new central wavelengths and the minimum transmission values of the attenuation bands were recorded. The results of this investigation are shown in Figures 5.13 and 5.15. The RI values given in Figures 5.13 and 5.15 are those quoted at a wavelength of 589.3nm and at 25°C 33], the effects of the dispersion of the RI liquid including the dependence of the RI value on the temperature and the measuring wavelength were not taken into account. The change in the central wavelengths of the attenuation bands is illustrated in Figure 5.13. Where the actual wavelength of attenuation band 3 is plotted as a function of increasing RI. As the RI of the liquids was increased from 1.400 - 1.456, the principal effect was the decrease in the central wavelengths of the attenuation bands. The magnitude of the wavelength shift changes as the RI of the surrounding medium approaches that of silica because of the non-linear change in dn_{cl}/dn_{ext}, equation 3.3 in Chapter 3. The largest sensitivity was shown by the attenuation band at the longest wavelength, for attenuation band 6 this was (24.3nm). For further increase in the RI the wavelengths show no response owing to the absence of modal confinement by the surrounding medium [24]. The result will be then a wavelength selective coupling to the attenuated cladding modes [24]. As the RI increases to 1.460 the attenuation bands shift to higher wavelengths compared with those in air, 828.3nm for attenuation band 3, because of the difference in the nature of the Frensel and total internal reflection conditions [23].

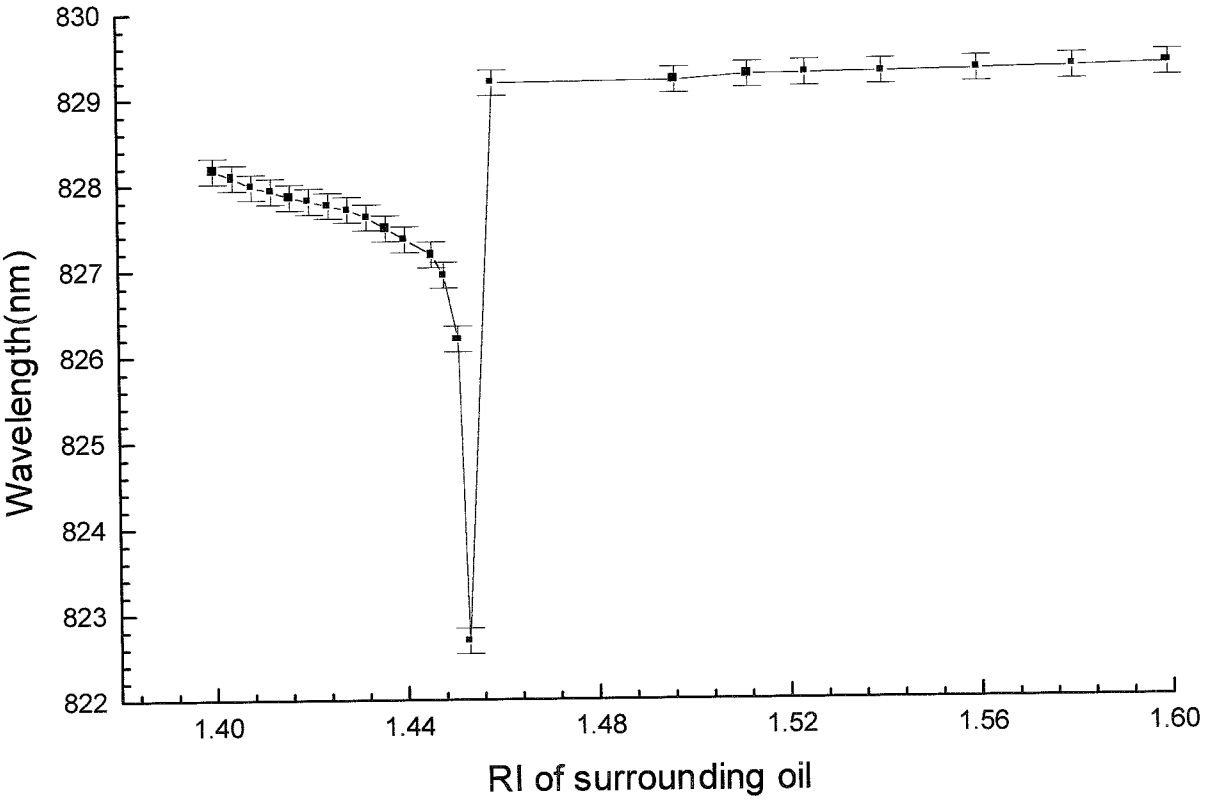

Figure 5.13: *Plot of actual wavelength as a function of the RI of the medium surrounding the LPG for attenuation band 3.*

The maximum changes in the central wavelengths of the attenuation bands 3-6 were determined and are presented in the Table 5.7.

Table 5.7: *The maximum wavelength shift of attenuation bands 3-6 induced by the RI liquids.*

Attenuation Band	Maximum Wavelength Shift (nm)
3	6.8 ± 0.3nm
4	10.7 ± 0.3nm
5	11.4 ± 0.3nm
6	24.3 ± 0.3nm

During the immersion of the LPG in the RI liquids, it was also observed that, as the RI increased, the attenuation bands responded with a simultaneous change in their minimum transmission values. This observation is illustrated in Figure 5.14, which shows the LPG's transmission profiles when the LPG was immersed in a liquid of RI 1.400 and then in liquid of RI 1.456.

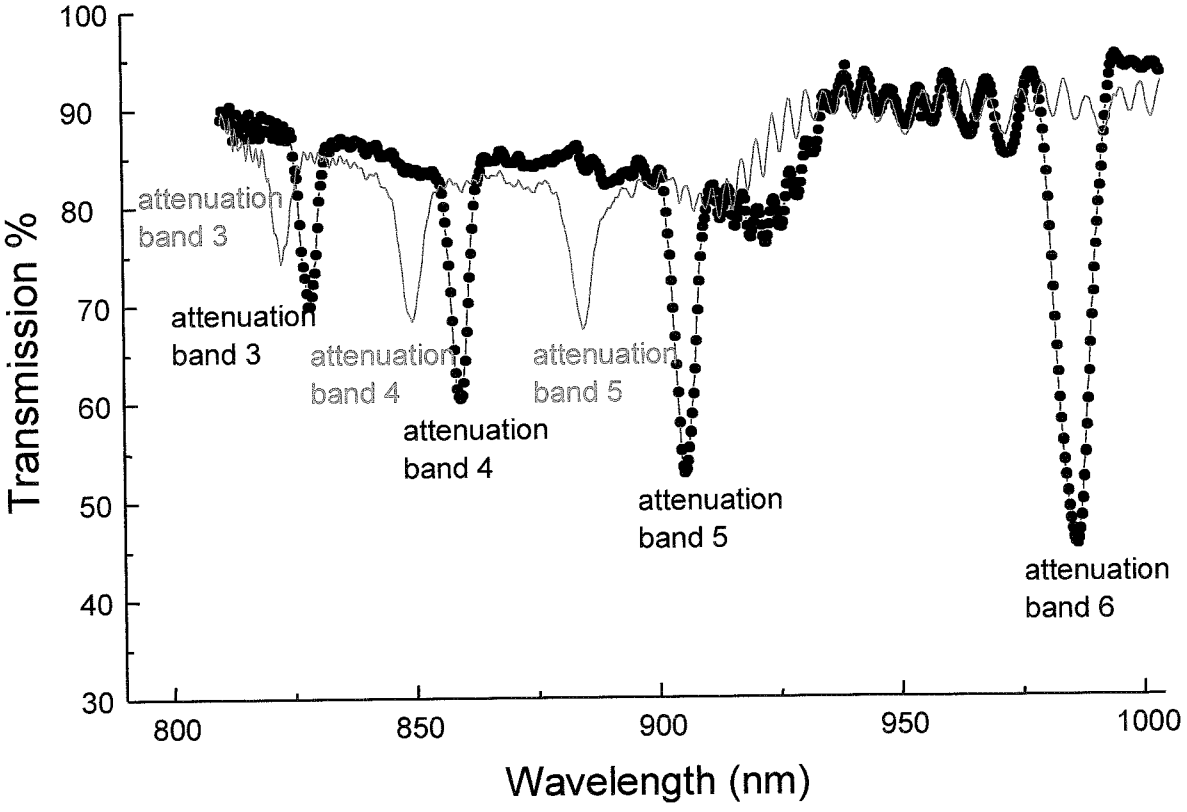

Figure 5.14: *A plot of the transmission spectrum for the LPG when it was immersed in liquids of RI,* • *1.400 and* —— *1.456.*

From Figure 5.14 it is clearly seen that attenuation bands 3-6, at n = 1.400 have a greater coupling strength than when compared to n = 1.456. The oscillations seen in the transmission spectra are due to a cavity forming between the ends of the connectors. The depth of attenuation band 3 is plotted as a function of RI in Figure 5.15.

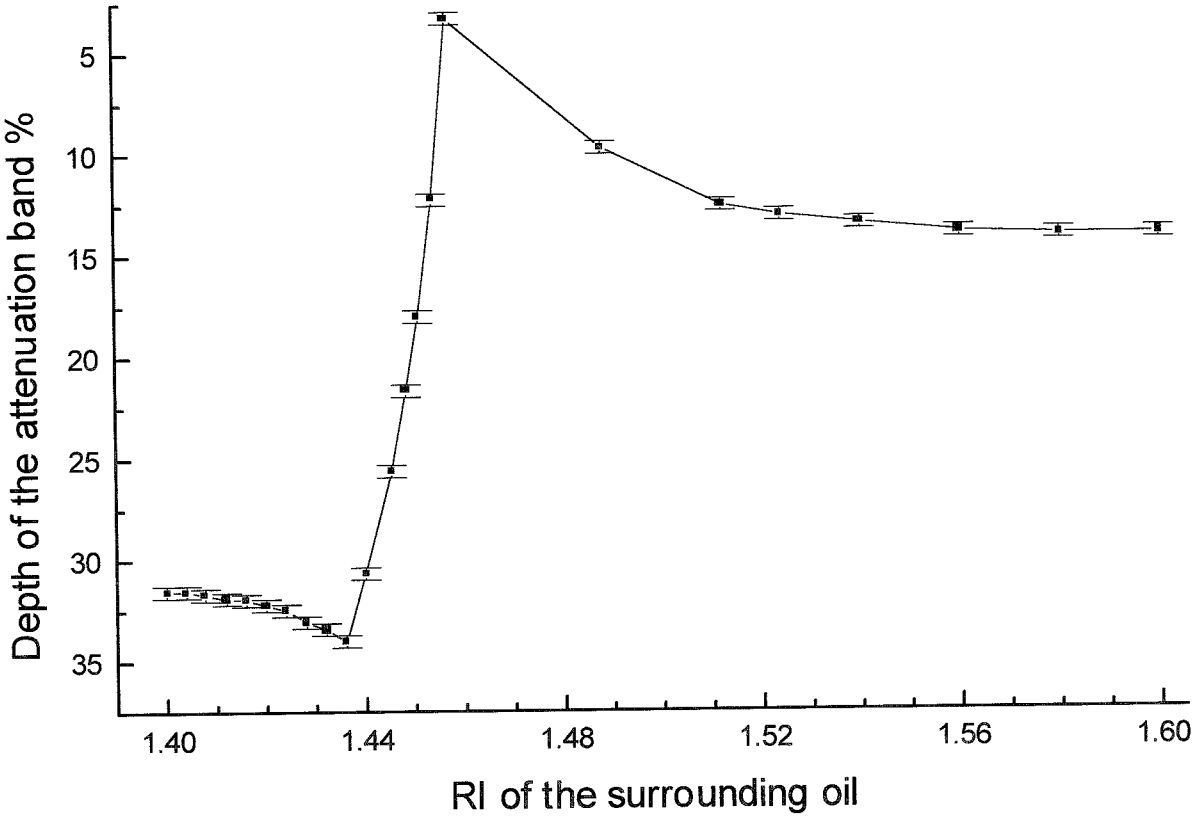

Figure 5.15: *A plot of the depth of the attenuation band as a function of RI for attenuation band 3. The line is a guide for the eye only.*

Between the RI's of 1.456 and 1.460, it was noted that the spectrum broadened and the depth of the attenuation bands reduced abruptly, for attenuation band 3 the depth is reduced from approximately 33% to 4%. As the RI of the surrounding medium increases, the cladding mode field penetrates deeper into the medium. Consequently, the overlap integral decreases thus reducing the coupling efficiency [25]. When the RI is greater than that of the cladding there is an absence of a guided regime in the cladding, which avoids the existence of guided cladding modes and entails that the phase matching relation, equation 2.18 of Chapter 2, is no longer valid and the cladding mode propagates in accordance with Fresnel reflection from the cladding boundary, which is accompanied by the reappearance of the higher order attenuation bands [25]. For further increase in the RI the depth of the attenuation bands is observed to increase but does not

go back to its original value. It was also observed that the attenuation bands at the longest wavelengths disappeared and those at the shortest wavelengths remain visible throughout the full range of the RI. Since each cladding mode has a unique effective index the higher order cladding modes had encountered their matched cladding interface at a lower value of RI, and the corresponding attenuation band disappeared, as compared to the lower order-cladding mode [34].

5.4.4 Discussion

As the RI of the liquid surrounding the LPG was increased from 1.400 - 1.456, Figures 5.13 and 5.15 showed that the principal effects was the decrease in the central wavelengths of the attenuation bands. The maximum wavelength shift was observed for a RI of 1.456, which corresponds to the RI of the fibre's cladding at a wavelength of 589.3nm [35]. The highest sensitivity, a wavelength shift of 24.3nm, was demonstrated by attenuation band 6. For further increases in the RI of the liquid in which the LPG was immersed, the wavelengths did not show a response, however a change in the minimum transmission values of the attenuation bands was still observed.

The magnitude of the RI induced wavelength shift is a function of the LPG's periodicity and the order of the cladding mode [23, 34]. The RI of the medium surrounding two LPGs, which had been fabricated in hydrogen loaded DSF fibre, was changed from 1.000 to 1.450. The highest order attenuation bands, situated in the 1200 - 1600nm wavelength range, for the two LPGs with periods of 200μm and 350μm exhibited a wavelength shift of 35nm and 8.5nm respectively [23]. The results obtained from the characterisation work fall into the same order of magnitude.

The characterisation carried out here has shown that the change in the RI of the liquids surrounding the LPG brought about two distinct changes, a shift of the attenuation bands to shorter wavelengths and the change in the minimum transmission value. This feature allows the LPG to be used as a RI sensor and these observations will be exploited in Chapter 6 to present three novel sensing schemes.

5.5 Bending characterisation

5.5.1 Introduction

The transmission spectrum of a LPG is highly sensitive to bending and responds in one of two ways. The first is the displacement of the attenuation bands to longer wavelengths and a reduction of the attenuation band's amplitude [36]. The second is the development of coupling to additional asymmetric cladding modes evidenced by the formation of extra attenuation bands [37]. The wavelength separation between these split attenuation bands increases with increasing bend curvature [37]. This section investigates the effects of bending a LPG.

5.5.2 Experiment

A series of bends of various radius of curvatures were introduced into the fibre containing the LPG, using the fibre bending module shown in Figure 5.16. The bending module is an adaptation of the system shown in Figure 5.10. One of the v-grooved blocks was fixed and the other was mounted on a linear translation stage that was manually driven by a micrometer screw gauge which could be set with an accuracy of ± 0.5μm. A bend is introduced into the fibre by movement of the linear translation stage in steps of 20μm towards the fixed block. The response of the transmission spectrum was observed using the general experimental configuration that is detailed in section 4.7.3 of Chapter 4. The LPG's parameters are detailed in section 5.2.2. The processes for positioning and fixing the LPG onto the translation stages and testing the adhesion of the fibre into the v-grooved blocks is the same as described in section 5.3.2.

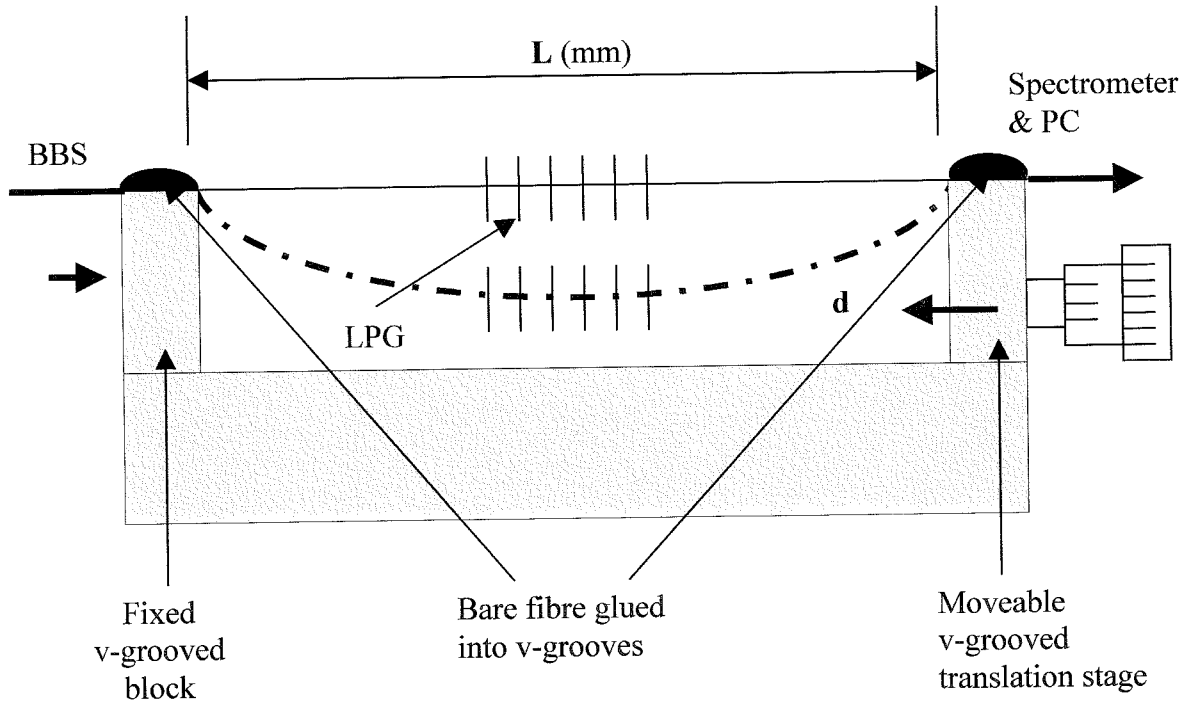

Figure 5.16: *The LPG bending module used to introduce a series of a bends of varying radius of curvature into the LPG.*

BBS: Broadband Source, LPG: Long period grating, L: Distance between the inner edges of the V-grooved blocks, d: distance that the moveable block moves.

The distance, L, between the inner edges of the two v-grooved blocks is measured using Vernier callipers and was found to be 185±0.5mm. By reducing L by a known amount, d, the bend curvature, the inverse of the radius of curvature, is estimated. The radius of curvature is estimated by approximating the bent fibre as the arc of a circle [36], which has a radius that is calculated using equation 5.2,

$$\text{Radius} = \frac{1}{\left(\frac{4}{d.L}\right)\sqrt{d.L - d^2}} \tag{5.2}$$

The uncertainty in the fibre's length and the accuracy of the step size resulted in a systematic error of ± 0.5%. The LPG bending module was surrounded by a thermal enclosure to reduce the effects of variance in the surrounding temperature.

5.5.3 Results

Bend curvature in the range 0.25 m^{-1} to 2.5 m^{-1} were applied to the fibre using the LPG bending module. For each applied bend, the transmission spectrum and the changes in the individual attenuation bands were recorded. It was observed that the attenuation bands 4-6 responded to bending by dividing into two closely separated attenuation bands, these bands were also reduced in depth. The divided attenuation bands were observed to increase in wavelength separation for increasing bend curvatures. The possible mechanism of the splitting of the attenuation bands in the LPG studied here is that when the fibre is bent this breaks the symmetry between the two normally degenerate spatial cladding modes of the straight circular fibre thus introducing a RI difference between them. The phase matching condition for the cladding mode could then be satisfied at two discrete wavelengths [38]. This effect results in two cladding modes with their fields predominantly on the outer and inner sides of the cladding relative to the centre of the bend, respectively [38]. Thus, with increasing bend curvature, the two split cladding modes propagate in a strained and compressed cladding with a shift to longer and shorter wavelengths [39]. Figure 5.17 illustrates the splitting of an attenuation band by plotting the transmission spectra of attenuation band 6, with curvature at 0 m^{-1} (straight) & 1.55m^{-1}.

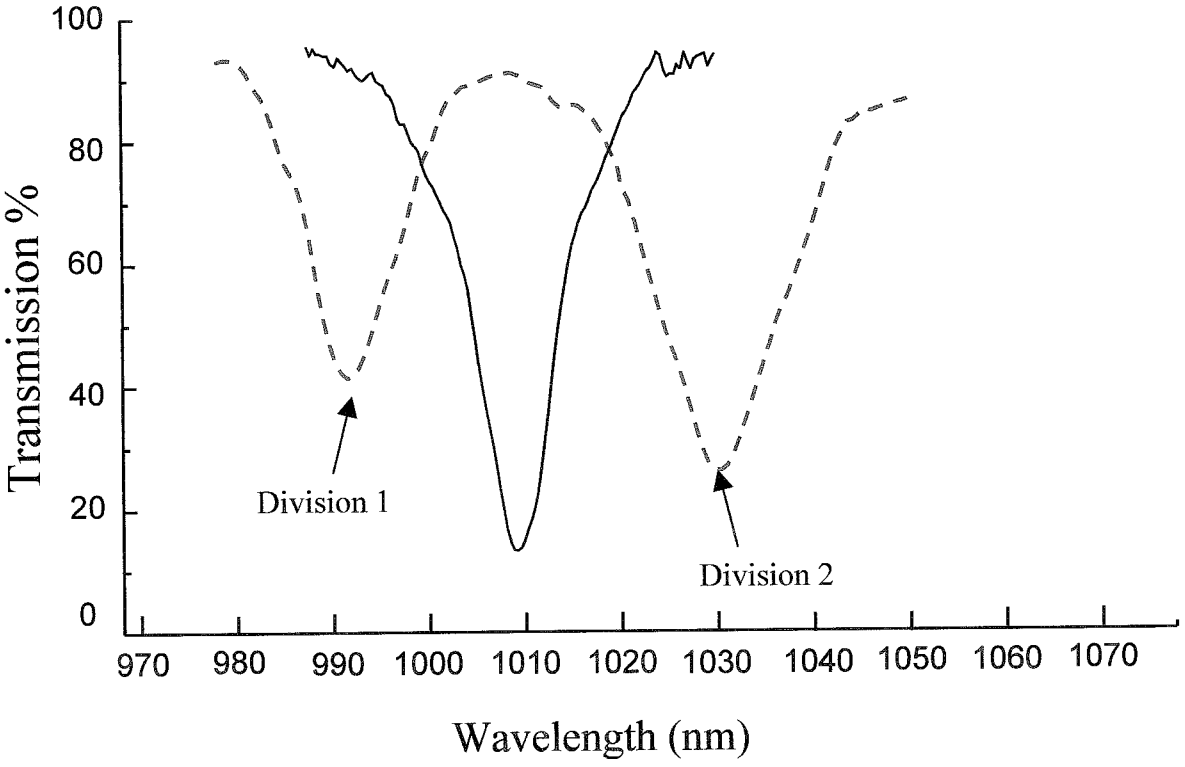

Figure 5.17: *A plot of the transmission spectra of attenuation band 6, for different bend curvatures.* ——— *0.00m^{-1},* ------ *curvature of 1.55m^{-1}.*

Attenuation band 6 is observed to have a single central wavelength at approximately 1010nm when the fibre was straight. The single attenuation band is divided in two when a bend of curvature 1.55m^{-1} is applied to the LPG and the divisions 1 & 2 are reduced in depth. When the LPG is bent with a curvature of 1.55m^{-1} the divisions are separated by approximately 40nm.

It was observed that the divided attenuation bands' wavelength separation increased significantly with increasing bend curvature. This observation is represented in Figure 5.18, which plots each division's central wavelength as a function of increasing bend curvature for attenuation band 6.

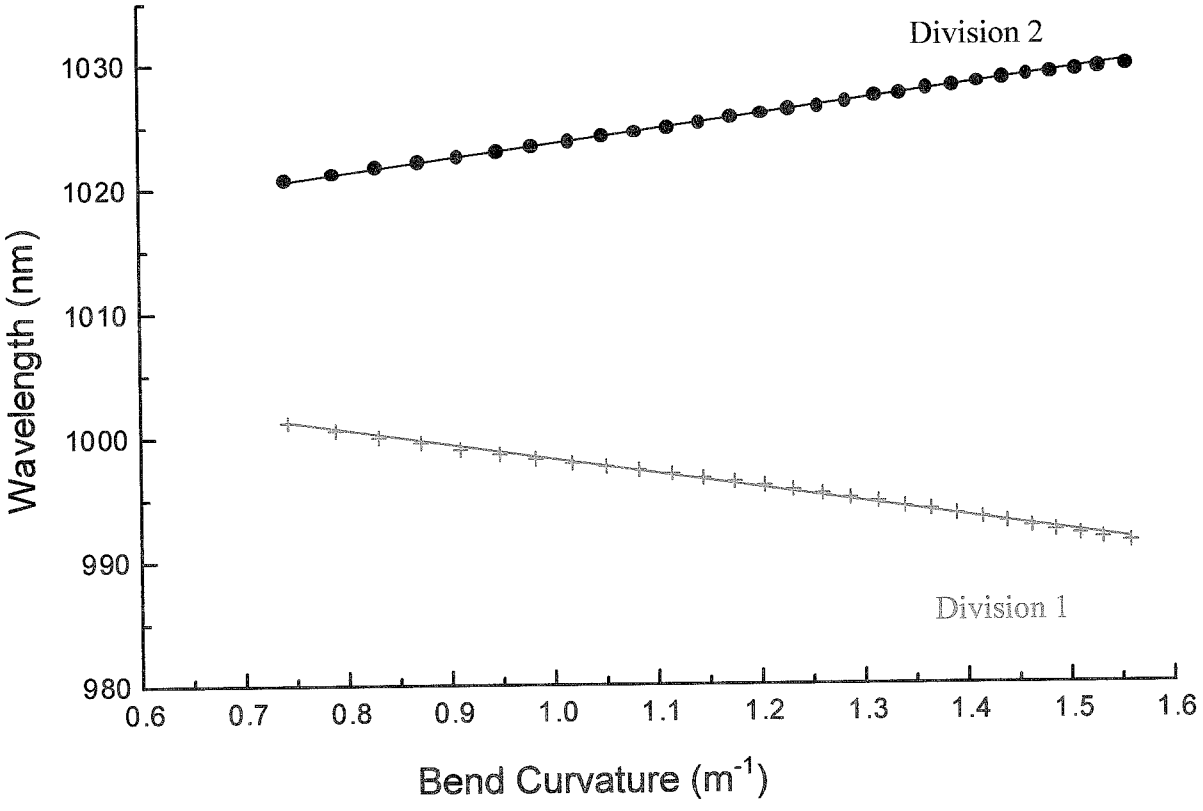

Figure 5.18: *Graph of the measured wavelengths against increasing bend curvature for the divisions of attenuation band 6, + Division 1, • Division 2.*

Figure 5.18 illustrates that the division's central wavelengths were observed to increase linearly with increasing bend curvature. A high bending sensitivity has been reported previously that uses the wavelength separation of the split attenuation band as the sensed information [37]. The wavelength separation between the splits of attenuation band 6 as a function of bend curvature over a range of 0.30 m^{-1} to 2.5m^{-1} is plotted in Figure 5.19.

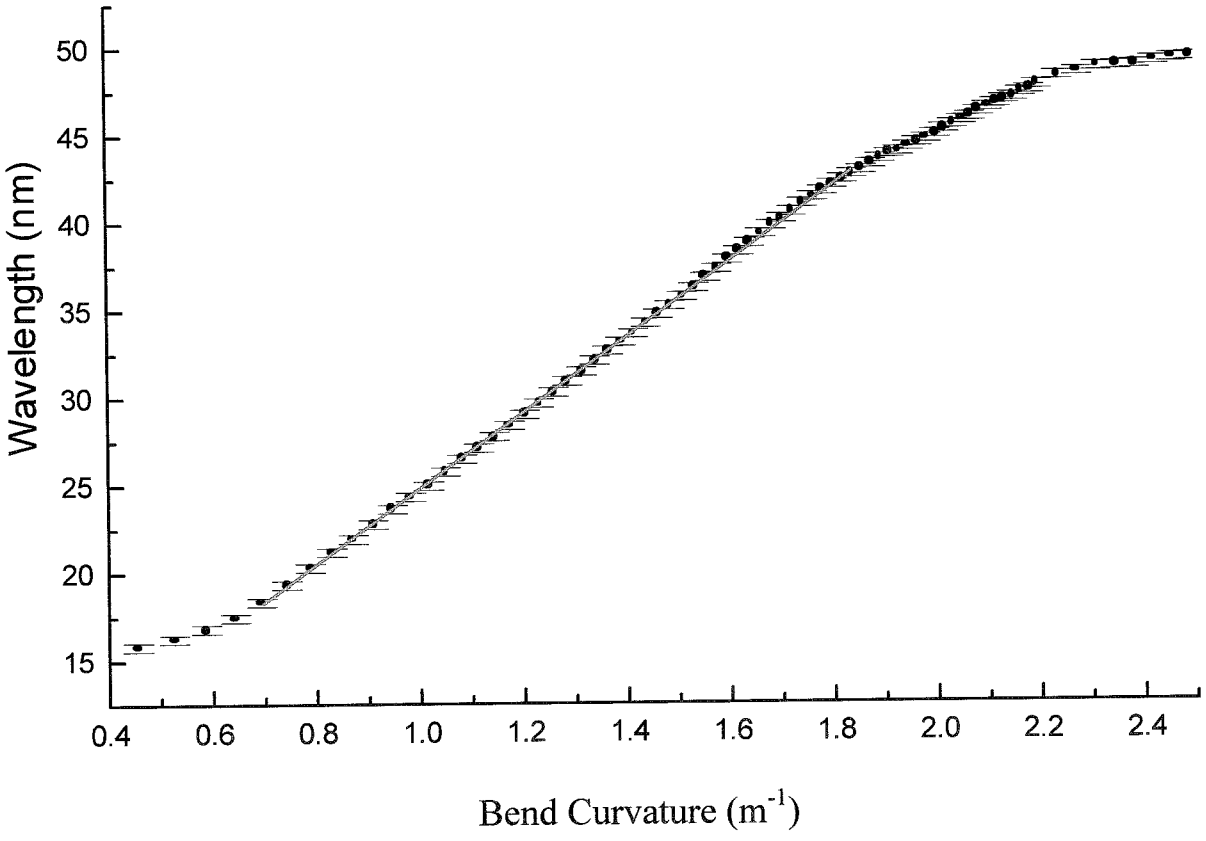

Figure 5.19: *Plot of wavelength separation between the divisions as a function of increasing bend curvature for attenuation band 6. The line is a fit over the linear region of 0.70m^{-1} to 1.80m^{-1}.*

Figure 5.19 illustrates that the wavelength separation of the divisions is linear over the limited bend curvature range of 0.70m^{-1} - 1.80m^{-1}. The bend curvature range under further investigation is within this linear region. The bend sensitivity in the region was determined to be 21.61nm/m^{-1}, this is approximately one and a half times the sensitivity reported previously in [40] and nearly six times the sensitivity demonstrated by the wavelength shift detection method [36]. When a bend curvature in range 0 to $\approx$ 0.4m^{-1} was applied to this particular LPG its attenuation bands did not show a response. Measurements in this region can be conducted by using a LPG with an attenuation band with a higher sensitivity. This can be achieved by specifically tailoring parameters such as choosing the highest order-cladding mode, the periodicity of the LPG and the operating wavelength [6].

The other attenuation bands responded in a similar manner and a comparison between their bend sensitivities was performed. Figure 5.20 plots the wavelength separation as a function of increasing bend curvature for attenuation bands 4-6. The bend sensitivity of each of the attenuation bands was calculated.

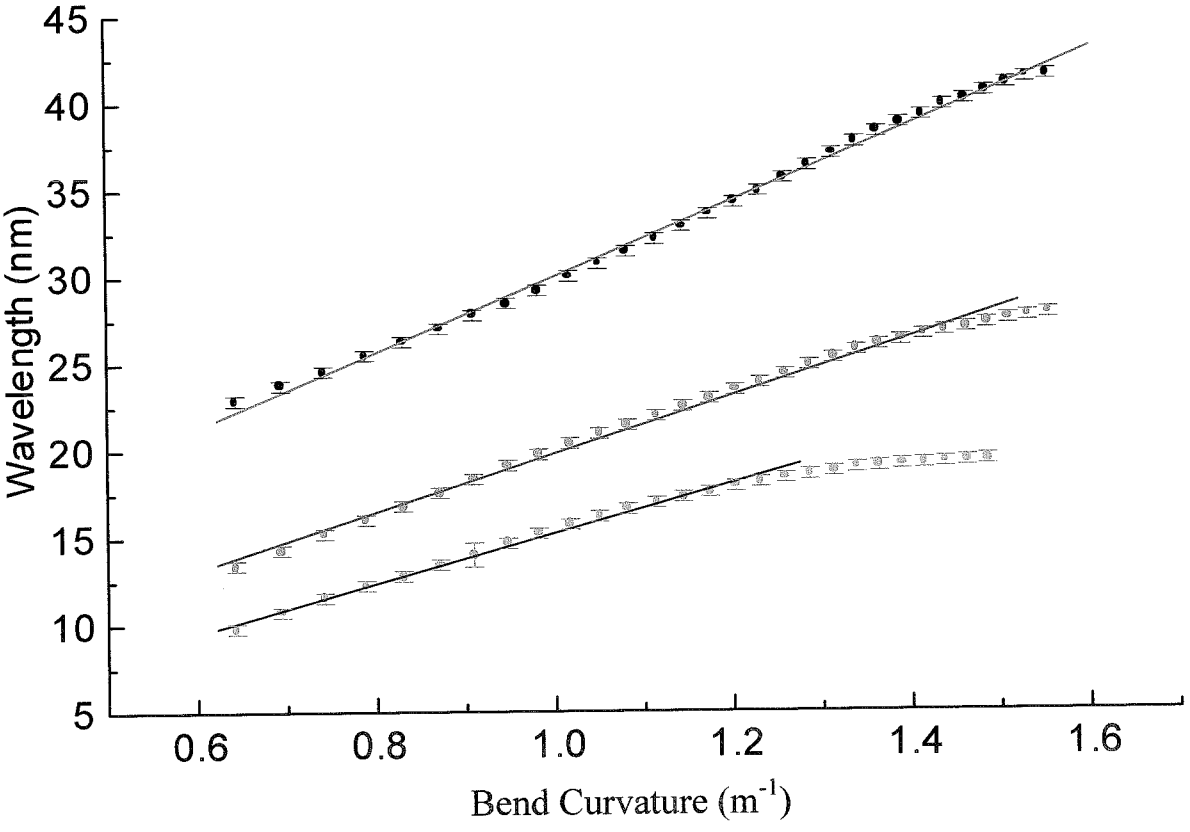

Figure 5.20: *Plot of wavelength separation of the divisions as a function of increasing bend curvature for the three attenuation bands ◍ attenuation band 4, ◍ attenuation band 5 and,● attenuation band 6.*

Figure 5.20, shows that within their linear regions the different attenuation bands have a different bend sensitivity. The bend sensitivity of the attenuation bands were, 14.28nm/m^{-1} for attenuation band 4, 16.59nm/m^{-1} for attenuation band 5 and 21.61nm/m^{-1} for attenuation band 6

5.5.4 Discussion

The attenuation bands of a LPG show sensitivity to bending. The attenuation bands in the transmission spectrum of the LPG have been observed to divide into two closely separated attenuation bands, with reduced depth. The divided attenuation bands division 1 and division 2 showed a negative and a positive linear response respectively, to the applied bend in the range $0.70m^{-1}$ to $1.65m^{-1}$. The wavelength separation between the divisions was observed to increase linearly for increasing bend curvatures, over a limited range. Each attenuation band had a different bend sensitivity. Within their linear regions the bend sensitivity of the attenuation bands ranged, from 14.28nm/ m^{-1} for attenuation band 4 to 21.61nm/ m^{-1} for attenuation band 6. The attenuation bands can be used as bend sensors.

5.6 Bend sensing of LPGs with rotation of the UV exposed face of the fibre.

5.6.1 Introduction

The bend sensitivity has been reported previously to be dependent upon the orientation of the plane in which the fibre is bent with respect to the orientation of the fibre during the LPG's fabrication [18]. Rotational dependence of the bend sensitivity of LPGs has been observed in highly Ge-doped fibre [36] and in fibre with a large concentricity error [41]. However, in normal single mode B-Ge photosensitive fibre this dependency has not been observed [40]. The dependency of the bend sensitivity on the orientation of the plane in which the fibre is bent with respect to the orientation of the UV irradiated side of the fibre during the LPG's fabrication is investigated in this section.

5.6.2 Experiment

During the fabrication of the LPG, the side of the fibre that was exposed to the UV beam was marked using two scotch tape flags as shown in Figure 5.21(a). When the fibre was rotated and bent such that the fibre's side that was exposed to the UV was on the inner surface of the curvature, the direction was defined as 0°, as shown in Figure 5.21(b). When the fibre was bent such that the fibre's side that was exposed to the UV was on the outer surface of the curvature, the direction was defined as 180°, as shown in Figure 5.21(c).

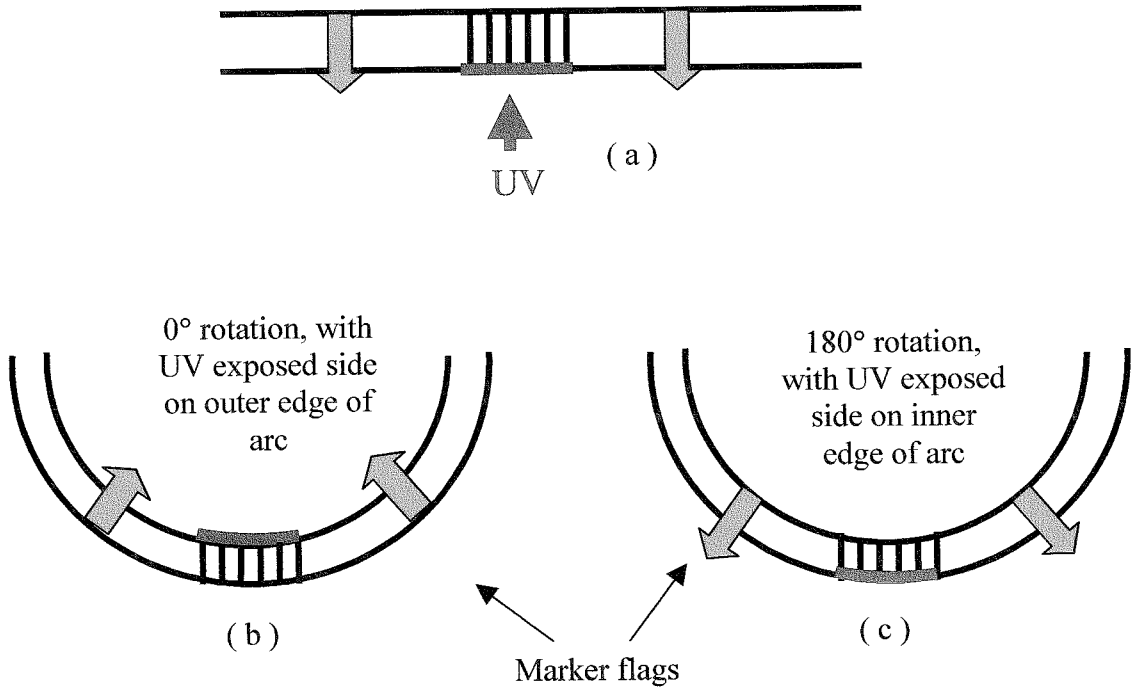

Figure 5.21: *Showing the fibre marked with tape (a) indicating the direction of UV irradiation, (b) UV exposed side of the fibre bent with a bend direction of 0° and (c) 180°.*

To facilitate the characterisation work the LPG bending module shown in Figure 5.16 was adapted, to that shown in Figure 5.22, to accommodate the rotation of the LPG's UV exposed face and the bending of the LPG through a series of bend curvatures.

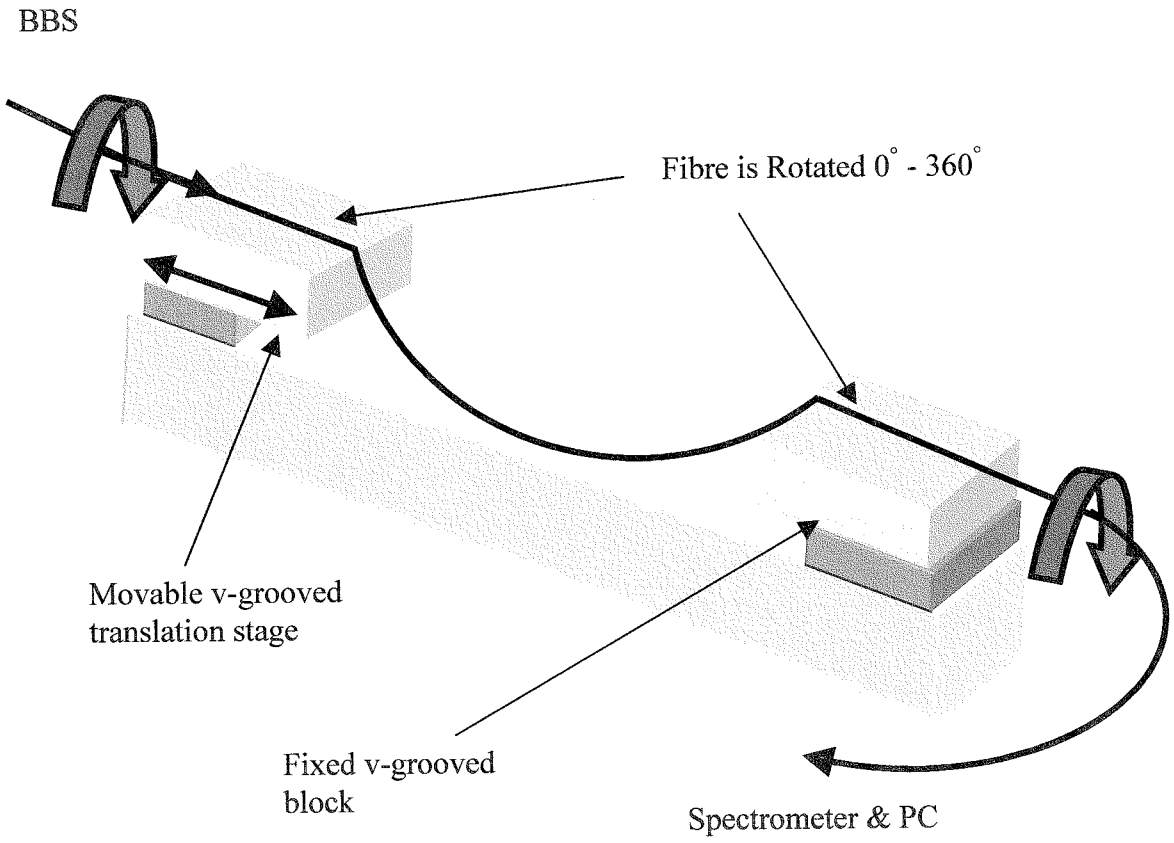

Figure 5.22: *LPG bending module adapted for applying a bend curvature to the LPG with respect to rotation of UV exposed side of the fibre.*

The bare fibre was held into the v-grooved blocks using magnets. The LPG was held with the UV exposed side at a known starting angle of 0°. The LPG was then bent through a series of bend curvatures over the range 0.6 – 1.6m^{-1}. The process was repeated rotating the LPG, in 30° increments, over the range 0° - 360° and at each angle the fibre was bent through the same bend curvature. The response of the transmission spectrum was observed using the general experimental configuration which was detailed in section 4.7.3 of Chapter 4 and the LPG's parameters are detailed in section 5.2.2. For each applied bend at every angle of rotation of the UV exposed side of the fibre, the central wavelengths of the associated divisions of attenuation bands 4-6 were recorded.

5.6.3 Results

The wavelength separation of the splits of the attenuation bands showed a linear response to the applied bend curvature over a curvature range of $0.6m^{-1}$ to $1.6m^{-1}$. The observation is illustrated in Figure 5.23, which plots the wavelength separation of attenuation band 6's splits, for a series of applied bend curvatures at bend directions of 0° and 180°.

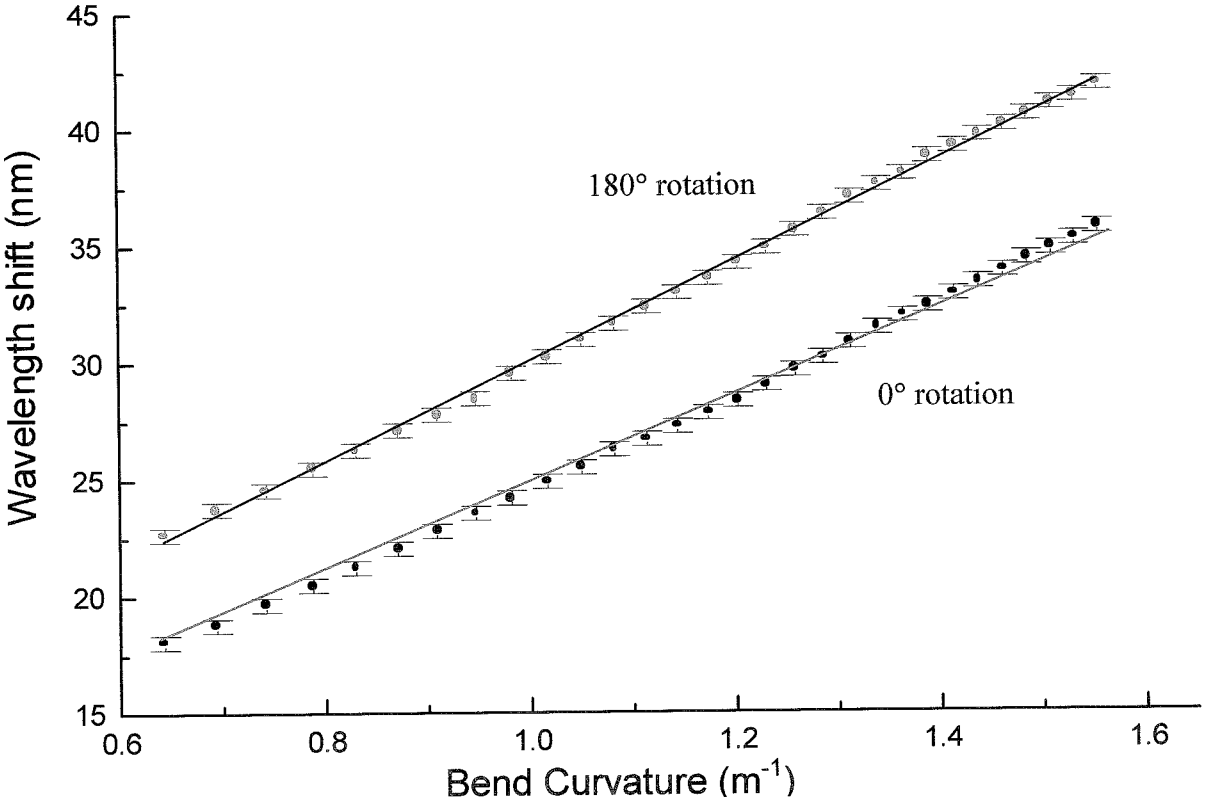

Figure 5.23: *Plot of wavelength shift as a function of increasing bend curvature for attenuation band 6 at two bend directions.* • *0°,* ◦ *180°.*

Figure 5.23 shows that the wavelength separation depends upon the orientation of the plane in which the fibre is bent relative to the orientation of the fibre during UV irradiation. The attenuation band has different bend sensitivity at the different angles of rotation. The bend sensitivity of the attenuation band was $20.45nm/m^{-1}$ at 180° and $21.87nm/m^{-1}$ at 0°.

Figure 5.24 plots for attenuation band 6 the wavelength separation of the splits as a function of angle of rotation at three increasing bend curvatures.

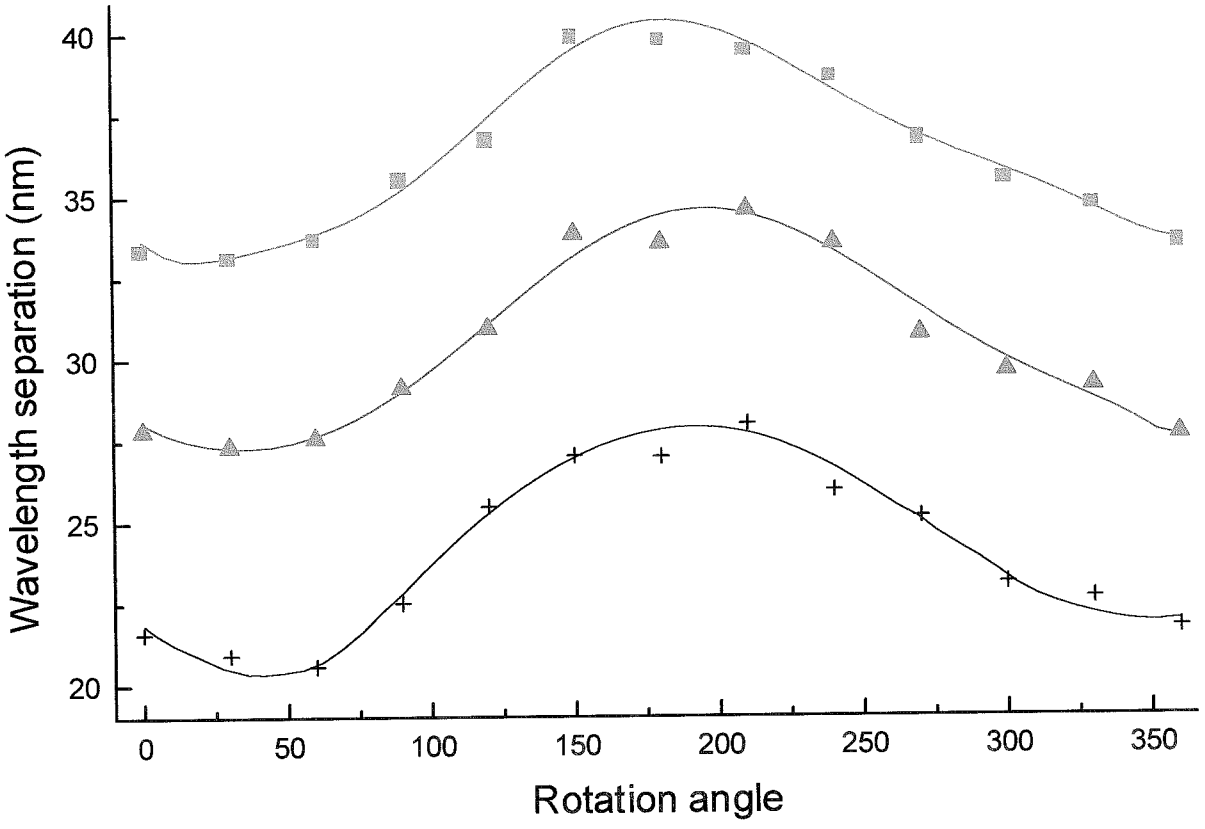

Figure 5.24: *Plot of wavelength separation between the divisions of attenuation band 6 plotted as function of rotational angle at three applied bend curvatures and their respective sine wave fits.* + *Response to an applied bend curvature of* $0.871m^{-1}$ *and associated sine fit* —— , ▲ *response to an applied bend curvature of* $1.174m^{-1}$ *and associated sine fit* —— *and* ■ *response to an applied bend curvature of* $1.438m^{-1}$ *and associated sine fit* ——.

The graph shows a sinusoidal response and a sine wave was fitted to each plot. The minimum point of the sine waves is at 30° instead of a 0°, the exact reason for this is not fully understood, however there are two possible explanations. The first is that the core concentricity error is responsible for the asymmetry in the splitting of the LPG's

attenuation bands for different bend directions [41]. The second is that the UV illumination direction has had an effect on the direction of the asymmetry [41]. Consequently, the experiment was repeated using 6 other LPGs that had been fabricated sequentially from the same roll of fibre. The orientation of the fibre in the translation stage prior to its exposure to UV and marking with 'flags' was random. Therefore, the effects of any core eccentricity would have been reduced. The plots, of the wavelength separation of the split attenuation bands as a function of rotational angle, for each LPG showed a minimum point at a rotation of 30°. Therefore, it can be concluded that the asymmetry in the splitting of the LPG's attenuation bands for different bend directions was an effect of the UV illumination direction. However, the exact effect of the UV illumination direction is not fully understood but is thought to be a result of an asymmetry introduced by a radially non-symmetric UV induced RI modulation. Such asymmetries have been used to account for similar effects in LPGs formed by CO_2 laser irradiation, where the asymmetry is more pronounced due to heating of the surface facing the laser beam [42].

It can be seen from Figure 5.24 that each of the wavelength separation against angle of rotation plots are displaced from each other and so this displacement, or wavelength offset, must be taken into account when sine waves are fitted to each of the plots. Each sine wave fit has a general form expressed in equation 5.3.

$$Y = A\sin(bx) + d \tag{5.3}$$

Where Y is the Wavelength separation, $\Delta\lambda$, of the split attenuation bands (nm), A is the amplitude of the fitted sine wave, b is the period of the response, x is the rotational angle expressed in radians and d is the offset wavelength due to the applied bend curvature. The relationship between offset wavelength and the applied bend curvature is determined by plotting Figure 5.25. Where the offset wavelength values for attenuation band 6 are plotted as a function of applied bend curvature.

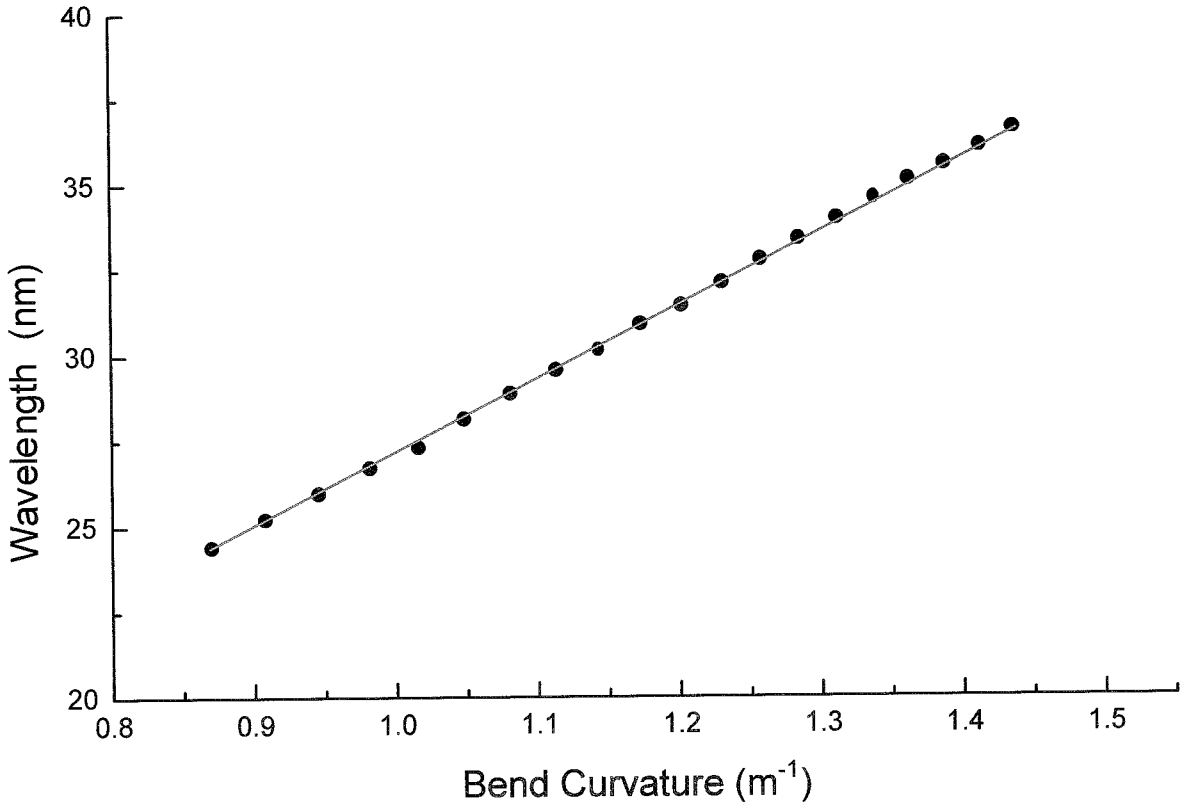

Figure 5.25: *Plot of the offset wavelength as a function of applied increasing bend curvature for attenuation band 6.*

Figure 5.25 shows that there is a constant wavelength offset for an increasing applied bend curvature. There is a linear relationship between the offset wavelength and the applied curvature a linear fit yields a gradient of 21.7 nm per m^{-1} and it crosses the offset axis at the point, 5.4 nm. The general form of the fitted sine wave equation, equation 5.3, can be rewritten as in equation 5.4.

$$\Delta\lambda = A\sin(bx) + (21.7 \times \text{curvature} + 5.4) \qquad (5.4)$$

Equation 5.4 can be used to determine the wavelength separation between the split attenuation bands for a known applied bend curvature.

The sinusoidal behaviour and the eccentricity demonstrated by attenuation band 6 in Figure 5.24 can be plotted onto a radial graph as shown in Figure 5.26.

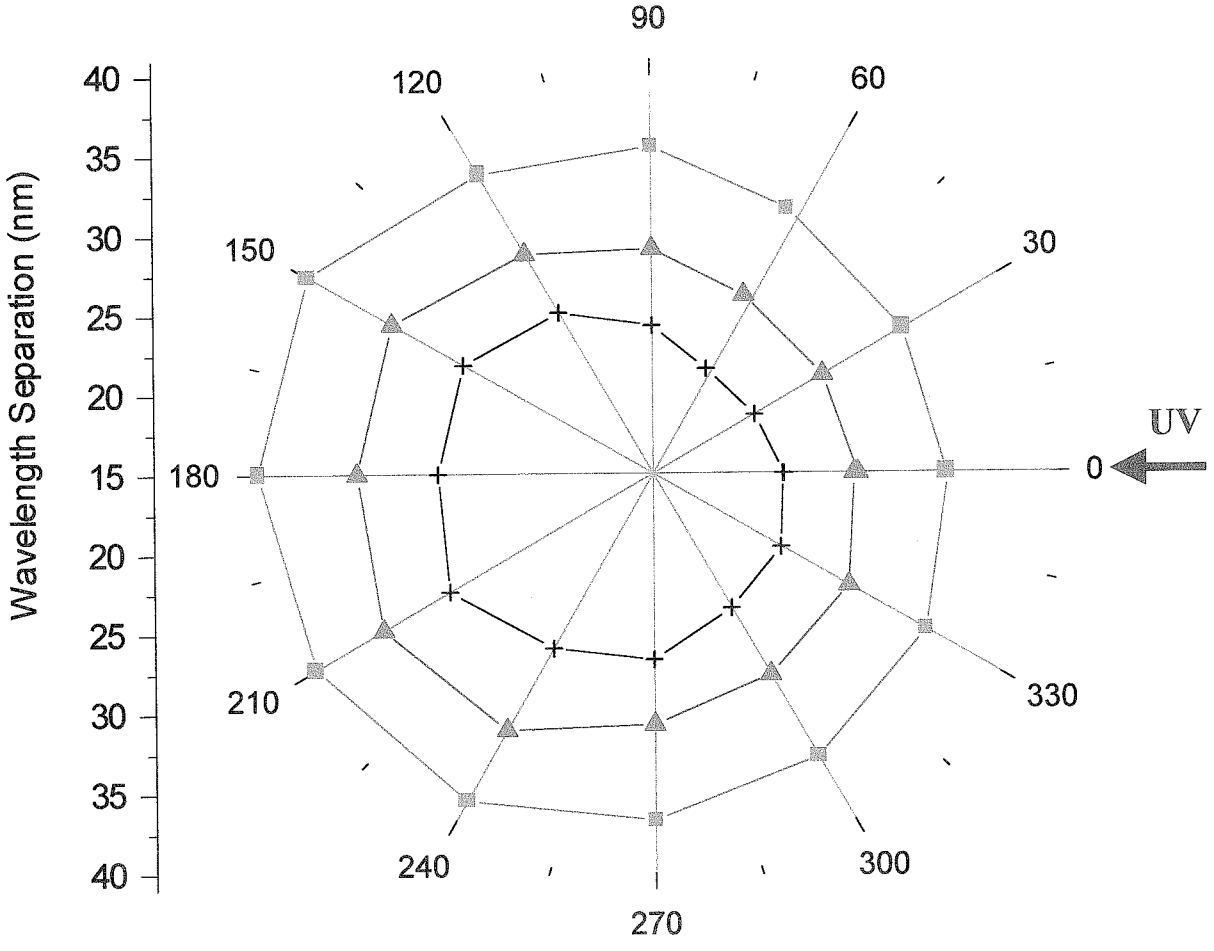

Figure 5.26: *Radial plot of wavelength shift as a function of the rotation for attenuation band 6 at three of the applied bend curvatures, + 0.871 m^{-1}, ▲1.174 m^{-1} and ■ 1.438 m^{-1}.*

Figure 5.26 illustrates that the wavelength separation of the divided attenuation bands is the same at 0 and 360° and that there is a minimum wavelength separation at 30°.

The dependence of the sensitivity on the order of the cladding modes, coupled to attenuation bands 5 and 6, to the measurand was also investigated. A graph of wavelength separation between the split attenuation bands of attenuation bands 5 and 6 as a function of bend rotation for a constant applied bend curvature is plotted in Figure 5.27.

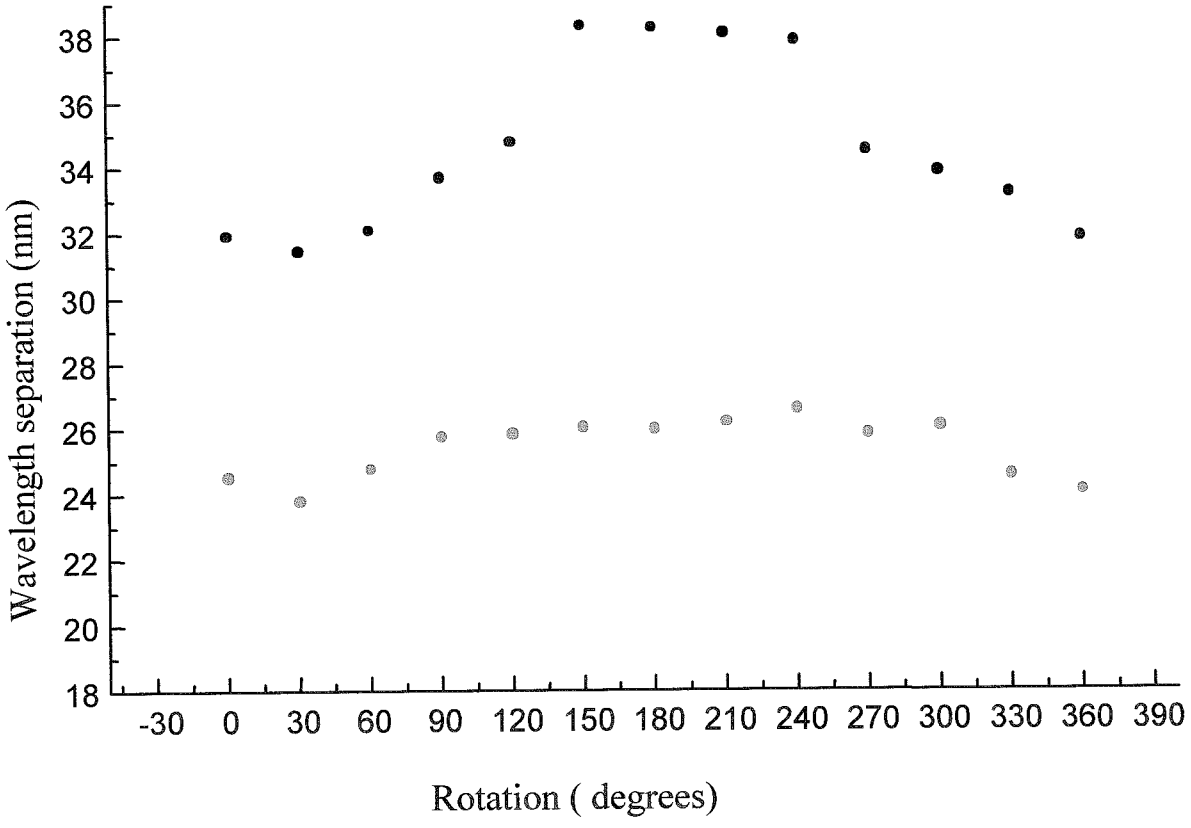

Figure 5.27: *Plot of the wavelength separation between the split attenuation bands of attenuation bands 5 and 6 as a function of rotation of bending at an applied bend curvature of 1.364m^{-1}, ◦ attenuation band 5 and • attenuation band 6.*

Figure 5.27 illustrates that for the same applied bend curvature the wavelength separation between the split attenuation bands of attenuation bands 5 and 6 have a sinusoidal response but with different amplitudes.

5.6.4 Discussion

The sensitivity of the wavelength separation of the divided attenuation bands shows a dependence on the orientation of the plane in which the fibre is bent relative to the orientation of the UV exposed side of the fibre. At each bending curvature the wavelength separation between the divided attenuation bands has a sinusoidal response when it is plotted as a function of the rotation angle of the UV exposed side of the fibre, this is illustrated in Figure 5.24. The sinusoidal response at each bending curvature has an offset wavelength that is dependent on the magnitude of the bending curvature, which is illustrated in Figure 5.25. The minimum point at a rotation of 30° is believed to be a result of the UV illumination direction. At the same bending curvature, the sinusoidal response of the wavelength separation between the divided attenuation bands of attenuation bands 5 & 6 have different amplitudes for rotation of the UV exposed side of the fibre, which is illustrated in Figure 5.27.

5.7 Chapter summary

A series of experiments have been performed to characterise the response of the LPG's transmission spectrum for the monitoring of variations in temperature, strain, RI and bending. Such characterisation experiments are important in order to forecast the behaviour of the LPG's transmission spectrum to the measurands when the LPG is utilised for sensing applications. It is important that the LPG is annealed, before use as a sensor, so that its transmission spectrum is 'fixed'. The annealing process has demonstrated to have an effect on the temperature sensitivity of the LPG. The temperature sensitivity of the LPG was reduced from 0.19nm/°C to 0.14nm/°C, after annealing at 200°C for 3 hrs. The post annealing response was stabilised provided the measurement range remained below the annealing temperature.

The strain sensitivity of the LPG's attenuation bands was found to be in the range 0.52pm/με to -0.06pm/με. Two of the attenuation bands demonstrated a positive response to strain whilst two others demonstrated a negative response. One of the attenuation bands, attenuation band 4, was found to be insensitive to strain. Attenuation

band 4 has demonstrated a sensitivity to temperature of 0.11nm/°C. This attenuation band could be used to measure temperature, the effect of which could be subtracted from attenuation band 6 to facilitate independent measurements of strain.

The sensitivity of the LPG to changes in the RI of its surrounding medium manifests itself as a decrease in the central wavelengths and in the minimum transmission value of the attenuation bands, as illustrated in Figure 5.13 and 5.14. The decrease in the central wavelengths was limited to when $n_{Ext} \leq n_{clad}$. The highest sensitivity was shown by the highest order mode and occurred when n_{Ext} approached n_{clad}, attenuation band 6 demonstrated a wavelength shift of 24.3nm. When $n_{Ext} = n_{clad}$, the cladding appears to be of infinite extent, and thus supports no discrete modes. Broadband radiation-mode coupling losses are then observed, with no distinct attenuation bands. For surrounding RI > than that of the cladding, the central wavelengths of the attenuation bands show a considerably reduced sensitivity, but a change in the form of the transmission spectrum is observed, in that the extinction of the attenuation bands is reduced, as illustrated in Figure 5.15. The presence of attenuation bands in this situation, where the cladding is no longer acting as a waveguide, is attributed to the existence of attenuated cladding modes, arising from Fresnel reflection, rather than total internal reflection, from the cladding/air interface.

The bend sensitivity of the LPGs manifested itself as a dividing in two of each attenuation band, as illustrated in Figure 5.17. Where the dividing of the attenuation bands is attributed to a breaking of the symmetry of the system that results in two degenerate spatial modes of the cladding becoming non-degenerate. The wavelength separation of the divided components increased with increasing bend curvatures, as illustrated in Figure 5.18. The wavelength separation of the divided components showed a linear dependence of 21.61nm/m^{-1} within a range of bend curvatures of 0.70m^{-1} to 1.80m^{-1}, as illustrated in Figure 5.19. This effect was also exhibited a dependence upon the orientation of the fibre. In this case the reference plane was defined by the orientation of the fibre during fabrication of the LPG, with the largest sensitivity corresponding to the surface of the fibre orientated towards the UV source on the outer surface of the bend, as illustrated in Figure 5.23. The wavelength separation of the

divided components plotted as a function of rotational angle showed a sinusoidal response with a minimum wavelength separation at 30°and not at 0°, this was thought to be a result of an asymmetry introduced by a radially non-symmetric UV induced RI modulation. The sinusoidal responses had a constant offset for increasing bend curvatures. The attenuation bands showed that for a fixed curvature their individual sinusoidal responses had different amplitudes. The wavelength separation of the divided components of the attenuation bands show high sensitivity to the external measurand and has been exploited to perform bend sensing, offering sensitivities of up to fifty times that previously reported LPG bend sensing [43].

References:

1 S.A. Vasiliev and O.I. Medvedkov, 'Long period refractive index fibre gratings: properties, applications and fabrication techniques', In Advances in Fibre Optics, Proc. of SPIE, **4083**, pp. 212 –223, (2000).

2 A.A. Abramov, A. Hale, R.S. Windeler and T.A. Strasser, 'Widely tuneable long period fibre gratings', Electron. Lett., **35**, pp. 81-82, (1999).

3 C.C. Ye, S.W. James and R.P. Tatam, 'Private Communication'.

4 Private communication with Carbolite Ltd.

5 V. Bhatia, D. Campbell and R.O. Claus, 'Simultaneous strain and temperature measurement with long period gratings', Opt. Lett., **22**, pp. 648-650, (1997).

6 V. Bhatia, A.M. Vengsarkar, 'Optical fibre long period grating sensors', Opt. Lett., **21**, pp. 692-694, (1996).

7 V. Bhatia, 'Applications of long period gratings to single and multi-parameter sensing', Opt. Exp., **4**, pp. 457- 466, (1999).

8 T. Erdogan, V. Mizrahi, P.J. Lemaire and D. Monroe, 'Decay of ultraviolet induced fibre Bragg gratings', J. Appl. Phys., **76**, pp. 73-80, (1994).

9 K.E. Chisholm, K. sugden and I. Bennion, 'Effects of thermal annealing on Bragg fibre gratings in boron/germania co-doped fibre,' J. Phys. D: Appl. Phys., **31**, pp. 61-64, (1998).

10 A. Othonos, 'Fibre Bragg gratings', Rev. Sci. Instrum., **68**, pp. 4309-4341 (1997).

11 A.M. Vengsarkar, P.J. Lemaire, J.B. Judkins, V. Bhatia, T. Erdogan and J.E. Sipe, 'Long period fibre gratings as rejection filters', IEEE, J. Lightwave Technol., **14**, pp. 58-64, (1996).

12 H. Patrick, S.L. Gilbert, A. Lidgard, M.D. Gallagher, 'Annealing of Bragg gratings in hydrogen loaded optical fibre', J. Appl. Phys., **78**, pp. 2940 – 2945, (1995).

13 Qin-Li, Wei-Zhan-Xiong, Wang-Quing-Ya, Li-Hui-Ping, Zhang-Yu-Shu, Goa-Ding-San, 'Abnormal shift of center wavelength in annealing long period gratings', Chinese Phys. Lett., **17**, pp. 28-30, (2000).

14 F. Bakhti, J. Larrey, P. Sansonetti, 'Annealing of long period gratings in standard hydrogen loaded fibre', Bragg Gratings, Photosensitivity, and Poling in Glass Fibres and Waveguides: Applications and Fundamentals. Tech. Dig. Williamsburg, VA. USA, pp. 350-354, Oct. 1997.

15 A.D. Kersey, M.A. Davis, H.J. Patrick, M. leBlanc, K.P. Koo, C.G. Askins, M.A. Putman and E.J. Friebele, 'Fibre grating sensors' J. Lightwave Technol., **15**, pp. 1442 – 14663, (1997).

16 C.C.Ye, ' Private Communication'.

17 C. Chaterjee, 'Laser Diode based FMCW Interrogation of Fibre Bragg Grating sensor array', Ph.D. thesis, Cranfield University, February 2000.

18 C.C. Ye, S.W. James and R.P. Tatam, 'Long period fibre gratings for simultaneous temperature and bend sensing', Opt. Lett., **25**, pp. 1007 - 1009, (2000).

19 D. Varelas, H.G. Limberger, R.P. Salathe and C. Kotrotsios, 'UV induced mechanical degradation of optical fibres', Electron. Lett., **33**, pp. 804-806, (1997).

20 R. Feced, M. P. RoeEdwards, S.E. Kanellopoulos, N.H. Taylor and V.A. Handerek, 'Mechanical strength degradation of UV exposed optical fibres', Electron. Lett., **33**, pp. 157-159, (1997).

21 D. Varelas, H.G. Limberger and R.P. Salathe 'Enhanced mechanical performance of single mode optical fibres irradiated by a CW UV laser, Electron. Lett., **33**, pp. 704-705, (1997).

22 D. Varelas, D.M. Costantini, H.G. Kimberger and R.P. Slathe 'Fabrication of high mechanical resistance Bragg gratings in single mode optical fibres with CW UV laser side exposure', Opt. Lett., **23**, pp. 397-399, (1998).

23 H.J Patrick, A.D. Kersey and F. Bucholtz, 'Analysis of the response of long period fibre gratings to external index of refraction', J. Lightwave Technol., **16**, pp. 1606-1612, (1998).

24 O. Duhem, J.F. Henninot, M. Warengham and M. Douay, 'Demonstration of long period gratings efficient couplings with an external medium of a refractive index higher than that of silica', Appl. Opt., **37**, pp. 7223-7228, (1998).

25 B.H. Lee, Y. Liu, S.B. Lee, S.S. Choi and J.N. Jang 'Displacements of the resonant peaks of a long period fibre grating induced by a change of ambient refractive index', Opt. Lett., **22**, pp. 1769 – 1771, (1997).

26 R. Hou, Z. A. Ghassemboy, A. Hassan, C. Lu and K.P. Doeker, 'Modelling of long period fibre grating response to refractive index higher than that of cladding', Meas. Sci. Technol., **12**, pp. 1709-1713, (2001).

27 B. H. Lee and J. Nishii, 'Cladding surrounding interface insensitive long period grating, ' Electron. Lett., **34**, pp. 1129-1130, (1998).

28 T. Erdogan and D. Stegall, 'Impact of dispersion on the bandwidth of long period fibre grating filters', Optical fibre Comm. Conf., **2**, pp. 280-282, OSA Tech. Dig. Series, (1998).

29 R.P. Espindola, R.S. Windeler, A.A. Abramov, B.J. Eggleton, T.A. Strasser and D.J. DiGiovanni, 'External refractive index insensitive air-clad long period grating', Electron. Lett., **35**, pp. 327-328, (1999).

30 T. Allsop, L. Zhang and I. Bennion, 'Detection of organic aromatic compounds in paraffin by a long period fibre grating optical sensor with optimised sensitivity', Optics Comm., **191**, pp. 181-190, (2001).

31 H.J Patrick, A.D. Kersey, F. Bucholtz, K.J. Ewing, B. Judkins and A.M. Vengsarkar, 'Chemical sensor based on long period grating response to index of refraction', in Proc. Conf. Laser Electro-opt., **11**, pp. 420-423, (1997).

32 R. Falciai, A.G. Mignani and A. Vannini, ' Long period gratings as solution concentration sensors', Sensors and Actuators B, **74**, pp. 74-77, (2001).

33 Data sheets supplied by Cargille for series 'A' liquids of RI 1.400 – 1.600

34 V. Bhatia, ' Properties and applications of long period gratings', PhD. Thesis Virginia Polytechnic and State University, Blacksburg, Virginia (1998).

35 Private conversation with the manufacturers of the fibre, Fibrecore Ltd.

36 H.J. Patrick, C.C. Chang and S.T. Vohra, 'Long period fibre gratings for structure bend sensing', Electron. Lett.,. **34**, pp. 1773-1775, (1998).

37 C.C.Ye, C. Wei, S. Khaliq, S.W. James, P.E. Irving and R.P. Tatam, 'Bend sensing in structures using long period optical fibre gratings', SPIE, 5th European Conf. on Smart Structures and Materials, Proc. SPIE, **4073**, pp. 311-315, Glasgow, Scotland, (2000).

38 V.V. Steblina, J.D. Love, R.H. Stolen, J.S. Wang, 'Cladding mode degeneracy in bent W- fibres beyond cut-off ', Opt. Comm. **156**, pp. 271-274, (1998).

39 Y. Liu, L. Zhang, J.A.R. Williams and I. Bennion, 'Bend sensing by measuring the resonance splitting of long period fibre gratings', Opt. Comm., **193**, pp. 69-72, (2000).

40 Y. Liu, L. Zhang, J.A.R. Williams and I. Bennion, 'Optical bend sensor based on measurement of resonance mode splitting of long period fibre gratings', IEEE Photon. Technol. Lett., **12**, pp. 531 – 533, (2000).

41 J. Rathje, M. Kristensen and J. Hubner, 'Effects of core concentricity error on bend direction asymmtery for long period fibre gratings', in Proc. BGPW '99, Fl, pp. 283-285, (1999).

42 G.D. VanWiggeren, T.K. Gaylord, D.D. Davies, E. Anemogiannis, B.D. Garrett, M.I. Braiwish and E.N. Glytsis, 'Axial rotation dependence of resonances in curved CO_2 laser induced long period fibre gratings', Electron. Lett., **36**, pp. 1354-1355, (2000).

43 Y.G. Han, B.H. Lee, W.T. Han, U.C. Paek and Y. Chung, 'Resonance peak shift and dual peak separation of long period fibre gratings for sensing applications', IEEE, Photon. Technol. Lett., **13**, pp. 699-701, (2001).

Chapter 6 Novel long period grating based sensor applications

6.1 Introduction

The characterisation of a LPG's sensitivity to the RI of its surrounding medium, achieved by total immersion of the LPG into different RI oils is detailed in section 5.6 of Chapter 5. The sensitivity was represented by the induction of a change in the attenuation bands' central wavelengths and minimum transmission values. The sensitivity has been previously reported [1, 2, 3, 4, 5, 6, 7, 8, 9] and exploited to demonstrate the measurement of the concentration of chemicals, for example, solutions of sodium chloride [10], calcium chloride [10], antifreeze with water [10, 11, 12] and of organic aromatics such as benzene and xylene [13]. The sensitivity has also been employed to tune the transmission spectrum of a LPG [14, 15]. This chapter exploits the sensitivities of a LPG's transmission spectrum to the RI of its surrounding medium to demonstrate three novel LPG based sensors.

6.2 A liquid level sensor

6.2.1 Introduction

Liquid level sensing is a requirement in many applications in which knowledge of the volume of a liquid is necessary, for example, in fuel storage systems and chemical processing. A wide range of liquid level sensing techniques have been reported based around mechanical [16], electrical [17], and optical [18, 19, 20, 21, 22, 23] methods. The mechanically based sensing techniques are usually unsuitable because of the limited durability of the moving parts and this is particularly undesirable in heavily used remote sensing areas. The electrical techniques are limited to use outside the oil and gas industries. The currently available optical techniques are either limited to monitoring one liquid level or are overly complicated and cumbersome. The aim of this

section is to investigate the sensitivity of a LPG's transmission spectrum to partial immersion of the LPG in bulk RI material with a view to demonstrating a liquid level sensor.

6.2.2 Existing fibre optic based liquid level sensors

Electrical liquid level sensors are widely employed but their applicability is compromised if the liquid to be monitored is conductive or if the environment is potentially explosive [24]. Optical fibre sensors offer well-established advantages under these conditions. The optical fibre is a dielectric and thus is non-conducting and the sensor may be configured so that the light is confined within the fibre, reducing the likelihood of ignition in a flammable environment [24].

One of the previously reported fibre optic liquid level sensing technique is based on the bend loss induced attenuation of the transmission through coils of multimode fibre [20]. The sensor is formed by coils of successively decreasing radius of curvature, orientated in two opposite directions and immersed vertically in the liquid, as illustrated in Figure 6.1.

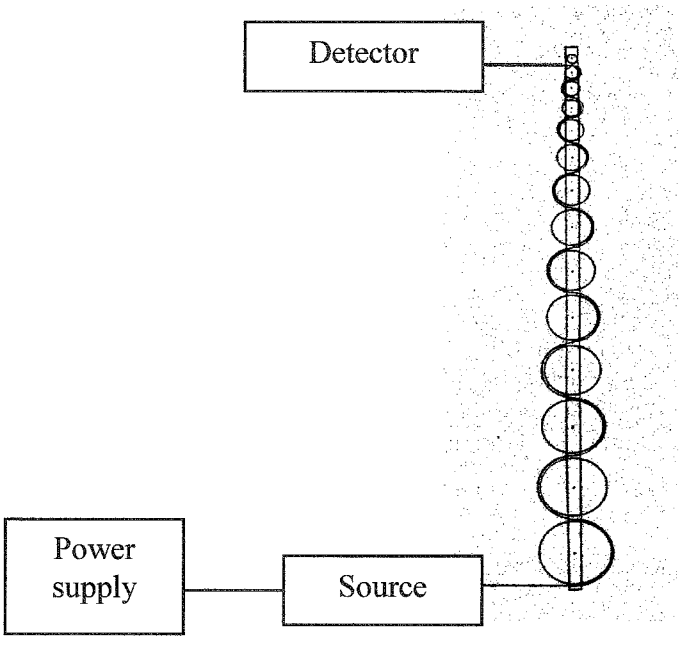

Figure 6.1: *The multimode fibre coils of successively decreasing radius of curvature are orientated in two opposite directions and immersed vertically in the liquid.* Diagram reproduced from [20].

The bend loss is a function of the radius of curvature and of the RI of the surrounding liquid provided the RI of the liquid is higher than that of the fibre's cladding [20]. As the liquid level increases so, the attenuation increases [20]. If the RI of the liquid is lower than that of the fibre's cladding then the cladding modes would continue to propagate in the fibre and would not be lost into the liquid. Therefore, there would be no attenuation of the transmitted power. The sensitivity is limited by the bend curvature that can be applied to the fibre without compromising its integrity and by the dimensions of the liquid's container. The measurement range of the sensor is limited by the number of successive multiple bends in the fibre [20]. This liquid level sensor is an example of an intrinsic intensity modulated sensor with indirect sensing. Intensity based sensing schemes generally suffer from interference of fibre bending loss and from unwanted fluctuations in the optical signals. Measurand induced intensity modulations in the measurement signal cannot be distinguished from anomalous intensity variations resulting from fluctuations in the source output power or from variable losses within optical components in the sensing system. [20].

Other level sensing techniques generally rely upon the interaction of the tip of the fibre with the surface of the liquid [22, 23], or upon the transmission of light to, and reception of the reflected light from, the surface of the liquid [21]. The techniques that rely on the interaction of the sensor's tip with the liquid are based on the total internal reflection, TIR, of light, which is disturbed by contact with a liquid [22, 23]. The principle of operation of such sensors is illustrated in Figure 6.2(a) and 6.2(b).

When the tip is surrounded by air the light travelling in the transmitting fibre for which the TIR conditions at the interface between the fibre cladding and the air is met, will travel into the core of the receiving fibre and onto a detector. When the tip is immersed in a liquid, the TIR at the tip of the sensor is no longer fulfilled. In this case, light will be lost into the liquid and consequently the optical power at the detector will decrease.

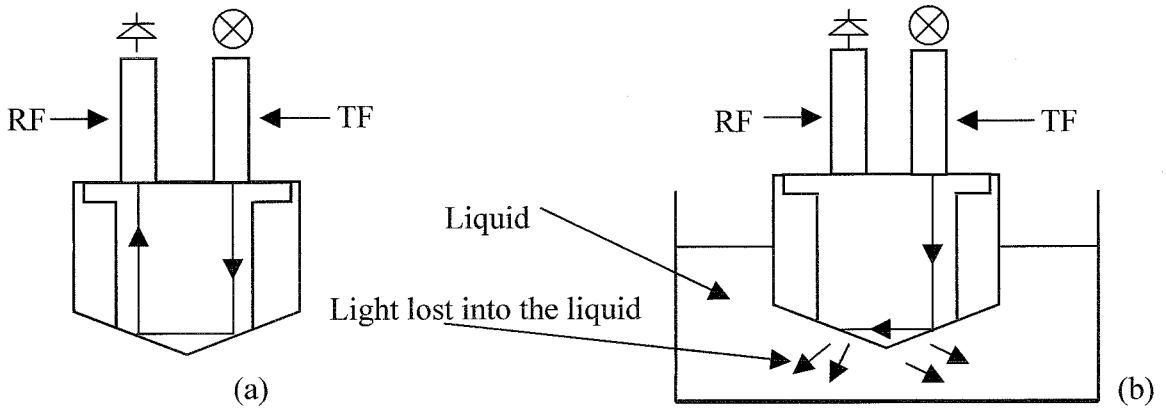

Figure 6.2: *Principle of operation of a sensor based on the TIR of light: (a) the sensor in air (b) the sensor in liquid:* ⊗ *light source,* ⏄ *: detector, TF: transmitting fibre & RF: receiving fibre.*

A liquid level sensing system incorporating a light source, 5 photodiode detectors and 5 sensor tips has been previously reported [22]. Each sensor tip consists of two spliced multimode fibres one termed the lead-in, transmitting, fibre and the other termed the lead-out, receiving, fibre. A schematic of the sensor is shown in Figure 6.3. Light from the source propagates to the sensor tip through the lead-in fibre. At the sensor tip, the light is partially reflected. The reflected light travels along the parallel lead-out, fibre to the detector.

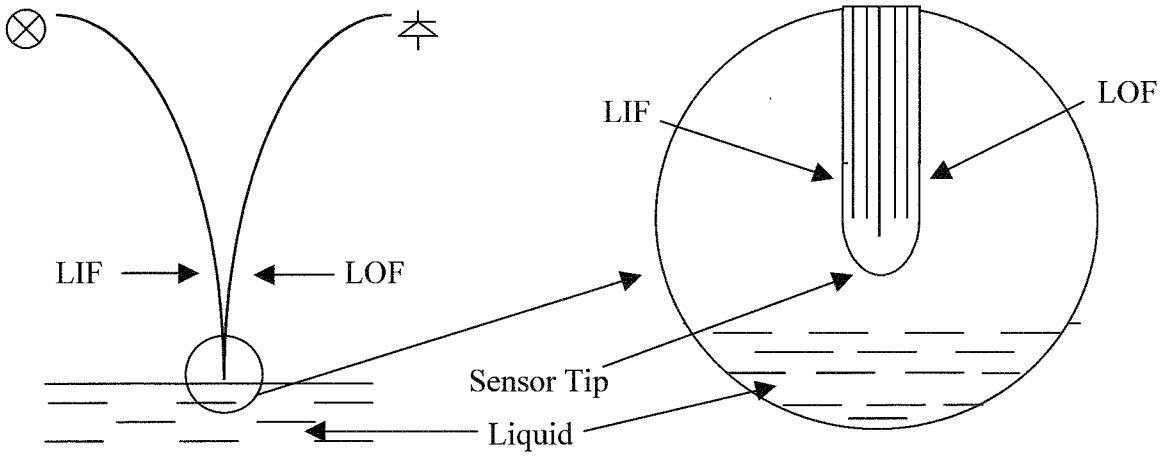

Figure 6.3: *Schematic of a multi-mode fibre optic based liquid level sensor. LIF: Lead-in fibre, LOF: Lead-out fibre,* ⊗ *Light source,* ⏄ *photodiode.* Diagram reproduced from [22].

Therefore, when the tip is surrounded by air the light for which the TIR conditions at the interface between the fibre cladding and the air is met, will travel in the core of the lead-out fibre and onto the detector. If the tip is immersed into a liquid, part of the incident light travelling in cladding modes will be lost at the sensor tip and the reflected power will decrease. The accuracy of the liquid level is limited to the distance between the sensor tips, which were located vertically at 200mm intervals in the container of liquid. In addition, when the liquid level falls below any of the sensor tips a drop of the liquid may adhere to it, thus providing an inaccurate reading [18]. These effects depend strongly on the viscosity of the liquid being measured [22, 23].

The change in the intensity of light that has been transmitted to, and is reflected from, the surface of the liquid has been used to determine the height of a liquid [21]. Light from a LED is transmitted onto the surface of the liquid, via two transmitting fibres, light which is reflected back from the surface is collected using two receiving fibres. One of the receiving fibres is used to provide as reference signal, as is illustrated in Figure 6.4.

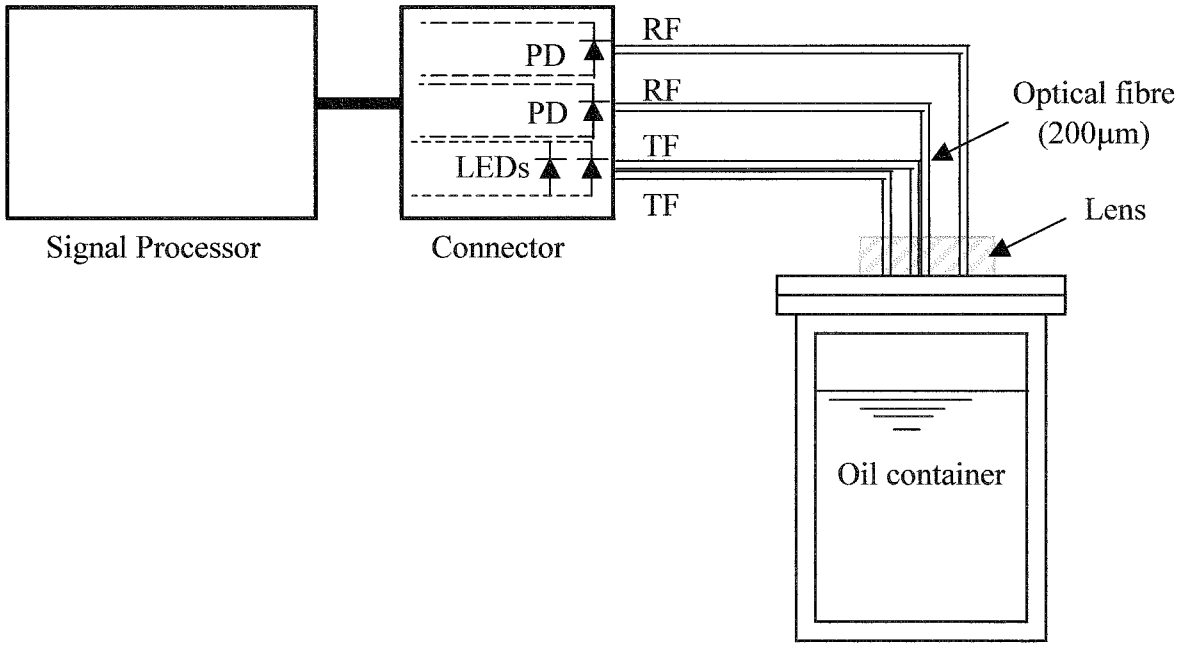

Figure 6.4: *Arrangement of an intensity based liquid level sensor, PD: Photodiode, TF: Transmitting fibre & RF: Receiving fibre.* Diagram reproduced from [21].

The height of the liquid is determined by the power collected by the remaining receiving fibre, measured by a photodiode. The discrepancy in measured height due to the variations in the intensity of the received light, which may be caused by external disturbances and temperature changes, is eliminated by division of the power of the reflected and reference signals. The sensing technique makes continuous measurements and is non-intrusive, as the sensor is positioned above the liquid, in the lid of the container. The measurement range is limited to 100mm with an accuracy of 1% at full-scale deflection [21].

However, to date none of the liquid level sensors exploit the influence of the liquid upon the fibre modes as the means of transduction. The next section presents a liquid level sensor where the form of the LPG's transmission spectrum is dependent upon the fraction of the length of the LPG that is surrounded by the liquid.

6.2.3 Principle of operation of the proposed liquid level sensor

When a LPG is partially immersed within a liquid then it can be considered as two separate gratings, one surrounded by air and the other surrounded by the liquid. This is illustrated in Figure 6.5, where the effective length of the two gratings is determined by the height of the liquid (l), which is determined from the position of the bottom of the liquid's meniscus. The effect of partially surrounding the LPG with the liquid is that for each cladding mode the transmission spectrum will contain two attenuation bands. One of the attenuation bands is centred at the coupling wavelength of the core mode with the cladding mode under the influence of the air surrounding (A), while the other is at the coupling wavelength of the core mode to the same cladding mode under the influence of the RI of the liquid (B). This effect is shown in the schematic diagram, Figure 6.6, which illustrates the splitting of the attenuation band into two bands.

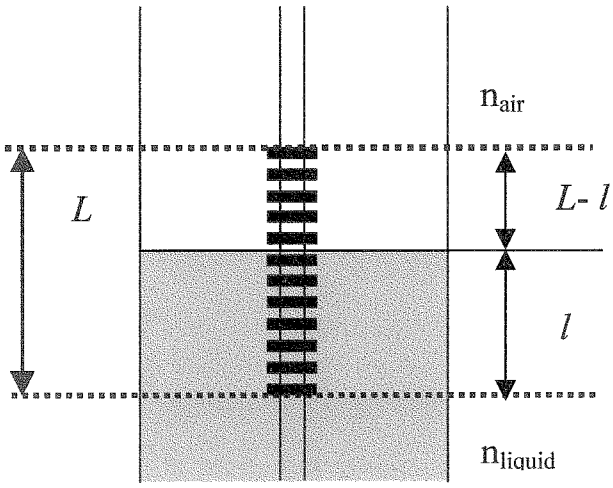

Figure 6.5: *Schematic of the LPG partially immersed in liquid of RI 1.456. This effectively creates two LPGs; the effective length of each of the two gratings is determined by the height of the liquid (l) when the length of the LPG is (L).*

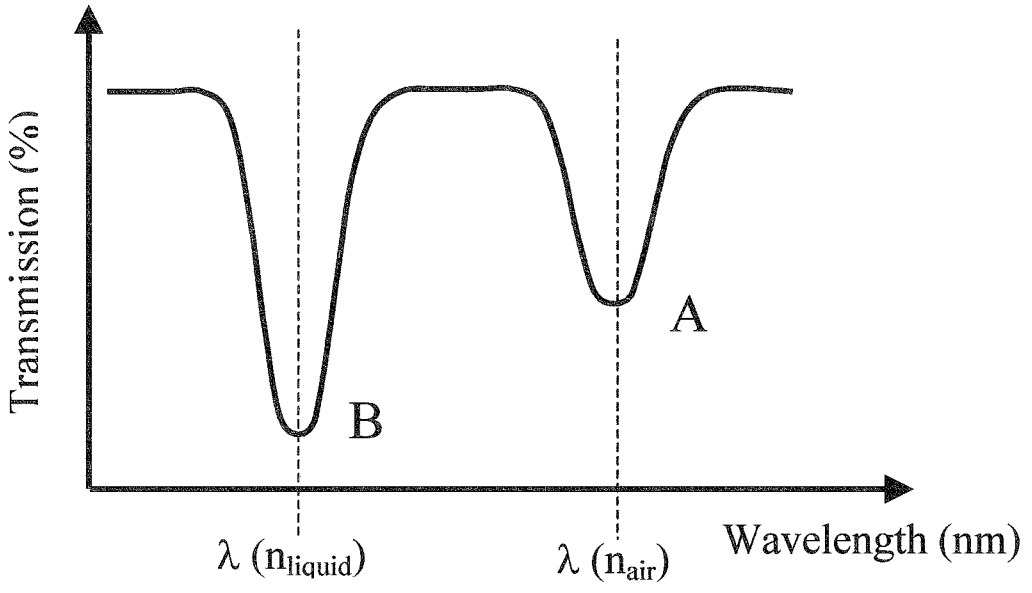

Figure 6.6: *The splitting of the attenuation band into two smaller attenuation bands located at the wavelengths corresponding to the coupling conditions for the LPG surrounded by the liquid and by air respectively.*

This liquid level sensor exploits the RI sensitivity of the LPG and the dependence of the minimum transmission values of the attenuation bands upon the length of the LPG that is immersed in the liquid. The minimum transmission value and width of the attenuation band are determined by the coupling efficiency between the core and cladding modes [2] and by the length of the LPG. The minimum transmission value of the attenuation band is related to the length of the LPG [2] as discussed in section 2.6.1 of Chapter 2. The RI sensitivity of the central wavelength of the attenuation bands of the LPG arises from the dependence of the cladding mode's effective RI upon the RI of the surrounding material. This allows the use of the LPGs as RI sensors based on the changes in the wavelength and/or the minimum transmission, of the attenuation bands in the LPG's spectrum.

For the attenuation band A to be fully developed the LPG it totally surrounded by air and similarly for attenuation band B to be fully developed the LPG has to be totally surrounded by the RI liquid. The LPG is being considered as two separate LPGs, using equation 2.24 in Chapter 2, the minimum transmission values of the attenuation bands A and B, T_A and T_B respectively are dependent upon the length of the LPG immersed in the liquid l, as given by equations 6.1 and 6.2. Where the coupling efficiency between the core and cladding mode at the central wavelength of attenuation bands A & B are given by κ_A & κ_B, respectively.

$$T_A = 1 - \sin^2(\kappa_A(L - l)) \tag{6.1}$$

$$T_B = 1 - \sin^2(\kappa_B l) \tag{6.2}$$

Equation 2.25 of Chapter 2, shows that for the condition of complete power transfer from core to cladding modes at the central wavelength of the attenuation bands corresponds to $\kappa L = \pi/2$. Substituting this value into equations 6.1 & 6.2 thus yields

$$T_A = T(L)\sin^2\left(\frac{\pi}{2}\left(\frac{L - l}{L}\right)\right) \tag{6.3}$$

$$T_A = T(L)\sin^2\left(\frac{\pi}{2}\left(\frac{l}{L}\right)\right) \tag{6.4}$$

where the expressions are valid in the range $0 < l < L$.

6.2.4 Experiment - Liquid level sensor

The LPG used in the experimental work was fabricated in boron-germanium co-doped photo sensitive silica single mode optical fibre (Fibrecore PS750), which had a cut off wavelength of 650nm. The RI of the fibre had been modulated by exposure to UV irradiation, at a wavelength of 266nm, through an amplitude mask, as detailed in section 4.8 of Chapter 4. Whilst the LPG was still in position behind the amplitude mask the approximate beginning and the end of the LPG were marked with coloured permanent ink. The LPG had a length of 40mm and a periodicity of 400μm; had previously been annealed at 200°C for 3 hours. The transmission spectrum of the LPG was monitored by coupling the output of a broad band light source into an optical fibre containing the LPG. The output from the fibre was coupled into a PC interfaced CCD spectrometer, Ocean Optics S2000, with a resolution of 0.7nm, and a minimum integration time of 1sec. The general experimental configuration is shown in Figure 4.8 of Chapter 4.

The response of the LPG's transmission spectrum to partial immersion into the liquid was investigated using the experimental configuration shown in Figure 6.7. The 1.00ml dispensing, upper, and receiving, lower, syringes were graduated in 0.01ml increments. A travelling microscope was used to measure the distances between the lower edges of 60 adjacent graduations on the receiving syringe, the average distance was calculated to be 0.57mm. The supports were designed to securely hold the syringe centrally with respect to the v-grooves of blocks 1 and 2 so when the LPG was fixed in position it would be equidistant from the syringe walls. The fibre containing the LPG was passed down centrally inside the body and out through the nozzle of the receiving

medical syringe. The bare fibre was temporarily secured in the v-grooves using magnets, such that the mark indicating the approximate beginning of the LPG coincided with the graduation labelled 0.05ml. The straight and taut fibre was fixed into the v-grooved blocks using wax. This was to avoid any bend induced distortion of the LPG's transmission spectrum [25]. The wax, supplied by Radio Spares, melted at approximately 80°C. The bare fibre was secured centrally within the lower part of the nozzle using the wax. The wax in the nozzle served two purposes, firstly to hold the fibre so that it did not touch the inner wall of the syringe and secondly to seal the nozzle so that the liquid did not flow out. A test tube stand and clamp were used to position and hold the dispensing syringe such that its needle was inside the receiving syringe. The needle was orientated so that the dispensed liquid would not fall directly onto the fibre nor run down the inner wall of the syringe. If the liquid fell directly onto the fibre and covered the LPG, this would provide a false measurement. In addition, if the liquid ran down the inner wall of the syringe then a delay would occur in taking that measurement of the liquid level as the dose of liquid settled in the syringe. The liquid was introduced into the recipient syringe in doses of approximately 0.01ml. The transmission spectrum, the attenuation bands' minimum transmission values and central wavelengths were recorded as a function of the liquid level.

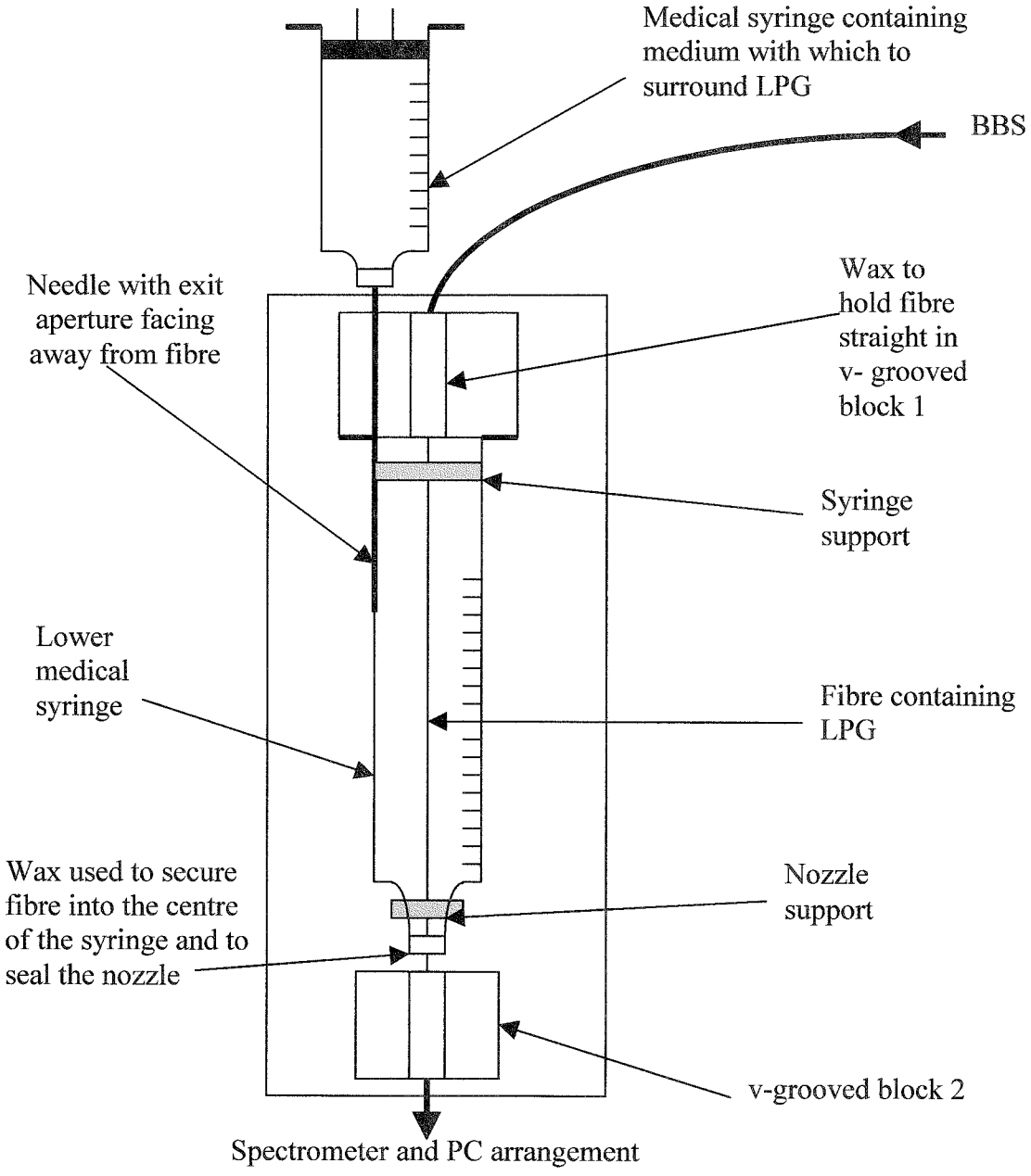

Figure 6.7: *Experimental configuration used to investigate the use of a LPG as a liquid level sensor.*

6.2.5 Results

The RI liquid selected for the investigation had a RI of 1.456, as it had produced the greatest wavelength shift in the attenuation bands during the characterisation work detailed in section 5.6 of Chapter 5. The RI was quoted as being measured at a wavelength of 589.3nm at 25°C. The liquid had a negative RI temperature coefficient of 0.000391nm/°C within a temperature range of 15°C - 35°C [26].

When the LPG was surrounded by air, the attenuation band corresponding to coupling to the 6^{th} order cladding mode was centred at 1032 nm. When the LPG was totally immersed in the liquid, the attenuation band was centred at 1008 nm. Figure 6.8 illustrates the development of the attenuation bands at three liquid levels. The change in the minimum transmission value and width of the attenuation bands with increasing liquid level can be observed, which is in agreement with Figure 6.6. The value of T_B at $l = L$ does not equal that of T_A at $l = 0$, the difference arises due to the coupling efficiency between the core and cladding mode at the central wavelength of attenuation band B.

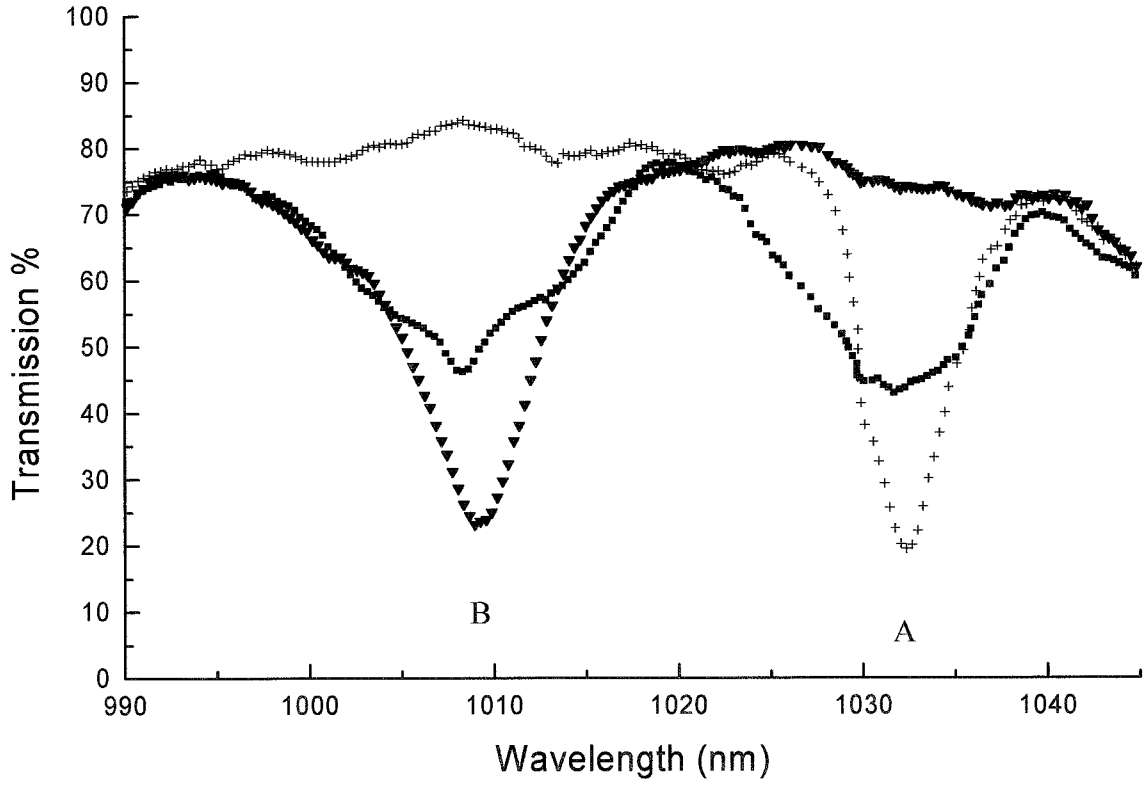

Figure 6.8: *Transmission spectra of the LPG, showing the response of the attenuation band corresponding to coupling to the 6th cladding mode under the following conditions, + surrounded by air, ■ with 60 % of the LPG surrounded by liquid of RI 1.456 and▲ the total immersion of the LPG in liquid of RI 1.456. The attenuation band **A** is observed when the LPG is surrounded by air and the attenuation band **B** is observed when the LPG is totally immersed in liquid of RI 1.456.*

When recording the transmission spectrum of a LPG, the measured transmission is generally normalised to the transmission prior to the LPG's inscription. This method is, however, prone to noise resulting from inconsistency in the coupling of light into the fibre, losses and misalignment at connectors, and also to losses induced by the UV exposure which are prominent at the longer wavelengths of our measurement range. To overcome these problems a reference transmission spectrum was recorded with the LPG surrounded by air, which was subtracted from the subsequent spectra to yield a difference spectrum such as that shown in Figure 6.9.

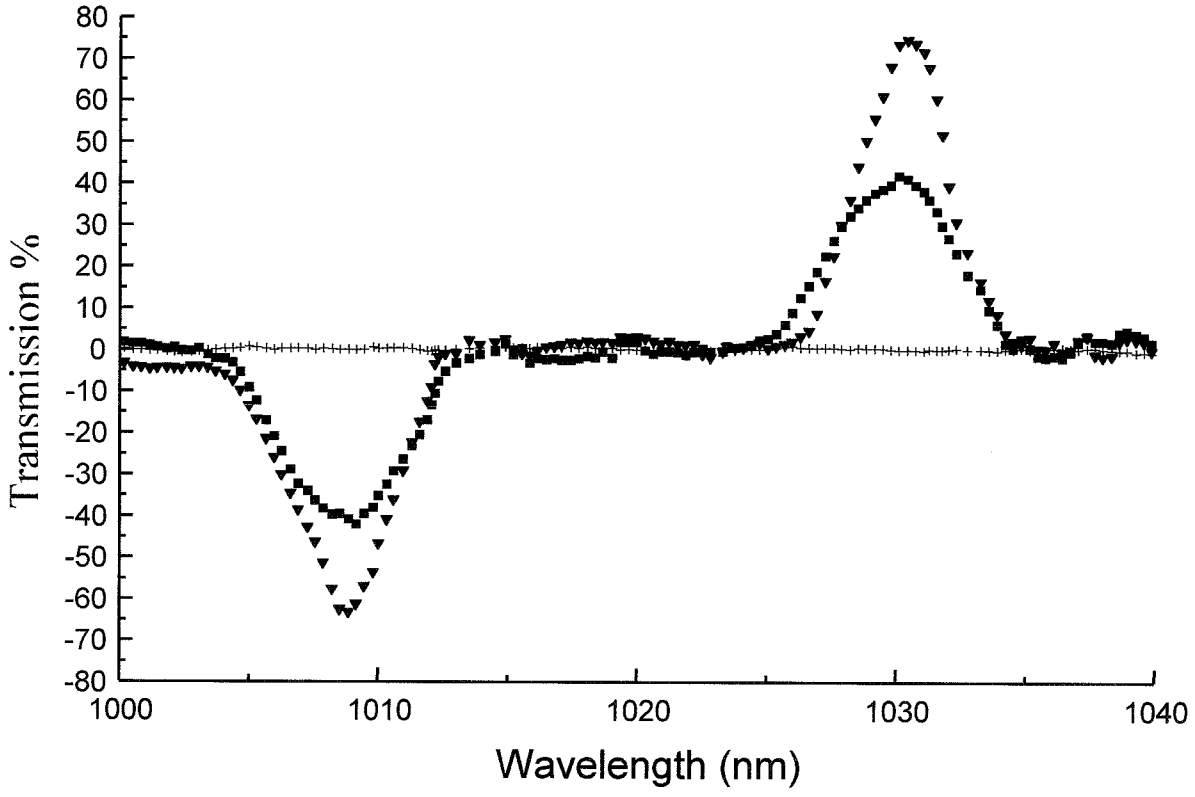

Figure 6.9: *Change in the normalised transmission spectrum of the LPG for three different liquid levels. + in air, ■ 60 % of the LPG surrounded by liquid of RI 1.456, ▲ total immersion of the LPG in liquid of RI 1.456. The normalisation was performed by subtraction of a reference spectrum recorded with the LPG surrounded by air.*

The noise present on the spectra of Figure 6.8 has been largely removed by this procedure. The peak, in Figure 6.9, arises from the decrease in the attenuation at the coupling wavelength corresponding to the LPG being surrounded by air, while the trough arises from the increased attenuation at the coupling wavelength corresponding to the LPG being surrounded by the liquid. In Figure 6.10, the change in the minimum transmission value of the LPG at the two wavelengths are plotted as a function of the % of the LPG immersed in the RI oil. Also plotted are the theoretical predictions using equations 6.4 and 6.5.

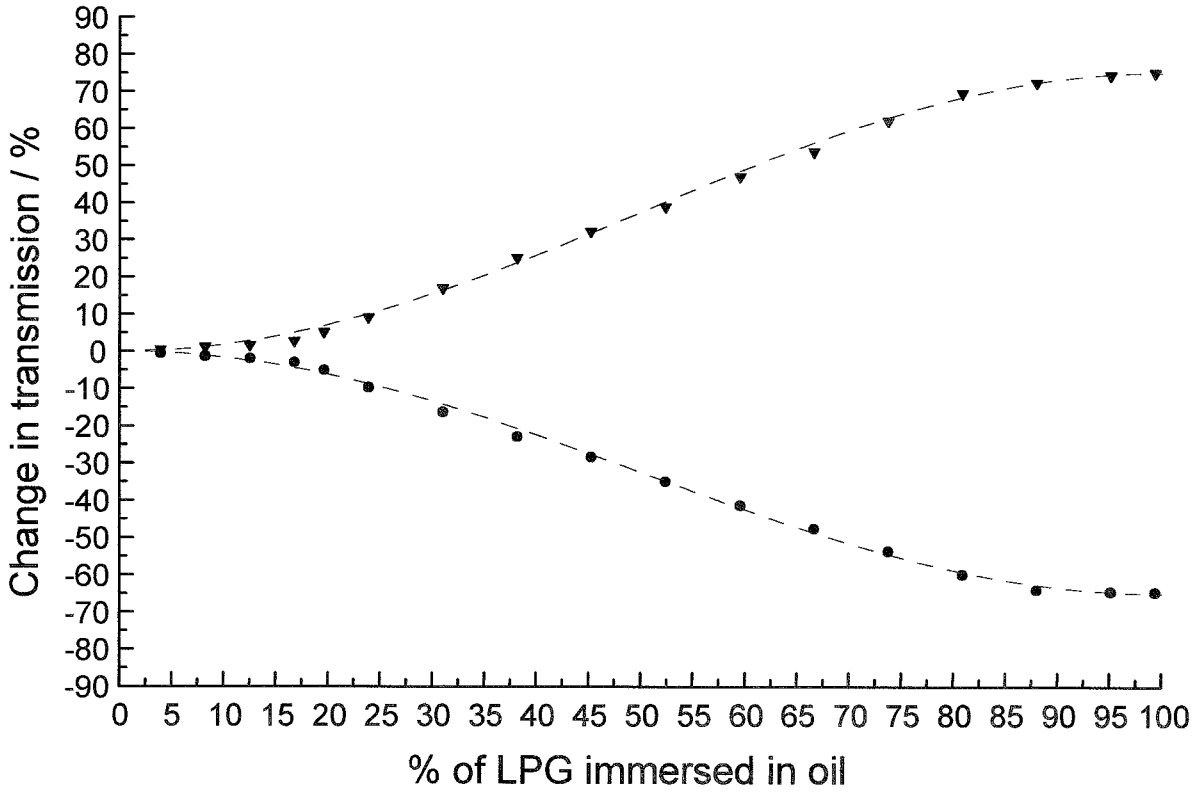

Figure 6.10: *Plot of the change in transmission measured at the two coupling wavelengths as a function of the % of the LPG immersed in the liquid of RI 1.45,* ● *Amplitude of the trough,* ▲ *Amplitude of the peak,* - *Theoretical predictions.*

The behaviour of attenuation bands A & B as a function of l is in accordance with the expected decrease and increase in the values of T_A and T_B respectively. The experimental results are in good agreement with the theoretical prediction. The relative changes in the extinction of the attenuation bands (ΔT) was calculated using simple subtraction. Figure 6.11 plots the relative changes in the extinction of the attenuation bands (ΔT) as a function of the % of the LPG immersed in the RI liquid.

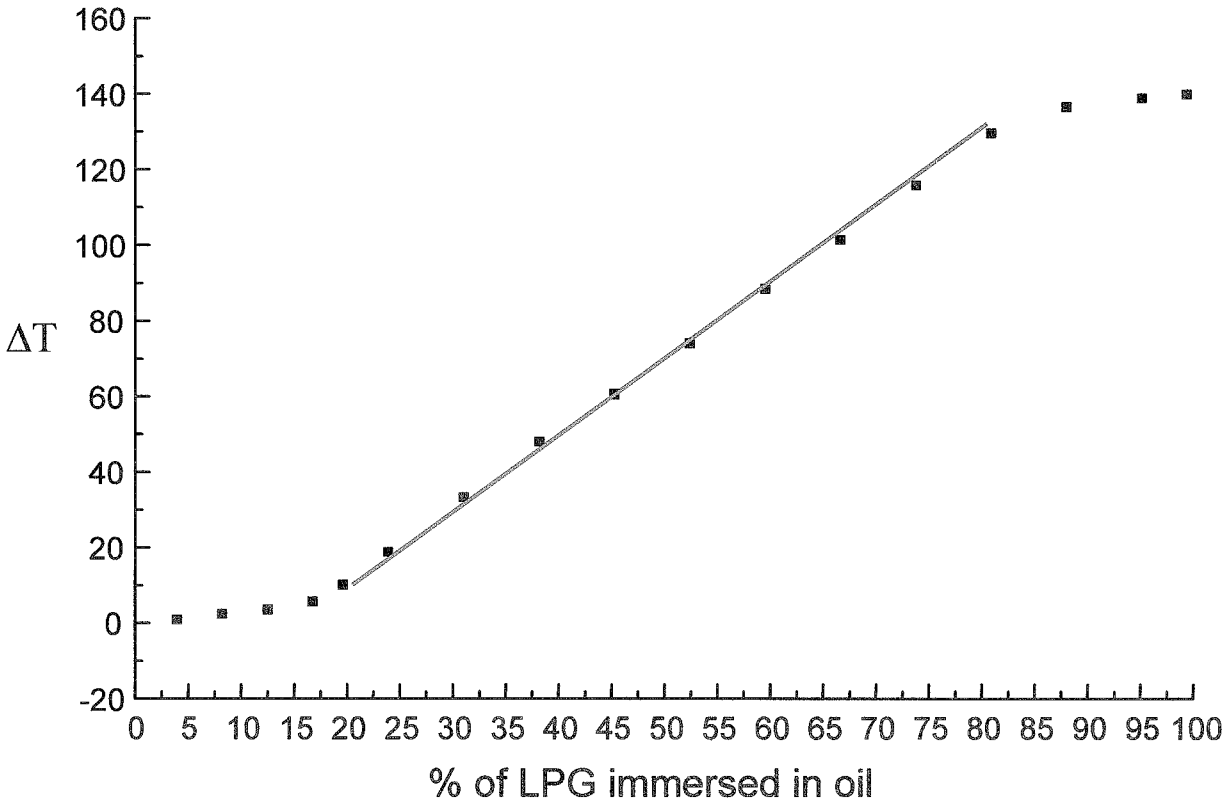

Figure 6.11: *Plot of the difference in the two curves shown in Figure 6.6, ΔT, as a function of the % of the LPG immersed in the liquid.*

This provides a large linear response over ≈ 62% of the overall length of the LPG with a sensitivity of 2% ±0.02 change in the transmission / % length of the LPG. This corresponds to a sensitivity of 4.8% change in transmission / mm length of the LPG.

6.2.6 Discussion

LPGs are known to possess large temperature sensitivities [27], and the liquid's RI will show a temperature sensitivity, both of which will induce a change in the coupling wavelengths. It is possible to ensure that this system is insensitive to these effects by using a reference spectrum that is continually updated, by employing a reference LPG that is fully covered by the liquid and experiences the same thermal environment. In this way, the extinction provides the measurement of the liquid level

while the central wavelengths and their separation, ΔT, allow the temperature and RI of the liquid to be determined. Alternatively, this information may be determined directly from the spectrum. A method of reducing the temperature sensitivity may be to use liquids with small thermo-optic coefficients however this might not be feasible for applications where the chemical composition of the test liquid is fixed. A second method is to design special fibres where the contribution due to the index change of the surrounding liquid is compensated by the temperature induced wavelength shift of the LPG. However, these LPGs are expected to have a limited dynamic range of RI measurements since the above condition will be satisfied for a small index range [28].

The optical fibre used to demonstrate this novel liquid level sensor is limited to use with liquids that have a RI of between 1.400 and 1.456. The lower limit is set by the RI of the liquid when the attenuation bands cannot be resolved. The upper limitation is due to the RI of the fibre's cladding, from Figure 5.7 of Chapter 5, it can be seen that the greatest wavelength shifts occur when the RI of the surrounding medium is equal to that of the fibre's cladding. However, this upper limit can be increased by using a fibre which has a cladding RI greater than 1.456. An additional limitation of this sensor is the length of the LPG that can be used. The best performance from the liquid level sensor is achieved when the coupling for the attenuation band resident at the highest wavelength is optimised. If the length of the LPG is extended then the condition of complete power transfer to the particular cladding mode is no longer being met, $\kappa^{(m)}L > \pi/2$. The cladding mode is over coupled and the minimum transmission value of the attenuation band begins to recede as the power in the cladding mode couples back into the fundamental guided mode. Therefore, when the level of the liquid around the LPG is increased the change in the minimum transmission value of the attenuation band no longer behaves as illustrated in Figure 6.10, but is expected to behave as illustrated in Figure 6.12, where the same change in transmission % has two corresponding liquid levels.

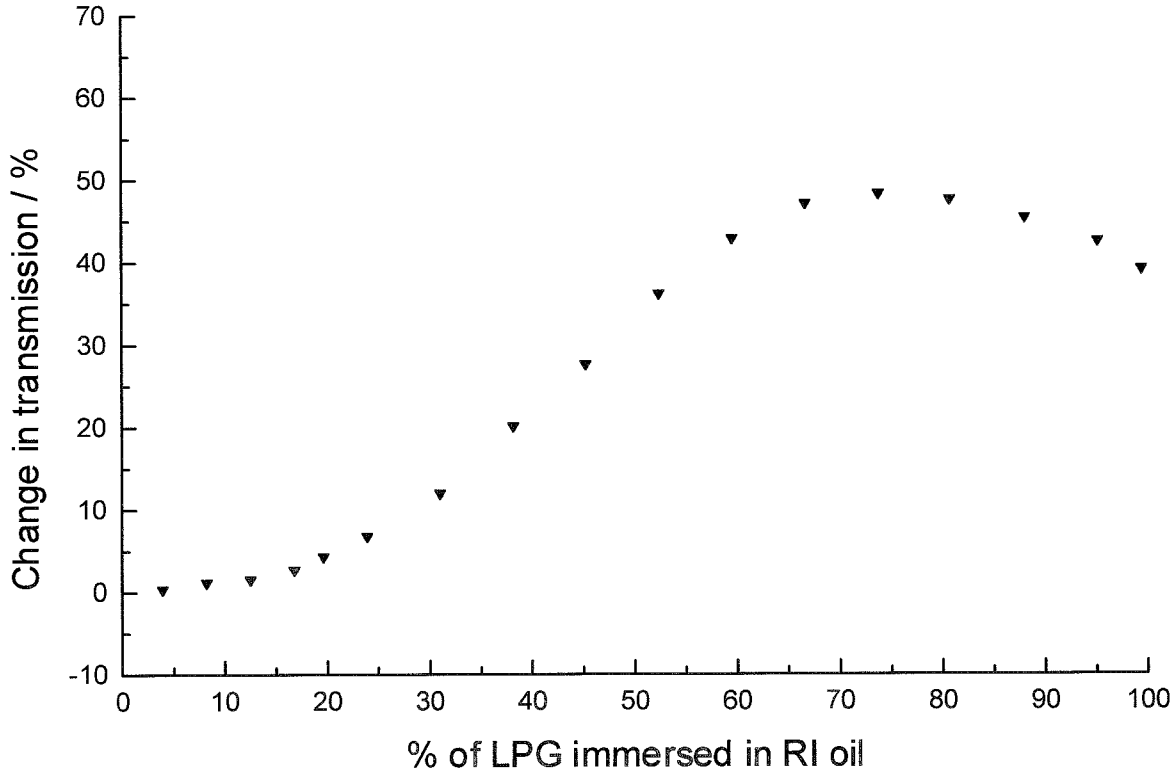

Figure 6.12: *Expected plot of the change in transmission of an over coupled attenuation band A as a function of the % transmission of the LPG immersed in the liquid of RI 1.456.*

The liquid level sensor relies on the LPG only measuring the increasing level of its surrounding liquid. When the LPG has been surrounded by the liquid, any decrease in the liquid level will expose a part of the LPG that has already been wetted by the liquid. The wetting of the LPG will lead to an error in the measurement of the liquid's new reduced level. The LPG could be chemically treated so that the surrounding liquid does not wet the LPG.

The system is also capable of measuring the height of mixtures of liquids that form stratified layers, which may be useful for determining the presence of impurities within containers, e.g. water in petrol tanks.

A liquid level sensor based upon the LPG's sensitivity to the RI of its surrounding medium has been proposed and demonstrated. The sensor displays a large

linear range and may be configured to be independent of temperature. In addition, it is also possible to use the LPG for the multi-parameter sensing of temperature, RI and the level of the surrounding medium.

An important factor in the mechanical strength of optical fibres is the buffer jacket. The polymer buffer jacket provides mechanical protection, allowing the fibre to survive unsympathetic handling. Removal of the buffer jacket in the region of the LPG may act to accelerate the fibre ageing and corrosion effects associated with unprotected optical fibres [29]. The buffer jacket affords protection against water corrosion and optical fibres are known to be weakened by prolonged exposure to moisture [29]. Therefore, when the level of an aqueous solution is to be measured, the absence of the buffer jacket will introduce an issue with respect to the lifetime of the sensor.

6.3 LPG based sensor with enhanced temperature sensitivity

6.3.1 Introduction

The temperature sensitivity of a LPG has already been enhanced by expoliting the LPG's sensitivity to the RI of its surrounding medium [30, 31]. Surrounding the LPG with a medium with a large thermo-optic coefficient results in the LPG responding to both changes in temperature and to the temperature induced RI change of the surrounding medium [30, 31]. The RI oils used during the investigations of the response of the LPG's transmission profile to increasing the RI of the surrounding external medium, discussed in section 5.5 of Chapter 5, are known to posses a large thermo-optic coefficient which is detailed in the relevant specification sheets [26]. The thermal cross sensitivity of a LPG based refractive index sensor has been separately measured using water, RI=1.33, and oil, RI=1.42 [28]. The water and oil were heated from room temperature to 80°C. The temperature sensitivity of the observed attenuation band increased linearly from 0.076nm/°C, in air, to 0.085nm/°C, in water and in oil the temperature sensitivity of the wavelength shift was calculated to be 0.14nm/°C, which is almost twice the sensitivity in air. The change in sensitivity was attributed in the main

to the reduction of the RI of water and oil with increasing temperature [28]. However, the influence of the thermo-optic response of the oils has not been previously investigated in detail. In this section the temperature sensitivity of a LPG is investigated by surrounding it with two RI oils with high thermo-optic coefficients and increasing their temperature over a range of ≈ 30°C. The investigation leads to the demonstration of a LPG based temperature sensor with enhanced sensitivity, of up to 19.2nm/°C. This technique thus exploits both the temperature and external RI sensitivity of the LPG. These techniques are discussed in the following section.

6.3.2 Existing long period grating based sensors with enhanced temperature sensitivity

LPGs fabricated in standard telecommunications optical fibre exhibit temperature sensitivities, in air, in the range -0.14nm/°C to -0.34nm/°C, depending on the attenuation band being monitored. This temperature sensitivity is approximately 2 orders of magnitude larger than that of FBG sensors [32]. For the fabrication of high resolution temperature sensors or to create widely thermally tunable filters, a number of techniques for further enhancing the sensitivity have been reported, including the use of fibres of different composition [33, 34, 35], different geometries [36, 37] and the use of polymer coatings [30, 31, 38, 39].

The sensitivity of LPGs to environmental parameters is influenced by the order of the cladding mode to which coupling occurs, the periodicity and by the composition of the optical fibre [33, 34, 35]. This combination of influences allows the fabrication of LPGs that have a range of responses to a particular measurand. By carefully choosing the order of the cladding mode, the periodicity of the LPG and the operating wavelength, the temperature sensitivity of LPGs has been enhanced [33, 34]. Using these chosen parameters, the temperature sensitivity of LPGs, fabricated in photosensitive B-Ge co-doped optical fibre, has offered sensitivities of upto 2.75nm/°C [35].

Other temperature sensitivity enhancing methods have relied on changing the structure of the fibre [36, 37] or upon surrounding the LPG with materials having a large thermo-optic coefficient [30, 31, 38, 39]. In LPGs with a periodicity < 100 μm, the change of the wave-guide effect due to temperature variations is negligible when compared to that of the material effect, where the induced wavelength shift can be of either polarity [28]. The magnitude of the material effect is related to the change in the differential effective index of the core and the cladding arising from the thermo-optic effect, and so the temperature dependence of the attenuation bands that have a negative sensitivity can be controlled by doping the fibre with dopants that have a negative temperature dependence of the refractive index, such as B_2O_3 [37]. Adjusting the doping levels of B_2O_3 into the depressed inner cladding of a silica-core fibre has enhanced the temperature sensitivity from –0.14nm/°C to 0.28nm/°C [37].

Temperature sensitivity enhancing techniques that are based upon surrounding the fibre by a material of large thermo-optic coefficients result in the LPG responding to both changes in the temperature and to the temperature induced refractive index change of the surrounding medium [30, 31, 38, 39]. If the material has a negative thermal expansion coefficient, then, for increasing temperature, the wavelength shift induced by the change in refractive index of the coating causes a red shift in the wavelength of the attenuation band. If the attenuation band itself has positive temperature sensitivity, the two effects add to increase the temperature response. Coating the LPG with an UV curable acrylate based polymer has enhanced the sensitivity of a LPG fabricated in a conventional dispersion shifted fibre from 0.05nm/°C to 0.8 nm/°C [31]. The polymer had a refractive index that was approximately equal to that of the cladding and a negative thermal expansion coefficient. In addition, it has been reported that using a LPG fabricated in a novel fibre cladding structure consisting of an ultra thin inner silica cladding layer and a low RI liquid crystal outer layer produced a temperature sensitivity of 2.10nm/°C [30]. This method relies on the fact that the RIs of the core and cladding change due to variations in temperature and much higher sensitivities are achieved because the ultra-thin cladding makes the LPG extremely sensitive to the environmental changes outside the cladding [30].

6.3.3 Experimental demonstration of a highly sensitive long period grating based temperature sensor

The parameters of the LPG and the general experimental configuration are discussed in section 6.2.3 of Chapter 6. The temperature of the RI liquid in which the LPG was to be immersed was increased using the liquid receptacle illustrated in section 5.6 of Chapter 5. The liquid receptacle was fixed to the middle of a thermo-electric heater/cooler, which was now used to increase the temperature of the liquid. A cross section of the experimental configuration is shown in Figure 6.13.

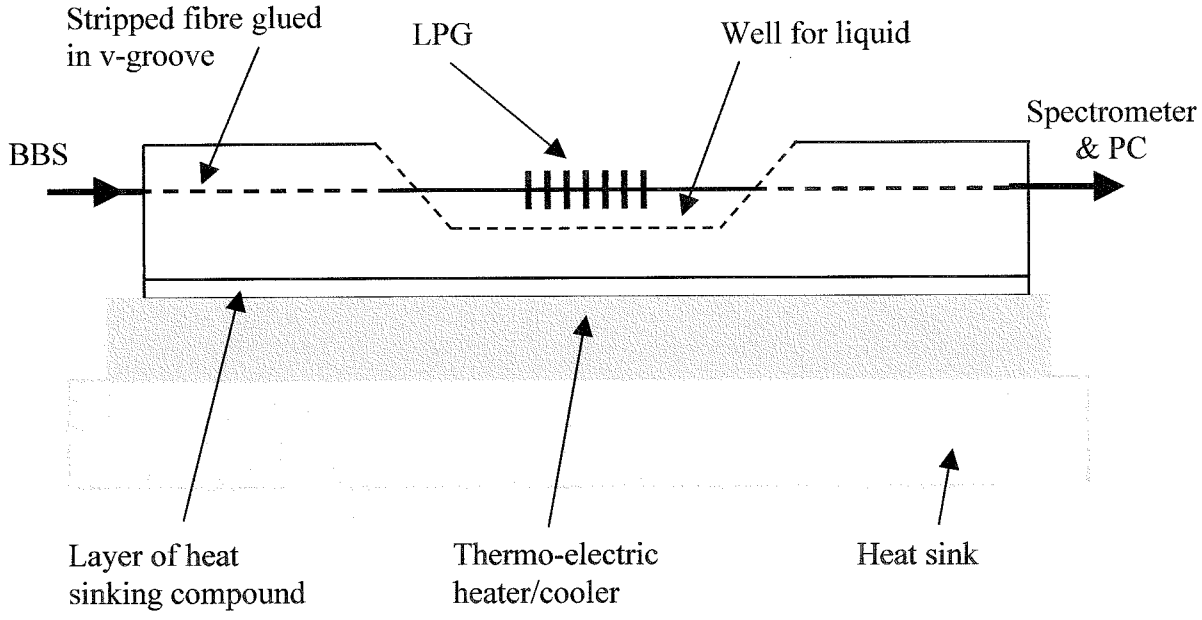

Figure 6.13: *Cross section of the experimental configuration used to increase the temperature of the liquid surrounding the LPG.*

The LPG was positioned into the middle section of the 5mm deep and 50mm long well. The LPG was held straight and taut to avoid any distortion of the LPG's transmission spectrum due curvature of the LPG [25]. The bare fibre either side of the LPG was secured into the v-grooves using a Cyanocrylate super glue, the v-grooves ran longitudinally into the well from either end of the block. Wax was used to seal the ends of the well so that the RI liquid did not flow out. The wax, supplied by Radio Spares,

had a melting point of approximately 80°C, which was approximately 30°C above the maximum temperature to which the RI liquid would be heated. A thin layer of heat sinking compound was laid between the base of the well and the thermo-electric heater to assist in the uniform heating of the RI liquid.

The temperature of the liquid was to be measured using a K-type thermocouple and an AD590 temperature sensor. The measuring devices were positioned into recesses, which would be filled with the RI liquid, located on either side of the LPG. The K-type thermocouple used in association with a digital thermometer, Keithley 740 scanning thermometer. The scanning thermometer had a resolution of 0.1°C. The AD590 was used in a feedback loop by a thermoelectric temperature controller, a TED 200 supplied by Profile, to maintain the thermo-electric heater at the required temperatures ± 1°C. The temperature range of the thermo-electric heater was limited by the size of the heat sink and the maximum output current of the TED 200, 2A. The TED 200 was able to maintain a temperature with a stability of ≤0.01°C. The settling behaviour of the TED 200 for a change in temperature was determined by the proportional, integral and derivative, PID, parameters which were adjusted to an aperiodic temperature settlement. Temperature changes in the environment immediately surrounding the experimental configuration were minimised by enclosing it within a thermal enclosure.

The attenuation bands' central wavelengths and minimum transmission values were recorded when the LPG was surrounded by air at 25°C. The liquid was introduced to the receptacle, via a syringe, through a purpose made access panel in the top of the thermal enclosure. When the temperature of the liquid had also settled at 25°C, the same parameters were recorded again. The temperature of the liquid was increased in steps of 0.5°C, up to a maximum of 54°C. When the temperature of the liquid had reached each set temperature ± 0.1°C, the liquid was allowed to remain at the temperature for a further minute to ensure that thermal equilibrium had been achieved. A plan view of the experimental configuration is shown in Figure 6.14.

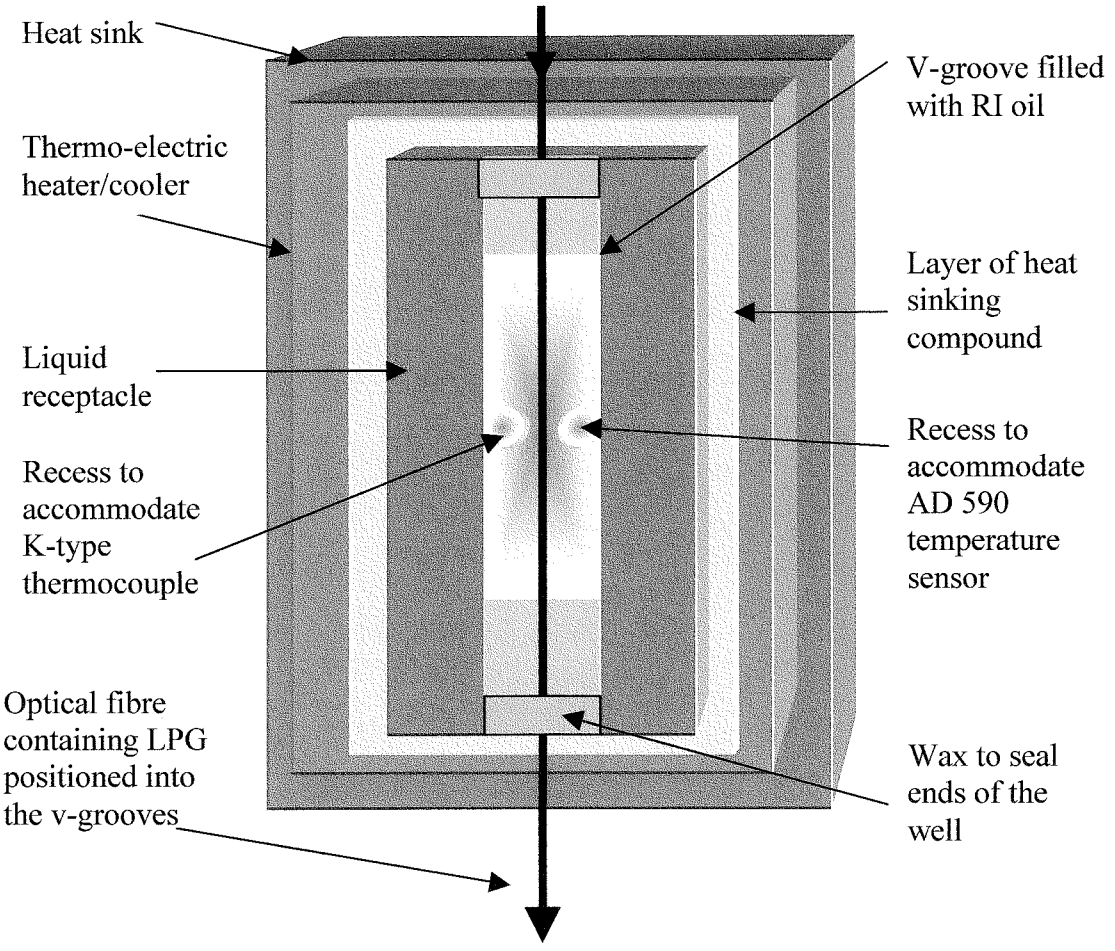

Figure 6.14: *Plan view of the configuration used to change the temperature of the RI oil that surrounded the LPG. The locations of the AD590 temperature sensor and K-type thermocouple are shown.*

6.3.4 Results

The liquids chosen for the experimental work, Cargille's Series 'A', had RIs of 1.460 and 1.462. These nominal RI values are quoted at 25°C and measured at a wavelength of 589.3nm. These particular liquids had temperature coefficients of –0.000389 and –0.000391 respectively over a temperature range 15-35°C [40]. These liquids were selected because their thermo-optic coefficient results in a decrease in RI with increasing temperature. When the RI of the liquids is less than or approximately equal to that of the fibre's cladding (1.456) the attenuation bands show maximum

sensitivity to changes in RI, as shown in section 5.5 of Chapter 5. The RI of the liquid at the central wavelength of each of the attenuation bands was calculated using the Cauchy equation which takes into account the material dispersion and the thermo-optically induced RI change [40]. The Cauchy equations for the liquids of nominal RI, 1.460 and 1.462 are given by equations 6.5 and 6.6 respectively.

$$n(\lambda)=1.44792+\frac{407363}{\lambda^2}+\frac{4.15330\times10^{11}}{\lambda^4} \tag{6.5}$$

$$n(\lambda)=1.44969+\frac{414215}{\lambda^2}+\frac{4.67247\times10^{11}}{\lambda^4} \tag{6.6}$$

where λ, the central wavelength of the attenuation band, is expressed in angstroms. The temperature of the liquid was increased in increments of 0.5°C, up to a maximum of 54°C. The attenuation bands' central wavelengths, minimum transmission values and the LPG's transmission spectrum were continually logged at a rate of 1Hz. The scanning thermometer provided a temperature value that was logged, via a GPIB card, in association with the LPG's transmission spectrum.

Attenuation bands 2-6 exhibited a decrease in their central wavelengths and a change in their minimum transmission values in response to the increase in temperature and the corresponding decrease in the RI of the liquid. The results of the observed spectral changes are plotted in Figures 6.15 and 6.16. Figure 6.15 illustrates the wavelength shift of attenuation bands 2-6 as a function of temperature over a range 25°C to 52°C when the LPG was immersed in oil of RI 1.460. The wavelength shift of attenuation bands is calculated with respect to their individual central wavelengths when the LPG was surrounded by air at 25°C.

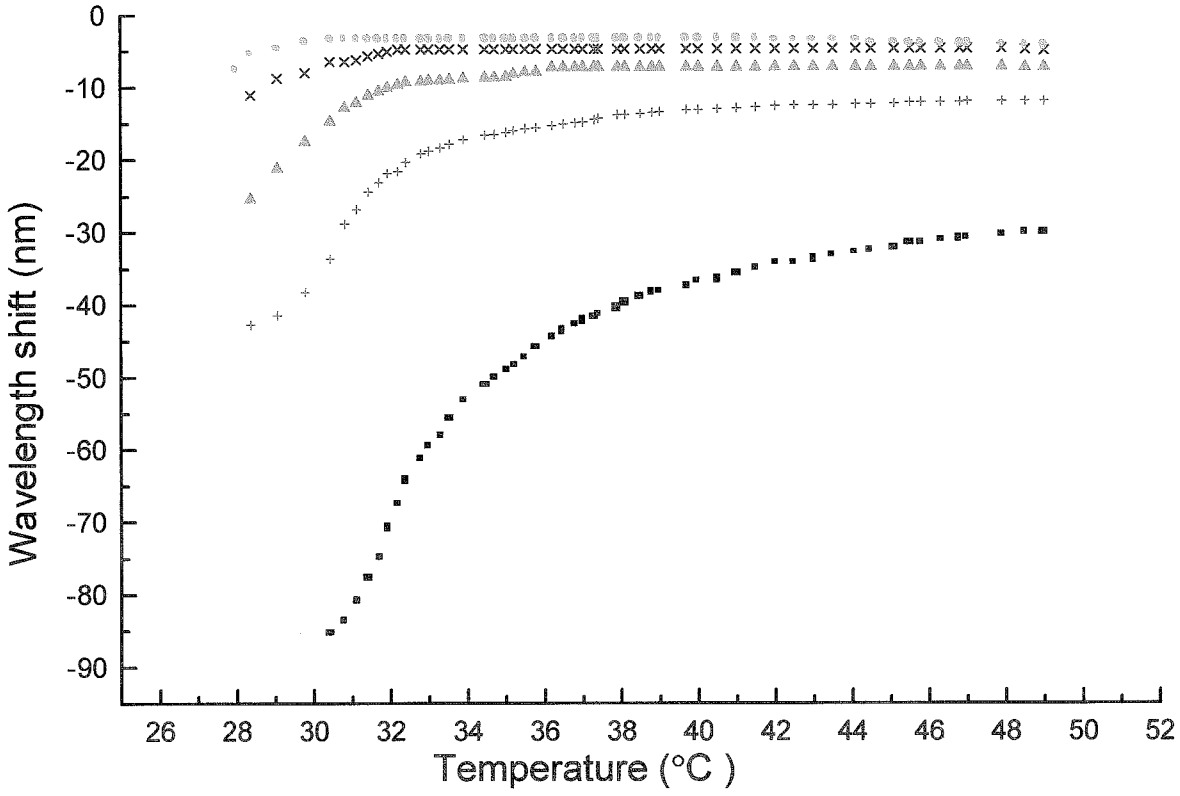

Figure 6.15: *Plot of the wavelength shift in the central wavelengths of the 5 attenuation bands, attenuation bands 2-6, as a function of temperature when the LPG was immersed in oil of RI 1.460.* ◍ *attenuation band 2,* x *attenuation band 3,* ▲ *attenuation band 4,* + *attenuation band 5 and* ■ *attenuation band 6.*

Figure 6.15 shows that each attenuation band has different temperature sensitivity and that, over a limited range, very high temperature sensitivities are achieved (for attenuation band 6 this is upto 19.2nm/°C over a temperature range of 1.1°C). It is also interesting to note that the temperature range is different for each attenuation band. This is a result of the dispersion of the liquid and of the cladding modes of the fibre.

The attenuation bands 2-6 also exhibited a change in their minimum transmission values. This is illustrated in Figure 6.16 which shows the change in the minimum transmission values of the attenuation bands as a function of increasing temperature, over the range 25°C to 54°C. The change in minimum transmission value of each attenuation band is calculated with respect to its minimum transmission value in the liquid at 25°C.

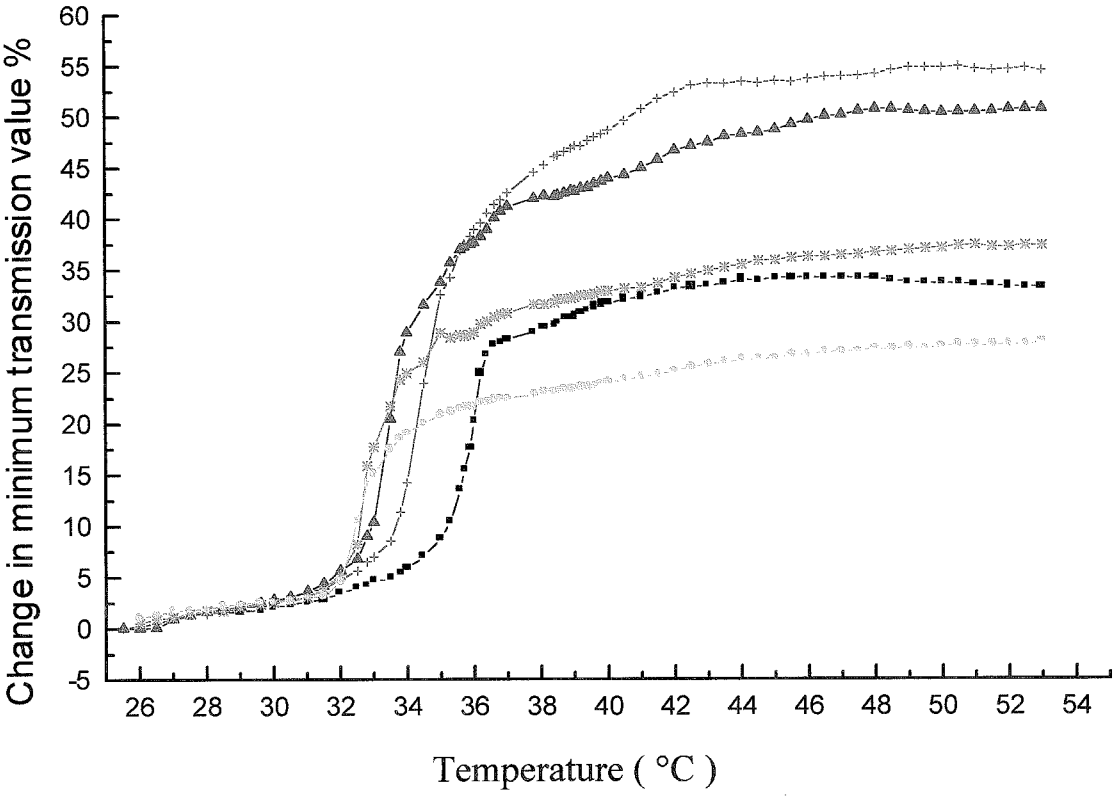

Figure 6.16: *Plot of the change in the minimum transmission value of the 5 attenuation bands, attenuation bands 2-6, as a function of temperature.* ⁘ *attenuation band 2,* ✳ *attenuation band 3,* ▲ *attenuation band 4,* + *attenuation band 5 and* ■ *attenuation band 6.*

The minimum transmission value of the attenuation band also demonstrates a large temperature sensitivity of upto 14.8 % /°C over a temperature range of 2.0°C for attenuation band 5 and again, offers different operating ranges for the different attenuation bands.

When the LPG was surrounded by the liquid of RI 1.462, it was noted again that the attenuation bands responded with a shift in wavelength and a change in their minimum transmission values in a similar way to that shown in Figures 6.15 and 6.16. To illustrate the different temperature ranges and the assosiated RI range for the two RI liquids, the wavelength shift of attenuation band 6 is plotted as a function of increasing temperature in Figure 6.17 and decreasing RI, calculated using the negative temperature coefficient of the liquid at each temperature, in Figure 6.18. Attenuation band 6 was

selected for observation as it had shown, in Figure 6.15, the largest wavelength shift for increasing temperature. Figure 6.17 plots the wavelength shift of attenuation band 6 as a function of increasing temperature, over a range of 30°C to 54°C, when the LPG was surrounded by the liquids of RI 1.460 and 1.462 respectively.

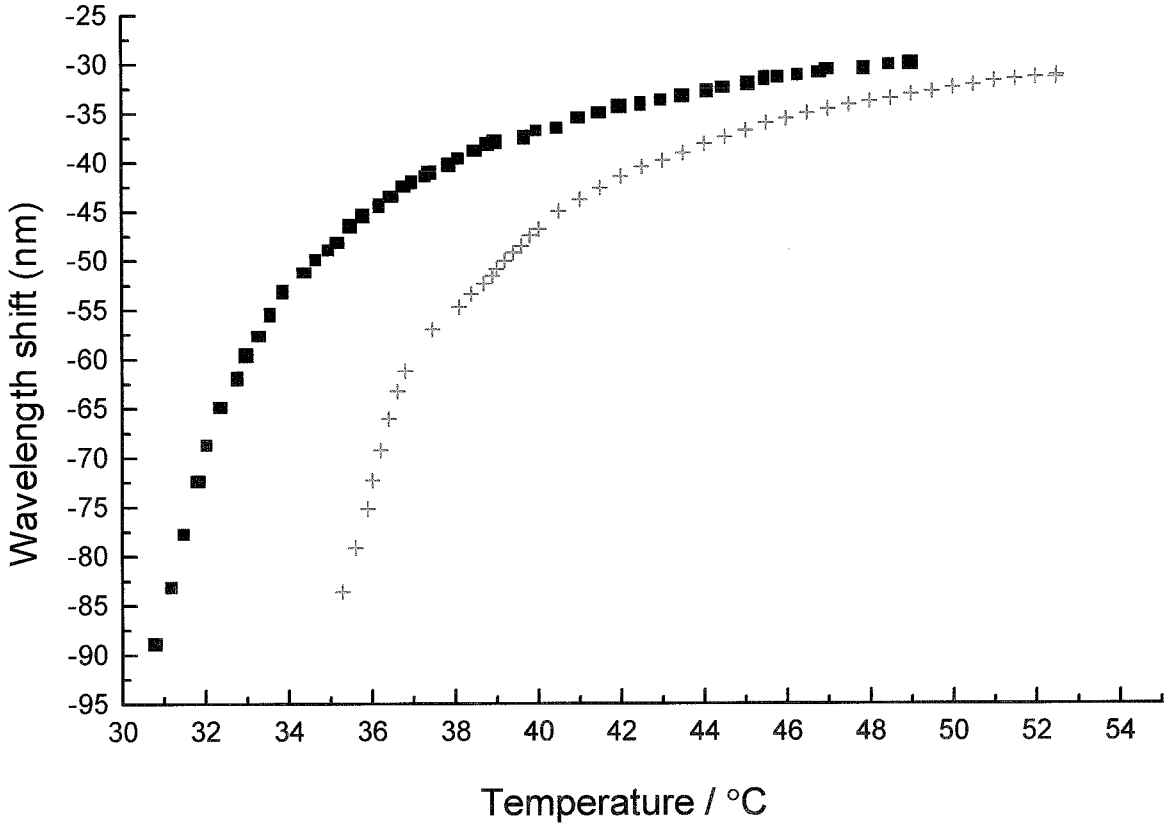

Figure 6.17: *Plot of wavelength shift of attenuation band 6 against increasing temperature, when the LPG was immersed separately in liquids of RI 1.460 and 1.462.* ■ *liquid of nominal RI 1.460 and* + *liquid of nominal RI 1.462.*

Figure 6.17 shows that the attenuation band operates over a different temperature range depending on the properties of the surrounding RI liquid. Attenuation band 6 demonstrates a high temperature sensitivity calculated to be up to 19.2nm/°C over a limited temperature range of 1.1°C. The 1.460 and 1.462 RI liquids can be used to monitor linear responses over temperature ranges of approximately 31°C to 32.5°C and 35°C to 36.1°C respectively with high accuracy in temperature critical environments.

Figure 6.18 illustrates the wavelength shift of attenuation band 6 as a function of decreasing RI, calculated using the temperature coefficient of the liquids at each temperature, over a range of 1.451 to 1.441 when the LPG was separately immersed in liquids of RI 1.460 and 1.462.

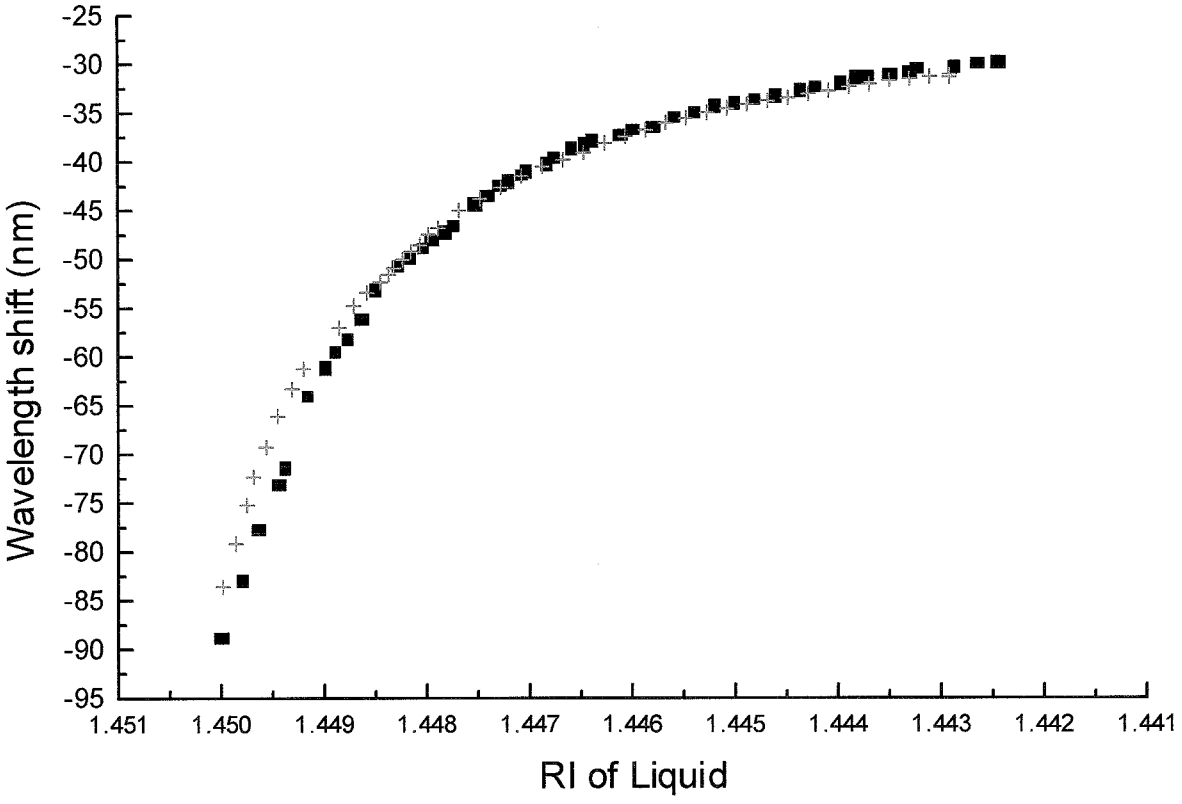

Figure 6.18: *Plot of wavelength shift of attenuation band 6 against decreasing RI of the liquid when the LPG was immersed separately into liquids of RI 1.460 and 1.462. The wavelength shift of attenuation band 6 is calculated with respect to its position in air at 25 ℃.* ■ *liquid of nominal RI 1.460 and* + *liquid of nominal RI 1.462*

Figure 6.18 illustrates good agreement of the central wavelength responses of the attenuation band to both RI oils, over a RI range of 1.450 to 1.441. It should be noted that the attenuation band does not respond with a wavelength shift until the RI is ≤ that of the cladding of the fibre. The sensitivity of the attenuation band, over the linear region is determined to be –31nm/ 0.001change in RI of the liquid.

The changes in the minimum transmission values of the attenuation band as a function of temperature and corresponding decreasing RI, when the LPG was separately immersed in the two RI liquids, are shown in Figures 6.19 and 6.20 for attenuation band 5. Attenuation band 5 was selected as it had shown, in Figure 6.16, the greatest change in its minimum transmission value. Figure 6.19 plots the change in the minimum transmission value, of attenuation 5, as a function of temperature over a range of 25°C to 54°C. The change in minimum transmission value of attenuation band 5 is calculated with respect to its minimum transmission value in the liquid at 25°C.

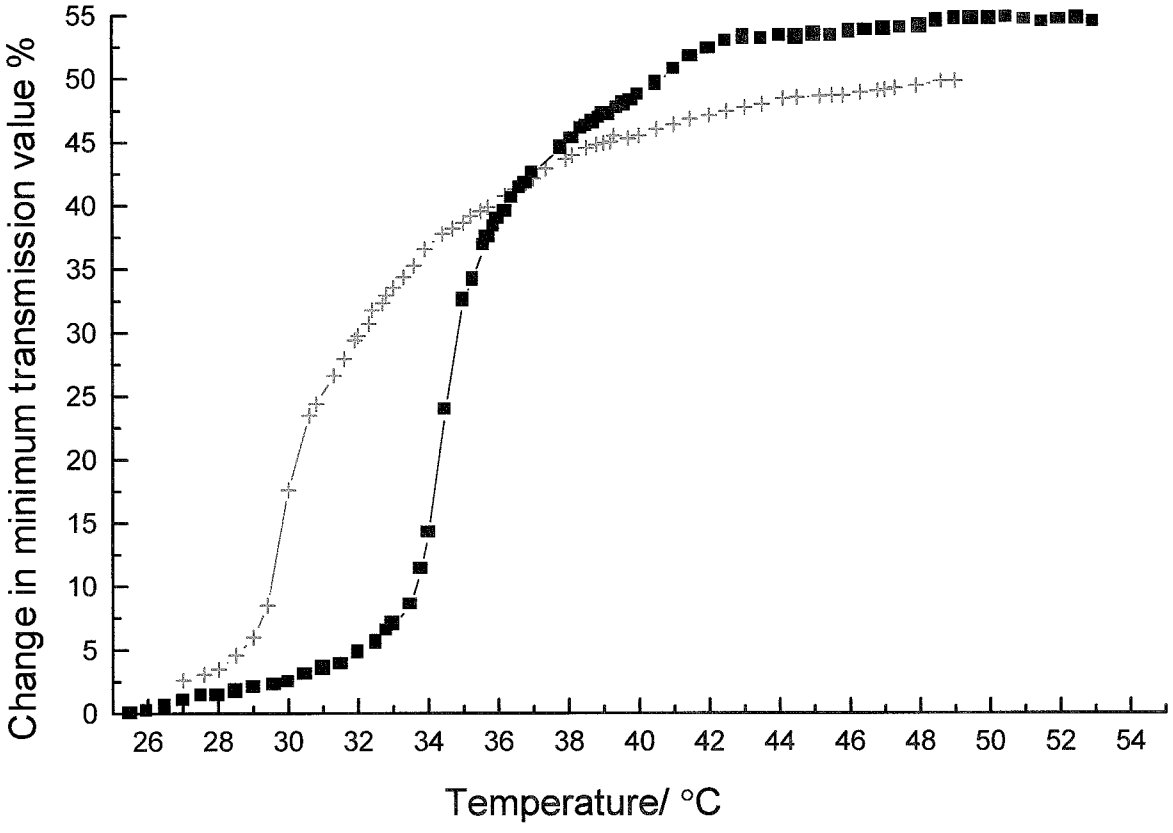

Figure 6.19: *Plot of change in minimum transmission value, of attenuation band 5, as a function of the temperature of the liquid.* ■ *liquid of nominal RI 1.460 and* + *liquid of nominal RI 1.462.*

It should be noted that the change in the minimum transmission value of the attenuation bands responds over a larger temperature range when compared to the response of the

central wavelengths, illustrated in Figure 6.17. When the LPG was surrounded by the liquid of RI 1.460, the response of the minimum transmission value began at ≈ 25.5°C, which was 5.5°C earlier than the commencement of the wavelength shift. Similarly, when the LPG was surrounded by the liquid of RI 1.462 the response of the minimum transmission value began 8.0°C earlier when compared to the initiation of the wavelength shift. At 25°C RI liquids, 1.460 and 1.462 had a higher RI than that of the fibre's cladding. An increase in temperature induced a decrease in the RI of the liquids. During increases in temperature for which the RI values of the surrounding liquids was ≥ to that of the fibre cladding only the minimum transmission values of the attenuation bands were sensitive to the changes in the RI. Therefore, change in the minimum transmission values of the attenuation bands was noted sooner than the response in wavelength shift. At higher temperatures when the RI of the liquids were < than that of the cladding, only then did the central wavelength of the attenuation band begin to respond. This was as expected since it had already been demonstrated in the characterisation experiments, section 5.5 of Chapter 5.

Figure 6.20 plots the change in the minimum transmission value of attenuation band 5 as a function of the decreasing RI of the liquids over a range 1.455 to 1.442.

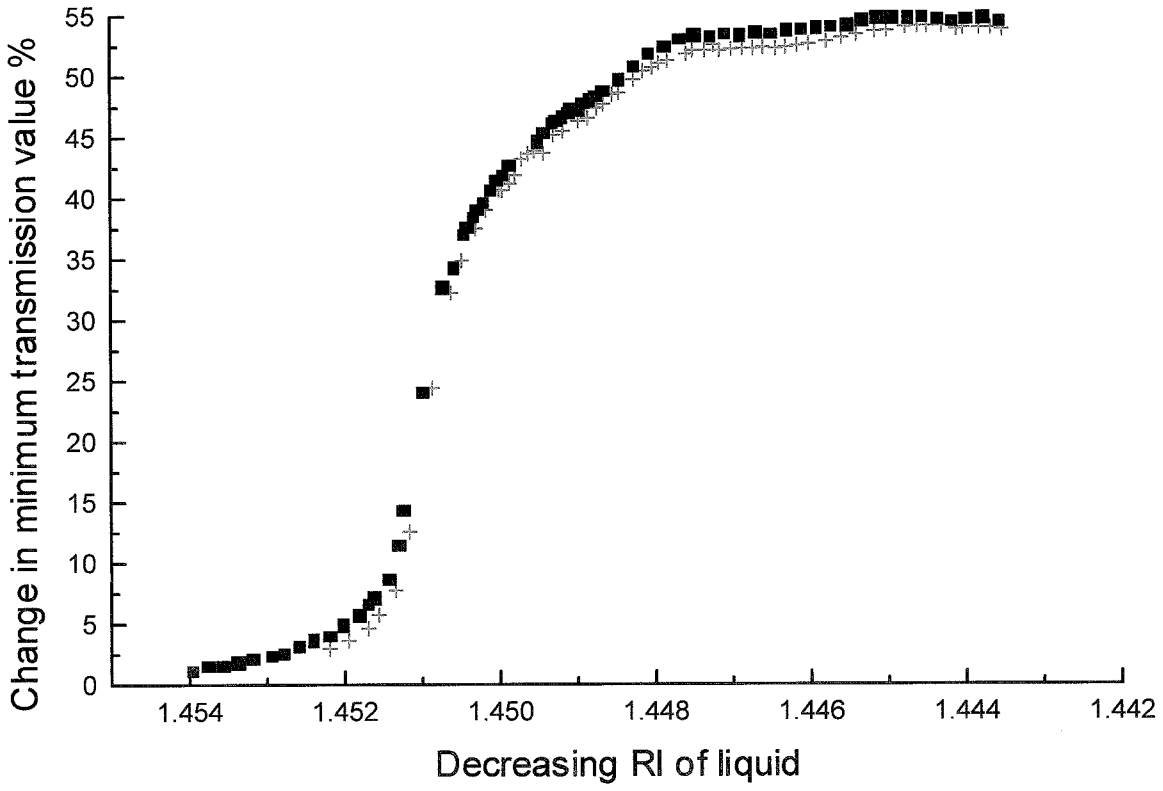

Figure 6.20: *Plot of change in minimum transmission value against decreasing RI of the liquid.* ■ *liquid of nominal RI 1.460 and* + *liquid of nominal RI 1.462.*

Figure 6.20 was expected to show, as already demonstrated from the characterisation experiments, that the change in the minimum transmission value is the same over the RI range.

6.3.5 Discussion

A method for enhancing the temperature sensitivity of a LPG has been demonstrated. There are no requirements for novel coating materials [31, 38, 39] or novel fibre structures [30]. The LPG fabricated in standard optical fibre is surrounded by a Cragille, RI oil of high thermo-optic coefficient. A sensor based on the demonstrated principle could be readily constructed using a capillary tube filled with the appropriate oil. The tube would also provide support for the LPG thus avoiding bend-induced changes to the transmission spectrum [25]. The attenuation bands have shown

two responses to the temperature-induced changes in the RI of the liquid in which the LPG is immersed. These changes occur in the central wavelengths and the minimum transmission values of the attenuation bands.

For both of the RI liquids investigated the changes in central wavelengths with respect to increasing temperature is linear, with high sensitivity of up to 19.2nm/°C in a very limited range of 1.1°C. The change in the minimum transmission value with respect to the increasing temperature have shown a temperature sensitivity of up to 14.8%/°C over a temperature range of 2°C. The temperature range is different for each of the attenuation bands, this is the result of the dispersion of the RI liquid and of the fibre modes, and each attenuation band has a different sensitivity in its linear region. Thus, the appropriate attenuation band can be selected for measurement in the required range. The temperature range for each RI is different but the LPG is influenced by a common RI range. If a different operating range is required, it is possible to choose a material with a different RI at room temperature, such that its RI lies within the sensitivity range of the LPG over a different range of temperatures. This is illustrated by the result shown in Figure 6.17, where the temperature responses of the attenuation band corresponding to coupling to the 6^{th} cladding mode surrounded by two different liquids (n = 1.460, n =1.462) are compared, demonstrating the tuning of the operating temperature range by change of material. The operating temperature and the sensitivity are determined by the properties of the surrounding oil allowing optimisation of the sensor for a given application.

The measurements reported were reproducible and no hysteresis was observed during temperature cycling. The temperature sensitivity enhancement discussed here would be of use in temperature critical systems, for example in chemical and material processing, where optimum processing temperature range may be limited. In addition, the high temperature sensitivity is of interest for thermally tuned optical filters.

6.4 Monitoring the cure of an epoxy resin using a long period grating

6.4.1 Introduction

Real time, in-situ monitoring for quality control of the cure process of an epoxy resin is of great interest [41]. High performance composite materials are generally made of stacked laminate or woven fabrics of continuous carbon or glass or aramid fibre pre-impregnated with an epoxy resin (matrix) pre-polymer system. They have the potential to find widespread use across a range of industries, including the civil and military aviation industries, the civil engineering industries and the automotive industries [41, 42, 43, 44]. The composites are good candidates for making smart materials because their manufacturing process allows sensors to be embedded within the structure [44]. Smart composites provide 'health monitoring' in real time and in-situ [41]. Due to their extensive use, there is a high demand to study their time dependent behaviour from a chemical and physical point of view [44]. In particular, epoxy resin reinforced with fibre is a system with high specific mechanical properties such as performance against weight ratio, corrosion resistance, electrical insulating properties and low density [44].

However, the cost of these materials must be reduced so that they can be competitive against traditional materials such as wood and metal. One strategy is to optimise the manufacturing process and hence reduce the amount of scrap so that the material becomes cheaper to buy [45]. An integral part of the manufacturing process is the curing of the resin, which is used to fix the many layers of the composite materials together. Epoxy and thermoset polyester adhesives are commonly used for composite matrices. The RI of these types of adhesives appears in the range 1.47-1.52 [46]. A characteristic of epoxy resins is that they achieve their final properties during a process in which the molecular structure of the resin is transformed into a ridged cross-linked network. This cross-linking is known as the 'cure'. Cure comprises of a complex set of chemical reactions, usually heat activated and performed under elevated pressure, which gradually elongate and cross-link the original uncured molecules [43]. The epoxy resin

runs the risk of being under-cured or over-cured which plays an important role in product quality [47]. If the epoxy resin is under-cured or over-cured then the mechanical strength of the material is compromised. Additionally for over-cured epoxy, the extra cost in the consumption of resources and associated energy must be met. It is very important for the final application that the curing of the epoxy resin is optimised.

Fibre optic sensors are suitable candidates for monitoring purposes due to their immunity from electromagnetic, interference, their sort response time and their compatibility with the manufacturing process [44]. Previously reported work has shown that it is possible to insert a fibre-optic sensor into a fibrous composite laminate without significant modification of the material's mechanical properties [42, 43]. Additionally the sensors offer the advantage of providing both the signal path and the sensing element. One of the ways in which to detect the curing process with a fibre-optic sensor is based on the knowledge that the RI of an epoxy resin increases during the cross-liking process [48, 49, 50]. The transmission spectrum of a LPG has shown two responses to the change in the RI of its surrounding medium [2, 3, 12]. This section demonstrates a LPG based optical fibre sensor, which utilises the RI change of a curing single component epoxy resin to investigate its state of cure.

6.4.2 Existing cure monitoring techniques

Many techniques are available for monitoring the resin's state of cure. In principle methods showing the propagation of chemical reaction are suitable. They can be divided into techniques that are directly sensitive to the chemical reaction and those that detect changes in the microscopic material parameters. The chemical reaction is sometimes exothermic and can be detected by thermoanalysis such as differential scanning calorimetery, DSC [51, 52]. Infrared spectroscopy [53], nuclear magnetic resonance spectroscopy NMR [54] and chromatography [55] are also typical methods used in research and development. DSC is a method that is directly sensitive to the chemical reaction that has occurred during curing but can only give a qualititive indication of the degree of curing of the resin [56]. A sample is required that is tested in the laboratory where qualified personnel are needed to perform the measurements. The

measurement in the laboratory also excludes the possibility for making measurements at the place of production or application [56]. For practical reasons, the other typical monitoring processes are also difficult to incorporate in the production process [54].

The microscopic attributes that change during the cure are mechanical and electrical material parameters [44, 57]. Typical mechanical parameters are complex elastic or shear modulus and viscosity. These quantities can be measured by dynamic mechanical analysis DMA [52], ultrasound propagation [44, 52] and viscosimetry [58]. Typical electrical parameters are ac conductivity, dielectric permittivity and loss [44, 59]. However, at present, there are no reliable tools that can be used to obtain real-time quantitative information on the rate, extent and homogeneity of the cure [60].

Using in-situ sensors to monitor the cure of an epoxy resin in an industrial process can allow processing decisions to be taken in light of the real time analysis of cure parameters such as temperature, pressure, resin viscosity, resin position, resin gelation point, degree of cure, presence of moisture and the types of polymerisations occurring within the resin [42]. As a consequence, the cure cycle can be tailored to produce desired properties in the material being processed. For example, in-situ sensors might be used to detect when the resin has achieved minimum viscosity so that the perfect time for injecting into a mould can be determined [45]. Thus, in-situ sensors can lift material processing from the realm of a trial and error procedure to a more scientific operation [42]. There is a growing need for sensors that can provide real-time, in-situ monitoring of the curing process. Only two types of micro-sensors are used reasonably widely in both academic research and industrial research and development to monitor the state of cure in real time: dielectric and optical fibre sensors. Both types of sensors can be embedded in selected locations of a composite prior to use [61]. Dielectric cure monitoring has been established since the late 1950's [60]. Some possible disadvantages of this technique are: (i) the operation of the dielectric cure sensor can be affected by electromagnetic interference (ii) the dielectric cure sensor can only give qualitative information on the cure kinetics of the resin system (iii) the sensor system is expensive to buy (iv) the output from the sensor may be influenced by the concentration of impurities in the resin system, the moisture content and the presence of conducting

materials in the composite [60]. Sensors embedded into the composite material into critical areas, such as thick areas and joints, do not adversely affect the quality of the material and provide more accurate status for active or intelligent cure monitoring and control systems. Additionally, sensors that remain in the cured material may be valuable to access the quality or integrity of the material for inspection purposes in production and in the field [62]. The types of in-situ sensors that are of particular interest are those based on optical fibre technology. FBGs and LPGs have been used as a means of inferring the state of cure of a thermoset resin [63, 64, 65, 66, 67].

6.4.3 In - situ optical based cure monitoring techniques

Optical fibre based cure monitoring in composites or in resin systems used in the production of composites can be classified into quantitative or qualitative techniques. The quantitative approach involves obtaining information on the relative chemical concentrations of the active or chemical species, which participate in the reaction. This approach usually involves spectroscopy-based optical fibre interrogation techniques. In the qualitative approach, correlation is sought between a specified property of the resins as a function of processing time and conditions. For example, the change in the refractive index of the system as a function of cure. The use of optical fibre sensors for cure monitoring of epoxy resin systems has gained considerable interest [68]. This is in part due to the increased interest in online and in-situ techniques that can determine the cure state and the mechanical properties of the resin during cure, as an aid to processing. Additionally, optical fibre sensors offer a number of unique advantages for cure monitoring when compared with other techniques such as the measurement of dielectric properties, viscosity, etc. This is because the optical fibre based sensor techniques can give information on the actual chemical concentrations of the constituent chemicals in the resin system, whereas the other techniques can only infer chemical concentration and/or composition [69]. Non-optical techniques require a vast database of information in order to establish a correlation between the sensor data and the state of cure. However, the results from some of these techniques may be affected by moisture, the relative volume fractions of the fibres in the carbon fibre reinforced epoxy, the orientation of those fibres and electrical interference from the processing equipment [68]. Optical fibre sensors are immune to these factors and can give additional

information on moisture content and temperature [69]. Techniques as diverse as near IR [70, 71, 72, 73], Raman [74, 75, 76, 77] and fluorescence [78, 79, 80, 81, 82] spectroscopy, ultrasound [83, 84, 85, 86, 87, 88] have all been applied as monitoring methods.

When light is incident on a medium the radiation can be absorbed, transmitted, reflected or scattered. The nature of the interaction will depend on the frequency of the radiation and the chemical composition of the medium [89]. The absorbed energy can then be lost to the surroundings in the form of heat or re-radiation. Plotting the absorbency or transmittance as a function of frequency produces an infra red spectrum and is measured using a spectrometer [68]. Interest in near IR spectroscopy has increased because of the availability of standard telecommunications grade optical fibre that transmits light near the IR wavelength range, 750nm to 10^5nm, and spectrometers with integrated fibre-optic ports for transmitting and receiving light [73].

Optical Raman spectroscopy has been used to monitor the cure of epoxy resin. The sensor usually consists of two fibres bonded side by side [74, 75, 76]. Light is launched into one fibre end and the scattered light is collected by the second optical fibre. Light emerging from the second fibre is passed to a spectrometer. Data collected from the Raman sensor during cure are compared with transmission near IR spectroscopy results, with good correlation. A single fibre has been used for both transmission and collection of the excitation wavelength of the Raman scattered light [77].

Another interesting development is the observation that the wavelength and efficiency of fluorescence of certain molecules exhibit viscosity dependence [82]. The explanation for this is that if the molecule can undergo non-radiative decay by intermolecular twisting, or torsional motion then the fluorescence efficiency is low. If, however, the molecule is constrained by a viscous polymer network, the radiative fluorescence efficiency increases. Certain epoxy molecules themselves exhibit viscosity dependent fluorescence. Other epoxies can be doped with trace levels of a fluorescent dye molecule, both distal and evanescent mode fibres optic fluorescence methods have been used to measure the state of cure of epoxy [78, 79, 80, 81].

Fibre optic based ultrasonic sensing has been used to monitor the cure process [83, 84, 85, 86]. The sensor is based on guided ultrasonic waves in an unconstrained small diameter optical fibre [84]. The ultrasonic pulse will propagate along the length of the fibre as a guided wave when the frequency of the investigating ultrasound is selected so that its corresponding wavelength is much smaller than the fibre's diameter. The attenuation and phase velocity of ultrasonic waves propagated through fibre ultrasonic wave-guides, embedded in composite materials, vary during the cure [84, 88]. The largest effect occurs in the attenuation, which increases at certain ultrasound frequencies by two orders of magnitude during the initial curing phase [83]. Ultrasound has the attraction of enabling study of the adhesive material when it is formed into components such as panels [87].

During the cure of an epoxy, there is a decrease in volume as the reaction progresses. Associated with this change in density, of approximately 1%, of the sample is a change in the RI. The change in RI can serve as a measure of the extent of cure [48, 49, 50]. This effect has begun to receive greater interest and a fibre optic based sensor has been developed [90]. The sensor consists of an adapted extrinsic Fabry-Perot interfrometer, whereby a single mode fibre was used as the input/output fibre and an unclad high RI fibre was used as the reflector. The sensor arrangement was embedded in curing epoxy, a decrease in the light intensity was observed as the RI of the curing epoxy resin approached the RI of the reflection fibre. The RI of curing epoxy has been monitored by other methods such as using an optical fibre Fresnel reflectrometer and artificial neural networks [91] and using a side-polished single mode fibre with a dielectric wave-guide overlay [92]. The RI of curing epoxy has also been monitored by an sensor based on fibre that has its cladding removed over a small region [44, 73, 93]. The principle of such a RI sensor is based on monitoring the intensity of the light that reaches the detector as the resin cures around the stripped region of the fibre. The intensity of the light at the detector is dependent upon the RI changes at the resin/core boundary as the resin cures changes. The change in the RI alters the guiding characteristics of the sensor in the region of the stripped fibre [44, 73, 93]. LPGs have shown a sensitivity to the RI of their surrounding medium [1-12]. However, cure-monitoring investigations conducted thus far do not make full use of their features [94].

In-situ LPGs have been used as flow sensors in a mould filling application [94, 45]. When the higher index resin covers the LPG sensor, the light that would have been attenuated is coupled back into the core and so there is no corresponding attenuation band in the transmission spectrum. The LPG provides a yes/no response to the presence of epoxy resin [94, 45]. The technique presented here also utilises the LPG's same unique response to the change in the RI of the medium surrounding it. However, here it is used to monitor the RI change in a curing, single component, epoxy resin as a means of investigating its state of cure.

6.4.4 Experimental demonstration of monitoring the cure of an epoxy resin using a long period grating based sensor

The parameters of the LPG are detailed in section 6.2.4 and the general experimental configuration is detailed in section 4.7.3 of Chapter 4. The LPG was secured into the receptacle, the K-type thermocouple and the AD590 temperature sensor were positioned into their respective recesses as previously detailed in section 6.3.3. The thermocouple monitored the temperature of the curing epoxy resin, whilst the AD590 temperature sensor provided a feedback signal for the circuit in order to maintain the stability of the epoxy's temperature via the thermo-electric heater/cooler's temperature that had been set to 25°C. The configuration was positioned within a thermal housing to avoid the influence of variations in the surrounding temperature.

6.4.4.1 Choosing the epoxy resin

The results of the RI characterisation experiments detailed in section 5.4 of Chapter 5, show that the attenuation bands of the LPG show wavelength shifts when the RI of the medium surrounding the LPG is in the range 1.400 to 1.456. The RI values are quoted at temperature of 25°C and measured at a wavelength of 589.3nm. Therefore, it is important that the epoxy resin that is selected has an uncured RI that is in the range 1.400 to 1.456 and a cured RI < 1.456. The majority of epoxy resins that are available either typically have a RI > 1.50 or the data is unavailable. To use epoxy resins with a

RI > 1.50 the LPG would have to be fabricated in a single mode fibre where the cladding has a RI > 1.600 and this is not commercially available. Several resins with an uncured R.I < 1.456 are available. Previously conducted characterisation experiments have shown that EPO-TEK OG 125, a single component epoxy resin supplied by Promatech Ltd, exhibits a definite RI change during curing. It has an uncured RI of 1.435, measured at a wavelength of 589.3nm, and its cured index of refraction is not known [95]. The epoxy resin was introduced around the LPG by means of a medical syringe, through a purpose made entry port in the thermal insulator. The well was filled with the epoxy resin to ensure that the LPG had been totally immersed in it and then the configuration was again allowed to reach a thermal equilibrium at 25°C. The epoxy resin can be cured within 2 minutes by exposure to UV irradiation at 100mW/cm^2.

The UV lamp, Norland, had a 5cm long UV tube that emitted 0.5mW of power per cm^2. It was chosen because the low UV power would extend the curing cycle of the epoxy resin. The curing cycle was extended to over 7 hours by adjusting the distance between the UV tube and the surface of the epoxy resin to approximately 150mm. Before the resin was exposed to the UV, the lamp was switched on and allowed to reach its normal operating conditions. The curing process was initiated by placing the UV lamp over the LPG and the experimental configuration was positioned back under a thermal insulator and was allowed to reach an environmental equilibrium.

6.4.5 Results

The central wavelengths of the attenuation bands their minimum transmission values, the temperature of the epoxy resin and the temperature stability of the thermo-electric heater/cooler were continually recorded at a rate of 0.1Hz. The curing epoxy resin induced a decrease in the central wavelengths and a change in minimum transmission values of attenuation bands 2-6. Figure 6.21 plots the transmission spectra for attenuation band 4 as a function of time. Figure 6.21 illustrates the decrease in the central wavelength and the change in the minimum transmission value of attenuation band 4. The change in the central wavelength and the minimum transmission value is induced by the change in the RI of the epoxy as it cures. Attenuation band 4, central

wavelength at ≈ 850nm in air at 25°C, was selected for observation because during the earlier conducted characterisation experiments it demonstrated the highest sensitivity of the attenuation bands that remained visible throughout the entire experiment.

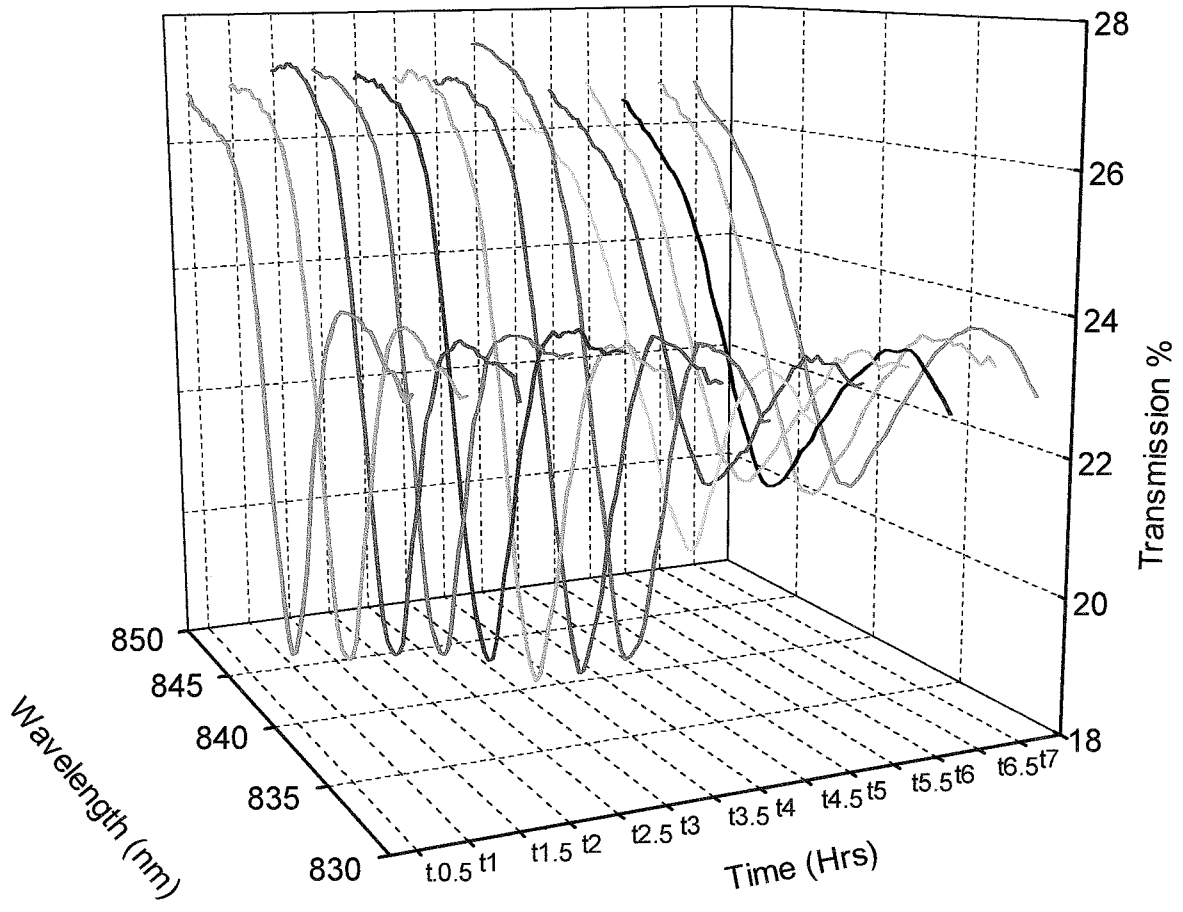

Figure 6.21: *Transmission spectra for attenuation band 4, as the epoxy is curing, plotted as a function of time.*

The actual change in the central wavelength of an attenuation band is illustrated in Figure 6.22, which plots the wavelength shift as a function of time for attenuation band 4. The wavelength shift of attenuation band 4 is calculated with respect to the central wavelength of attenuation band 4 when the LPG was surrounded by air at 25°C.

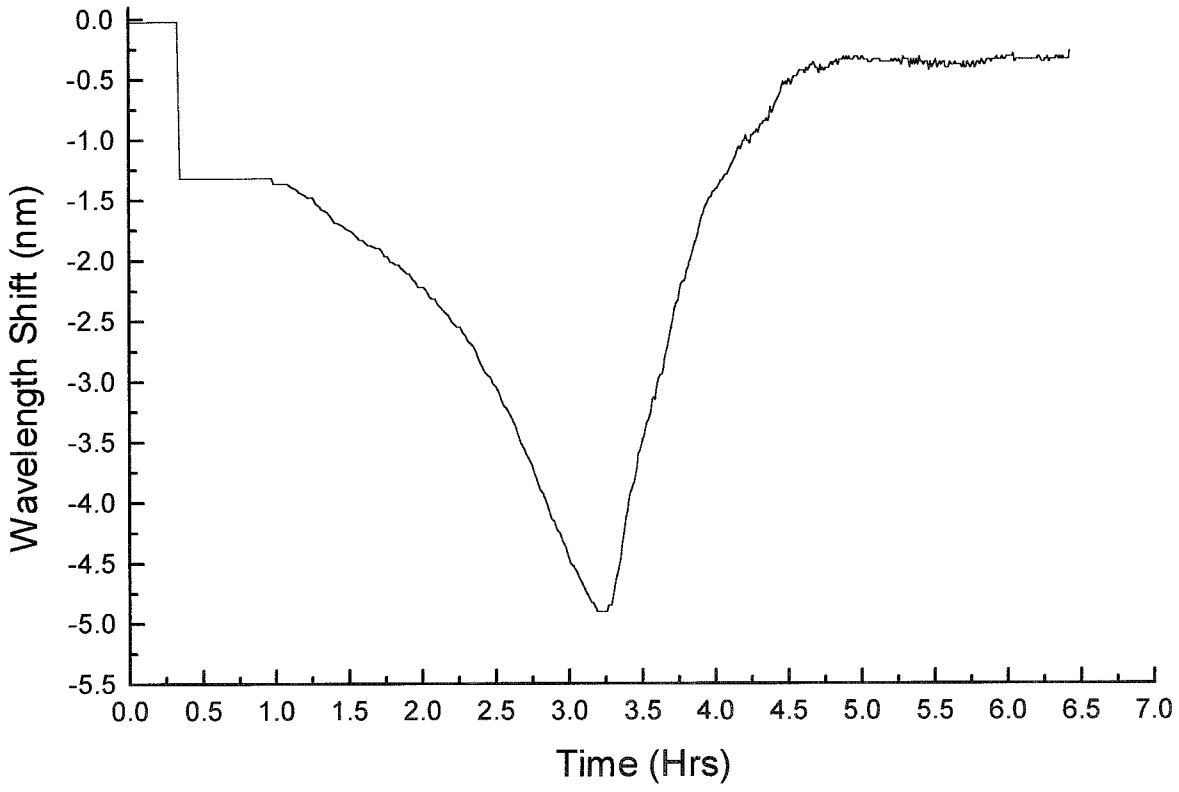

Figure 6.22: *A plot of the wavelength shift of attenuation band 4 as a function of time.*

Initially the LPG, surrounded by air at 25°C, was allowed to reach equilibrium with its surrounding environment. The epoxy, at 25°C, was introduced around the LPG and was allowed to settle and reach equilibrium with its surrounding environment again. The temperature of the epoxy resin was stabilised at 25°C using a TEC. The presence of the epoxy induced a wavelength shift corresponding to a RI of 1.404. The exposure of the epoxy to the UV irradiation initiated the curing process and the increase in RI, which is signified by the continuous decreasing wavelength shift of the attenuation band. The RI of the epoxy reaches that of the fibre's cladding, which is ≈1.453 at ≈ 850.00nm [96]. Further exposure of the epoxy to the UV induces additional increases in the RI of the epoxy. When the RI of the epoxy is greater than that of the cladding the wavelength of the attenuation bands will be slightly shifted compared with those in air and will be insensitive to the RI of the surrounding medium.

During the experiment discussed in section 6.3.3 data was also collected for attenuation band 4 when the LPG was immersed in the RI liquids. A 6th order polynomial was fitted to the data in the region of RI ≈1.404 -1.453 which allowed the RI of the heated RI liquids to be calculated for a given wavelength shift. A 6th order polynomial was fitted to the data illustrated in Figure 6.22, in the region 1.0-3.25 hours. This allowed the time to be calculated for a given wavelength shift of attenuation band 4. Figure 6.23 plots the calculated RI of the curing epoxy resin as a function of time.

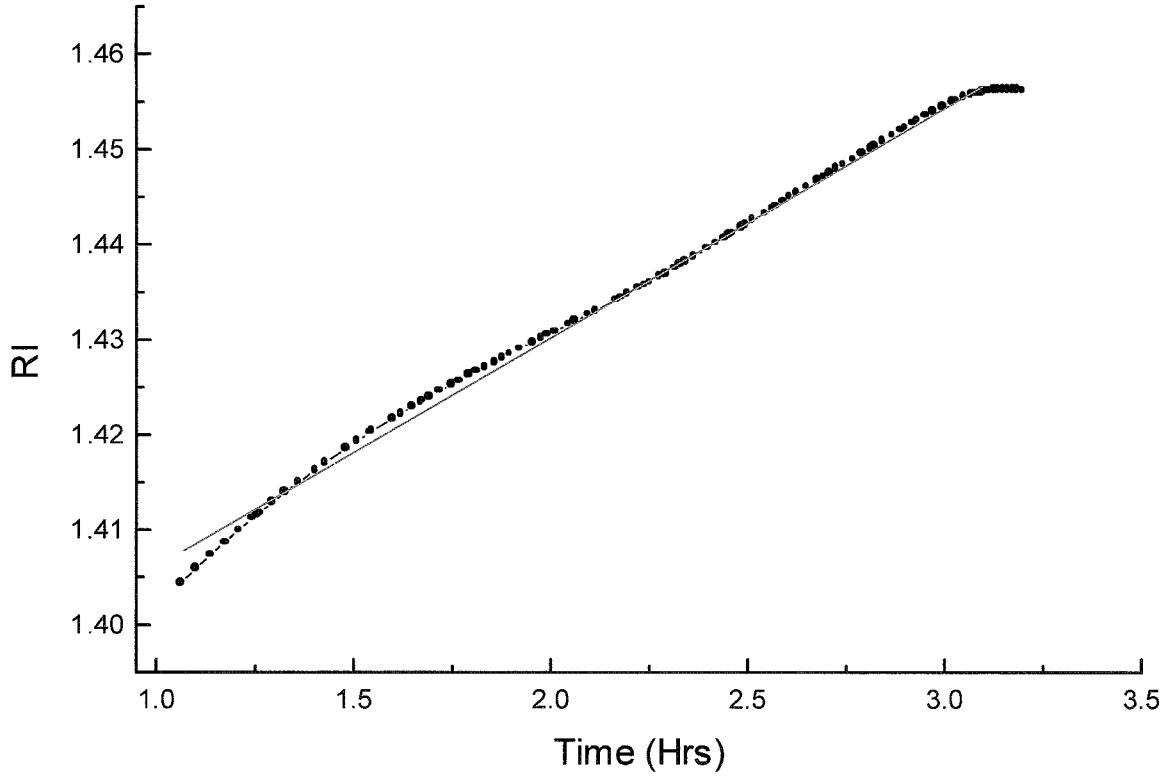

Figure 6.23: *Plot of the calculated RI of the curing epoxy resin, for attenuation band 4, as a function time. The straight line is a guide for the eye only.*

Figure 6.23 is only plotted in the region from when the LPG was first exposed to the UV lamp up to when the RI of the curing epoxy reached that of the cladding. This was because data for the epoxy was available in this region. The plot shows a linear response over the region 1-3 hours. However, it should be noted that the curing time of the epoxy had been artificially extended and that the response of the RI with respect to time is unknown in the other regions. These results need to be investigated further when the

epoxy is cured under ideal conditions.

The change in the minimum transmission values of the attenuation bands is illustrated in Figure 6.24. Figure 6.24 plots the minimum transmission value as a function of time for attenuation band 4.

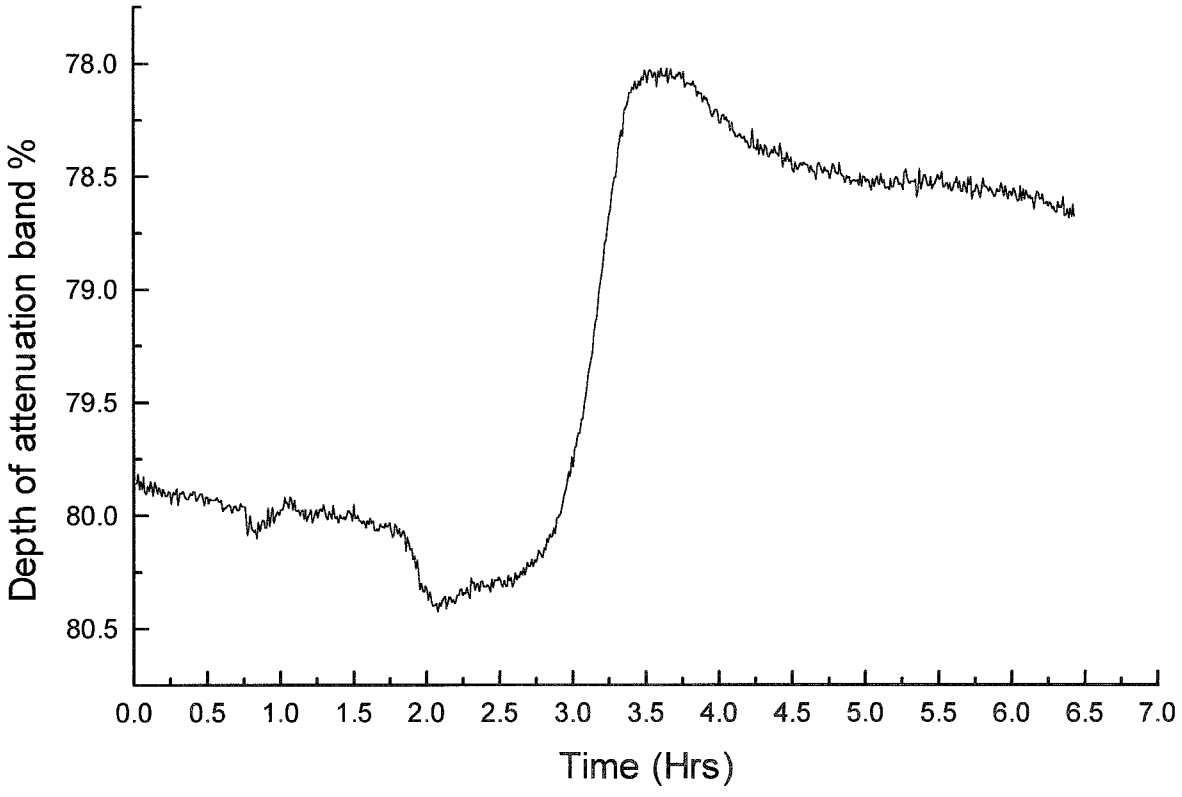

Figure 6.24: *Plot of the change in the depth of attenuation band 4 as a function of time.*

The depth of the attenuation band increases with the introduction of the epoxy and with its initial curing. The minimum transmission value of the attenuation band is a function of the coupling efficiency and further increases in RI around the LPG correspond to a loss in the coupling efficiency and hence a decrease in the depth of the attenuation band.

6.4.6 Discussion

The demonstrated technique is sensitive to the state of cure and so could be used within the body of large composite structures undergoing a curing process. It is further expected that the sensor may be left in the final product without detrimental effects to the eventual application and be used for the monitoring of other parameters such as temperature, strain and bending. However, the demonstrated technique does not utilise the optimum fibre and epoxy combination as the RI of the cured epoxy is greater than that of the fibre's cladding. Ideally, the maximum wavelength shift of the attenuation band would indicate the RI of the cured epoxy. This could be achieved by lowering the RI of the cured epoxy using a blend of epoxies or by using a fibre with a cladding of higher RI [68, 97]. The experiment is never the less a useful first attempt.

If the demonstrated technique were used in a thermoset epoxy, then the temperature changes will cause shifts in the central wavelengths of the attenuation bands, due to the inherent temperature sensitivity of the LPG and additionally due to any temperature dependant RI changes of the epoxy. The wavelength shifts due to temperature can be addressed by using a simultaneous measurement technique such as employing a FBG as a temperature monitor, since FBGs are insensitive to changes in RI, and correcting for the sensitivity of the LPG [98]. Alternatively, a LPG's temperature insensitive attenuation band could be used to monitor the RI change in the thermoset or more than one attenuation band of the LPG could be used to monitor the environmental changes.

6.5 Chapter summary

This chapter has presented three LPG based sensors, a liquid level sensor, an enhanced sensitivity temperature sensor and a sensor for monitoring the cure of an epoxy resin. The sensors utilised the RI sensitivity of LPGs.

The liquid level sensor demonstrated that the transmission spectrum of a LPG is dependent upon the fraction of the length of the LPG that is surrounded by the liquid. The sensor showed a large linear range, with sensitivity of 4.8% change in transmission per millimetre of the 40mm long LPG. LPGs possess large temperature sensitivities and the liquid's RI will show temperature sensitivity, both of which will induce a change in the coupling wavelengths. This information may be determined directly from the spectrum where the central wavelengths and their separation allow the temperature and RI of the liquid to be respectively determined.

The optical fibre used to demonstrate the novel liquid level sensor is limited to use with liquids that have a RI of between 1.400 and 1.456. However, if a higher RI material is to be monitored then this limitation can be overcome by using a fibre that has a cladding of higher RI. The liquid level sensor is also limited to measuring increasing liquid levels. If the liquid level were to fall then the sensor would give an incorrect reading as the fibre above the liquid level would still be wet with the liquid. This limitation can be overcome by treating the fibre so that the liquid does not adhere to it. The system is also capable of measuring the height of mixtures of liquids that form stratified layers, which may be useful for determining the presence of impurities within containers, e.g. water in petrol tanks.

The temperature sensitivity of a LPG has been enhanced by surrounding it with RI oil of high thermo-optic coefficient. The attenuation bands have shown two responses to the temperature-induced changes in the RI of the liquid in which the LPG is immersed. The changes in central wavelengths with respect to increasing temperature is linear, with high sensitivity of up to 19.2nm/°C over a limited range of 1.1°C. The change in the minimum transmission value with respect to the increasing temperature

have shown a temperature sensitivity of up to 14.8%/°C over a temperature range of 2°C. The temperature range is different for each of the attenuation bands. Thus, the appropriate attenuation band can be selected for measurement in the required range. The temperature range for each RI is different but the LPG is influenced by a common RI range. If a different operating range is required, it is possible to choose a material with a different RI at room temperature, such that its RI lies within the sensitivity range of the LPG over a different range of temperatures.

There are no requirements for novel coating materials or novel fibre structures. A sensor based on the demonstrated principle could be readily constructed using a capillary tube filled with the appropriate oil. The tube would also provide support for the LPG thus avoiding bend-induced changes to the transmission spectrum.

The measurements reported were reproducible and no hysteresis was observed during temperature cycling. The temperature sensitivity enhancement discussed here would be of use in temperature critical systems, for example in chemical and material processing, where optimum processing temperature range may be limited. In addition, the high temperature sensitivity is of interest for thermally tuned optical filters.

A LPG has been demonstrated to monitor the RI change during the cure of an epoxy resin. The wavelength shift induced by the uncured epoxy resin corresponded to a RI of 1.404 and this changed by 0.049 when the RI of the curing epoxy resin had reached that of the fibre's cladding. The demonstrated technique could be used within the body of large composite structures undergoing a curing process. It is further expected that the sensor may be left in the final product without detrimental effects to the eventual application and be used for the monitoring of other parameters such as temperature, strain and bending. However, the demonstrated technique does not utilise the optimum fibre and epoxy combination as the RI of the cured epoxy is greater than that of the fibre's cladding [68, 97]. Ideally, the maximum wavelength shift of the attenuation band would indicate the RI of the cured epoxy. This could be achieved by lowering the RI of the cured epoxy using a blend of epoxies or by using a fibre with a cladding of higher RI [68, 97]. The experiment is never the less a useful first attempt.

References:

1 H.J. Patrick, A.D. Kersey, F. Bucholtz, K.J. Ewing, .B. Judkins and A.M. Vengsarkar, 'Chemical sensor based on long period grating response to index of refraction', in Proc. Conf. Laser Electro-Opt. OSA, **11**, pp. 420 – 423, (1997).

2 O. Duhem, J.F. Henninot, M. Warenghem and M. Douay, 'Demonstration of long period grating efficient couplings with an external medium of a refractive index higher than that of silica', Appl. Opt., **37**, pp. 7223 - 7228, (1998).

3 B.Y. Lee, Y. Liu, S.B. Lee, S.S. Choi and J.N. Jang, 'Displacements of the resonant peaks of a long period fibre grating induced by a change of ambient refractive index', Opt. Lett., **23**, pp. 1769 – 1771, (1997).

4 L.R. Chen, 'Tunable phase shifted long period gratings by refractive index shifting', Canadian Conf. on Electrical and Computer Eng. **1**, pp. 453 – 457, (2001).

5 X. Shu and D. Huang, 'Highly sensitive chemical sensor based on the measurement of the separation of dual resonant peaks in a 100μm period fibre grating', Opt. Comms., **171**, pp. 65 – 69, (1999).

6 R.P. Espandola, R.S. Windeler, A.A. Abramov, B.J. Eggleton, T.A. Strasser and D.J. DiGiovanni, 'External refractive index insensitive air clad long period fibre grating', Electron. Lett., **35**, pp. 327 – 328, (1999).

7 K.S. Chiang, Y. Liu, M.N. Ng and X. Dong, 'Analysis of etched long period fibre gratings and its response to external refractive index', Electron. Lett., **36**, pp. 966 – 967, (2000).

8 X. Shu, X. Zhu, S. Jiang, W. Shi and D. Huang, 'High sensitivity of dual resonant peaks of long period fibre gratings to surrounding refractive index changes', Electron. Lett., **35**, pp. 1580 – 1581, (1999).

9 B.H. Lee and J. Nishii, 'Cladding surrounding interface insensitive long period grating, 'Electron. Lett., **34**, pp. 1129 – 1130, (1998).

10 R. Falciai, A.G. Miganai and A. Vannini, 'Long period gratings as solution concentration sensors', Sensors and Actuators B, **74**, pp. 74 – 77, (2001).

11 R. Falciai, A.G. Miganai and A. Vannini, 'Solution concentration measurements by means of optical fibre long period gratings', Eurosensors, XII, Optical Sensors session pp. 339 – 342, (1998).

12 H.J. Patrick, A.D. Kersey and F. Bucholtz, 'Analysis of the response of long period fibre gratings to external index of refraction', J. Lightwave Technol. Vol. **16**, pp. 1606 – 1612, (1998).

13 T. Allsop, L. Zhang and I. Bennion, 'Detection of organic aromatic compounds in paraffin by a long period grating optical sensor with optimised sensitivity', Opt. Comms., **191**, pp. 181 – 190, (20001).

14 K. Zhou, H. Liu and X. Hu, 'Tuning the resonant wavelength of long period fibre gratings by etching the fibre's cladding', Opt. Comms., **197**, pp. 295 – 299, (2001).

15 S. Yin, O. Leonov, K.W. Chung, P. Kurtz, K. Richard, H. liu and Q. Zhang, 'Wavelength tuning range enhanced single resonant band fibre filter using a long period grating with ultra thin cladding', Optical Fibre Communications Conference, pp. 23 –25, (2000).

16 B.W. Northway, N.H. Hancock and T. Cong-Tran, 'Liquid level sensors using thin walled cylinders vibrating in circumferential modes', Meas. Sci. Technol., **6**, pp. 85 - 93, (1995).

17 F.N. Toth, G.C.M. Meijer, and M. van-der-Lee, 'A new capacitive precision liquid level sensor', IEEE, Proc. of Conf. on Precision Electromagnetic Measurements, June 1996, Braunschweig, Germany, WE1B-5, pp. 356 – 357, (1996).

18 K. Spenner, M.D. Singh, H. Schulte and H.J. Boehnel, 'Experimental investigations on fibre optic liquid level sensors and refractometers', IEEE, Proceedings of the 1st International Conference on Optical Fibre Sensors, London, pp. 96-99, (1983).

19 D.A. Jackson, 'High precision remote liquid level measurement using a combination of optical radar and optical fibres,' IEEE, Proceedings of the 1st International Conference on Optical Fibre Sensors, London, pp. 100-103, (1983).

20 M. Belkerdid and N. Ghandeharioum, 'Fibre optic fluid level sensor', in Fibre Optic and Laser Sensors III, Proc. SPIE , **566**, pp. 153-158, (1985).

21 K. Iwamoto and I. Kamata, 'Liquid level sensor with optical fibres', Appl. Opt., **31**, pp. 51- 54, (1992).

22 A. Wang, M.F. Gunber, K.A. Murphy and R.O. Claus, 'Fibre optic liquid level sensor', Sensors and Actuators A, **35**, pp. 161- 164, (1992).

23 P. Raatikainen, I. Kassamakov, R. Kakankov and M. Luukkala, 'Fibre optic liquid level sensor', Sensors and Actuators, A, **35**, pp. 93 – 97, (1997).

24 J.D. Weiss, 'Fluorescent optical liquid level sensor', Opt. Eng., **39**, pp. 2198 – 2213, (2000).

25 C.C. Ye, S.W. James and R.P. Tatam, 'Long period fibre gratings for simultaneous temperature and bend sensing', Opt. Lett., **25**, pp. 1007 - 1009, (2000).

26 Data sheets for liquid of RI 1.456, from the 'A' series of RI liquids, supplied by Cargille.

27 V. Bhatia, D.K. Cambell, D. Sherr, T.G. D'Alberto, N.A. Zabaronick, G.A. Ten Eyck, K.A. Murphy and R.O. Claus, 'Temperature insensitive and strain insensitive long period grating sensors for smart structures', Opt. Eng., **36**, pp. 1872 – 1876 (1997).

28 V. Bhatia, 'Properties and sensing applications of long period gratings', PhD. Thesis, Virginia Polytechnic and State University, Blacksburg, Virginia, 1996.

29 J. Rayss, W.M. Podkoscielny, A. A. Gorgol, J. Widomski and J. Ryczkowski, 'The properties of polymer protective coatings of optical fibres: II The influence of curing time adhesion of UV curable coatings to fused silica surface', Applied Polymer Sci. **57**, pp. 1119-1125, (1995).

30 S. Yin, K-W. Chung and X. Zhu, 'A novel all optic tuneable LPG using a unique double cladding layer', Opt. Comm., **196**, pp. 181-186, (2001).

31 A.A. Abramov, B.J. Eggleton, J.A. Rogers, R.P. Espindola, A. Hale, R.S. Windeler and T.A. Strasser, 'Electrically tunable efficient broad band fibre filter', IEEE, Photon. Technol. Lett., **11**, pp. 445-447, (1999).

32 S. Magne, S. Rougeault, M. Viela and P. Ferdinand, 'State of strain evaluation with fibre Bragg grating-rosettes: Application to discrimination between strain and temperature effects in fibre sensors', Appl. Opt., 36, pp. 9437 – 9447, (1997).

33 V. Bhatia and A.M. Vengsarkar, 'Optical fibre long period grating sensors', Opt. Lett., **21**, pp. 692 – 694, (1996).

34 E.M. Dianov, A.S. Kurkov, O.I. Medvedkov, S.A. Vasiliev, 'Photo induced long period gratings as a promising sensor element', Proc. of Eurosensors X, The 10th European Conf. on Solid State transducers, Leuven, Belgium, P5, pp. 126 - 128, (1996).

35 X. Shu, T. Allsop, B. Gwandu, L. Zhang and I. Bennion, 'High temperature sensitivity of long period gratings in B-Ge co-doped fibre', IEEE - Photon. Technol. Lett., **13**, pp. 818 – 820, (2001).

36 M.N. Ng, K.S. Chiang, 'Thermal effects on the transmission spectra of long period fibre gratings, Opt. Comm. **208**, pp. 321-327, (2002).

37 Y. G. Han, C.S. Kim, K.Oh, U.C. Paek and Y. Chung, 'Performance enhancement of strain and temperature sensors using long period fibre grating', Proc. 13th OFS Conf., SPIE, Vol. **3746**, Tu2-7, pp. 58-61, Kyongju, Korea, (1999).

38 A.A. Abramov, A. Hale, R.S. Windeler and T.A. Strasser, 'Widely tunable long period fibre gratings', Electron. Lett., **35**, pp. 81- 82, (1999).

39 C.G. Atherton, A.L. Steele, and J.E. Hoad, 'Resonance conditions of long period gratings in temperature sensitive polymer ring optical fibre,' IEEE - Photon. Technol. Lett., **12**, pp. 65-67, (2000).

40 Data sheets for liquids of RI 1.460 and 1.462 from the 'A' series of RI liquids supplied by Cargille.

41 R. O. Claus, K. A. Murphy, M. S. Miller, B. R. Fogg and M. F. Gunther, 'Sense-able structure' in IEEE, Optical fibre sensors for smart materials and structures, pp. 548 – 550, (1992).

42 M. J. O'Dwyer, 'Implementation and Appraisal of an In-Fibre Bragg Grating Quasi-Distributed Health and Usage Monitoring System with Applications to Advanced Materials', Chapter 5, Ph.D. Thesis, Cranfield University, (2000).

43 M. J. O'Dwyer, G.M. Maistros, S.W. James, R.P. Tatam and I.K. Partridge, 'Relating the state of cure to the real time internal strain development in a curing composite using in-fibre Bragg gratinggs and dielectric sensors', Meas. Sci. Technol., **9**, pp. 1153-1158, (1998).

44 E. Chailleux, M. Silvia, N. Jaffrezic-Renault, Y. Jayet, A. Maazouz, G. Seytre and I. Kasik, 'Process monitoring of composites using multidetection techniques', ' Non-destructive Evaluation of Materials and Composites V, Proceedings of SPIE, **4336**, pp. 204-210, (2001).

45 J.P. Dunkers, J. L. Lehart, S. R. Kueh, J.H. van Zanten, S.G. Advani and R.S. Parnas, 'Fibre optic flow and cure sensing for liquid composite molding', Optics and Lasers in Eng., **35**, pp. 91-104, (2000).

46 C.C. Ye, C. Wei, S.Khaliq, S.W. James, P.E. Irving and R.P. Tatam, 'Bend sensing in structures using long period fibre gratings', 5th European Conf. on Smart structures and materials, Proc. SPIE, **4073**, pp. 311-315, Glasgow (U.K.), (2000).

47 W. Stark, J. Döring, V. Bovtun, Ch. Kürten, Proc. ECNDT '98, session: 'Monitoring of curing reaction of polycondensating thermosets at press and injection mouldings', **3**, pp. 185 – 191, (1998).

48 M.A. Afromowitz and K.Y. Lam, 'The optical properties of curing epoxies and applications to the fibre optic epoxy cure sensor', Sensors and Actuators A, **21-23**, pp. 1107 – 1110, (1990).

49 M.A. Afromowitz, 'Fibre optic polymer cure sensor', J. Lightwave Technol., **6**, pp. 1591-1594, (1988).

50 K.Y. Lam and M.A. Afromowitz, 'Fibre optic epoxy composite cure sensor, dependence of refractive index of an autocatalyic reaction epoxy system at 850nm on temperature and extent of cure', Appl. Opt., **34**, pp. 5635-5638, (1995).

51 C.J. DeBakker, N.A. St. John and G.A. George, 'Simultaneous differential scanning calorimetery and near-infrared analysis of the curing of tetraglcidyl-diminodiphenylmethane with diainodiphenylsulphone', Ploymer, **34**, pp. 716-725, (1993).

52 S.R. White, P.T. Mather and M.J. Smith, 'Characterisation of the cure-state of DGEBA-DDS epoxy using Ultrasound, Dynamic Mechanical and thermal probes', Polymer Eng. and Science, **42**, pp. 51- 67, (2002).

53 B. Chabert, G. Lachenal and C. V. Tung, 'Epoxy resins and epoxy blends studied by near-infrared spectroscopy', Macromolecular Symposia, **94**, pp. 145-158, (1995).

54 D.J. Dare and D.L. Chadwick, 'A low resolution pulsed nuclear magnetic resonance study of an epoxy during cure', Inter. J. of Adhesion and Adhesives, **6**, pp. 155-163, (1996).

55 W. Dong, M. Kubouchi, S. Yamamoto, H. Sembokuya, K. Arai and K. Tsuda, 'Decomposition mechanism of epoxy resin in nitric acid for recycling', Procc. EcoDesign 2001, 2nd International Symposium on Environmentally Conscious Design and Inverse Manufacturing, pp. 980-985, (2001).

56 Internet article by Dutch company, 'Know how for in-situ cure monitoring of epoxy resin types',

57 S. Wu, S. Gedeon and R.A. Fouracre, 'The measurement and modelling of dielectric response of molecules during curing of epoxy resin', IEEE, Trans. On Electrical Insulation,. **23**, pp. 409-417, (1988).

58 D.J. O'Brien, P.T. Mather and S. R. white, 'Viscoelastic properties of an epoxy resin during cure', J. of Composite Mater. pp. 883-904, (2001).

59 Li Li, C. Lizzul, H. Kim, I. Sacolick and J. E. Morris, 'Electrical, structural and processing properties of electrically conductive adhesives', IEEE, Trans. On Components, Hybrids and Manufacturing Technol.,. **16**, pp. 843-851, (1993).

60 K.T.V. Grattan and B.T. Meggitt, 'Optical fibre sensor technology: Applications and systems', Volume 3, Kluwer Academic Publishers 1999, Chapter 3, pp. 57-86.

61 Private Communication with Dr. Ivana Partridge, Cranfield University, also at www.cranfield.ac.uk/sims/materials/polymers/cure monitoring.

62 N. Hager III and R. Domszy, 'Time-domain reflectrometry cure monitoring', of Material sensing and Instrumentation, at www.msi-sensing.com.

63 P.A. Crosby, C. Doyle, C. Tuck, M.Singh and G.F. Fernando, 'Multifunctional fibre optic sensors for cure and temperature monitoring', Smart Structures and Materials 1999, Proc. SPIE, **3670**, pp. 144 - 153, (1999).

64 J.R. Dunphy, G. Meltz, F.P. Lamn and W.W. Morey, 'Multifunction, distributed optical fibre sensor for composite cure and response monitoring', Fibre optic Smart Structures and Skins III, Proc. SPIE, **1370**, pp. 116 - 118, (1990).

65 V.M. Murukeshan, P.Y. Chan, L.S. Ong and L.K. Seah, 'Cure monitoring of smart composites using fibre Bragg grating based embedded sensors', Sensors and Actuators, A, **79**, pp. 153 - 161, (2000).

66 V. Dewynter-Marty and P. Ferdinand, 'Embedded fibre Bragg grating sensors for industrail composite cure monitoring', J. Intell. Mater. Sys. Struct., **9**, pp. 785 - 787, (1998).

67 T. Liu, G.F. Fernando, Y. Rao, D.A. Jackson, L. Zhang and I. Bennion, 'A multiplexed optical fibre based extrinsic Fabry Perot sensor system for in-situ strain monitoring in composites', J. Smart Mater. Struct., 7, pp. 550 - 554, (1998).

68 B. Degamber and G.F. Fernando, 'Process monitoring of fibre reinforced polymer composites', MRS Bulletin, pp. 370 – 380, (2002).

69 C. Doyle, A. Martin, T. Liu, M. Wu, S. Hayes, P.A. Crosby, G.R. Powell, D. Brooks and G.F. Fernando, 'In-situ process and condition monitoring of advanced fibre reinforced composite materials using optical fibre sensors' Smart Mater. Struct., 7, pp. 145 – 158, (1998).

70 B. Zimmermann, M. DeVries and R. Claus, 'Composite cure monitoring using optical fibre sensors', Conf. on Optical Fibre Sensor-Based Smart Materials and Structures, Blacksburg, VA. pp. 182-187, April 1991.

71 G.A. George, P. Cole-Clarke, N. St. John and G. Friend, ' Real-time monitoring of the cure reaction of a TGDDM/DDS epoxy resin using fibre optic FT-IR', Polymer, **42**, pp. 643-657, (1998).

72 B.P. Rice, 'Composite cure monitoring with a tool-mounted UV-VIS-NIR fibre optic sensor', 39th Int. SAMPE Symp., pp. 893-904, (1994).

73 G.R. Powell, P.A. Crosby, D.N. Waters, C.M. France, R.C. Spooncer and G.F. Fernando, 'In-situ cure monitoring using optical fibre sensors – a compartaive study', Smart Mater. Struct., **7**, pp. 557 – 568, (1998).

74 R.E. Lyon, K.E. Chike and S.M. Angel, 'In-situ cure monitoringof epoxy resins using fibre optic Raman spectroscopy', J. Applied Polym. Sci. and Eng., **53**, pp. 1805-1812, (1994).

75 C.M. Stellman, J.F. Aust and M.L. Myrick, 'Remote cure monitoring of polymeric resins by laser Raman spectroscopy', Proc. 38th Intl. SAMPE Symposium, pp. 427 – 430, (1993).

76 J.F. Aust, K.S. Booksh, A.R. Muroski, M.P. Nelson and M.L. Myrick, 'Novel in-situ probe for polymer curing', Appl. Spectroscopy, **49**, pp. 392-394 (1995).

77 J.F. Aust, K.S. Booksh, C.M. Stellman, R.S. Parnas and M.L. Myrick, 'Precise determination of percent cure of epoxide polymers and composites via fibre optic Raman spectroscopy and multivariate analysis', Appl. Spectroscopy, **51**, pp. 247-252, (1997).

78 H-J Paik and N.H. Sung, 'Fibre optic intrinsic fluorescence for in-situ cure monitoring of amine cured epoxy and composites', Polym. Eng. Sci., **35**, pp. 1025-1028, (1994).

79 D.L. Woerdman, J.K. Spoerre, K.M. Flynn, R.S. Parnas, 'Cure monitoring of the liquid composite moulding process using fibre optic sensors', Polym. Comp., **18**, pp. 133-137, (1997).

80 W. Dang and N.H. Sung, 'In-situ cure monitoring of diamine cured epoxy by fibre optic fluorimetery using extrinsic reactive fluorophone', Polym. Eng. Sci., Vol. **34**, pp. 709-711, (1994).

81 A. Fuchs and N.H. Sung, 'Composite interphase study by evanescent wave fibre optic fluorescence', ANTEC Conf. Proc. pp. 2347-2349, Boston, MA, (1995).

82 R.O. Loutfy 'Fluorescence probes for polymerisation reactions: Bulk polyermerisation of styrene, n-butyl, methacrylate, etheyl methacrylate and ethyl acrylate', J. Polymer Sci.,: Polymer Physics Ed., **20**, pp. 825, (1982).

83 M.M. Ohm, A. Davis, K. Liu and R.M. Measures, 'Embedded fibre optic detection of ultrasound and its application to cure monitoring', SPIE, Fibre Optic Smart and Structures and Skins V, **1798**, pp. 134-143, (1992).

84 R.M. Kent, 'Fibre ultrasonics for health monitoring of composites', The 19th Digital Avionics Systems Conferences, 2000, Procc. DASC pp. 6D3/1-6D3/6, (2000).

85 B. Mitra and D.J. Booth, 'Remote cure monitoring of epoxy materials using optical techniques', Ultrasonics, **35**, pp. 569 -572, (1998).

86 J.Y. Chen, S.V. Hoa, C.K. Jen and H. Wang, 'Fibre optic and ultrasonic measurements for in-situ cure monitoring of graphite epoxy composites', J. Compos. Mater., Vol. **33**, pp. 1860 -1881, (1999).

87 R.J. Freemantle and R.E. Challis, 'Combined compresion and shear wave ultrasonic measurements on curing adhesive', Meas. Sci. Technol. **9**, pp. 1291-1302, (1998).

88 M. Matsukawa and I. Nagai, 'Ultrasonic characterisation of a polymer epoxy resin with imbalanced stoichiometry', J. Acoust. Soc. Am., **99**, pp. 2110 – 2115, (1996).

89 Josė Miguel López-Higuera, 'Handbook of Optical Fibre Sensing Technology', Wiley, USA, (2002).

90 R.G. May, J.M. Sanderson and R.O. Claus, 'Combined fibre optic strain sensor and composite cure monitor for smart structure applications', Proc. SPIE, **2191**, pp. 46-57, (1994).

91 C. Ganesh, P.J. Steele, H. Zhang, D. Mishra and J. Jones, 'Predicting degree of cure of epoxy resins with fibre optic sensors and artificial networks', 39th Intl. SAMPE Symposium, pp. 883-892, (1994).

92 G. Fawcett, W. Johnstone and W.L.K. Yim, 'Design and experimental optimisation of an evanescent field fibre optic refractometer', Conf. on Lasers and Electro-optics, Amsterdam, pp. 372-373, (1994).

93 R.O. Claus, K.D. Bennett, A.M. Vengsarkar, K.A. Murphy, 'Embedded optical fibre sensors for material evaluation', J. Non-Destructive Evaluation, **8**, pp. 135-145, (1989).

94 S.R.M. Kueh and S.G. Advain, 'Long period grating as a flow sensor for resin transfer moulding', Non-destructive Evaluation of Materials and Composites IV, Proc. SPIE, **3993**, pp. 204-210, (2000).

95 Data Sheet for EPO-TEK OG 125. Promatech Ltd.

96 Private communication with fibre supplier, Fibrecore Ltd.

97 G.F. Fernando, T. Liu, P. Crosby, A. Martin, D. Brooks, B. Ralph and R. Badcock, 'A multi-purpose optical fibre sensor design for fibre reinforced composite materials', Meas. Sci. Technol., **8**, pp. 1065-1079, (1997).

98 X. Shu, B. Gwandu, Y. Liu, L. Zhang and I. Bennion, 'Sampled fibre Bragg grating for simultaneous refractive index and temperature measurement', Opt. Lett., **26**, pp. 774 – 776, (2001).

Chapter 7 Conclusions and future research

This final chapter presents a synopsis of the study on long period grating, LPG, sensors and proposes directions for future investigations in this field.

7.1 Summary of the study on fibre optic long period gratings

In Chapter 6 the partial immersion of a 40mm long LPG in a liquid created two LPGs, one surrounded by air and the other by the liquid. The length of each LPG was dependent upon the liquid level. This acted to split the attenuation bands into two these were located at the wavelengths corresponding to the coupling conditions for the LPG surrounded by the liquid and by air. The minimum transmission values of the two attenuation bands were dependent on the length of each LPG. Measurement of the relative extinction of the bands facilitated the determination of the liquid level. Plotting the relative changes in the extinction of the attenuation bands showed a linear response over 60% of the length of the LPG. LPG's possess a large temperature sensitivity. The RI of the liquid also showed a temperature sensitivity by exhibiting a change in the coupling wavelengths. The central wavelengths then provide a measurement of the temperature and the RI, while the extinction gave a measure of the liquid level. The sensor is currently limited to use with liquids that have a RI of between 1.400 and 1.456, but this may be modified by use of a fibre with a different RI.

A method for enhancing the temperature sensitivity of a LPG was also presented in chapter 6. A LPG was immersed in oil with a high negative thermo-optic coefficient. The LPG's inherent temperature sensitivity and its response to temperature induced changes in the oil's RI were exploited. Once the RI of the oil was ≤ that of the cladding of the fibre, the central wavelengths of the attenuation bands responded to the change in RI. Each attenuation band demonstrated a different temperature sensitivity. For attenuation band 6 a very high temperature sensitivity of up to 19.2nm/°C over a range of 1.1°C was achieved. The temperature range for each attenuation band was different. The depths of the attenuation bands also responded to the temperature induced change

in the RI of the oil. A temperature sensitivity of up to 14.8%/°C over a temperature range of 2.0°C was shown by attenuation band 5. The temperature range was again different for each attenuation band, therefore by monitoring a number of attenuation bands in the spectrum of a single LPG allows measurements to be performed over different temperature ranges. The operating temperature and the sensitivity are determined by the properties of the surrounding oil, thus allowing optimisation of the sensor for a given application.

The transmission spectrum of a LPG embedded into an epoxy resin was demonstrated to respond to the RI changes that occur during the cure cycle of the resin. The central wavelengths and the minimum transmission values of the attenuation bands responded as expected from the characterisation experiments. However, the demonstrated technique did not utilise the optimum fibre and epoxy combination as the RI of the cured epoxy was greater than that of the fibre's cladding. Ideally, the maximum wavelength shift of the attenuation band would indicate the RI of the cured epoxy. This could be achieved by lowering the RI of the cured epoxy using a blend of epoxies or by using a fibre with a cladding of higher RI. The experiment is nevertheless a useful first attempt. Since, the demonstrated technique is sensitive to the state of cure it could be used within the body of large composite structures undergoing a curing process. It is further expected that the sensor may be left in the final product without detrimental effects to the eventual application and be used for the monitoring of other parameters such as temperature, strain and bending.

LPGs are versatile devices that can be used for a number of sensing applications. Large shifts in the central wavelength of a LPG's attenuation bands are induced by changes in the surrounding temperature, strain and RI. A bend is seen to divide the attenuation bands into two. The separation of the divided bands is observed to increase for bends with increasing radius of curvatures. LPGs greatest advantage is their potential for implementation with simple demodulation schemes. The amplitude mask based fabrication techniques allows batches of LPGs to be economically produced, an inexpensive system with low cost sensors and signal processing will make them more attractive to the end user. The versatility of LPGs can be employed in many different

applications, for example a temperature insensitive LPG could be used as a strain sensor. A LPG based RI sensor may be implemented without the need for etching the cladding. LPGs can be adapted for multi-parameter sensing for example, simultaneously measuring temperature and bend, temperature and strain and temperature, RI as well as liquid level. The multiple attenuation bands in a LPG's transmission spectrum can be used to distinguish between the effects of two or more changes acting on the same system. The limiting effects of cross-sensitivities and non-linearities can be overcome by designing special fibres or by fabricating LPGs with specific periodicities.

LPGs offer a number of advantages over conventional sensors, however, they also possess certain drawbacks which need to be addressed before a successful sensing system can be made commercially viable. One of the drawbacks is the bend sensitivity of LPGs, which is of major concern in applications such as the sensing of strain and during the measurements of the three demonstrated sensors. The LPG is expected to remain taut over the duration of the measurements. For other applications such as RI sensors, where constant access to the fibre cladding is required, the bend sensitivity may be a major limiting factor. The large number of attenuation bands also limits the number of LPGs that can be multiplexed using a broadband source.

7.2 Future research

A number of areas of future research have arisen from the experimental work and the review of LPGs as sensors in this thesis, the most significant of which are now outlined.

Where the LPG's sensitivity to bend is a problem it may be addressed by modifying the properties of the host fibre or by using grating periods that couple to lower order cladding modes [1]. However, the sensitivity to bend and to bend with respect to the orientation of the UV exposed face of the LPG can be used to devise a sensor from which the magnitude and direction of bend can be determined. The sensitivity of the LPG to the RI of the medium surrounding it has in the main concentrated on immersion into bulk RI liquids, however, it has been shown that the LPG responds to partial immersion in RI liquid [2] and to the thickness of the overlay

on its cladding [3]. If a film of the appropriate thickness is laid onto the surface of the cladding, then a small RI change could induce a large wavelength shift, this offers the possibility of developing a highly sensitive sensor, or if the overlay material is electro-optic then a voltage controlled optical modulator could be produced [3].

The monitoring of the RI changes in a curing epoxy resin has been demonstrated in this thesis. It has opened the door into the realm of possibilities by which the state of cure of an epoxy resin could be determined from its RI. Investigations into using LPGs with complementary technology such as dielectric sensors could provide collaborating information on particular points in the cure, such as gelation.

Composite materials have the potential to find widespread use across a range of industries, including the civil and military aviation industries, the civil engineering industries and the automotive industries [4, 5, 6]. The final mechanical properties of composite materials result from the complex variety of chemical and rheological events that occur during the curing cycle. An important issue is the development of residual strain in curing composite coupons [5]. The final strain in the composite coupons results possibly from the onset of liquification, gelation, and vitrification of the matrix resin within the composite coupons [5]. The net shrinkage of the cured resin has lead to the warping of the coupons [7]. In order to optimise the properties of the material, improve product yield, and reduce processing costs, adequate process monitoring must be implemented. LPGs could be used in conjunction with IFBGs sensors as integral parts of the composite coupons. These in-situ sensors could then be used to provide information during the fabrication of the composite coupons thus allowing processing decisions to be taken in light of the real-time analysis of cure parameters like temperature, pressure, resin viscosity, resin position, resin gelation-point, degree of cure, presence of moisture, and the types of polymerisations occurring within the composite. Consequently, the cure cycle can be tailored to produce desired properties in the material being processed. For example, in-situ sensors might be used to detect when the resin has achieved minimum viscosity so that the perfect time for injecting into a mould can be determined. Thus, in-situ sensors can lift materials processing from the realm of a trial and error procedure to a more scientific operation. Once the coupons are in use the combination of sensors could be used to provide 'in use' data, such as

variations in temperature, bending, moisture content, strain and for the detection of any impact that the structure may suffer.

References:

1 A.M. Vengsarkar, P.J. Lemaire, J.B. Judkins, V. Bhatia, J.E. Sipe and T.E. Erdogan, 'Long period gratings as band rejection filters', J. Lightwave Technol., **14**, pp. 58 – 65 (1996).

2 S. Khaliq, S.W. James and R.P. Tatam, 'Fibre optic liquid level sensor using a long period grating', Optics Lett., **26**, pp. 1224-1226 (2001).

3 S.W. James, N.D. Rees, R.P. Tatam and G.J. Ashwell, 'Optical fibre long period gratings with thin film overlay', Opt. Lett., **27**, pp. 686-688, (2002).

4 R. O. Claus, K. A. Murphy, M. S. Miller, B. R. Fogg and M. F. Gunther, 'Sense-able structure' in IEEE, Optical fibre sensors for smart materials and structures, pp. 548 – 550, (1992).

5 M.J. O'Dwyer, 'Implementation and Appraisal of an In-Fibre Bragg Grating Quasi-Distributed Health and Usage Monitoring System with Applications to Advanced Materials', Ph.D Thesis, Cranfield University, (2000).

6 M. J. O'Dwyer, G.M. Maistros, S.W. James, R.P. Tatam and I.K. Partridge, 'Relating the state of cure to the real time internal strain development in a curing composite using in-fibre Bragg gratinggs and dielectric sensors', Meas. Sci. Technol., **9**, pp. 1153-1158, (1998).

7 T.D. Kim and C.A. Rotz, 'Warping of flat composite isogrid Panels', Aerospace Conference, Procc. IEEE, **1**, pp. 271-277 (1997).

Publications arising from this research work

Journals:

1 S. Khaliq, S.W. James and R.P. Tatam, 'Fibre optic liquid level sensor using long period gratings' Optics Lett., Vol. **26**, pp. 1224-1226, (2001).

2 S. Khaliq, S.W. James and R.P. Tatam, 'Enhanced sensitivity fibre optic long period grating temperature sensor', Meas. Sci. & Technol., Vol. **13**, pp. 792-795, (2002).

Conference Presentations:

3 S. Khaliq, S.W. James, C.C. Ye, C. Wei, P. E. Irving and R.P. Tatam, 'Structural bend sensing using optical fibre long period gratings', Presented at the IOP, Applied Optics and Opto-electronics Conf., Loughborough University (U.K.), Sept. 17th – 21st (2000). Published in the Proc. of the IOP, pp. 20-23.

4 S.W. James, S. Khaliq and R.P. Tatam, 'Liquid level sensing using a long period fibre grating', Presented at the IOP meeting, In fibre Bragg gratings and Special fibres, Coventry (U.K.), Oct. 17th –18th (2001).

5 C.C. Ye, C. Wei, S. Khaliq, S.W. James, P. E. Irving and R.P. Tatam, 'Bend sensing in structures using long period optical fibre gratings', Presented at the 5th European Conf. on Smart Structures and Materials Glasgow (U.K.), (2000). Published in the Proc. SPIE,Vol. **4073**, pp. 311- 315.

6 S.W. James, C.C. Ye, S. Khaliq and R.P. Tatam, 'Bend sensing using optical fibre long period gratings', Presented at the 14th International Conf. on Optical Fibre Sensors Venice (Italy), (2000). Published in the Proc. SPIE, Vol. **4185**, pp. 66- 69.

7 S.W. James, S. Khaliq and R.P. Tatam 'Fibre optic long period grating liquid level sensor', Presented at the 15th International Conf. on Optical Fibre Sensors, Portland, Oregon, USA, (2002). Published in the IEEE Tech. Dig. pp. 139-142.

8 S.W. James, S. Khaliq and R.P. Tatam 'Enhanced temperature sensitivity long period grating sensor', Presented at the 15th International Conf. on Optical Fibre Sensors, Portland, Oregon, USA, (2002). Published in the IEEE Tech. Dig. pp. 127-130.